ISTANBUL TECHNICAL UNIVERSITY ★ GRADUATE SCHOOL OF SCIENCE ENGINEERING AND TECHNOLOGY

INVESTIGATION AND ENHANCEMENT OF THE MECHANICAL PROPERTIES OF THE FABRIC REINFORCED HYBRID COMPOSITES

Ph.D. THESIS

Hande SEZGİN

Department of Textile Engineering

Textile Engineering Programme

FEBRUARY 2018

ISTANBUL TECHNICAL UNIVERSITY ★ GRADUATE SCHOOL OF SCIENCE ENGINEERING AND TECHNOLOGY

INVESTIGATION AND ENHANCEMENT OF THE MECHANICAL PROPERTIES OF THE FABRIC REINFORCED HYBRID COMPOSITES

Ph.D. THESIS

Hande SEZGİN
(503112801)

Department of Textile Engineering

Textile Engineering Programme

Thesis Advisor: Prof. Dr. Ömer Berk BERKALP

FEBRUARY 2018

İSTANBUL TEKNİK ÜNİVERSİTESİ ★ FEN BİLİMLERİ ENSTİTÜSÜ

KUMAŞ TAKVİYELİ HİBRİT KOMPOZİTLERİN MEKANİK ÖZELLİKLERİNİN İNCELENMESİ VE İYİLEŞTİRİLMESİ

DOKTORA TEZİ

Hande SEZGİN
(503112801)

Tekstil Mühendisliği Anabilim Dalı

Tekstil Mühendisliği Programı

Tez Danışmanı: Prof. Dr. Ömer Berk BERKALP

ŞUBAT 2018

Hande Sezgin, a Ph.D. student of ITU Graduate School of Science Engineering and Technology student ID 503112801, successfully defended the thesis/dissertation entitled "INVESTIGATION AND ENHANCEMENT OF THE MECHANICAL PROPERTIES OF THE FABRIC REINFORCED HYBRID COMPOSITES", which she prepared after fulfilling the requirements specified in the associated legislations, before the jury whose signatures are below.

Thesis Advisor :	**Prof. Dr. Ömer Berk BERKALP** İstanbul Technical University	.....
Jury Members :	**Prof. Dr. Hale KARAKAŞ** Istanbul Technical University	.....
	Prof. Dr. Recep EREN Uludag University	.....

Date of Submission : 06.02.2018

To my family,

FOREWORD

First of all, I would like to express my gratitude to my advisor, Prof. Dr. Omer Berk BERKALP for his guidance during toilsome thesis process while encouraging me to proceed to the next step everytime.

A substantial part of my thesis was shaped in Liberec Technical University, Department of Material Engineering. Therefore, I would like to show gratitude to Prof. Dr. Jiri MILITKY and Assoc. Prof. Dr. Rajesh MISHRA for offering me such an opportunity and sharing their experiences with me.

I also would like to express my gratitude to Semih OZKUR, Shahrukh SHAHBAZ and Erdal DINC for their suppport in laboratory works.

I would like to thank to Erasmus Mobility Programme and Tincel Cultural Foundation for funding visiting scholarship to abroad.

The research presented in the thesis was supported by ITU Projects of Scientific Investigation (BAP; Project no: 37677 and 40030). Further more, I would like to thank to TUBITAK 2211, National Scholarship Programme for PhD Students for supplying scholarship during my thesis period and TUBITAK 2214 Program for funding visiting scholarship to abroad.

February 2018

Hande SEZGİN
(MSc.)

TABLE OF CONTENTS

Page

ABBREVIATIONS

Adj MS	**:** Adjusted Mean Squares
Adj SS	**:** Adjusted Sum of Squares
Al_2O_3	**:** Aluminium Oxide
ANOVA	**:** Analysis of Variance
B_2O_3	**:** Boron Trioxide
C-glass	**:** Corrosive resistant glass made with calcium borosilicates.
CaO	**:** Calcium Oxide
CNC	**:** Computer Numerical Control
CNT	**:** Carbon Nanotube
CO_2	**:** Carbon Dioxide
CVD	**:** Chemical Vapor Deposition
DF	**:** Degrees of Freedom
DHBA	**:** Dihydroxybenzoic Acid
DMA	**:** Dynamic Mechanical Analysis
DSC	**:** Differential Scanning Calorimetry
DWCNT	**:** Double-walled Carbon Nanotube
DWCNT-NH_2	**:** Amide Functionalized Double-walled Carbon Nanotube
E-glass	**:** Electrically resistive glass
e.p.c.	**:** ends per centimeter
F_2	**:** Fluorine
Fe_2O_3	**:** Iron (III) Oxide
H_2SO_4	**:** Sulfuric Acid
HNO_3	**:** Nitric Acid
ILSS	**:** Interlaminar Shear Strength
K_2O	**:** Potassium Oxide
MEKP	**:** Methyl Ethyl Ketone Peroxide
MgO	**:** Magnesium Oxide
MWCNT	**:** Multi-walled Carbon Nanotube
MWCNT-COOH	**:** Carboxyl Functionalized Multi-walled Carbon Nanotube

MWCNT-NH_2 : Amide Functionalized Multi-walled Carbon Nanotube

MWCNT-OH : Hydroxyl Functionalized Multi-walled Carbon Nanotube

Na_2O : Sodium Oxide

NaOH : Sodium Hydroxide

PAN : Polyacrylonitrile

p.p.c. : picks per centimeter

SD : Standard Deviation

SEM : Scanning Electron Microscope

SiO_2 : Silicon Dioxide

SWCNT : Single-walled Carbon Nanotube

T_g : Glass Transition Temperature

TGA : Thermogravimetric Analysis

TiO_2 : Titanium Dioxide

TEM : Transmission Electron Microscope

TUBITAK : The Scientifc and Technological Research Council of Turkey

UPR : Unsaturated Polyester Resin

VARTM : Vacuum Assisted Resin Transfer Moulding

SYMBOLS

a_{cn}	: Charpy impact strength of notched specimen
bar	: Metric unit of pressure
b_n	: Remaining width at the notch base of the test specimen
°C	: Celcius
GPa	: Gigapascal
h	: Thickness of the impact test specimen
J	: Joule
kN	: Kilonewton
kV	: Kilovolt
MPa	: Megapascal
tan δ	: Damping factor
vol. %	: Volume percent
wt. %	: Weight percent
W	: Corrected energy absorbed by breaking the test specimen
W_j, W_g, W_c, W_p	: Weight ratios of the jute, E-glass, carbon and polyester
$\rho_j, \rho_g, \rho_c, \rho_p$	: Densities of jute, E-glass, carbon and polyester
ρ_{ct}, ρ_{ex}	: Theoretical and experimental densities of composite
µm	: Micrometer

LIST OF TABLES

Page

LIST OF FIGURES

Page

INVESTIGATION AND ENHANCEMENT OF THE MECHANICAL PROPERTIES OF THE FABRIC REINFORCED HYBRID COMPOSITES

SUMMARY

Since the discovery of steel, metal materials have been the most preferred types of materials for engineering applications. However in the last century, there has been an ever-inreasing demand for novel materials with high specific mechanical properties, high stiffness-to-weight ratio and high strength-to-weight ratio which especially led the researchers to discover new materials by combining existing materials, namely known as composites. Most of the composite structures used in advanced applications are textile reinforced composites.

The primary aim of this work is to create a novel generation hybrid composite structure with improved mechanical properties. When a hybrid structure comprising two or more different types of fibers is used, desirable properties of a fiber eliminate the undesirable properties of the other. As a result, a balance of performance and cost can be achieved with appropriate material design. It is also known that the fiber-matrix interface has a prominent role in the mechanical performance of textile reinforced composites. This contribution mainly relates to the ability of the interface to transfer mechanical load to the matrix reinforcement material during loading. It has been shown in the literature that the long-term performance and fatigue life of composites are effectively controlled by micromechanical damage processes occurring at the fiber-matrix interface.

In this thesis, hybrid composite structures were manufactured by vacuum assisted resin transfer molding method using three different woven fabrics (jute, E-glass and carbon) as the reinforcing material and polyester resin as the matrix material. It was aimed to reduce the cost by adding jute fabric while by using E-glass and carbon fabrics to improve the mechanical properties. In addition, it was observed that previous studies on textile reinforced composites have generally used fiber or unidirectional structures as the reinforcement material. In this study, woven fabric structures were preferred because they show better impact strength and more stable structure. By using these materials firstly one type of fabric reinforced composite materials and nine hybrid composite materials in the form of binary combinations of these three different fabrics were produced. All composite structures comprise four layers of fabric. The void ratios, mechanical properties (tensile and impact strength) and thermal properties (dynamic mechanical analysis, thermogravimetric analysis and differential scanning calorimetry analysis) of these twelve different composite structures were investigated.

When previous studies were examined, it was appeared that there were many studies about investigation of the mechanical properties of textile reinforced composites. In those studies, the effects of changing the reinforcement materials (different fiber types) and the alignment of the reinforcement material (fabric) on the mechanical properties of composite materials were investigated. Within the scope of this thesis, tests were performed with samples that taken from both directions of composite material, taking into consideration the weft and warp direction of the fabric, which is an important

factor for the woven fabrics. The obtained results showed that the analysis results of the samples taken from these directions had a big difference and the fact that there was not any study considering the weft and warp directions of reinforcing material displays the deficiency in the field of textile reinforced composites.

Since produced composite specimens were thought to be suitable for use in the automotive industry, it has been concluded that thermal analysis other than mechanical tests were also appropriate for these materials. These tests had been carried out in order to understand how the increase in the temperature of the internal parts during the operation of the automobiles influences the structure of the material and its thermo-mechanical properties.

The results of the mechanical tests showed that the highest tensile strength result was obtained with the carbon fabric reinforced composite structure while the E-glass reinforced composite material was attained for the highest impact strength. The jute fabric reinforced sample had the lowest values in both test results. When the hybrid specimens were examined, it was understood that the best results in tensile strength tests were obtained with constructions in which the high tensile strength fabrics placed to the outer layers of the composite structure, whereas the higher impact strengths were achieved by placing fabrics which have high impact strength to the inner layers.

At the second part of the thesis study, the effects of addition of nano filler materials on the mechanical properties of composite structures were examined. In this study, carbon nanotubes with a combination of excellent mechanical, electronic and thermal properties had been preferred as nanofiller materials. It was seen that in previous studies in order to improve the mechanical properties of composite materials, the most widely used type of multi-walled carbon nanotube (MWCNT) was pristine MWCNT and that there was not any study about MWCNTs with hydroxyl and carboxyl functional groups. In this thesis, pristine MWCNT, MWCNT-OH and MWCNT-COOH were used as the nano-filler material in order to determine how the MWCNTs with different functional groups affect the mechanical properties compared to pristine MWCNT. Thirty-six composite specimens were produced by adding these three nano-filler materials to twelve different constructions.

Mechanical and thermal analysis of those thirty-six samples were performed and the results were compared with those of not nano-filler added composite materials. When examining the changes in mechanical properties, it was found that all three types of MWCNTs positively affected the tensile and impact strengths, and it was understood that the best results were obtained with pristine MWCNT added samples. In addition, void ratios, which have major effects on the mechanical properties of composite materials, were also calculated and it was found that void ratios were decreased by the addition of different types of MWCNTs.

Dynamic mechanical analysis (DMA), thermogravimetric analysis (TGA) and differential scanning calorimetry (DSC) analysis were performed as thermal analysis. All three tests were applied to composite samples as well as polyester resin and fabric samples.

When the literature was examined, no study has been found on the application of dynamic mechanical analysis to fabric structures. It was seen from the DMA results that, the carbon fabric structure has higher moduli (storage and loss moduli) than the others and that with increasing temperature there is a decrease in the moduli of carbon and E-glass fabrics, while an increase in the modulus of jute fabric structure. Dynamic mechanical analysis results of composite specimens showed that the moduli were

higher in the samples taken from the warp direction of the material and the MWCNT addition affected the modulus values positively.

Thermogravimetric analysis of the fabrics revealed that the jute fabric structure was passed through two degradation stages at about 255°C and 345°C, and that the carbon fabric started to degrade at around 520°C, while E-glass fabric did not show any degradation till to 600°C. When the thermogravimetric analysis results of composite structures were considered, different types of MWCNTs had slightly increased the degradation temperature of composite materials.

DSC analysis of both fabric and composite materials showed that the jute-containing samples showed an endothermic reaction at around 55°C due to the impurities and humidity in the jute fabric. Apart from the TGA results, it has been determined that the addition of MWCNTs has nearly no effect on the degradation temperature of the samples.

The significance of the mechanical test results (tensile and impact strength) were examined by full factorial analysis method with the help of MINITAB software program and it was observed that the four selected factors (yarn material type, fabric direction, fabric stacking sequences and MWCNT type) had statistically significant effects on mechanical properties. It was seen that the most effective factor on the mechanical properties of the composite structure was the yarn (material) type, while the least effective one was the type of MWCNT. In addition, the bonding strength of reinforcement and matrix materials were investigated via scanning electron microscope images.

The hybrid composite structures that produced as a result of this work is expected to be a suitable material for the automotive industry due to its mechanical properties and lightweight. As it provides less energy and fuel consumption in vehicles, lightness has become a necessity for automobiles. By taking into account the decline in fossil fuel supplies and global warming, it is clear that how lightness of a vehicle is an important factor for the environment.

Within the scope of this doctoral dissertation, the below subjects that have not been carried out in previous works were studied on. These are;

- → Dynamic mechanical analysis of fabrics was carried out,
- → It has been proved that the mechanical and thermo-mechanical properties of the woven fabric reinforced composites vary considerably accordingly to the warp/weft directions of the fabric reinforcement,
- → Instead of epoxy resin that was used in almost all studies about E-glass and carbon reinforced composites, polyester resin which is lighter and cheaper than epoxy was utilized in this study to demonstrate that polyester based composites can also achieve sufficient mechanical properties for automotive industry.
- → It has been examined how the hydroxyl and carboxyl functionalized MWCNTs contribute to the mechanical properties of materials compared to pristine MWCNT and it has been proved that pristine MWCNT had higher effect on mechanical properties of textile reinforced hybrid composites.

In the light of these studies, it is thought that the results obtained from this doctoral dissertation will guide the following studies about fabric reinforced polymer composite materials.

KUMAŞ TAKVİYELİ HİBRİT KOMPOZİTLERİN MEKANİK ÖZELLİKLERİNİN İNCELENMESİ VE İYİLEŞTİRİLMESİ

ÖZET

Çeliğin keşfinden bu yana, metal malzemeler, mühendislik uygulamaları için en çok tercih edilen malzeme türleri olmuştur. Fakat günümüzde birçok uygulama alanında yüksek spesifik mekanik özelliklere, yüksek rijitlik/ağırlık oranına ve yüksek mukavemet/ağırlık oranına sahip malzemelere karşı artarak devam eden ihtiyaçların neticesinde yapılan araştırmalar, yeni ve üstün nitelikli kompozit malzemelerin ortaya çıkmasına ön ayak olmuştur.

Kompozit yapılar çoğu zaman alaşımlarla karıştırılsa da aslında alaşımlardan tamamen farklıdırlar. Malzemeler kompozit yapılarda makroskopik olarak birleştirilirken, alaşımlarda mikroskopik olarak birleşmektedirler. Bu nedenle, alaşımlar makroskopik boyutlarda homojen bir görünüm sergilerken, kompozitler homojen olmayan görüntüdedirler. Ayrıca, kompozit yapılardaki her bir bileşen kendi mekanik, kimyasal ve fiziksel özelliklerini korur. Gelişmiş kompozit malzemeler, askeri, sivil havacılık uygulamaları, otomotiv endüstrisi ve ulaşım gibi birçok farklı alanda kullanılmaktadır. İleri uygulamalarda kullanılan kompozit yapıların birçoğunun tekstil takviyeli kompozitler olması da önemli bir gerçektir.

Bu çalışmanın ilk amacı mekanik özellikleri geliştirilmiş yeni nesil hibrit bir kompozit yapı oluşturmaktır. İki veya daha fazla farklı lif türü içeren bir hibrit yapı kullanıldığında, bir lifin istenen özellikleri diğerinin istenmeyen özelliklerini yok etmektedir. Sonuç olarak, uygun malzeme tasarımı ile performans ve maliyet dengesi elde edilebilmektedir.

Ayrıca lif-matris arayüzünün, tekstil takviyeli kompozitlerin mekanik performansında belirgin bir role sahip olduğu bilinmektedir. Bu katkı esas olarak arabirimin yükleme esnasında matristen takviye malzemesine mekanik yük transfer edebilme yeteneği ile ilgilidir. Literatürden, kompozitlerin uzun süreli performansı ve yorulma ömrünün lif-matris arayüzünde meydana gelen mikromekanik hasar süreçleri tarafından etkili bir şekilde kontrol edildiği görülmüştür.

Bu doktora tezi kapsamında takviye malzemesi olarak üç farklı dokuma kumaş (jüt, E-camı ve karbon) ve matris malzemesi olarak da polyester reçine kullanılarak vakum infüzyon yöntemi ile hibrit kompozit yapılar elde edilmiştir. Malzeme seçiminde E-camı ve karbon kumaş kullanılarak mekanik özelliklerin iyileştirilmesi amaçlanırken jüt kumaş eklenerek maliyetin düşürülmesi hedeflenmiştir. Ayrıca, tekstil takviyeli kompozitlerle ilgili önceden yapılmış olan çalışmalarda genel olarak lif ve tek yönlü yapıların kullanıldığı görülmüştür. Bu çalışmada ise onlardan farklı olarak daha iyi darbe dayanımı ve daha stabil bir yapı göstermesinden dolayı dokuma kumaş yapısı tercih edilmiştir.

Bu malzemeler ile birlikte ilk olarak, üç adet tek tip lif içeren dört katlı kumaş takviyeli kompozit yapılar ve bu üç farklı kumaşın ikili kombinasyonları şeklinde dokuz adet dört kat kumaş takviyeli hibrit kompozit malzemeler üretilmiştir. Üretilen bu oniki

farklı kompozit yapının boşluk oranları, mekanik özellikleri (çekme ve darbe dayanımı) ve termal özellikleri (dinamik mekanik analiz, termogravimetrik analiz ve diferansiyel taramalı kalorimetri analizi) incelenmiştir.

Önceden yapılmış çalışmalar incelendiğinde, tekstil takviyeli kompozitlerin mekanik özelliklerinin araştırıldığı bir çok çalışma olduğu görülmektedir. Bu çalışmalarda, takviye malzemelerini (farklı lif tipleri) ve kullanılan bu malzemelerin sıralımlarını değiştirerek bu faktörlerin mekanik özellikler üzerindeki etkisi incelenmiştir. Gerçekleştirilmiş olan bu tez kapsamında ise, farklı lif tipi ve kumaş sıralımlarının yanı sıra dokuma kumaşlar için önemli bir faktör olan kumaşın atkı ve çözgü yönü de göz önünde bulundurularak testler her iki yönden alınan numunelerle gerçekleştirilmiş ve elde edilen sonuçlar bu iki yönden alınan numunelerin birbirinden oldukça farklı mekanik özellikler gösterdiğini gözler önüne sermiştir. Literatürde bugüne kadar takviye malzemesinin atkı ve çözgü yönlerini dikkate alarak yapılmış çalışmaya rastlanmaması tekstil takviyeli kompozitler alanında önemli bir eksikliğin olduğunu göstermektedir.

Üretilecek olan kompozit numunelerin otomotiv sektöründe kullanıma uygun olacağı düşünüldüğünden bu malzemelere mekanik testler dışında termal analizlerin de yapılmasının uygun olduğu sonucuna varılmıştır. Otomobillerin çalışması esnasında iç aksamlarda oluşan sıcaklık artışının malzemenin yapısına ve termo-mekanik özelliklerine ne derece etkide bulunduğunu anlamak amacıyla bu testler gerçekleştirilmiştir.

Elde edilen mekanik test sonuçları, en yüksek çekme dayanımının karbon kumaş takviyeli kompozit yapı ile elde edildiğini gösterirken, en yüksek darbe dayanımına ise E-camı takviyeli kompozit malzeme ile ulaşıldığını ispat etmiştir. Jüt kumaş takviyeli numune ise her iki test sonucunda da en düşük değerleri elde etmiştir. Hibrit numuneler incelendiğinde ise, çekme dayanımı testlerinde en iyi sonuçların çekme dayanımı daha yüksek olan kumaşların kompozit yapının dış katmanlarına yerleştirildiği konstrüksiyonlarla elde edildiği görülürken, darbe dayanımında ise bunun tam tersi olarak darbe dayanımı yüksek olan kumaşların kompozit yapının iç katmanlarına yerleştirildiği numunelerle yüksek darbe dayanımı elde edildiği anlaşılmıştır.

Elde edilen bu sonuçlardan sonra tez çalışmasının ikinci kısmında ise nano dolgu malzemelerinin üretilen bu kompozit yapıların mekanik ve termal özelliklerine etkisi incelenmiştir. Bu çalışmada, nano dolgu malzemesi olarak mükemmel mekanik, elektronik ve termal özelliklerin kombinasyonuna sahip olan karbon nanotüpler tercih edilmiştir. Kompozit malzemelerin mekanik özelliklerini geliştirmek için önceden yapılmış olan çalışmalarda en çok kullanılan çok duvarlı karbon nanotüp (ÇDKNT) tipinin saf ÇDKNT olduğu görülmüş ve ayrıca hidroksil ve karboksil fonksiyonel grubu eklenmiş ÇDKNT'lerle ilgili yapılmış hiç bir çalışma olmaması dikkat çekmiştir. Farklı fonksiyonel grup içeren ÇDKNT'lerin saf ÇDKNT'e göre mekanik özelliklere ne oranda etki ettiğini belirlemek amacıyla bu tez kapsamında nano dolgu malzemesi olarak saf ÇDKNT, ÇDKNT-OH ve ÇDKNT-COOH kullanılmıştır. Önceden üretilmiş olan oniki farklı konstürksiyona bu üç nano takviye malzemesi de eklenerek otuz altı kompozit numunesi daha üretilmiştir.

Üretilen bu otuz altı numunenin de mekanik ve termal analizleri yapılarak sonuçlar nano takviye uygulanmamış kompozit malzemelerin sonuçları ile karşılaştırılmıştır. Mekanik özelliklerdeki değişimlere bakıldığında her üç tipteki ÇDKNT'ün de çekme ve darbe dayanımlarını olumlu bir şekilde etkilediği görülmüş ve bu üç tip ÇDKNT

arasından en iyi sonuçların ÇDKNT-OH ve ÇDKNT-COOH'a kıyasla saf ÇDKNT ile elde edildiği anlaşılmıştır. Ayrıca, kompozit malzemelerin mekanik özellikleri üzerinde büyük etkisi olan boşluk oranları da hesaplanmış ve ÇDKNT ilave edilmiş numunelerde boşluk oranlarının azaldığı tespit edilmiştir.

Termal analiz testi olarak ise dinamik mekanik analiz (DMA), termogravimetrik analiz (TGA) ve diferansiyel taramalı kalorimetri (DSC) analizi gerçekleştirilmiştir. Her üç test, kompozit numunelerin yanında ayrıca polyester reçine ve kumaş numunelerine de uygulanmıştır.

Literatür incelendiğinde, dinamik mekanik analiz yönteminin daha önce kumaş yapılarına uygulandığı bir çalışmaya rastlanmamıştır. Karbon kumaş yapısının diğerlerine göre daha yüksek modüllere (depolama ve kayıp modülü) sahip olduğu ve artan sıcaklıkla birlikte karbon ve E-camı kumaşlarının modüllerinde azalma görülürken, jüt kumaş yapısının modülünde ise artış olduğu anlaşılmıştır. Kompozit numunelerinin dinamik mekanik analiz sonuçlarında ise mekanik analiz testlerinde olduğu gibi malzemenin çözgü yönünden alınan numunelerde modüllerin daha yüksek olduğu ve ÇDKNT ilavesinin modül değerlerini olumlu bir şekilde etkilediği görülmüştür.

Kumaş yapılarının termogravimetrik analiz sonuçlarından jüt kumaş yapısının 255°C ve 345°C civarlarında iki degradasyon evresinden geçtiği görülürken, karbon kumaşlarda 520°C civarında bir bozunmanın başladığı, E-camı kumaşlarda ise 600°C'ye kadar malzemede bir bozunmanın olmadığı anlaşılmıştır. Kompozit yapıların termogravimetrik analiz sonuçlarına bakıldığında ise üç farklı tip ÇDKNT ilavesi kompozit malzemelerin bozunma sıcaklığını bir miktar arttırmıştır.

Hem kumaşlara hem de kompozit malzemelere yapılan DSC analizlerinde ise jüt içeren numunelerin jüt kumaşın içerisinde bulunan safsızlıklar ve nemden dolayı 55°C civarında endotermik bir reaksiyon verdiği görülmüştür. TGA sonuçlarına kıyasla DSC'den elde edilen bozunma sıcaklıklarına ÇDKNT ilavesinin anlamlı bir etkide bulunmadığı saptanmıştır.

Yapılan mekanik testlerin (çekme ve darbe dayanımı) sonuçları MINITAB yazılım programında tam faktöriyel analiz metodu ile incelenmiş ve seçilen dört faktörün (İplik tipi, kumaş yönü, farklı kumaş sıralımları ve ÇDKNT tipi) de mekanik özellikler üzerinde istatiksel olarak anlamlı bir etkisi olduğunu gözler önüne serilmiştir. Mekanik özellikler üzerinde en çok etkili olan faktörün iplik tipi olduğu görülürken, en az etkiyi ise ÇDKNT tipinin gösterdiği anlaşılmıştır. Ayrıca taramalı elektron mikroskobu görüntüleri aracılığıyla takviye ve matris malzemelerinin birbirine tutunumları incelenmiştir.

Bu çalışmanın sonucu olarak üretilecek olan hibrit kompozit yapının, mekanik özellikleri ve hafifliği sayesinde otomotiv sektöründe uygun bir malzeme olacağı düşünülmektedir. Araçlarda daha az enerji ve yakıt tüketimini sağladığı için hafiflik, otomobil yapıları için bir zorunluluk halini gelmiştir. Fosil yakıt stoğundaki azalış ve küresel ısınma göz önünde bulundurulduğunda, araçların hafifliğinin çevre için ne kadar önemli bir faktör olduğu açıkça görülmektedir.

Bu doktora tezi kapsamında tekstil takviyeli kompozit malzemelerin mekanik özelliklerini geliştirmek amacıyla gerçekleştirilmiş olan önceki önceki çalışmalarda yapılmamış olan;

→ Kumaş yapılarının dinamik mekanik analizi gerçekleştirilmiş,

→ Dokuma kumaş takviyeli kompozitlerin mekanik ve termo-mekanik özelliklerinin kumaşın atkı/çözgü yönlerinden alınmış numunelerde oldukça farklılık gösterdiği ispat edilmiş,

→ E-camı ve karbon takviyeli kompozitlerin çoğunda kullanılan epoksi reçine yerine daha az maliyetli ve daha düşük yoğunluğa sahip olan polyester reçine tercih edilerek, polyester bazlı kompozit yapılarla da otomotiv sektörü için yeterli mukavemet elde edileceği görülmüş,

→ Hidroksil ve karboksil fonksiyonel gruplu ÇDKNT'lerin saf ÇDKNT'e göre malzemelerin mekanik özelliklerine ne oranda katkı sağladığı incelenmiş ve saf ÇDKNT'lerin mekanik özellikleri daha fazla geliştirdiği anlaşılmıştır.

Yapılan bu çalışmalar ışığında, bu doktora tezinden elde edilen sonuçların tekstil takviyeli kompozit malzemelerle ilgili bundan sonra yapılacak olan çalışmalara yol gösterici olacağı düşünülmektedir.

1. INTRODUCTION

Human population has almost reached 7.6 billion people in the world. While it continues to expand, our planet does not. On the other hand, human needs are also changing and expanding according to the growth in the global economy. In this perspective, composite materials that continue to progress rapidly has reached the quality of being the material of the future. They support the sustainable development and growth of the core industries and play a key role in meeting their future demands.

Composite structures, that are one of the most critical materials of today, are being improved day by day with high performances besides their lightness. Textile reinforced composite structures constitute a key share among all composite forms. In these structures, textile components provide strength and dimensional stability to the composite material. Since 1960s, textile reinforced composites is being used in diverse structural applications, for exhibiting high strength and hardness at low densities, high energy storage behavior and excellent fatigue performance.

In this perspective; the primary aim of this thesis is to seek answers for various solutions for enhancing the mechanical properties of fabric reinforced composites for the automotive industry. In order to reach our objective, one natural fiber (jute) based fabric and two inorganic man made fiber (E-glass and carbon) based fabrics were utilized as the reinforcement materials, whereas polyester resin as the matrix material. Vacuum assisted resin transfer molding technique was preferred as the manufacturing method.

Hybrid samples were produced with various fabric stacking sequences formed by binary combinations of these three fabric types. Four factors which were thought to have an influence on the mechanical properties of composite materials were established and the production was carried out accordingly. These factors were; yarn (material) type, fabric direction, fabric stacking sequence and multi-walled carbon nano tube (MWCNT) type.

- In the first factor, yarn (material) type, binary combinations (jute / E-glass, jute / carbon, E-glass / carbon) of the three different fabrics were selected. Hybrid samples with four layers of fabric plies have comprised two layers of each fabric.
- The second factor was the fabric direction, which was not unfortunately considered in the previous studies (according to our knowledge). On the other hand, as a textile engineer, we know that fabrics are not iso-structural units, therefore the mechanical properties of the woven fabric reinforced composite materials were examined in both directions and this significantly influences the mechanical properties of the composite materials. In this context, the tests were carried out based on the warp and weft directions of the woven fabrics in the composite material.
- The third factor was the fabric stacking sequence. The positions of four layers of the reinforcement material were altered in three different arrangements for each binary combination of yarn (material) types. In the first of these three combinations, the higher strength fabrics were placed in the inner layers of the sample (layers 2 and 3) whereas the higher strength fabrics were placed in the outer layers of the composite sample (layers 1 and 4) in the second arrangement type. In the final combination, two fabric types were aligned alternately.
- The fourth and final factor was the type of nano filler material added to the composite material (MWCNT type). Four different levels had been identified for this case. The samples without nanofiller material which was produced in the first stage of the study, constitute the first level whereas the samples with pristine MWCNT, MWCNT-OH and MWCNT-COOH form was manufactured at the second, third and fourth levels respectively.

By taking into account of these factors, forty-eight dissimilar composite configurations were manufactured and samples were considered from the machine and cross directions of these composite plates and at the end of the day; a total of ninety-six different test samples were obtained and evaluated in this research.

The effects of these four factors on the mechanical properties of the composite materials were investigated by various methods. Firstly, composite void ratio, which is an important factor on the mechanical properties of composite materials, were

evaluated by calculating the theoretical and experimental densities of the materials. Subsequently, the mechanical properties of the materials were measured by tensile and impact strength tests. Since the samples manufactured in this entire research were thought to be suitable for the automotive industry and automobile interior parts are exposed to high temperatures - besides the mechanical properties of these composite materials -, the thermo-mechanical properties (storage module, loss modulus and loss factor) were also measured and evaluated by dynamic mechanical analysis method. In addition, the thermal properties of the materials were investigated by differential scanning calorimetry analysis and thermogravimetric analysis methods. Moreover, the interfacial bonding strength between matrix and reinforcement materials was analyzed by scanning electron microscope images. Finally, to examine whether or not the mechanical results (tensile and impact strength) were statistically significant; a full factorial experimental design method through Minitab 18 program was utilized.

The mechanical, thermo-mechanical and thermal properties of the matrix material (polyester resin), thermo-mechanical and thermal properties of the reinforcement materials (jute, E-glass and carbon fabric) were also investigated separately and the properties of these materials were compared with those of the composite materials. The mechanical tests could not have been performed on the reinforcement materials because fabric structure is not a suitable material for the impact strength test and correspondingly; E-glass and carbon yarns have slipped over each other throughout the tensile strength tests and furthermore the fabrics have slid from the jaws during the testing due to the slippery properties of the filaments.

It was thought that some of the deficiencies (mechanical and thermo-mechanical tests according to fabric direction, the effects of hydroxyl and carboxyl functionalized MWCNTs on mechanical properties) which were not considered in previous studies related to the mechanical properties of fabric-reinforced composite materials have been attempted to be contemplated by this study and it is apparent that some of these factors (especially fabric directions) that were not realized in previous studies, should be taken into account from now on at the composite industry thus this research will be a guide for future studies.

2. COMPOSITE STRUCTURES

2.1 Composites

In today's world, the ever-evolving technology and the endless desires of people are increasing the demand for innovative materials (Raghavendra, Kumar, Kumar, RaghuKumar, & Ojha, 2015). In this perspective, composite materials seems to be one of the most preferred choices as novel materials when their outstanding properties are compared to conventional materials such as metal and wood (Agarwal, Patnaik, Sharma, & Agarwal, 2014; Gopinath, Kumar, & Elayaperumal, 2014; Jawaid, Khalil, Bakar, & Khanam, 2011; Ornaghi, Bolner, Fiorio, Zattera, & Amico, 2010). Their manufacturing methods consist of combining two or more different materials in macroscopic scale to form a new structure which have better features than the individual constituents (Campbell, 2010; Lee & Suh, 2006).

The first composite material is considered to be produced by ancient Egyptians 3000 years ago. It was a clay based composite material which was reinforced by straw and was used in building constructions (Sapuan & Maleque, 2005) . From that day to this, composite materials is being used in automotive, aerospace, marine applications, sporting goods, electrical equipments, defense industry and so on (Gopinath et al., 2014; Jawaid et al., 2011; Lee & Suh, 2006; Sapuan & Maleque, 2005).

Composite structures can be classified into three categories according to their matrix system. These are; metal matrix composites, ceramic matrix composites and polymer matrix composites (Campbell, 2010; Tucker & Lindsey, 2002).

2.2 Polymer Matrix Composites

During the last four decades, polymer matrix composites are gaining importance in both conventional and high technology application areas due to their high specific stiffness and strength, low cost, corrosive resistance and high dimensional stability properties. (Pandya, Veerraju, & Naik, 2011).

Composite materials are anisotropic materials and show different characteristics in different directions (Campbell, 2010). They are mostly confused with alloys but composite structures are completely different from alloys. While materials are being combined macroscopically in composite structures, they are being combined microscopically in alloys. Therefore, alloys exhibit a homogeneous appearance in macroscopic dimensions, while composites are inhomogeneous assemblies (Lee & Suh, 2006). Moreover, each constituent in the composite structures maintains its own mechanical, chemical and physical characteristics (Campbell, 2010).

The two main components of the composite structures are named as "reinforcement material" and "matrix material" (Gujjala, Ojha, Acharya, & Pal, 2014; Hasan, Islam, Morshed, Iqbal, & Wu, 2016). Reinforcement materials are mostly stronger and stiffer than the matrix materials (Campbell, 2010). On the other hand, matrix material is the continuous phase of the composite material which holds the reinforcement materials. It is the discontinuous phase of the structure. (Campbell, 2010; Lee & Suh, 2006). The main components of a composite structure are shown in Figure 2.1.

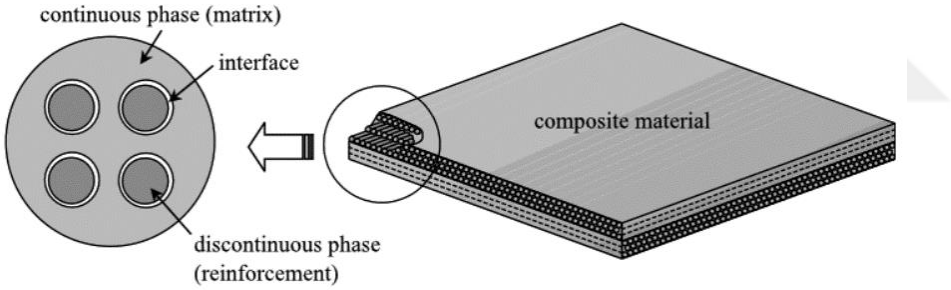

Figure 2.1 : Main components of a composite structure (Lee & Suh, 2006).

Figure 2.2 shows the relative effect of the reinforcement and the matrix material on several properties of the composites. It is seen that while the properties such as strength and stiffness of the composite are mostly associated with the reinforcement material; corrosion, temperature and chemical resistance of composite materials are directly related to the properties of the polymer matrix material. However, most of the mechanical properties of the composites are governed by both the reinforcement and the matrix material. By raising the amount of work that is needed to fracture the composite, the synergy of the reinforcement and the matrix material strengthen and toughen the composite material (Friedrich & Almajid, 2013).

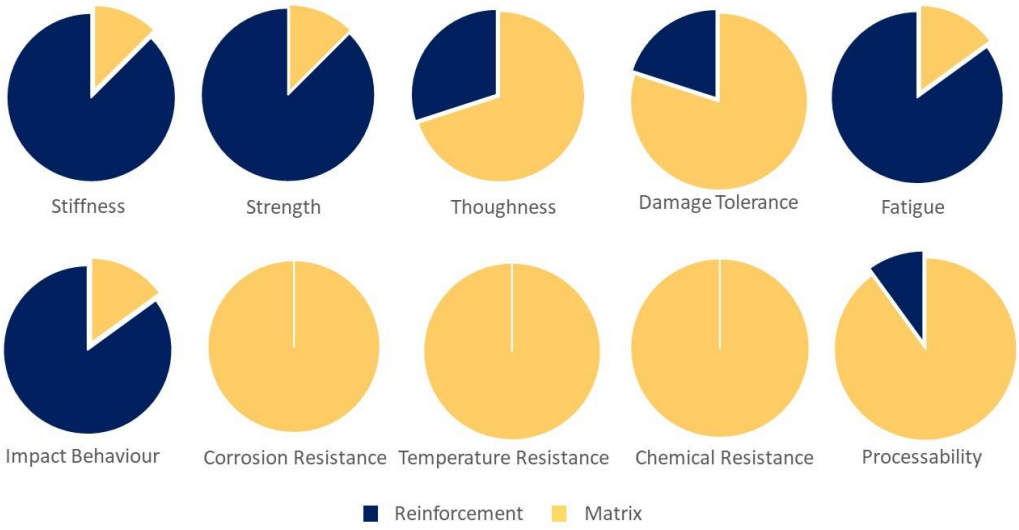

Figure 2.2 : Relative effect of reinforcement and matrix materials on properties of composites.

2.2.1 Reinforcement materials

Polymer matrix composites are mostly reinforced with textile structures. The utilization of textile materials in composite structures is increasing day by day under favour of excellent mergence of their relative low costs and high performances (Bodaghi, Cristóvão, Gomes, & Correia, 2016; Ding, Yan, McIlhagger, & Brown, 1995; Hasan et al., 2016; Mishra & Biswas, 2013). The first example of fiber reinforced composite was developed after World War II by embedding glass fibers in polymeric resin for petrochemical industry (Bakis et al., 2002).

Using low-cost, light-weight polymers with high strength and high modulus fibers provides good combination of mechanical and technological properties to composites and these properties enable them to find numerous application areas in many sectors such as; automotive, aerospace industry, medical, defense, marine and so on (Bakis et al., 2002; Bilisik & Yolacan, 2015; Bindal, Singh, Batra, & Khanna, 2013; Hasan et al., 2016; Hossain, Hossain, Dewan, Hosur, & Jeelani, 2013; Mishra & Biswas, 2013; Munikenche Gowda, Naidu, & Chhaya, 1999; Murugan, Ramesh, Padmanabhan, Jeyaraam, & Krishna, 2014; Sezgin & Berkalp, 2016; Shalin, 2012; Y. S. Song et al., 2012).

In composite structures, textile materials are used in different forms such as; unidirectional continuous fibers, bidirectional continuous fibers, multidirectional continuous fibers, unidirectional discontinuous fibers and random discontinuous fibers

(Mallick, 2007; Misnon, Islam, Epaarachchi, & Lau, 2013). Figure 2.3 shows the different forms of textile materials.

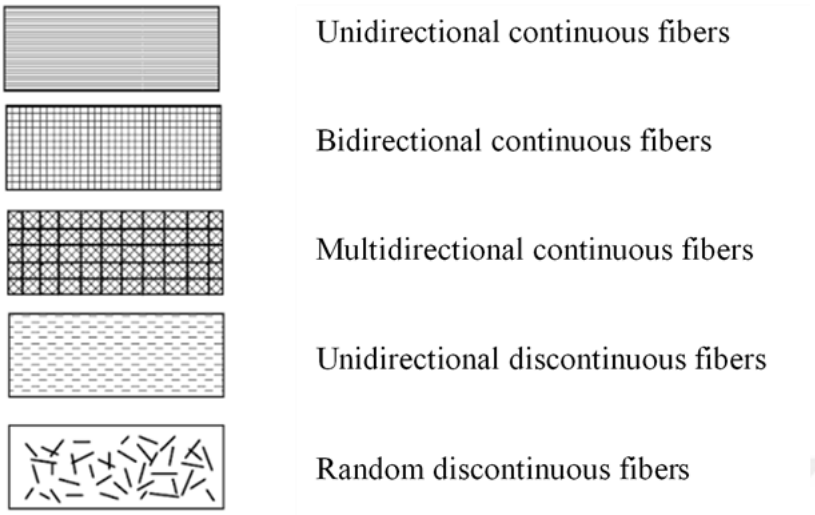

Figure 2.3 : Different forms of textile materials (Mallick, 2007).

While discontinuous fibers can be arranged in unidirectional or random form, continuous fibers can be arranged in the composite material in unidirectional, bidirectional or multidirectional forms (Lee & Suh, 2006; Mallick, 2007). The mechanical properties of discontinuous fiber reinforced composites are usually lower than those of continuous fiber reinforced composites due to their irregular alignment (Campbell, 2010).

At fiber reinforced composites, the length, orientation, cross sectional shape and the type of the fiber are the main factors that influence the mechanical properties (Ikbal, Ahmed, Qingtao, Shuai, & Wei, 2016). In structure while enabling new outstanding properties, fiber and the resin material also maintains their own physical and chemical features (Saha, Das, Bhatta, & Mitra, 1999). Fabric reinforced composites have superior properties than the fiber reinforced composites due to their orderly alignment, high load bearing capacity and good entirety concept (Su et al., 2006).

Bidirectional and multidirectional fiber structures are the fabrics that are obtained from weaving or other processes. In all these structures the mechanical properties can vary regards to direction of the material (Mallick, 2007). Among fabric structures (woven, knitted and nonwoven), woven fabric is one of the most preferred reinforcement material owing to their properties like easy formability to irregular shapes, deformation characteristics, integrity, dimensional stability and yarn packing density (Alavudeen,

Rajini, Karthikeyan, Thiruchitrambalam, & Venkateshwaren, 2015; Blackketter, Walrath, & Hansen, 1993; Kaka, Rongong, Hodzic, & Lord, 2015; Russo, Acierno, Simeoli, Iannace, & Sorrentino, 2013; Y. S. Song et al., 2012). Woven fabrics are divided into three main subclasses according to their patterns (Figure 2.4).

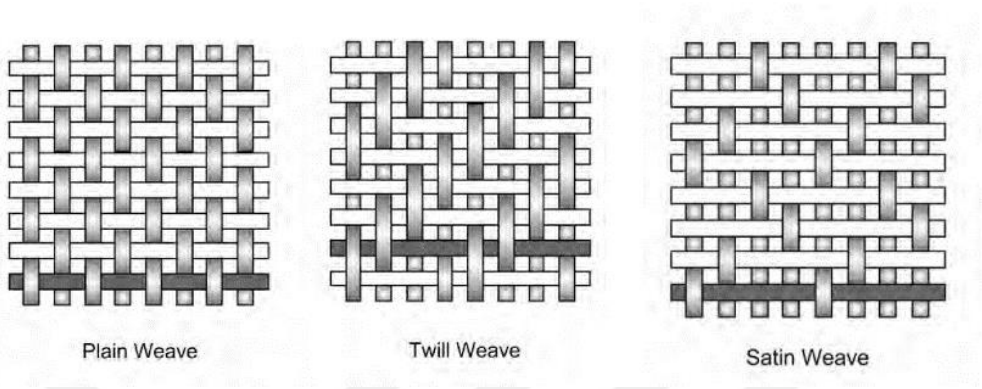

Figure 2.4 : Woven fabric types (Campbell, 2010).

Plain woven fabrics, which have the highest number of warp/weft interlaces per unit area, are more durable to in-plane shear movements and this makes them favourable materials as reinforcement (Campbell, 2010). Table 2.1 shows plain, twill and satin fabrics some features which have impact on mechanical properties of the material. Compared to others, plain-woven fabrics have higher stability and balance. Moreover, plain-woven fabrics are more symmetrical than other structures (Thomas, Joseph, Malhotra, Goda, & Sreekala, 2012).

Table 2.1 : Some features of woven fabrics (Thomas et al., 2012).

Property	Plain	Twill	Satin
Stability	****	***	**
Symmetrical	*****	***	*
Balance	****	****	**

***** =excellent, ****=good, ***=acceptable, **=poor, *=very poor

Fibers that are used in composite structures can be divided into two primary categories as natural and synthetic fibers (Jawaid, Khalil, Bakar, & Khanam, 2011).

2.2.1.1 Natural fibers for composite industry

Natural fibers are classified into two main groups; plant and animal fibers. The main difference between animal and plant fibers is their contents. While animal fibers are consist of protein, plant fibers are composed of cellulose. In composite industry,

cellulose based plant fibers are preferred as reinforcement material (Dicker et al., 2014).

Owing to their environmentally and economically beneficial features and their properties which are comparable to conventional materials, plant fiber reinforced composites become outstanding materials in the composite industry (Araújo, Correia, & Soares, 2015; Jabbar et al., 2017; Jabbar, Militký, Wiener, & Karahan, 2016; Mishra & Biswas, 2013; Rajesh, Jeyaraj, & Rajini, 2016; Rodrigues, Maia, & Mulinari, 2011; Sapuan & Maleque, 2005; Shahinur, Hasan, Ahsan, Saha, & Islam, 2015). In comparison to synthetic fiber reinforced composites, natural fiber reinforced composites cut down on the CO_2 emission in the atmosphere (Araújo et al., 2015). They also offer many benefits such as low cost, light weight, flexibility, renewability, enhanced energy recovery, high specific strength and stiffness, better thermal and insulation properties, relative non-abrasiveness, biodegradability and safer handling over synthetic fibers (Acha, Marcovich, & Reboredo, 2005; Ahmed, Vijayarangan, & Naidu, 2007; Das & Bhowmick, 2015; Gujjala et al., 2014; Jabbar et al., 2017; Jawaid, Abdul Khalil, Hassan, Dungani, & Hadiyane, 2013; Jawaid et al., 2011; Militký & Jabbar, 2015; Mishra & Biswas, 2013; Munikenche Gowda et al., 1999; Patel, Bhuva, & Parsania, 2008; Raghavendra, Kumar, Kumar, RaghuKumar, & Ojha, 2015; Ramesh, Palanikumar, & Reddy, 2013a; Shanmugam & Thiruchitrambalam, 2013; Tajvidi, Falk, & Hermanson, 2006). Physical properties of some natural fibers are given in Table 2.1.

Table 2.2 : Physical properties of some natural fibers (Holbery & Houston, 2006; Pandita et al., 2013).

Fiber	Density (g/cm3)	Elastic Modulus (GPa)	Tensile Strength (MPa)	Elongation at Break (%)
Jute	1.45	10-32	450-550	1.1-1.5
Sisal	1.45	26.32	580-610	3-7
Cotton	1.50-1.60	5.5-12.6	400	7-8
Flax	1.50	27.6	500-1500	2.7-3.2
Hemp	1.47	70	690	2-4
Ramie	-	61.4-128	400-938	3.6-3.8
Coir	1.20	4-6	593	30

Besides all these advantageous properties, natural fiber reinforced composites have some drawbacks. Their mechanical properties are not as high as synthetic fiber reinforced composites and also they have very high tendency to absorb moisture

(Ahmed & Vijayarangan, 2008; Alavudeen et al., 2015; Gujjala et al., 2014; Raghavendra et al., 2015; Romanzini, Lavoratti, Ornaghi Jr., Amico, & Zattera, 2013; Shanmugam & Thiruchitrambalam, 2013). The Young's modulus of natural fibers mostly decreases with increasing moisture content. When a natural fiber absorbs water, water goes to the pores and the amorphous parts of the fiber and this causes a reduction in interfibrillar bonding of the fiber (Baley, 2002). Besides, natural fibers have poor wettability and this fact causes unsatisfying bonding between fiber and the matrix material (Ashworth, Rongong, Wilson, & Meredith, 2016; Mohanty, Khan, & Hinrichsen, 2000; Patel et al., 2008; Tajvidi et al., 2006). Table 2.3 summarizes the advantageous and disadvantageous properties of natural fibers.

Table 2.3 : Advantages and disadvantages of natural fibers (Jawaid & Abdul Khalil, 2011).

Advantages	Disadvantages
Low specific weight, higher specific strength and stiffness than E-glass	Low strength (especially impact strength)
Renewable resources, low CO_2 emission	Variable quality
Production with low investment at low cost	Poor moisture resistant
No wear of tool and no skin irritation	Limited maximum processing temperature
High electrical resistant	Lower durability
Good thermal and acoustic insulating properties	Relatively Poor fiber matrix adhesion
Biodegradability	Poor fire resistant

By virtue of these disadvantageous properties, the technical necessities that are desired from a composite material is mostly insufficient in solely natural fiber reinforced composites (Hamouda, Hassanin, Kilic, Candan, & Bodur, 2015). To eliminate the relatively poor wettability of natural fibers, some chemical modifications are performed to the fibers (Alavudeen et al., 2015; Gujjala et al., 2014; Mohanty et al., 2000). Besides, some scientists take steps in the direction of hybridizing natural fiber reinforced composites with synthetic fibers. In this way, the economic advantages of natural fibers combine with the mechanical advantages of synthetic fibers, resulting in

a superior material (Ahmed & Vijayarangan, 2008; Alavudeen et al., 2015; Gujjala et al., 2014; Ornaghi, Bolner, Fiorio, Zattera, & Amico, 2010; Rajesh et al., 2016).

Natural fiber reinforced composites are mostly used in marine, construction, packaging, automotive and aerospace applications (Gopinath, Kumar, & Elayaperumal, 2014; Gujjala et al., 2014; Hasan et al., 2016; Manfredi, Rodríguez, Wladyka-Przybylak, & Vázquez, 2006; Ornaghi et al., 2010; Raghavendra et al., 2015).

Plant fibers, which consist of cellulose, hemicellulose, lignin and pectin, are divided into five main categories as follows: bast fibers, leaf fibers, seed fibers, grass fibers and all other fibers (wood fibers and etc.) (Raghavendra et al., 2015; Rodrigues et al., 2011; Shah, 2013). Fibers which belong to these five categories are given in Figure 2.5 (Célino, Freour, Jacquemin, & Casari, 2014; Romanzini et al., 2013; Smole, Hribernik, Kleinschek, & Kreže, 2013).

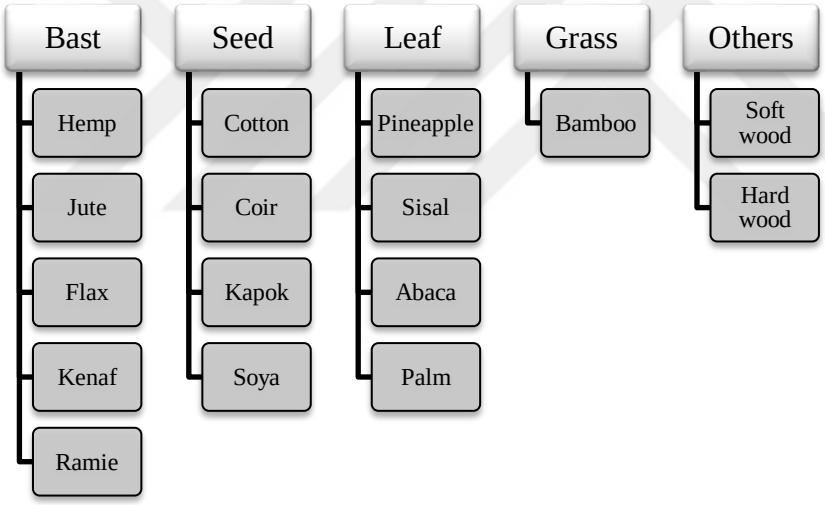

Figure 2.5 : Plant fiber categories.

Bast fibers are gathered from certain natural plants skin or inner shell of the stem (Ashworth et al., 2016). They have superior mechanical properties (such as high strength and rigidity) than other plant fibers and due to this fact they are the most used natural fiber reinforcement materials (Romanzini et al., 2013; Shah, 2013).

Jute fiber

Jute is a natural fiber which is obtained from jute plants (Raghavendra et al., 2015). It is the longest bast fiber (Shahinur et al., 2015). Jute fiber is mostly produced in Bangladesh, Latin America and India and are mostly 1-3.5 m in length (Das &

Bhowmick, 2015; Hasan et al., 2016). From the point of production and consumption, jute fiber is ranked as number two after cotton fiber and it contains one of the highest amount of cellulose among all natural fibers (Ashworth et al., 2016; Militký & Jabbar, 2015; Roe & Ansell, 1985). It contains 58-63% cellulose, 21-24% hemicellulose, 12-14% lignin, 0.8-1.5% nitrogenous substances, 0.6-1.2% inorganic substances and 0.4-0.8% fats and waxes. While lignin and hemicellulose are located in the amorphous region of the semi-crystalline structured jute, cellulose is mostly located in the crystalline region and they are all in the long chain molecule form (Acha et al., 2005; Hasan et al., 2016). The fundamental unit of cellulose is cellobiose, which is a combination of glucose units (Figure 2.6). Cellulose is an isotactic polymer of cellobiose (Suhas et al., 2016).

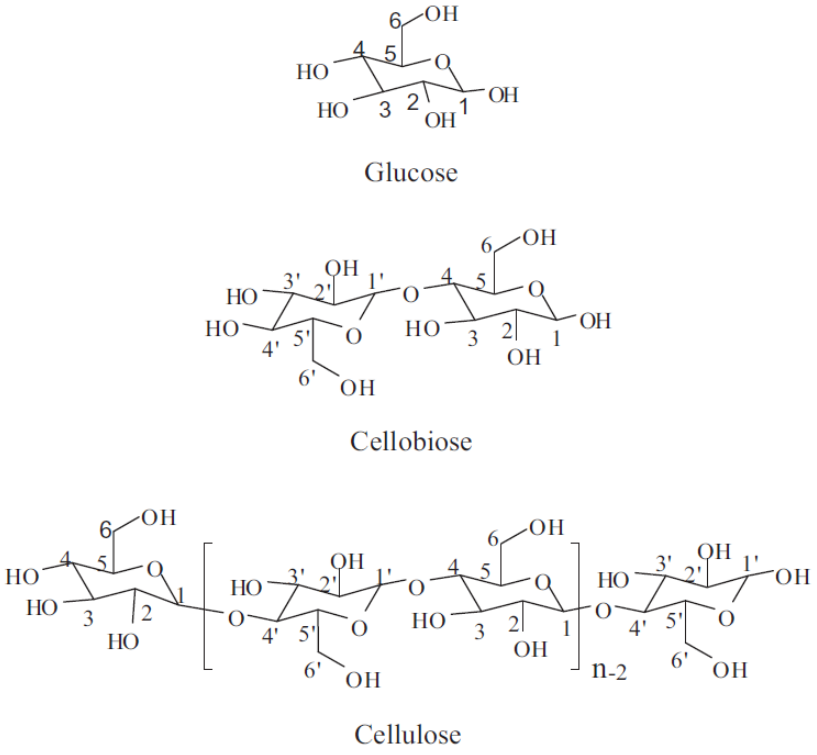

Figure 2.6 : Structure of glucose, cellobiose and cellulose (Suhas et al., 2016).

The characteristic properties of jute fibers are mostly related to the characteristics of the cellulose (Gassan & Bledzki, 1999). Jute, which is a strong fiber, has a brittle structure and low extension at break (Acha et al., 2005).

Jute is one of the most preferred natural fiber reinforcements owing to its properties such as; high modulus, low cost, good thermal and electrical insulation properties, moderate moisture regain, biodegradability, silky luster, high specific strength and

commercially availability (Acha et al., 2005; Ahmed & Vijayarangan, 2007; Hasan et al., 2016; Raghavendra et al., 2015; Shahinur et al., 2015; Shanmugam & Thiruchitrambalam, 2013; Tripathy, Di Landro, Fontanelli, Marchetti, & Levita, 2000). Apart from all these advantages, jute fiber also has some disadvantages like low extensibility, low abrasion resistance, highly non-uniformity, low moisture resistance, coarseness, poor protection against microbial attacks and poor wettability (Acha et al., 2005; Das & Bhowmick, 2015; Munikenche Gowda et al., 1999; Saha et al., 1999).

Jute fiber contains hydroxyl and some other polar groups and this gives them a hydrophilic characteristic. The poor wettability of jute fiber is mostly related to the mismatch between hydrophilic fiber and hydrophobic matrix material (Acha et al., 2005; Mohanty et al., 2000). Moreover, it is well known that like all plant fibers, properties of jute fiber changes according to its growth conditions, geographic origin and processing techniques (Gassan & Bledzki, 1999; Munikenche Gowda et al., 1999).

Jute fiber is mostly used as a woven form in the composite structures. Woven jute fabrics are denominated as Hessian cloth and a surface coating is applied to jute yarns before weaving to make its' manufacture easier and more efficient. (Acha et al., 2005; Hasan et al., 2016).

In composite structures, jute fiber is mostly used with thermoset resins like phenolic, vinyl ester, epoxy and unsaturated polyester. The usage with thermoplastic resins is limited because of the weak bonding between hydrophilic jute and hydrophobic thermoplastics (Das & Bhowmick, 2015; Roe & Ansell, 1985; Sapuan & Maleque, 2005).

Jute reinforced polyester composites are used in many structural and nonstructural applications where high mechanical properties are not required, such as suitcases, bio-gas containers, pipes, post-boxes, lampshades, helmets and electrical appliance covers (Acha et al., 2005; Ahmed et al., 2007; Gopinath et al., 2014; Sapuan & Maleque, 2005).

2.2.1.2 Synthetic fibers for composite industry

The textile reinforced composites are come to exist primarily using synthetic fibers. They have superior properties than natural fibers (Begum & Islam, 2013). Synthetic fibers used in the composite industry are stronger than plant fibers (Acha et al., 2005). They possess less variation compared to natural fibers. Also, they have high strength

and stiffness, high thermal stability and their lower density than the metal materials (Begum & Islam, 2013; Unterweger, Brüggemann, & Fürst, 2014). By using synthetic fibers in composite structures, long fatigue life, good corrosion and wear resistance and environmental stability can be obtained in composite structures (Begum & Islam, 2013).

However, their densities are higher than those of plant fibers and they have very high cost in comparison to natural fibers (Acha et al., 2005; Begum & Islam, 2013). Moreover, one of the most important drawbacks of synthetic fibers are their poor recycling and non-biodegradable properties (Begum & Islam, 2013)

Properties of some synthetic fibers used in the composite industry are given in Table 2.2.

Table 2.4 : Properties of some synthetic fibers used in the composite industry (Holbery & Houston, 2006; Mallick, 2007; Pandita et al., 2013).

Fiber	Density (g/cm3)	Elastic Modulus (GPa)	Tensile Strength (MPa)	Elongation at Break (%)
E-glass	2.60	73	1800-2700	2.5
Carbon	1.80	260	3500-5000	1.4-1.8
Kevlar	1.45	130	2700-4500	3.3-3.7
S-glass	2.50	86	4570	2.8

Figure 2.7 demonstrates the specific strength and specific modulus values of some synthetic fibers and conventional materials. As seen from the figure, while E-glass and S-glass have approximately same specific modulus with steel and aluminum, synthetic fibers such as carbon, E-glass, S-glass and Kevlar have higher specific strength than steel and aluminum (Lee & Suh, 2006).

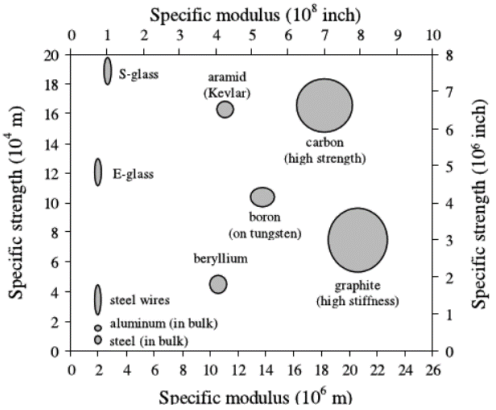

Figure 2.7 : Specific modulus and strength values of some synthetic fibers and conventional materials (Lee & Suh, 2006).

Carbon and E-glass fibers are the most popular synthetic fibers used as reinforcement materials in high strength composite materials (Elanchezhian, Ramnath, & Hemalatha, 2014). Synthetic fiber reinforced composites are mostly used in transportation industry, aerospace and military applications (Begum & Islam, 2013).

Carbon Fiber

Carbon and graphite fibers, both of which contain carbon element, are widely used in composite materials (Campbell, 2010). While graphite fiber contains 99% of carbon, carbon fiber contains 90%. This makes carbon fibers less stiffer and stronger than graphite fibers (Lee & Suh, 2006). Although rayon, polyacrylonitrile (PAN) and petroleum based pitch are the precursors that are used in carbon fiber production; PAN is the commonly used one (Campbell, 2010).

The carbon fiber production from PAN has three thermal stages; stabilization, pre-carbonization and carbonization steps (Figure 2.8). In stabilization stage, fibers are stabilize under low heat treatment (<300 °C) and in the pre-carbonization stage the non-carbon atoms are removed. Finally in the carbonization stage, the pre-carbonized fibers are heated at 1000–1800 °C for several minutes and crystals are ordered in the fiber axis direction (Khayyam et al., 2017).

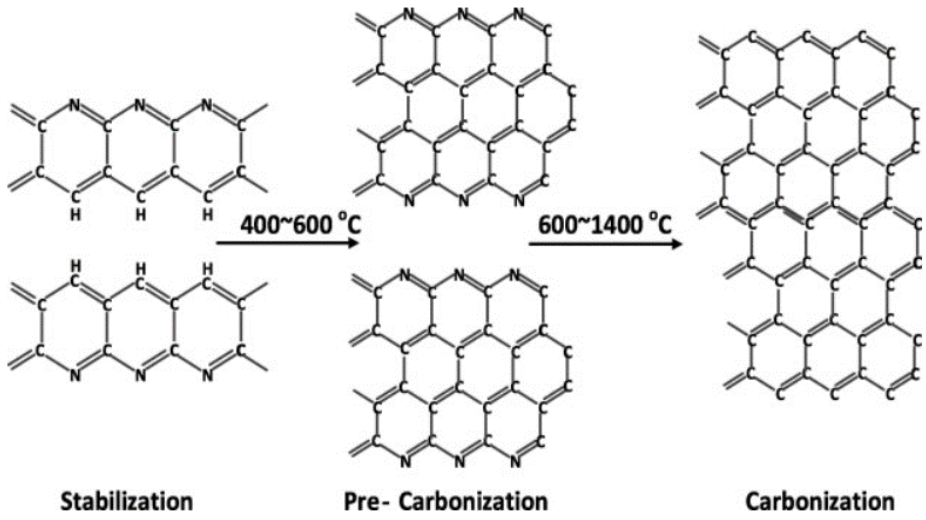

Figure 2.8 : PAN-based carbon fiber production stages (Khayyam et al., 2017).

The carbon fiber was discovered by Thomas Edison in 1879. He had produced a carbon filament from a cellulosic precursor to utilize in electrical lamps (Donnet & Bansal, 1998). Carbon fibers are acknowledged with their excellent tensile and compression strengths and high modulus value (Campbell, 2010; Ikbal et al., 2016; Su et al., 2006).

In a carbon fiber, carbon atoms are aligned parallel to the axis of the fiber and that provides the superior properties (Elanchezhian et al., 2014).

Figure 2.9 shows the layered and planar structure of crystalline carbon fibers. The carbon atoms are settled in a hexagonal lattice and they are bonded with strong covalent bonds in a layer. These individual layers are bonded together by weak van der Waals forces and the different bonding forces within and between the layers causes anisotropy in carbon fibers (Horoschenkoff & Christner, 2012).

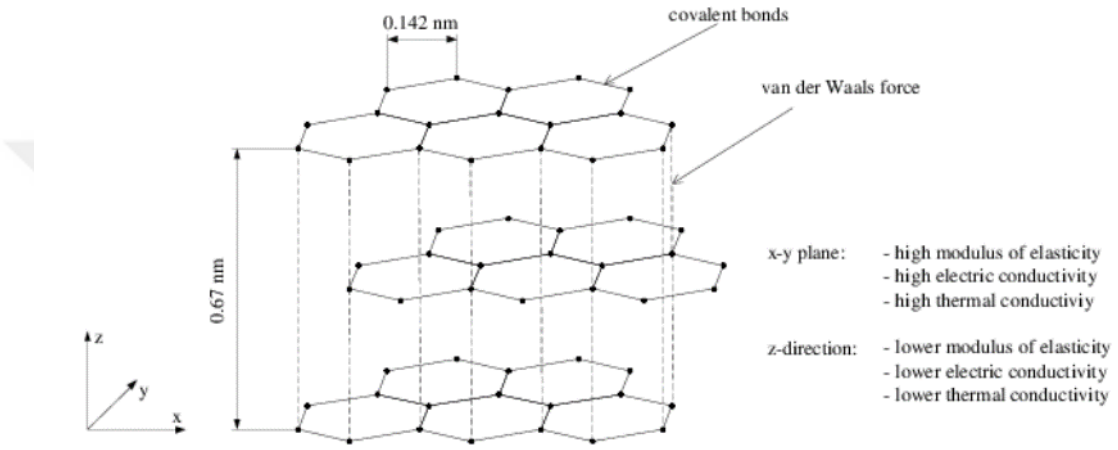

Figure 2.9 : Graphite structure of crystalline carbon fibers (Horoschenkoff & Christner, 2012).

The relatively low density of carbon fiber (1.8 g/cm^3), low thermal expansion value, high thermal stability value, anti-corrosion properties and superior fatigue characteristics make carbon fibers irreplaceable reinforcement materials for high value added composites (Campbell, 2010; Elanchezhian et al., 2014; Ikbal et al., 2016; Su et al., 2006). However, carbon fibers also have some disadvantages. They have higher brittleness and lower impact resistance than glass fibers and also due to their manufacturing techniques they have high cost (Ashworth et al., 2016; Campbell, 2010; Su et al., 2006).

Carbon fiber reinforced composites are mostly used in application areas where superior properties are needed like aerospace industry, robotic structures, motorsports, military, civil engineering applications, and etc. (Ahmed & Vijayarangan, 2007; Elanchezhian et al., 2014; Lee & Suh, 2006; Pandya et al., 2011).

E-glass fiber

Glass is a non-crystalline material which is composed of silica sand, boric acid, limestone, clay, coal and etc. (Campbell, 2010; Lee & Suh, 2006). Glass fiber had first came into being in the 1700s when Réaumur discovered that glass could be finely spun into fiber (Hearle, 2001). The atomic level structure of glass is demonstrated in Figure 2.10.

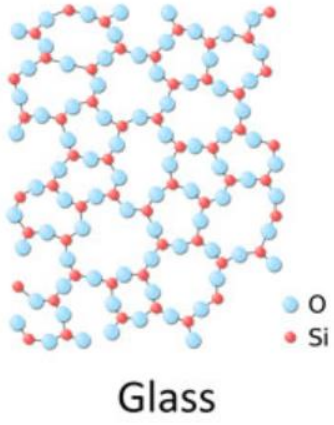

Figure 2.10 : Atomic level structure of glass (Bernstein & Carpi, 2015).

Glass fiber is produced by melting the raw material in three phases, extruding fine strands of glass into small diameter fibers and implementing a chemical size on them (Figure 2.11) (Campbell, 2010; Hasan et al., 2016).

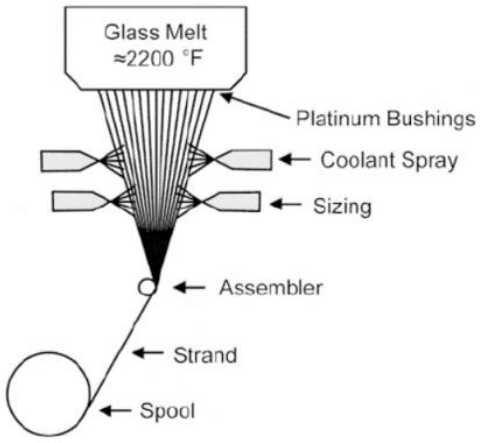

Figure 2.11 : E-glass production (Campbell, 2010).

There are different types of glass fibers. The most known ones are; E-glass, C-glass and S-glass fibers. While E represents the term electrical, C and S stand for corrosion and high silica content (Campbell, 2010; Lee & Suh, 2006) (Matthews & Rawlings,

1999). Among these three types of glass fibers, E-glass fibers are mostly used in composite structures owing to their moderate modulus, low cost and high strength values (Hameed, Sreekumar, Francis, Yang, & Thomas, 2007; Lee & Suh, 2006). Composition of E-glass fiber is given in Table 2.3.

Table 2.5 : E-glass fiber composition (Hearle, 2001) .

Constituent	Weight %
SiO_2	52-56
Al_2O_3	12-16
B_2O_3	5-10
TiO_2	0-1.5
MgO	0-5
CaO	16-25
$Na_2O + K_2O$	0-2
Fe_2O_3	0-0.8
F_2	0-1

One of the most important reasons that the E-glass fibers are widely used in the composite industry is their relatively low price compared to the synthetic fibers such as carbon fibers (Hasan et al., 2016; W. Li, Dichiara, Zha, Su, & Bai, 2014; Russo et al., 2013). Besides, they have relatively high chemical resistance, impact resistance and tensile strength (Campbell, 2010; Elanchezhian et al., 2014; Hameed et al., 2007; Ramesh, Palanikumar, & Reddy, 2013b; Russo et al., 2013). When the performance features of E-glass fibers are compared with those of carbon fibers, it can be said that they are weaker, non-rigid and more sensitive to fatigue loadings but on the other hand their brittleness is less.

One of the undistinguished properties of E-glass fiber is their higher weight compared to carbon fiber (Campbell, 2010; Hasan et al., 2016; Russo et al., 2013). For instance, while 40-60% weight reduction can be obtained by using a carbon reinforced composite in a vehicle, this percentage comes down to 20-35% with E-glass fiber reinforced composite (Jin Zhang, Chaisombat, He, & Wang, 2012).

E-glass fiber can be used with both thermoplastic and thermoset resins (Ramesh et al., 2013b). Automobiles, boats, pipes, water tanks and aircrafts are the main application areas of E-glass fiber reinforced composites (Elanchezhian et al., 2014; Lee & Suh, 2006; Ramesh et al., 2013b).

2.2.2 Matrix materials

Resins are divided into two main categories. These are; thermoplastic and thermoset resins (Campbell, 2010; Lee & Suh, 2006).

2.2.2.1 Thermoplastic resins

Thermoplastic resins are high viscosity resins that they soften and melt when they are heated and then get back to their original form when they are cooled down (Campbell, 2010; Lee & Suh, 2006). Acrylic, polyethylene terephthalate, polybutylene terephthalate, polypropylene, polyamide and polystyrene are the high-profile thermoplastic resins (Lee & Suh, 2006).

Although thermoplastic resins are also reinforced with continuous filaments, they are mostly reinforced with short fibers due to their viscous properties (Lee & Suh, 2006).

2.2.2.2 Thermoset resins

Thermosets are formed from monomers that have low viscosity and low molecular weight. Thermoset resins crosslink in the course of curing process and can not be reprocessed and reshaped by reheating. They will merely degrade or burn (Campbell, 2010; Lee & Suh, 2006).

In the composite industry, thermoset polymers comprise more than three quarters of all polymeric matrices owing to their higher chemical resistance, lower price, higher softening temperatures, better fiber impregnation and higher creep behavior than thermoplastic resins (Lee & Suh, 2006).

Table 2.6 : Properties of some thermoset resins (Campbell, 2010).

Resin Types	Characteristics
Polyester	High processing flexibility Can be used for both continuous and discontinuous composites Inexpensive
Epoxy	Relatively expensive Higher temperature resistance than polyester and vinyl ester resins.
Polyamide	Not easy to process High temperature resistance
Phenolic	High fire resistance Not easy to process
Vinyl Ester	Relatively inexpensive Tougher than polyester resin

Polyester, epoxy, phenolic, vinyl ester and polyamide resins are the primary thermoset resins (Campbell, 2010; Gujjala et al., 2014). Main characteristics of some thermoset resins are given in Table 2.4.

Unsaturated polyester

Unsaturated polyester resin is widely used in polymer matrix composites and they are mostly redominated as "polyester resins". Chemical structure of an unsaturated resin is given in Figure 2.12. According to their ingredients such as acids, glycols and monomers, there are different types of polyesters. Orthophthalic and isophthalic polyester are the most used polyester resins in composite production. While isophthalic polyester resin is usually preferred in marine applications, orthophthalic polyester resin is a standard affordable resin used in many fields ('Composite materials guide: Resin Systems - Polyester Resins | NetComposites', n.d.).

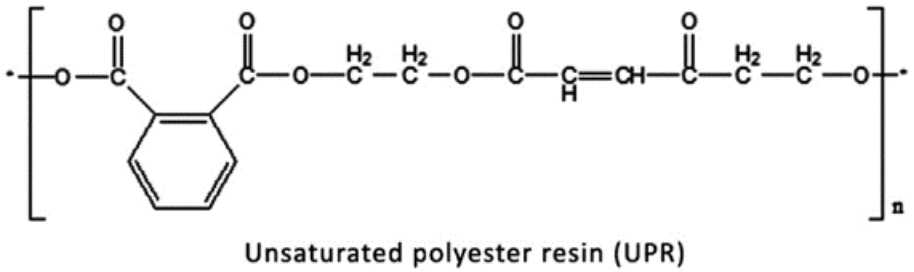

Figure 2.12 : Chemical structure of unsaturated polyester resin (Kargarzadeh, M. Sheltami, Ahmad, Abdullah, & Dufresne, 2015).

Polyester resins are quick curing resins but they have high cure shrinkage in comparison with epoxy (Seyhan, Gojny, Tanoğlu, & Schulte, 2007). Polyester resin has high resistant to chemical attacks and environmental effects. They have very low cost compared to epoxy resin and also have high dimensional stability and low viscosity (Lee & Suh, 2006; Manfredi et al., 2006; Pıhtılı & Tosun, 2002). Properties of polyester resin are given in Table 2.7.

Polyester resin is mostly reinforced with cellulosic and glass fibers (Aziz & Ansell, 2004; Pıhtılı & Tosun, 2002). To start the polymerization process, a catalyst must be added to the polyester and also an accelerator is added to expedite the reaction (Campbell, 2010).

Table 2.7 : Properties of polyester resin (Ku, Wang, Pattarachaiyakoop, & Trada, 2011).

Property	Polyester Resin
Density (g/cm^3)	1.2 - 1.5
Elastic modulus (GPa)	2 - 4.5
Tensile strength (MPa)	40 – 90
Compressive strength (MPa)	90 – 250
Elongation (%)	2
Cure shrinkage (%)	4 – 8
Water absorption (24h @20°C)	0.1 – 0.3
Izod impact strength (J/m)	0.15 – 3.12

Polyester matrix composites have usage areas in offshore applications, automotive industry, building constructions and waterlines. However, polyester has limited usage in high performance composites by virtue of their low mechanical properties, low thermal and weather resistance compared to epoxy resin (Campbell, 2010; Manfredi et al., 2006; Seyhan et al., 2007).

2.3 Advantages and Disadvantages of Textile Reinforced Composites

Lightness is the foremost property of composite structures. It is mostly crucial for transportation vehicles because by decreasing the weight of the structure, a great amount of energy consumption can be obtained (Jin Zhang et al., 2012). For instance, in a car structure by using a composite material instead of steel or aluminum, a weight saving of 60-80% and 20-50% can be achieved, respectively (Gopinath et al., 2014). Moreover, while a steel car hood is in need of 27 kg of crude oil equivalent, this value drops below 17 kg by using polymer matrix composite materials (Lee & Suh, 2006).

Composite structures gain the upper hand owing to their design flexibility. The flexibility of design provides the opportunity to produce materials with desired properties. Some of the design parameters are type and amounts of resin and matrix materials, production methods, the count and the stacking sequence of layers (Lee & Suh, 2006; Jin Zhang et al., 2012). The desired properties can be achieved by choosing appropriate manufacturing technique, matrix and reinforcement materials,

reinforcement ratio and orientation of the reinforcement material (Gujjala et al., 2014; Lee & Suh, 2006; Patel et al., 2008; Raghavendra et al., 2015).

Good mechanical properties, low density, high specific strength and stiffness are also the other main outstanding features of the composite materials (Campbell, 2010; Gopinath et al., 2014; Jawaid et al., 2011).

The main disadvantages of composite materials are their nonrecyclable properties, high cost and deficiency of qualified labour force (Lee & Suh, 2006; Jin Zhang et al., 2012). The high cost can be related to the raw material or fabrication technique (Campbell, 2010).

2.4 Composite Production Methods

The composite production technique is a significant parameter that affects the properties and the quality of the material (Huang & Talreja, 2005; Lee & Suh, 2006). For recent thirty years, there has been great improvements in composite manufacturing techniques to eliminate the process-based failings, to lower the cost of manufacturing and to improve the mechanical properties of composite materials (Advani & Hsiao, 2012).

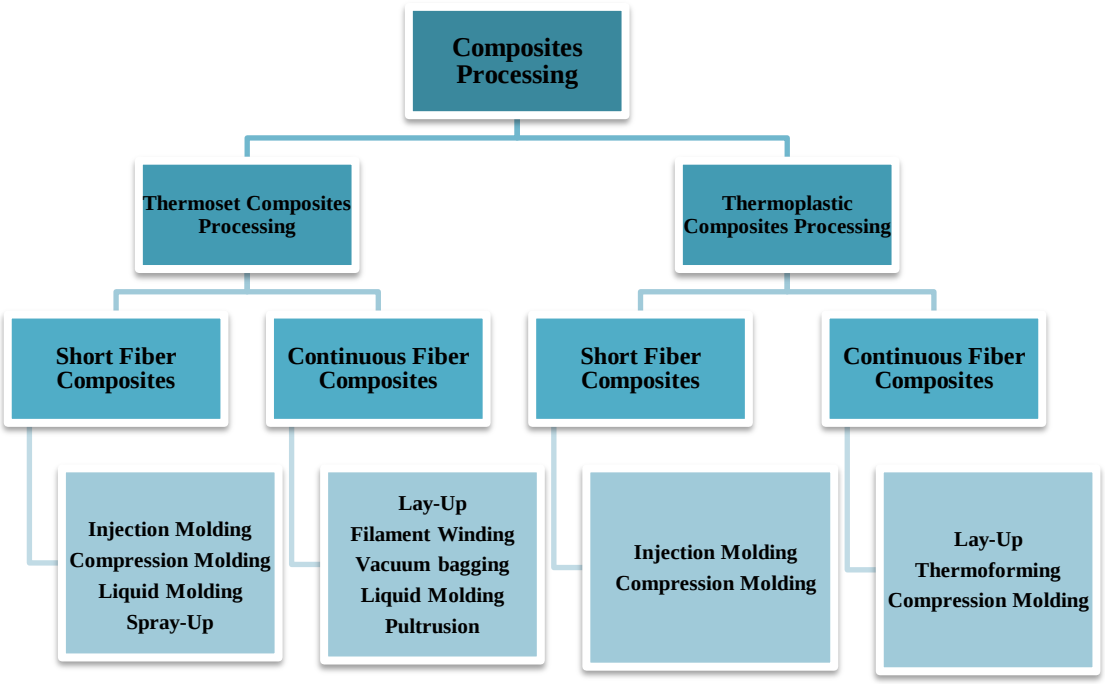

Figure 2.13 : Composite Processing Techniques (Campbell, 2010).

There are a great number of composite production methods like compression molding, vacuum assisted resin transfer molding, autoclave vacuum bag degassing, pultrusion, resin transfer molding, filament winding and etc. (Lee & Suh, 2006). The production method that will be used in composite manufacturing is mostly determined by the type of the matrix and reinforcement materials (Campbell, 2010; Lee & Suh, 2006). Figure 2.13 displays the composite processing techniques according to reinforcement and matrix materials.

The liquid molding process which is used with thermoset resins comprises resin transfer molding, resin film infusion and vacuum assisted resin transfer molding techniques (Campbell, 2010).

Vacuum assisted resin transfer molding

The vacuum assisted resin transfer molding (VARTM) is a process that uses pressure difference between the vacuum and environmental pressures to consolidate the composite structure. Compared to resin transfer molding method, VARTM is a cheaper and easier method (Advani & Hsiao, 2012; Campbell, 2010). It is mostly utilized in aerospace, marine and defence industries (Advani & Hsiao, 2012).

A typical VARTM process is given in Figure 2.14. It is a closed mold technique that uses dry preforms. VARTM technique has five main stages. These are; *i.* preparation of mold and fabric lay-up, *ii.* sealing the vacuum bag and creating the vacuum, *iii.* preparation of the matrix material, *iv.*impregnation of the resin, *v.*curing of the composite laminate (Ary Subagia, Kim, Tijing, Kim, & Shon, 2014). Resin is injected to the preform by vacuum pressure (Advani & Hsiao, 2012; Campbell, 2010). In this technique, a porous permeable structure is used to obtain homogeneity. By using this structure, resin flows easily to the each part of the preform (Campbell, 2010). Finally, the excess resin is pulled out from the preform again by the help of vacuum pressure (Advani & Hsiao, 2012).

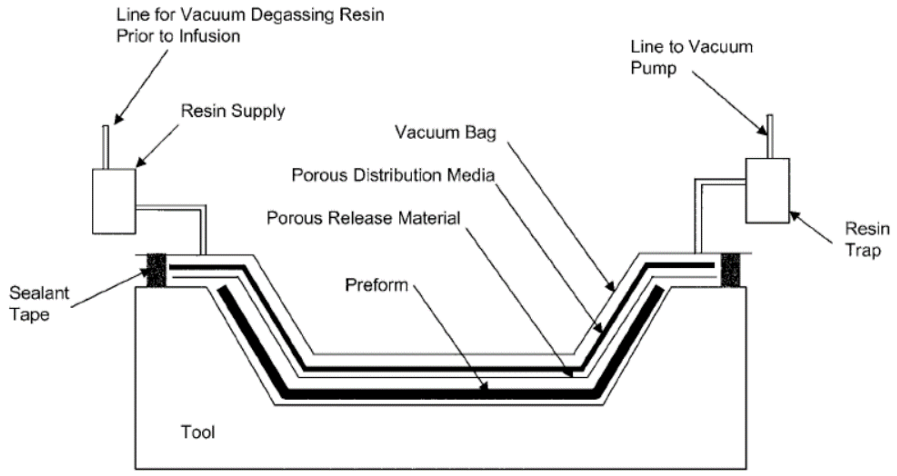

Figure 2.14 : Typical VARTM process (Campbell, 2010).

VARTM process has many benefits. Some of which are;

- Low volatile organic compound emission owing to closed mold construction.
- Opportunity to manufacture large and complex forms.
- Owing to transparent vacuum bag, nonimpregnated points can be easily detected and eliminated by inserting a vacuum needle.
- Ability to achieve high fiber loadings (up to 50%).
- Clean handling (Advani & Hsiao, 2012; Holbery & Houston, 2006).

VARTM process also has some drawback such as;

- Vacuum pressure is limited compared to autoclave and typical resin transfer molding process.
- Possibility of air gaps is high.
- Vacuum equipments (peel ply, vacuum bag, tubes and etc.) are all single use only (Advani & Hsiao, 2012).

3. MECHANICAL PERFORMANCE OF COMPOSITE STRUCTURES

3.1 Factors Affecting the Mechanical Properties

The mechanical properties are the main features that have impact on the end use area of the composite materials (Wang, Zheng, & Zheng, 2011a). The factors that affect the mechanical properties of composite structures can be divided into three main sections. These are; *i.* reinforcement and matrix material parameters, *ii.* interface characteristics and *iii.* voids (Shah, 2013; Wang et al., 2011a).

3.1.1 Reinforcement and matrix parameters

The mechanical properties of composite structures are mostly related to the properties of the reinforcement material (Wang et al., 2011a). The fiber length, orientation, shape and material type are the factors that influence the performance of the composites (Campbell, 2010; Huang & Talreja, 2005; Jin Zhang et al., 2012).

The fiber volume fraction is the foremost factor that have an impact on the mechanical properties of composite materials (Elanchezhian et al., 2014; Lee & Suh, 2006; Shah, 2013). By virtue of the fact that reinforcement material gives the strength and stiffness to the composite material, mechanical properties of the structure can be enhanced by decreasing the amount of matrix material (Wang et al., 2011a).

3.1.2 Interface characteristics

The composite interface is the area between the matrix and the reinforcement material that gives durability to the material (Peterson, Jensen, & Palmese, 2011; Wang, Zheng, & Zheng, 2011b). The schematic view of a composite interface is displayed in Figure 3.1. The interface is a layer that has a certain thickness and it is characterized as the middle-phase of the composite material (Wang et al., 2011b).

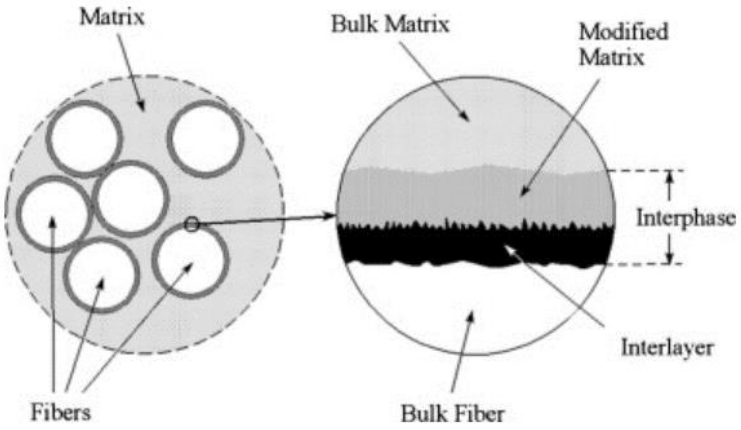

Figure 3.1 : Schematic display of the composite interface (Cech, Palesch, & Lukes, 2013).

Wetting is a process that the liquid matrix material flows over and cover the reinforcement material. The viscosity of the matrix material should not be too high to realize the wetting process (Lee & Suh, 2006). There is a direct proportion between wettability and interface bond strength of the material. The wetting property of a material can be changed by modifying the surface tension of the reinforcement (Wang et al., 2011b).

The bonding strength between the matrix and the reinforcement material is the most important factor that affects the mechanical properties of a composite structure because the reinforcement is the phase that can resist the applied load and load is transferred from the matrix to the reinforcement material from the interface. So, a good bonding between matrix and reinforcement material will result in high mechanical properties owing to high stress transfer from matrix to reinforcement (Acha et al., 2005; Hameed et al., 2007; Jabbar et al., 2016; Lee & Suh, 2006; Militký & Jabbar, 2015; Mohanty et al., 2000; Ornaghi et al., 2010; Patel et al., 2008; Peterson et al., 2011; Thomas et al., 2012; Tripathy et al., 2000; Wang et al., 2011b, 2011a). The bonding strength between matrix and the reinforcement material also depends on the polarity of the materials (Mohanty et al., 2000).

The different mechanical properties of the matrix and the reinforcement material makes the interfacial region a potential area for crack development, interfacial debonding and stress concentration (Peterson et al., 2011; Thomas et al., 2012). Furthermore, mechanically or thermally induced fatigue results in enlargement of cracks and so failure in mechanical properties (Peterson et al., 2011).

Impact and tensile strength of composite materials are the foremost mechanical properties that are affected from interfacial bonding strength. The bonding strength has a huge effect on the failure mode of the composite, which is directly related to the impact properties of the material. (Acha et al., 2005; Wang, Zheng, & Zheng, 2011c). The fracture resistance of a composite material is related to the interfacial bonding strength, as well. A strong interface results in a brittle structure. This means that a strong interface causes low fracture resistance (Lee & Suh, 2006; Ornaghi et al., 2010; Wang et al., 2011b).

The damping properties are also associated with interface strength. The energy dissipated from the composite material increases with the descending bonding strength which results in higher damping (Jabbar et al., 2016). When toughness of composites is taken into consideration, it can be said that bonding strength of the material should not be so strong to permit the toughening actions (Elanchezhian et al., 2014; Wang et al., 2011a).

Natural fibers have hydrophilic characteristics while polymer matrices have hydrophobic. This mismatch of characteristics leads to poor interfacial bonding between natural fibers and polymer matrices (Portella et al., 2016). Also, the pendant hydroxyl and polar groups of natural fibers cause poor adhesion of fiber and matrix (Patel et al., 2008; Tripathy et al., 2000).

3.1.3 Voids

The other parameter that affects the mechanical properties of composite structures is void. The terms void and porosity are mostly confused with each other. While porosity indicates more than one small pores, void indicates a one large pore. In composite studies, the term void is mostly used instead of porosity (Campbell, 2010).

Voids are the entrapped air or moisture in the composite structures. Although sometimes they have a positive effect on density (reduction of density), they have really adverse effect on the mechanical properties (tensile, flexural, shear strengths and etc.) of composite materials (Ashworth et al., 2016; Bodaghi et al., 2016; Chambers, Earl, Squires, & Suhot, 2006; Hagstrand, Bonjour, & Månson, 2005; Huang & Talreja, 2005; Jawaid et al., 2011; Lee & Suh, 2006). Voids can be both located in plies or in ply interfaces (Campbell, 2010).

The amount of voids in the composites are sometimes referred as void volume fraction but generally they are stated as void content (Huang & Talreja, 2005). Modelling of voids in a composite structure is given in Figure 3.2.

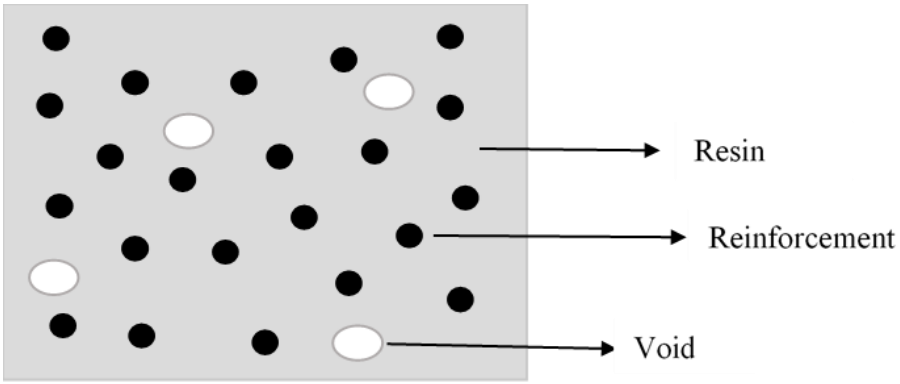

Figure 3.2 : Modelling of voids in a composite structure.

The primary factors of voids in the composite materials are the air gaps that originated during lay-up process, viscosity of resin, permeability of reinforcement material and the inadequate resin pressure which holds the remnant moisture in resin till solidification of resin starts (Campbell, 2010; Jawaid et al., 2011; Protz et al., 2015). Insufficient pressure will end up with low resin passage and so void formation (Chambers et al., 2006; Huang & Talreja, 2005).

The process parameters of the composite production techniques have strong effect on the occurrence of the void content. The air gaps may appear in the material due to incorrect process parameters which can result in voids (Ashworth et al., 2016).

Void content usually increases with the increment of fiber content (Sreekala, George, Kumaran, & Thomas, 2002). However, some studies declared that there is not a perceptible dependence between void content and fiber volume fraction (Roe & Ansell, 1985; Shah, Schubel, Licence, & Clifford, 2012; L. Zhang & Miao, 2010). Moreover, it is referred in the literature that void content of a composite material increases substantially when the fiber volume ratio is more than 40% (Protz et al., 2015).

The limit of void content differs according to the end-use area of composite structure. For example, while void content less than 1% is required for aerospace applications, 5% is acceptable for other applications such as automotive and marine (Huang & Talreja, 2005; Shah, 2013).

The void content can be measured by density measurements, ultrasonic attenuation and optical image analysis (Huang & Talreja, 2005; Lee & Suh, 2006). The amount of void content can be reduced by choosing the right manufacturing technique, process parameters, resin and the reinforcement material (Hagstrand et al., 2005; Huang & Talreja, 2005; Roe & Ansell, 1985).

3.2 Enhancement of Mechanical Properties of Composite Structures

There are a great number of methods to improve the mechanical properties of composite materials. The methods will be examined under three headings. These are; hybridization and changing the stacking sequence of fabric plies, addition of nanofillers and fiber surface treatments.

Due to the fact that interfacial strength is the primary factor that influences the mechanical properties, the properties of composites are mostly enhanced by interfacial treatments (Sapuan & Maleque, 2005). Incorporation of fillers and fiber surface treatments are the foremost interfacial treatment methods (Tugrul Seyhan, Tanoglu, & Schulte, 2008). Hybridization of low strength fibers with high strength fibers and also changing the stacking sequences of fabric plies have also great effect on mechanical properties.

3.2.1 Hybridization and changing the stacking sequence of fabric plies

Composite materials may be subjected to very different loading conditions and this situation sometimes forces the reseachers to utilize various types of reinforcement materials in the composite structure. Such composites which are reinforced with two or more types of materials are known as hybrid composites.

Hybrid composites are divided into two categories. These are; interply and intraply composites. In interply hybrid composites each fabric ply consists of one type of fiber, while in intraply hybrid composites each fabric ply consists of two or more types of fiber (Mallick, 2007; Pandya et al., 2011). Shematic diagram of interplay and intraply hybrid composites are given in Figure 3.3.

(a) (b)

Figure 3.3 : Schematic diagram of (a) intraply and (b) interply hybrid composites (Ha, Kim, Nasir, & Han, 2012).

By using two or more types of reinforcement materials, better mechanical properties and reduced material costs compared to the conventional composites can be achieved (Agarwal, Patnaik, Sharma, & Agarwal, 2014; Jawaid et al., 2011; Pandya et al., 2011; Romanzini et al., 2013; Sezgin & Berkalp, 2016). These hybrid composite structures combine the beneficial properties and eliminate the undesirable properties of each component (Hamouda et al., 2015; Hasan et al., 2016). Although in the definition of hybrid composite materials it is stated that two or more reinforcement materials can be used in hybrid structures, it is declared in the literature that the best properties are achieved by using only two types of reinforcement materials (Banerjee & Sankar, 2014).

Hybrid composites are mostly engineered by using one low modulus and one high modulus reinforcement material. The most preferred synthetic fibers used in hybrid composites are E-glass (low modulus), Kevlar (low modulus) and carbon (high modulus). While high modulus reinforcement material ensures stiffness and high load bearing capacity, low modulus reinforcement material gives a ductile characteristic to the composite structure (Ikbal, Ahmed, Qingtao, Shuai, & Wei, 2016).

The hybridization of a natural fiber with a high strength fiber provides a good balance of performance, cost and environmental facts (Ashworth et al., 2016). Different stacking sequences, type of matrix material, fiber volume fractions and fiber/matrix interfaces are the facts that affect the mechanical properties of the hybrid composites (Ikbal et al., 2016; Ornaghi Jr., da Silva, Zattera, & Amico, 2011; Pandya et al., 2011; Shanmugam & Thiruchitrambalam, 2013).

The design of a laminated composite material depends on selecting the best arrangement of the materials (Ghiasi, Fayazbakhsh, Pasini, & Lessard, 2010).

Changing the place of fabric layers have a great influence on the mechanical properties of the composites (Wang et al., 2011a; Ramesh et al., 2013a).

3.2.2 Addition of nanofillers (carbon nanotubes)

Nanofillers are priviledged filler materials to develop the properties of composite structures. They have very high specific surface areas (more than 1000 m^2/g) and aspect ratios compared to micro-scaled fillers (Gojny, Wichmann, Fiedler, Bauhofer, & Schulte, 2005). Nanoclays, nanofibers and nanotubes are the forms of nanofillers that are used in composite industry (Chandrasekaran, Advani, & Santare, 2010).

Four factors have crucial impact on the reinforcing effect of the nano filler. These are aspect ratio, interfacial stress transfer, alignment and dispersion (Coleman, Khan, Blau, & Gun'ko, 2006; Qiu, Zhang, Wang, & Liang, 2007). A good dispersion of nanoparticles in polymeric resins is a critical factor. Stress concentration points will be diminished by having a good dispersion (Coleman et al., 2006; Shokrieh, Saeedi, & Chitsazzadeh, 2013; Simsek, Ozyuzer, Seyhan, Tanoglu, & Schulte, 2007). By virtue of their high aspect ratio and surface area and van der Waals attractions, nanoparticles are liable to agglomeration and this causes reduction in the properties of the modified polymer (Gojny et al., 2005; W. Li et al., 2014; Shen et al., 2009; Shokrieh et al., 2013; Simsek et al., 2007; Tugrul Seyhan et al., 2008). The alignment of the nanoparticles has less influence on the properties of the composite materials. Alignment makes the material anisotropic and it enhances the mechanical properties of the composite structure only in one direction (Coleman et al., 2006). CNTs have sp^2 hybridized carbon bonds which gives their high strength (Bily, Kwon, & Pollak, 2010).

Carbon nanotubes are up and coming nanoparticles used in composite industry for enhancing their properties (Chen & Liu, 2004; W. Li et al., 2014; Liao, Wang, Fang, Liew, & Pan, 2011; Seyhan et al., 2007; Shen et al., 2009; J. Zhu et al., 2007). They are a class of materials that possess combination of excellent mechanical, electronic and thermal properties that no other material has been displayed until now (Chen & Liu, 2004; Coleman et al., 2006). They have two times higher thermal conductivity than diamond, 1000 times higher electric-current-carrying capacity than copper. Their strength is 10 to 100 times greater than steel, their thermal stability is up to 2800°C and they have elastic modulus more than 1 TPa (Thostenson, Ren, & Chou, 2001). It is an understanding thing that CNTs are the stiffest and strongest man-made materials

(Spitalsky, Tasis, Papagelis, & Galiotis, 2010). The only downside of CNTs is their high prices (Bily et al., 2010).

CNTs are very small tubes with nanometer size diameters and micron size lengths (Coleman et al., 2006; Seyhan et al., 2007; Shokrieh et al., 2013). They have densities of less than 1.3 g/cm^3 (Coleman et al., 2006).

There are two essential types of CNTs. These are; single-walled carbon nanotubes (SWCNT) and multi-walled carbon nanotubes (MWCNT). MWCNTs are the coalescence of coaxial SWCNTs. (Bily et al., 2010; Thostenson et al., 2001). Figure 3.4 shows the structures of SWCNT and MWCNT. Also, MWCNTs which consist of two concentric cylinders are entitled as double-walled carbon nanotubes (DWCNT).

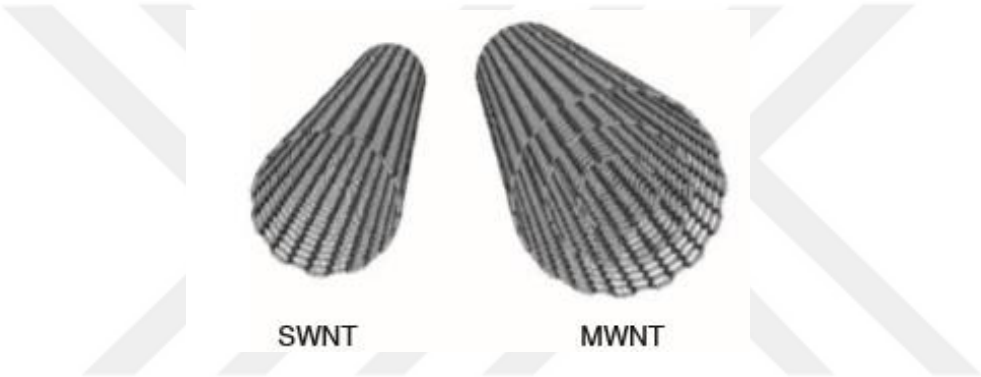

Figure 3.4 : Structures of SWCNT and MWCNT (Rachmadini, Tan, & Tay, 2010).

The simplest and the finest one is SWCNT. They are cylindrical shape materials that are formed by a single sheet of graphene that is rounded seamlessly and have diameters ranging from 0.4 nm to 3 nm (Coleman et al., 2006; Simsek et al., 2007). The MWCNTs are combination of these cylinders that are bonded to each other with van der Waals forces and have approximately 0.35 nm gap between them. The diameters of MWCNTs are in the range of 2 to 100 nm, while they have lengths in tens of microns (Coleman et al., 2006; Thostenson et al., 2001). Among CNT types, MWCNT has the smallest surface area and therefore exhibits better dispersibility (Gojny et al., 2005). In composite materials, MWCNTs are the most preferred filler compared to SWCNTs due to the fact that SWCNTs are relatively more expensive and have limited supply potential (Liao et al., 2011).

Figure 3.5 displays the transmission electron microscope (TEM) graph of a MWCNT with graphitic carbon layers and hollow core.

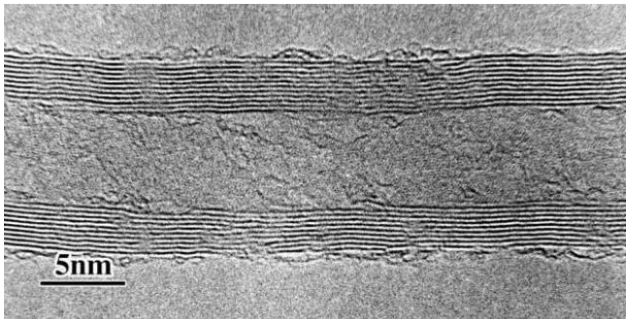

Figure 3.5 : TEM micrograph of a MWCNT (Thostenson et al., 2001).

The first CNT was a MWCNT discovered by Iijima in 1991. Two years later, SWCNT was synthesized by Iijima & Ichihashi and Bethune et al. (Karapappas, Vavouliotis, Tsotra, Kostopoulos, & Palpetis, 2009; Shokrieh et al., 2013).

Arc-discharge, laser-ablation and chemical vapor deposition are the production techniques of CNTs (Coleman et al., 2006; Karapappas et al., 2009).

The major properties that are improved by incorporation of very few amounts of CNTs are electrical conductivity, thermo-mechanical properties, tensile strength, stiffness, fracture toughness, elastic modulus and impact strength (Alexopoulos, Bartholome, Poulin, & Marioli-Riga, 2010; Gojny et al., 2005; Seyhan et al., 2007; Shokrieh et al., 2013; Tugrul Seyhan et al., 2008; Jie Zhang et al., 2010; J. Zhu et al., 2007). Incorporation of CNTs to composite materials enhances the toughness of the material by improving the energy absorption characteristics of the material (J. Zhu et al., 2007). Furthermore, addition of CNTs to composite material decreases the coefficient of thermal expansion and increases the glass transition temperature (T_g) of the matrix (Díez-Pascual et al., 2011).

CNTs can be incorporated to composite structures by two ways; applying directly to the fiber or mixing it into the matrix (Díez-Pascual et al., 2011; Warrier et al., 2010; Zhao et al., 2017). Figure 3.6 shows the schematic diagrams of fiber reinforced polymer composites and CNT based hierarchical polymer composites. While adding CNTs into the matrix results in matrix modification, attaching CNTs on fibers results in interface modification (Zhao et al., 2017). The most known method is the addition of CNTs directly to the matrix material (Boroujeni, Tehrani, Nelson, & Al-Haik, 2014).

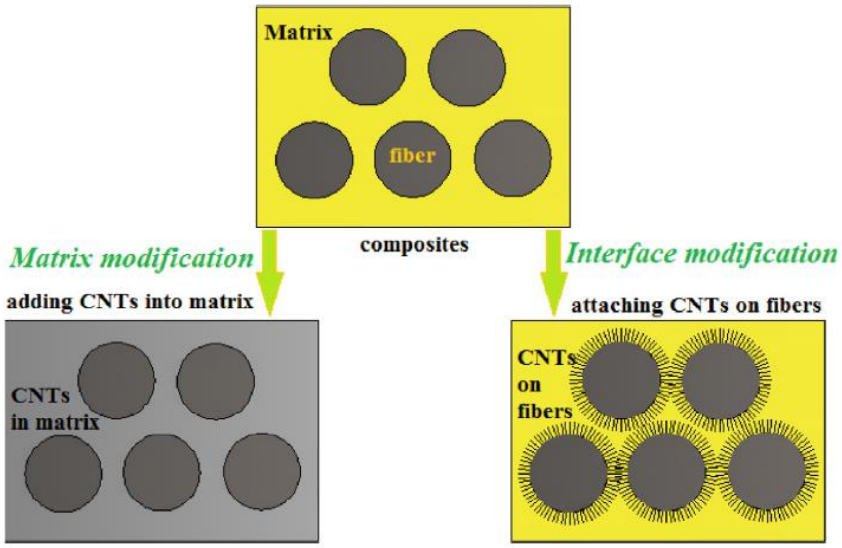

Figure 3.6 : Schematic diagrams of fiber reinforced polymer composites and CNT based hierarchical polymer composites (Zhao et al., 2017).

Materials adequacy to withstand stress can be enhanced by addition of CNTs (Bily et al., 2010).

Stirring, ultra-sonication and high shear mixing are the techniques that are used for dispersing CNTs homogenously in polymer resin (W. Li et al., 2014). Ultra-sonication is the chief method to solve the dispersion problem.(Qiu et al., 2007; Seyhan et al., 2007; Shokrieh et al., 2013).

The weak interfacial bonding between CNT and polymer minimizes the performance of the structures (Gamze Karsli, Yesil, & Aytac, 2014; W. Li et al., 2014). This can be enhanced by chemical functionalization of CNT surface by providing the formation of covalent bonds or dipole-dipole interactions between the resin and CNTs (Gojny et al., 2005). Also, the enhancement of the dispersion of CNTs in polymer resin can be achieved by surface treatment of CNTs by functional groups (Karapappas et al., 2009; Simsek et al., 2007). Functionalization changes the surface characteristics of CNT and gives higher polarity to them which ends up with improved load transfer performance and high interfacial shear strength (Coleman et al., 2006; Qiu et al., 2007).

The hydroxyl functionalized MWCNT (MWCNT-OH) and carboxyl functionalized MWCNT (MWCNT-COOH) are two of the examples of functionalized MWCNTs. The schematic diagram of the preparation of MWCNT-OH and MWCNT-COOH from pristine MWCNT is given in Figure 3.7.

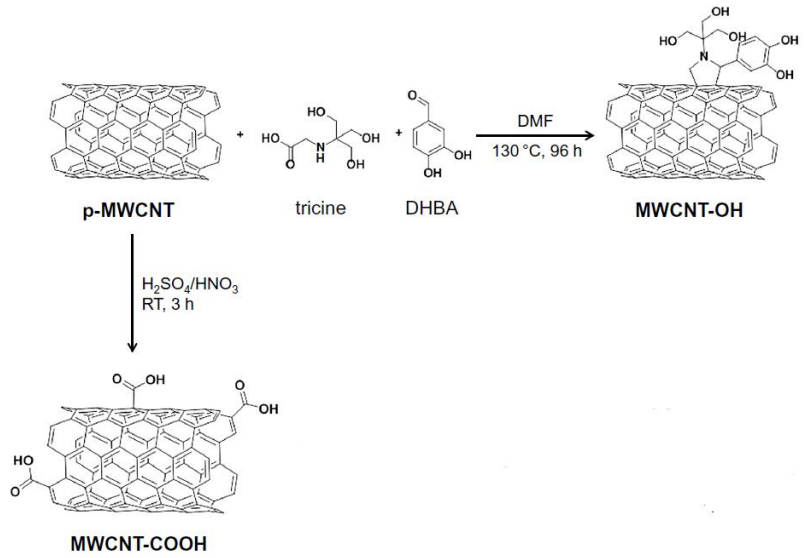

Figure 3.7 : Schematic diagram of the preparation of functionalized MWCNT from pristine MWCNT (Kaufmann et al., 2017).

For MWCNT-OH synthesis, hydroxyl groups are attached to the surface by 1,3-dipolar cycloaddition with tricine and 3,4-dihydroxybenzaldehyde (DHBA) as reactants. In MWCNT-COOH synthessis, MWCNTs are dispersed in H2SO4/ HNO3 in a sonication bath, filtrated and washed with distilled water (Kaufmann et al., 2017).

3.2.3 Fiber surface treatment

To improve the adhesion between natural fibers and synthetic polymers, chemical modifications are used (Patel et al., 2008; Tripathy et al., 2000). Surface treatment is a widely used method for improving interfacial strength and durability of composite structures (Peterson et al., 2011).

Coupling agents are mostly utilized to improve the compatibility of the matrix and the reinforcement materials (Demir et al., 2011; Tajvidi et al., 2006). They build a new interface to enable high bonding strength (Wang et al., 2011b).

In natural fibers, surface treatment is done to enhance the hydrophobic characteristics of fibers (Thwe & Liao, 2003). Alkaline treatment (NaOH) is one of the methods used to increase interfacial bonding in natural fiber reinforced thermoplastic and thermoset composite materials. It is known that this process also reduces the hydration. Sodium hydroxide prevents the hydroxyl groups on cellulose to bond with water molecules by reducing the hydrogen bonding capacity of these groups (Dittenber & GangaRao, 2012). A certain amount of lignin, wax and oils on the surface of fiber is removed with this treatment (X. Li, Tabil, & Panigrahi, 2007).

One of the common methods used for improving the mechanical properties of E-glass fiber reinforced composites is treatment of E-glass fibers with silane coupling agents (Liao et al., 2011). The silane coupling agents form siloxane bonds with silica glass and thus provide influential interfacial bonding (Haque et al., 2010). They minimize the number of cellulose hydroxyl groups in the interface (X. Li et al., 2007).

3.3 Previous Studies on Enhancement of Mechanical Properties of Composite Structures

Enhancement of the mechanical properties of composite structures attract the attention of scientist for a long while. In this study, the previous studies about enhancement of mechanical properties of composite structures are summarized in two sections according to the extent of the thesis. These are; studies on enhancement of the mechanical properties of composite structures by changing stacking sequence of fabric layers and by addition of CNT fillers.

Apart from these two methods there are also many studies about improvement of mechanical properties of jute, carbon and E-glass fiber reinforced composites.

One of the methods that is mostly used in jute fibers to enhance the mechanical properties of jute reinforced composites is NaOH treatment of jute fibers. Many studies can be found in the literature about this subject (Doan, Brodowsky, & Mäder, 2012; Karaduman & Onal, 2013; Liu, Yu, Cheng, & Qu, 2009; Mohanty et al., 2000; Ray, Sarkar, Rana, & Bose, 2001; Saha et al., 1999; Sinha & Rout, 2009). Besides, there are also some works about enzyme (Jabbar et al., 2016; Karaduman & Onal, 2013; Militký & Jabbar, 2015), acetone (Alves et al., 2010), maleic anhydride (Gassan & Bledzki, 1997) and potassium dichromate (Khan, Khan, Islam, & Gafur, 2010) treatments of jute fibers.

When enhancement of the E-glass fiber reinforced composites mechanical properties are taken into consideration, it comes out that most of the studies in the literature reports the effect of silane coupling agent on E-glass reinforced polymer composites (Cui & Kessler, 2014; Gorowara, Kosik, McKnight, & McCullough, 2001; Jensen & McKnight, 2006; H.-H. Kim, Kim, Kim, Oh, & Jo, 2014; J.-K. Kim, Sham, Sohn, & Hamada, 2001; Luo, Wang, Huang, & Fang, 2014; Park & Jin, 2001; Patel et al., 2008; Puska, Zhang, Matinlinna, & Vallittu, 2014; Wu, Dwight, & Huff, 1997).

.

3.3.1 Studies on enhancement of mechanical properties of composite structures by changing stacking sequence of fabric plies

The summary of some studies about enhancement of mechanical properties of composite structures by changing stacking sequence of fabric layers are given below. It was observed that epoxy resin was used as the matrix material in most of the studies. Studies about polyester resin based composites and epoxy resin based composites are given respectively.

In one of the studies, Gupta & Deep (2017) studied the dynamic mechanical and flexural properties of sisal and glass fiber reinforced polyester composites. Composite laminates were fabricated by hand lay-up method. Three hybrid composites with different stacking sequences were manufactured and results indicated that sample which has a fabric stacking sequence of glass/sisal/glass has the highest flexural strength, loss modulus and storage modulus in glassy region.

Hasan et al. (2016) used woven jute and non-woven E-glass fabrics to manufacture jute reinforced, E-glass reinforced and jute/E-glass hybrid reinforced polyester composites. Jute and E-glass fabric plies aligned consecutively in their hybrid composite structures. It was noticed that placing glass or jute fabrics at the outer layers of the sample has nearly no effect on the tensile strength of the hybrid composite structure. However, the sample which has glass fabric plies at the outer layers reached higher impact strength than the other hybrid samples.

In an another study, Portella et al. (2016) reinforced unsaturated polyester resin with cotton fiber wastes and E-glass fiber. They produced eight samples with varying stacking sequences of reinforcement materials (cotton reinforced, E-glass reinforced and six hybrid structures). The results indicated that hybrid samples have exhibited midlevel mechanical properties than the pure ones. Impact and flexural test results demonstrated that higher impact and flexural resistance were achieved by placing the E-glass plies to the outer layers. Besides, higher T_g values have been achieved with the hybrid structures and they have concluded that this could be due to the lower mobility of the polymer molecules owing to the fully package of the different fibers at the interface.

Ahmed & Vijayarangan (2008) investigated the effect of stacking sequence on the mechanical properties such as tensile, inter-laminar shear and flexural strength of untreated woven jute and E-glass fabric-reinforced composites. Hand lay-up technique was used to produce the composite laminates. Laminates were composed of 10 plies of fabric and polyester resin was preferred as the matrix material. Their results showed that hybrid laminate which has two E-glass plies at outer layers has the best property/cost balance.

In one of the studies, Bukhari et al. (2017) examined the effect of stacking sequence on tensile strength, displacement and flexural strength properties of carbon/E-glass hybrid composites. They produced four plied glass fabric reinforced, four plied carbon fabric reinforced and two carbon/glass fabrics reinforced epoxy composites with different stacking sequences. It was revealed that carbon fabric reinforced sample has the highest tensile strength value (269 MPa). Moreover, when hybrid samples were compared, it was seen that the sample which has carbon fabrics at the inner layers and glass fabrics at the outer layers has a higher tensile strength (262 MPa) than the sample which has glass fabric at the inner layers (220 MPa).

Jusoh et al. (2016) studied the effect of stacking sequence on the tensile and flexural properties of glass fiber reinforced epoxy composites hybridized with basalt, flax or jute fabrics. Composite samples were reinforced with seven plies of fabric. They have used two stacking sequences; sandwich-like and intercalation. Tensile strength results indicated that samples hybridized with basalt fabric have the highest tensile strength, whereas jute fabric hybridized samples have the lowest. In view of stacking sequences of fabric plies, it was appeared that instead of arranging fabric plies in a consecutive sequence, placing glass fabrics to the outer layers of the hybrid composite structures provided higher tensile strength.

Song (2016) has analyzed the influence of several stacking sequences of fabric plies on the bending properties of carbon/glass and carbon/aramid fabric reinforced hybrid composites. VARTM method was used for manufacturing the epoxy based composite samples. It was concluded that, carbon/glass reinforced samples have higher bending strength than carbon/aramid samples. It was also observed that while four carbon/four glass/four carbon/four glass fabric reinforced sample has the highest bending strength among carbon/glass reinforced samples, five carbon/ten aramid/five carbon fabric

reinforced sample has the highest bending strength among carbon/aramid reinforced samples.

In an another study, Behnia et al. (2016) has fabricated hybrid composite structures and investigated the influence of different stacking sequences and notch angles on low-velocity impact properties. Aramid, glass, basalt and carbon fabrics were utilized to reinforce the epoxy matrix by hand lay-up method. While placing basalt fabric to the midlayer enhanced the energy absorption capacity of glass/basalt reinforced samples, it was improved by placing basalt fabric plies to the outer layers in basalt/carbon hybrid samples. Moreover, energy absorption capacity of samples decreased with increasing notch angle from 45° to 75°.

Gujjala et al. (2014) have searched the effect of hybridizing E-glass fabric with jute fabric and also the stacking sequence on the density, tensile, flexural and interlaminar shear properties of woven jute/glass fiber hybrid composites. They prepared the samples by hand lay-up process and they preferred epoxy resin as matrix material. According to the results, the maximum interlaminar shear strength and tensile strength were obtained with the composite prepared with E-glass fabric at extreme layers; however, the maximum flexural strength was obtained with composite sample, which has a fabric stacking sequence of ‘‘glass-jute-glass-jute.

In a study, Agarwal et al. (2014) have examined the effect of different stacking sequences on the mechanical properties of glass/carbon hybrid composites. Epoxy resin was reinforced by seven plies of woven fabrics. Their results showed that while the sample which has consecutive glass/carbon alignment has the highest tensile strength, the sample which has carbon fabrics at the outer layers and glass fabric at the inner layers has the highest impact strength among those hybrid composite samples.

Murugan et al. (2014) fabricated interply hybrid composite structures by reinforcing epoxy resin with E-glass and carbon plain woven fabrics. Hand lay-up and compression molding methods were used to manufacture four plied fabric reinforced laminates. The static (tensile, flexural and impact strength) and dynamic mechanical properties (loss factor, storage and loss modulus) of the structures were measured. Static mechanical results showed that except impact strength carbon fabric reinforced sample has higher mechanical strength than E-glass reinforced sample. When the hybrid structures were examined, it was observed that sample which has E-glass fabric

plies at the outer layers has higher tensile and impact strength while sample which has carbon fabric plies at the outer layers has higher flexural strength, loss factor, storage and loss modulus.

At their study, Pandita et al. (2013) produced jute and jute/glass reinforced epoxy composites to investigate the effect of hybridizing on the mechanical properties of jute composites. They used resin infusion under flexible tooling method for manufacturing. From the results, it was observed that adding thin layers of E-glass fabric to the outer layers has increased the tensile, bending, and impact properties of the jute-reinforced composites.

Zhang et al. (2012) analyzed the effect of changing the stacking sequence of fabric plies on the tensile strength of glass/carbon hybrid composites with varying ratios of glass woven fabric and carbon woven fabric in an epoxy matrix. They indicated that the tensile strength of hybrid composite laminates can be improved with glass/carbon (50:50) fibre reinforcement not only by placing the carbon layers at the exterior, but also placing different fibre types alternatively.

Pandya et al. (2011) investigated the tensile strength of hybrid composites reinforced with eight-harness satin weave carbon fabric and plain weave E-glass fabric with two different stacking sequence configurations. Epoxy resin was utilized as matrix material. It was seen that hybrid composite having carbon fabrics at the outer layers and glass fabrics at the inner layers showed higher tensile strength and ultimate tensile strain.

In one of the studies, Hosur et al. (2005) studied the low velocity impact response characteristics of four different hybrid laminates. In hybrid structures while epoxy resin was used as matrix material, 2/2 twill carbon fabric and plain weave S2 glass fabric were used as reinforcement. Results showed that by placing S2 glass fabric on the back surface, impact responses of hybrid laminates were enhanced.

When the above-mentioned studies are examined, it has been seen that epoxy resin is used as the matrix material of the majority of the studies that have been done primarily. Looking at the reinforcement materials, it is seen that there are many studies using synthetic and natural fiber based fabrics. One of the most noticeable elements in these studies is that no information is given as to whether the directions of these fabrics have been taken into consideration during both production and mechanical tests. The facts

that woven fabrics generally exhibit different mechanical properties in the warp and weft directions and it is not taken into consideration in composite studies show a critical deficiency about this subject in the literature.

3.3.2 Studies on enhancement of mechanical properties of composite structures by addition of CNT fillers

In the literature survey, it comes out that the enhancement of mechanical properties of composite structures by addition of CNTs was mostly implemented to epoxy based composites. Tensile strength, interfacial shear strength and flexural strength are the foremost mechanical properties that improved by supplementation of CNTs.

In one of the studies, Mohan & Rajmohan (2017) have fabricated MWCNT treated banana, jute and flax fabric reinforced hybrid composites by compression moulding method and examined their mechanical properties. MWCNT dispersion was procured by ultrasonic probe sonicator. It was noticed that sample which has jute fabric plies at the outer layers (JBFBFBFJ) has higher tensile, compressive and hardness properties than the sample which have flax fabric plies at the outer layers (FBJBJBJF). Moreover, it was observed that while the impact energy of the sample which has flax fabric plies at the outer layers was improved by increasing the amount of MWCNT, it was decreased at samples which has jute fabrics at the outer plies.

Zhao et al. (2017) included CNTs to carbon fiber reinforced epoxy composites by two methods (mixing directly with matrix and attaching on the fiber) to compare the effects of two different methods. It was observed that matrix treated samples have 10.41%, 10.22% and 15.14% higher tensile strength, flexural strength and flexural moduli compared to carbon fiber reinforced epoxy sample while the fabric treated samples have 24.42%, 18.43% and 27.01% higher tensile strength, flexural strength and flexural moduli compared to carbon fiber reinforced epoxy sample, respectively. Besides, fabric treated samples reached slightly higher T_g values than matrix treated samples.

Zhang et al. (2016) designed and fabricated glass fabric reinforced epoxy based composite structures for sport equipment. They added MWCNTs (0.4 wt.%, 0.75 wt.% and 1.1 wt.%) to the resin and examined their effects on the mechanical properties. The higher tensile fracture work with fewer damages was observed with 0.75 wt.%

MWCNT added sample, whereas highest flexural strength was observed with 0.4 wt.% MWCNT added sample.

In an another study, Boroujeni et al. (2014) utilized CNTs to improve the in-plane and out-of-plane properties of composites. They used a relatively low temperature synthesis to build up different surface treated CNTs on carbon fibers. The results indicated that thermal barrier coated CNT grown samples show higher on-axis tensile strength, ductility and off-axis stiffness.

Shokrieh et al. (2013) added different amounts of MWCNTs (0.05, 0.1 and 0.5 wt.%) to unsaturated polyester resin to investigate their effects on mechanical properties. Mechanical stirring and ultrasonic mixing technique were used for dispersion of the MWCNTs. It was noticed from the results that better mechanical properties were achieved with 0.05 wt.% MWCNT added sample. The tensile and flexural strengths of 0.05 wt.% MWCNT added sample increased 6% and 20%, respectively. Besides, SEM images indicated that when the amount of MWCNT comes up to 0.05 wt.%, a large amount of agglomeration was procured.

Godara et al. (2010) investigated the effect of different CNT incorporation methods on interfacial shear strength of unidirectional glass fiber reinforced epoxy composites. These methods were addition of CNTs to (i) fiber sizing, (ii) matrix material and (iii) fiber sizing and matrix material simultaneously. Results indicated that interfacial shear strength of samples in all three cases were higher than the those of pristine sample and also it was observed that the maximum interfacial shear strength was achieved in the composite sample where CNTs were added to the fiber sizing.

To analyze the effect of amount of MWCNT on the mechanical properties, Chang (2010) added MWCNTs (0.5 wt.%, 0.75 wt.%, 1 wt.%, 1.5 wt.% and 2 wt.%) to epoxy resin, carbon fiber reinforced epoxy composite and glass fiber reinforced epoxy composite. From the results, it was acquired that by addition of 2 wt.% MWCNT to the samples, the impact strengths of epoxy resin, carbon fiber reinforced epoxy composite and glass fiber reinforced epoxy composite were increased at an amount of 154.1%, 35.9% and 44.3%. In addition, tensile strength of carbon fiber reinforced sample increased from 580.1 MPa to 781.4 MPa by addition of 0.5 wt.% MWCNT.

Shen et al. (2009) incorporated CNTs (up to 4 wt.%) into glass fabric reinforced polyamide 6 composite and investigated its influence on mechanical and thermal

properties. Hot press technique was used for manufacturing the samples. It was occurred that incorporation of CNTs up to 2 wt.% has a positive effect on the thermal stability, thermal conductivity and mechanical features of the sample. The flexural stress was improved up to 17%, 32% and 36% by incorporation of 0.5 wt.%, 1 wt.% and 2 wt.% CNTs, respectively.

In an another study, Fan et al. (2008) analyzed the interlaminar shear strength of glass fiber reinforced MWCNT treated epoxy composites. Three different amounts of MWCNTs (0.5 wt.%, 1 wt.% and 2 wt.%) were added to epoxy resin by high speed mechanical stirring, ultrasonic agitation and acid oxidation methods. They used traditional VARTM technique for production of samples that includes 0.5 wt.% MWCNT and a novel injection and double vacuum assisted resin transfer molding method for manufacturing of other samples due to the fact that with concentrations more than 0.5 wt.%, the insufficient permeability across the fiber layers causes VARTM method to break down. It was concluded that ILSS increased by 9.7%, 20.5% and 33.1% with addition of 0.5, 1 and 2 wt.% of MWCNT to the composite samples.

Seyhan et al. (2007) added CNTs to the polyester resin to examine their influence on the viscosity and the tensile strength of the composite material. They utilized four different CNTs (MWCNT, MWCNT-NH_2, DWCNT, DWCNT-NH_2) with three different amounts (0.1 wt.%, 0.3 wt.% and 0.5 wt.%). Three-roll milling process was used for mixing polyester resin and CNTs. It was seen that viscosity of resin increased with ascending amount of CNT and NH_2 functionalized CNT added samples displayed higher tensile strength than the others. Besides, the highest tensile strengths were achieved with 0.5 wt.% CNT added samples.

Zhu et al. (2007) were the first that integrated single-wall carbon nanotubes (SWCNT) to glass fiber reinforced vinyl ester composites and analyzed its effect on the interlaminar shear strength on the composite. SWCNTs were coated on the glass fabrics and VARTM process was used for composite manufacturing. It was concluded that, 45% increase of shear strength was procured by coating midplane ply of composite with 0.015 wt.% SWCNT.

At one of the studies, Qiu et al. (2007) integrated MWCNTs to the epoxy resin to enhance the mechanical properties of glass fabric reinforced epoxy composites. Pristine and strong acid functionalized MWCNTs were used. VARTM technique was

utilized as the composite production method. The tensile strength, Young's modulus, shear strength and short beam modulus of composite samples improved by 14%, 20%, 5% and 8%, respectively with 1 wt.% loading of functionalized MWCNTs. Furthermore, SEM images have supported these results by showing enhanced interfacial bonding.

Bekyarova et al. (2007) deposited MWCNTs and SWCNTs to the surface of carbon fabric by electrophoresis method to fabricate composite structures with enhanced interlaminar shear strengths. VARTM method was preferred to produce epoxy based composites. Results demonstrated that CNT integrated samples reached 30% higher interlaminar shear strengths than untreated sample.

Gojny et al. (2005) investigated the effect of addition of amino-functionalized double-wall carbon nanotubes (DWCNT-NH_2) on the mechanical properties of glass fiber reinforced epoxy composites. The highest matrix dominated properties (such as interlaminar shear strength) were observed with 0.3 wt.% DWCNT-NH_2 added sample. It was also indicated that tensile strength was not affected from CNT addition due to the interrelatedness of tensile properties and reinforcement material (fiber).

When preliminary studies on MWCNT reinforced textile based composites are examined, it has been found that there are not many studies utilizing polyester resin as the matrix material. It is also noteworthy that in general, pristine MWCNTs are used instead of functionalized MWCNTs and in the case of composites with functional group-treated MWCNTs, the studies using MWCNT-OH and MWCNT-COOH are rarely found.

4. EXPERIMENTAL STUDY

4.1 Materials

4.1.1 Reinforcement materials

In this study, jute (supplied by Ege Izmir Cuval, Izmir, Turkey), E-glass (supplied by Omnis Kompozit, Istanbul, Turkey), and carbon plain weave fabrics (supplied by Spinteks, Denizli, Turkey) were used as the reinforcement materials. Fabric parameters are given in Table 4.1.

Table 4.1 : Fabric parameters.

	Jute	E-glass	Carbon
Areal density (± SD) (g/m^2)	200 (±15.2)	200 (±5.3)	200 (±2.4)
Thickness (± SD) (mm)	0.99 (±0.10)	0.41 (±0.01)	0.29 (±0.005)
Fabric count (e.p.c. x p.p.c)	4 x 4	4 x 3	5 x 5
Warp yarn count (± SD) (Tex)	375 (±36.3)	288 (±10.3)	206 (±6.2
Weft yarn count (± SD) (Tex)	234 (±25.8)	409 (±11.5)	203 (±5.9)

SD: standard deviation, e.p.c.: ends per cm; p.p.c: picks per cm

4.1.2 Matrix materials

The matrix system consists of POLRES PRE-62 unsaturated orthophthalic polyester resin. Also, accelerator and hardener were obtained from Ada Elektrik. While cobalt was used as accelerator, methyl ethyl ketone peroxide (MEKP) was utilized as hardener.

4.1.3 Nanofillers

Three different MWCNTs were added to the matrix material to enhance the mechanical properties. MWCNTs that were used in this study were supplied by US Research Nanomaterials. Technical parameters of MWCNT, MWCNT-OH and MWCNT-COOH that are provided from the supplier are given in Table 4.2.

Table 4.2 : Technical parameters* of MWCNT, MWCNT-OH and MWCNT-COOH.

Parameters	MWCNT	MWCNT-OH	MWCNT-COOH
Purity (wt. %)	>95	>95	>95
Outside diameter (nm)	< 7	< 7	< 7
Inside diameter (nm)	2-5	2-5	2-5
Length (μm)	10-30	10-30	10-30
Specific surface area (m^2/g)	500	500	500
Tap density (g/cm^3)	0.27	0.27	0.27
True density (g/cm^3)	2.1	2.1	2.1
Manufacturing method	CVD	CVD	CVD
-OH content (wt.%)	-	5.58	-
-COOH content (wt.%)	-	-	3.86

*provided from the supplier

4.2 Methods

4.2.1 Preparation of the matrix material

One of the most critical jobs in the fabrication of composites is to determine the amount of the accelerator and hardener that should be added to polyester resin. If these chemicals are less than needed, it will prevent the adhesion of fabric and resin and thus the hardening of the sample. On the other hand, if they are used more than needed, it may cause the resin to be solidified before vacuum pump sucks the excess resin.

Literature review was carried out to decide the amount of accelerator and hardener. It was observed that there are different ratios at different studies. Some of the ratios of polyester:cobalt:MEKP found in the literature are;

- 1:0.015:0.015 (Ahmed & Vijayarangan, 2006, 2008; Ahmed et al., 2007)
- 1:0.01:0.01 (Ataş, 2017; Varga, Miskolczi, Bartha, & Lipóczi, 2010)
- 1:0.02:0.026 (Munikenche Gowda et al., 1999)
- 1:0.05:0.02 (Balcioğlu, Kaya, Akyildiz, & Aktas, 2013)
- 1:0.02:0.01 (Yasar & Aslan, 2000)

But it was not stated if these ratios are by weight or volume in those studies. According to the ratios, it was decided to use the ratio of 1:0.015:0.015 (by weigth), as an optimum value for composite production by using vacuum infusion system.

→ *First Trial (Resin Ratio: 1:0.015:0.015)*

First of all, 1 kg polyester resin was mixed with 15 g cobalt. Then, 15 g MEKP was added to the resin. And it was seen that after 5 minutes resin solidified.

→ *Second Trial (Resin Ratio: 1: 0.007:0.007)*

At the second trial, the ratios of MEKP and cobalt lessened half and half. 1 kg polyester resin mixed with 7 g cobalt and 7 g MEKP. Resin didn't solidified as at the first trial but after applying the resin on to the fabric layers it was again solidified. And because of this, the vacuum pump couldn't suck the excess resin. Also it was observed that 1kg resin was not enough for the four-ply jute composite production.

→ Third Trial (Resin Ratio: 1:0.003:0.003)

At the third trial, the ratios of MEKP and cobalt lessened half and half again. Also the amount of resin increased to 2 kg. 2 kg polyester resin mixed with 6 g cobalt and 6 g MEKP. As at the second trial, resin solidified after applying the resin on to the fabric layers and the vacuum pump couldn't sucks the excess resin.

→ *Fourth Trial (Resin Ratio: 1:0.00075:0.001)*

At the fourth trial, 2 kg polyester resin mixed with 1.5 g cobalt and 2 g MEK. The resin did not get solidified both during applying the resin on to the fabric and while vacuum sucks the excess resin. But when the vacuum bag was opened after 24 hours, it was seen that sample didn't cured and not turned into a composite plate.

→ *Fifth Trial (Resin Ratio: 1:0.00175:0.002)*

At the last trial, 2 kg polyester resin mixed with 3.5 g cobalt and 4 g MEK. The resin did not get solidified neither during applying the resin on to the fabric nor vacuum sucks the excess resin. Also when the vacuum bag was opened after 24 hours, it was seen that composite plate was properly formed.

All resin ratio trials were done by using jute fabric which has an areal density of 200 g/m^2. Eventually, according to those trials it was observed that resin ratio of 1:0.00175:0.002 is acceptable for composite production by vacuum infusion technique.

MWCNT addition to matrix material

To improve the interfacial strength and mechanical properties of composite structures, MWCNTs were added to the matrix material. CNT amounts that were added to the polymer composites were mostly ranging from 0.015 wt.% to 4 wt.% in the literature (Fan et al., 2008; Gojny et al., 2005; Mao Sheng Chang, 2010; Qiu et al., 2007; Seyhan et al., 2007; Shen et al., 2009; Shokrieh et al., 2013; X. Zhang et al., 2016; J. Zhu et al., 2007).

It was stated in the literature that agglomeration of CNTs increases with ascending amount of CNT (Shokrieh et al., 2013). In this study, to investigate the effect of addition of very few amounts of CNTs on mechanical properties of composite materials and also to minize the agglomeration of CNTs 0.5 g of MWCNT was added to 1 kg of polyester resin (0.05 %). Mixing of the MWCNT and polyester was performed by ultrasonic mixer (Figure 4.1). MWCNT was added little by little to avoid agglomeration and ultrasonic mixer was run for 2 hours for each resin preparation to acquired a homogenous dispersion.

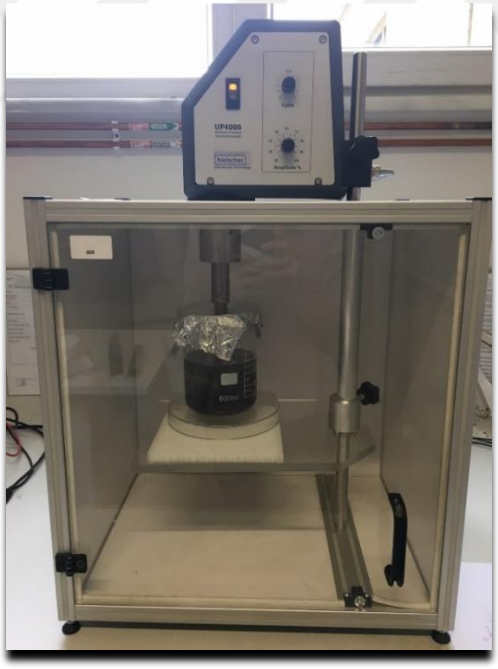

Figure 4.1 : Ultrasonic mixer.

4.2.2 Composite fabrication

Vacuum assisted resin transfer molding technique was used for the preparation of four-plied composite specimens. Composite fabrication was realized at room temperature

(20°C±2°C). During the process, ventilator located above the table was in working order. The schematic diagram of vacuum assisted resin transfer molding is given in Figure 4.2.

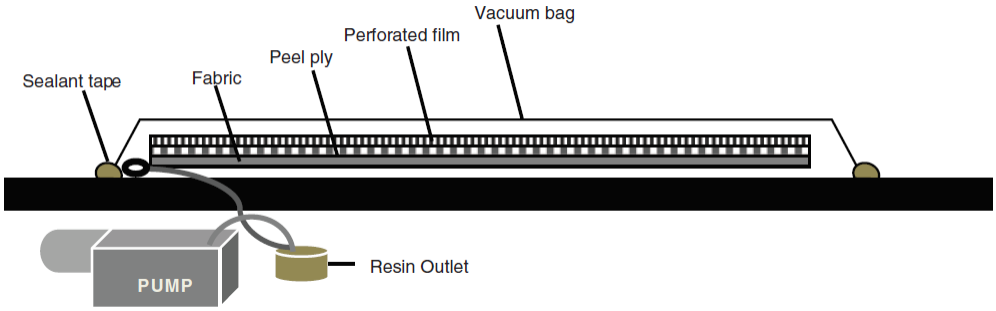

Figure 4.2 : Schematic diagram of vacuum assisted resin transfer molding technique.

Production steps of the vacuum infusion technique

1) First of all, surface of the vacuum table was cleaned with acetone and 1 layer of releasing agent was applied.
2) Fabric plies were superposed and then peel ply fabric (Figure 4.3) layed on the fabric layers. Peel plies are tightly woven fabrics (often nylon) and impregnated with some types of releasing agent. The peel ply fabric sticks to the laminate, but it can be pulled away without too much difficulty.
3) Then, perforated film (Figure 4.3) put on peel ply. This film holds the resin in laminate, when high vacuum pressure is used with slow curing resin system or thin laminates.

Figure 4.3 : Arrangement of peel ply and perforated film.

4) Spiral hoses were attached to the two sides of the fabric plies to enable a homogenous flow of resin.

5) Finally, vacuum sealant tape was pasted around the sample and vacuum bag attached on it. Two small holes were opened for resin inlet and outlet.
6) Vacuum pump was started up to test if is there any air leakage or not.
7) Then vacuum pump was started up again to suck the required amount of resin and then again to suck the excess resin from the sample. Figure 4.4 shows the resin inlet and outlet of the system.
8) Vacuum pump worked for 2 hours (about 1 bar) and then it was switched off. Also vacuum tube was cut and closed with sealant tape to prevent air entrance. Sample waited for 24 hours at that position for curing.
9) After 24 hours, vacuum bag was opened and composite plate separated from both tempered glass, peel ply and perforated film. And excess resin which was stored at resin container was cleaned out after process.

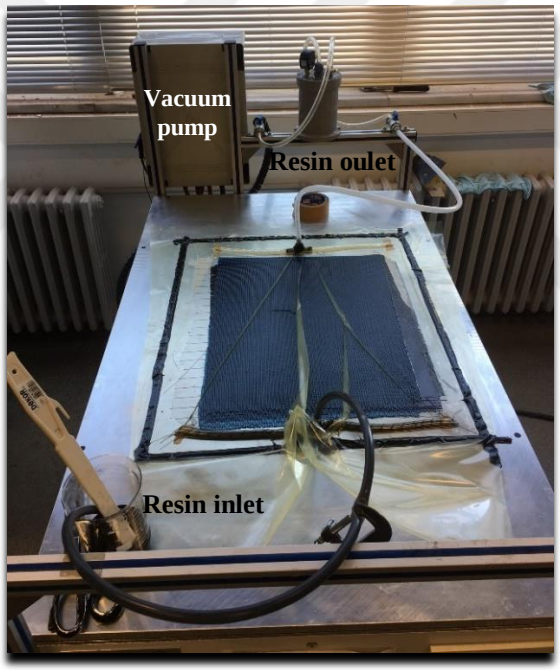

Figure 4.4 : Resin inlet and outlet of VARTM system.

By using this method, twelve different four-plied fabric reinforced composites were manufactured (Table 4.3). Three of them were pure jute, pure cotton and pure E-glass reinforced composites and other nine composites were hybrid structures of these three fabrics. At specimen codes J, G and C indicate jute, E-glass and carbon fabric plies, respectively.

Table 4.3 : Composite samples.

Specimen Code	Layer Sequence	Fabric Types
JJJJ		Jute/Jute/Jute/Jute
GGGG		E-glass/E-glass/E-glass/E-glass
CCCC		Carbon/Carbon/Carbon/Carbon
JGGJ		Jute/E-glass/E-glass/Jute
GJJG		E-glass/Jute/Jute/E-glass
JGJG		Jute/E-glass/Jute/E-glass
JCCJ		Jute/Carbon/Carbon/Jute
CJJC		Carbon/Jute/Jute/Carbon
JCJC		Jute/Carbon/Jute/Carbon
GCCG		E-glass/Carbon/Carbon/E-glass
CGGC		Carbon/E-glass/E-glass/Carbon
GCGC		E-glass/Carbon/E-glass/Carbon

Table 4.4 : Sample codes of all composite samples.

Sample Codes			
GGGG	GGGG-MWCNT	GGGG-MWCNTOH	GGGG-MWCNTCOOH
CCCC	CCCC-MWCNT	CCCC-MWCNTOH	CCCC-MWCNTCOOH
JJJJ	JJJJ-MWCNT	JJJJ-MWCNTOH	JJJJ-MWCNTCOOH
GCGC	GCGC-MWCNT	GCGC-MWCNTOH	GCGC-MWCNTCOOH
GCCG	GCCG-MWCNT	GCCG-MWCNTOH	GCCG-MWCNTCOOH
CGGC	CGGC-MWCNT	CGGC-MWCNTOH	CGGC-MWCNTCOOH
GJGJ	GJGJ-MWCNT	GJGJ-MWCNTOH	GJGJ-MWCNTCOOH
GJJG	GJJG-MWCNT	GJJG-MWCNTOH	GJJG-MWCNTCOOH
JGGJ	JGGJ-MWCNT	JGGJ-MWCNTOH	JGGJ-MWCNTCOOH
CJCJ	CJCJ-MWCNT	CJCJ-MWCNTOH	CJCJ-MWCNTCOOH
CJJC	CJJC-MWCNT	CJJC-MWCNTOH	CJJC-MWCNTCOOH
JCCJ	JCCJ-MWCNT	JCCJ-MWCNTOH	JCCJ-MWCNTCOOH

After production of these twelve samples, MWCNT, MWCNT-OH and MWCNT-COOH added to these twelve configuration and thirty six samples were manufactured. Table 4.4 shows the sample codes of all samples. Apart from these samples, neat polyester plate was also manufactured to see the reinforcement effect on the properties of polyester resin.

4.2.3 Fiber volume ratio and void fraction

The fiber volume ratio was calculated using equation 4.1.

$$V = \frac{\frac{w_j}{\rho_j} + \frac{w_g}{\rho_g} + \frac{w_c}{\rho_c}}{\frac{w_j}{\rho_j} + \frac{w_g}{\rho_g} + \frac{w_c}{\rho_c} + \frac{w_p}{\rho_p}} \tag{4.1}$$

where Wj, Wg, Wc, and Wp represent the weight ratios of the jute, E-glass, carbon, and polyester, and ρ_j, ρ_g, ρ_c, and ρ_p are the densities of jute, E-glass, carbon, and polyester, respectively.

Void fraction was calculated from the theoretical and experimental density of the composite through equation 4.2, according to ASTM D2734-94 standard.

$$\Delta v = \frac{\rho_{ct} - \rho_{ex}}{\rho_{ct}} \tag{4.2}$$

where ρ_{ex} and ρ_{ct} are the experimental density and theoretical density of the composite laminate. Experimental density of composite laminates was measured by dividing the measured weight (g) by the measured volume (cm^3). While the dimensions of the samples were measured by micrometer, the samples were weighed by a precision balance.

Equation 4.3 was used to calculate the theoretical density of the composites.

$$\rho_{ct} = \frac{1}{(W_f/\rho_f) + (W_m/\rho_m)} \tag{4.3}$$

where W_f and W_m represent weight fractions of fabric and matrix, and ρ_f and ρ_m are the densities of fabric and matrix, respectively.

4.2.4 Thermal analysis

In this study, dynamic mechanical analysis, thermogravimetric analysis and differential scanning calorimetry were used to analyze the thermo-mechanical and other thermal properties of fabric reinforcements, polyester matrix and composite structures.

4.2.4.1 Dynamic mechanical analysis

Dynamic mechanical analysis (DMA) is a technique that measures both the mechanical and viscoelastic properties of materials (Gupta & Deep, 2017; Shanmugam & Thiruchitrambalam, 2013). DMA is a method that applies sinusoidal force to samples to study their viscoelastic properties and structures. It measures the modulus and damping properties of materials (Goertzen & Kessler, 2007; Pothan, Oommen, & Thomas, 2003; Saha, Das, Bhatta, & Mitra, 1999). Fibre-reinforced composites are exposed to different types of dynamic stresses during handling, which demonstrates the importance of analysing the viscoelastic properties of composite materials (Ornaghi, Bolner, Fiorio, Zattera, & Amico, 2010).

DMA has different mechanical deformation modes. These are; compression, tension, shear, torsion, single cantilever, dual cantilever and three point bending modes (Figure 4.5) (Price & Duncan, 2016).

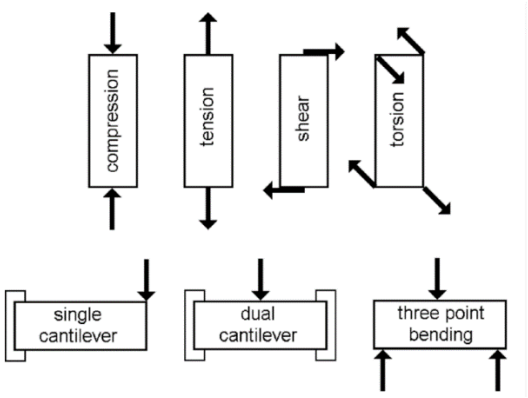

Figure 4.5 : Mechanical deformation modes of DMA (Price & Duncan, 2016).

An RMI DX04T dynamic mechanical analyzer with a three-point bending (Figure 4.6(a)) configuration was used for the dynamic mechanical analysis of composite samples, while tension mode (Figure 4.6(b)) was used for fabric samples.

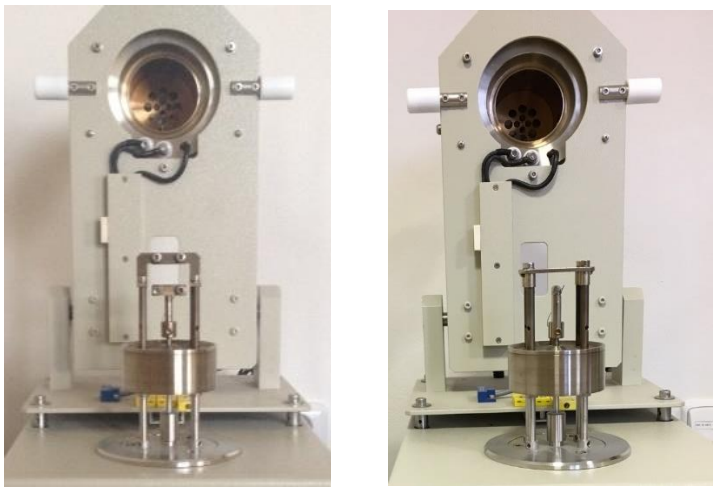

Figure 4.6 : (a) Tension and (b) three-point bending configurations of dynamic mechanical analyser.

Samples measuring 10 mm x 50 mm were cut from warp and weft directions of composite plates. Tests were performed at a frequency of 1 Hz, while temperature programs were run from 30 to 150 °C under a controlled sinusoidal strain, at a heating rate of 3 °C/min.

For DMA analysis of reinforcement materials, thickness of the samples were needed. For this purpose, thicknesses of fabrics were measured with Schmidt Textile Digital Thickness Gauge (Figure 4.7). Same measuring standards were applied to the fabric samples.

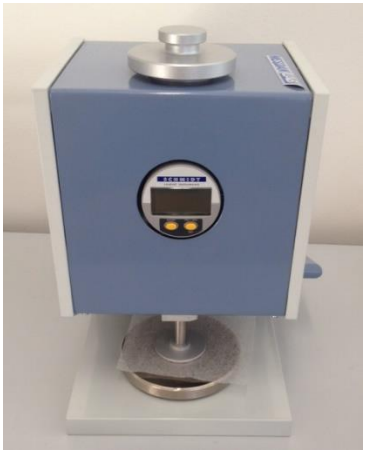

Figure 4.7 : (a) Tension and (b) three-point bending configurations of dynamic mechanical analyser.

4.2.4.2 Thermogravimetric analysis

Thermogravimetric analysis (TGA) shows the degradation temperature and amount of weight materials lose as temperature is increased (Joseph et al., 2003; Mei & Chung, 2000; P. Zhu, Sui, Wang, Sun, & Sun, 2004).

Mettler Toledo TGA/SDTA851^e analyzer was used to conduct the thermogravimetric analysis (Figure 4.8). Samples that have weight between 6-7 mg were prepared and put into aluminium oxide crucibles. After that, closed crucibles put into heating tunnel and experiment was started. Samples were heated from 25 °C to 600 °C with a heating rate of 5°C/min in a nitrogen atmosphere.

Thermogravimetric analysis of pure solidified resin, fabrics and composite samples were realized at same measurement standards.

Figure 4.8 : Mettler Toledo TGA analyzer.

4.2.4.3 Differential scanning calorimetry analysis

Differential scanning calorimetry (DSC) is a thermal analysis method that measures heat flow rate as a function of time and temperature (Joseph et al., 2003). By using a reference material, it computes the required amount of heat to make the temperature difference between sample and reference material zero. This heat provides information regarding the physical and chemical transformations of material (Mei & Chung, 2000; P. Zhu et al., 2004).

Figure 4.9 shows the preparation and analysis steps of DSC measurement. While executing DSC analysis, first of all aluminium crucibles with lids were prepared with the apparatus. Then samples which have a weight between 8-10 mg were cut from

fabrics and composite panels. They were weighed with precision balance and put into aluminium crucible with a tweezers and lid was put on it.

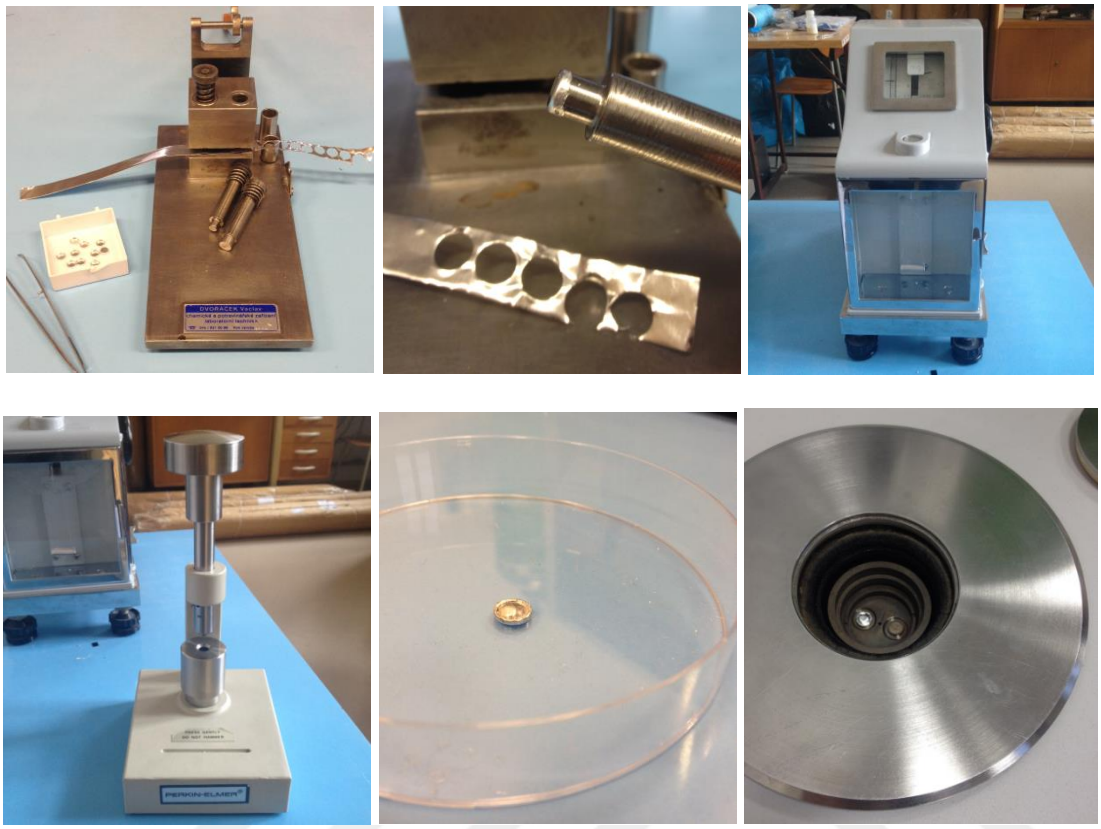

Figure 4.9 : Steps of sample preparation and analysis of DSC.

By using crucible press, samples were enclosed in this small cups. Then, substance was loaded into DSC. Tests were carried out in dynamic condition with the following standard procedure:

A DSC-6 Perkin–Elmer differential scanning calorimeter was used for differential scanning calorimetry. Composite samples weighing approximately 8 mg were heated from 25 °C to 400 °C at a heating rate of 10 °C /min, with a pause of one minute at 25 °C. They were then cooled to 25 °C at a rate of 10 °C /min.

Apart from this standards, fabric samples were heated from 25°C to 200°C at a heating rate of 10°C /min and then, the samples were cooled to 25°C at a rate of 10°C /min. Samples waited 1 minute at 25°C and then heated to 200°C at a heating rate of 10°C /min and the samples were cooled to 25°C.

4.2.5 Mechanical analysis

4.2.5.1 Sample preparation for mechanical analysis

The mechanical properties of composite samples were evaluated by tensile strength and v-notched Charpy impact testing. Before starting mechanical tests,

- ✓ AUTOCAD software program was used to draw the forms of test specimens according to related standards. The forms of tensile strength test specimen (ASTM D638-10) and impact strength test specimen (BS EN ISO 179:1997) are given in Figure 4.10 and 4.11, respectively.

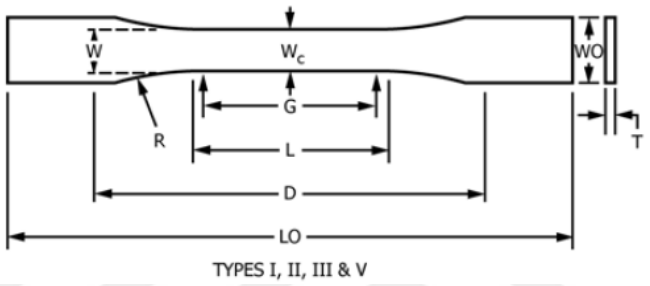

Figure 4.10 : Tensile strength test specimen form [W:13 mm, L: 57 mm, WO: 19 mm, LO:165 mm, G: 50 mm, D: 115 mm, R : 76 mm].

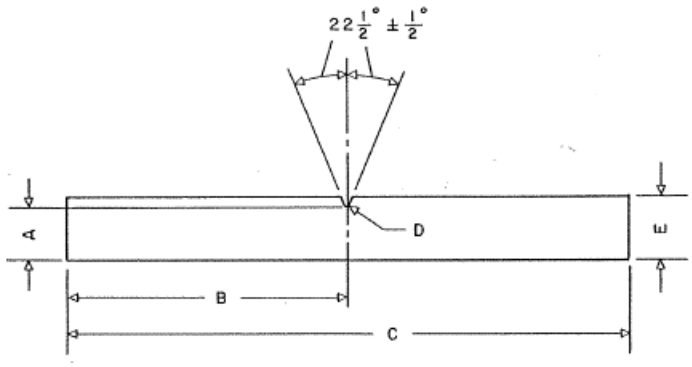

Figure 4.11 : Impact strength test specimen form [A: 10.16 mm, B: 63.5 mm, C: 127 mm, D:0.25R mm (Radius of notch), E: 12.7 mm].

- ✓ Then, these drawings were arranged by ISYCAM program.
- ✓ Finally, drawings send to the REMOTE program which was connected to Computer Numerical Control (CNC) milling machine (Figure 4.12).

Samples were cut from both warp and weft directions according to related standards by CNC milling machine. For each test, 3 warp specimen and 3 weft specimen were cut.

Figure 4.12 : CNC milling machine.

4.2.5.2 Tensile strength analysis

Tensile testing was realized by Shimadzu AG-IS test machine (Figure 4.13(a)) according to ASTM D638-10 standard. A load cell of 10 kN at cross-head speed of 6 mm/min was used.

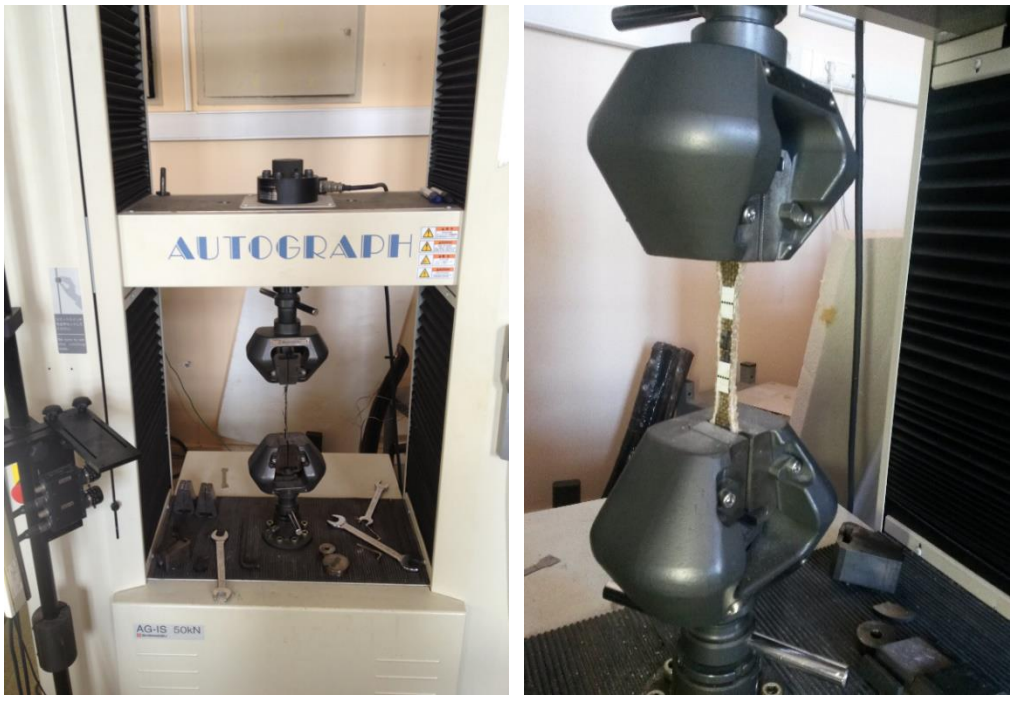

Figure 4.13 : (a) Shimadzu AG-IS test machine, (b) testing sample.

Programs DVE-201 and Trapezium 2 were utilized to evaluate the tensile strength of composite samples. Before testing, width and depth of all test specimens were measured. Two white papers which had a black line on them were pasted to the samples at 50-mm intervals (Figure 4.13(b)). The distance between these black lines were also measured by DVE-201 program by using two cameras that were integrated to the testing machine. Then, this distance, width and depth values were entered to the Trapezium 2 program and testing was started.

4.2.5.3 Impact strength analysis

Devotrans Charpy Impact Test Machine (Figure 4.14(a)) was utilized to evaluate the impact resistance of the composite samples according to BS EN ISO 179:1997 standard. Before testing, a notch was opened at the middle of each sample by a notching apparatus (Figure 4.14(b)). The notched sample was placed on the testing machine and the notched part was adjusted to be at the level of the pendulum of the machine. Then, the pendulum was fixed at the top of the machine and then released. The energy that was applied to the sample was 12 J.

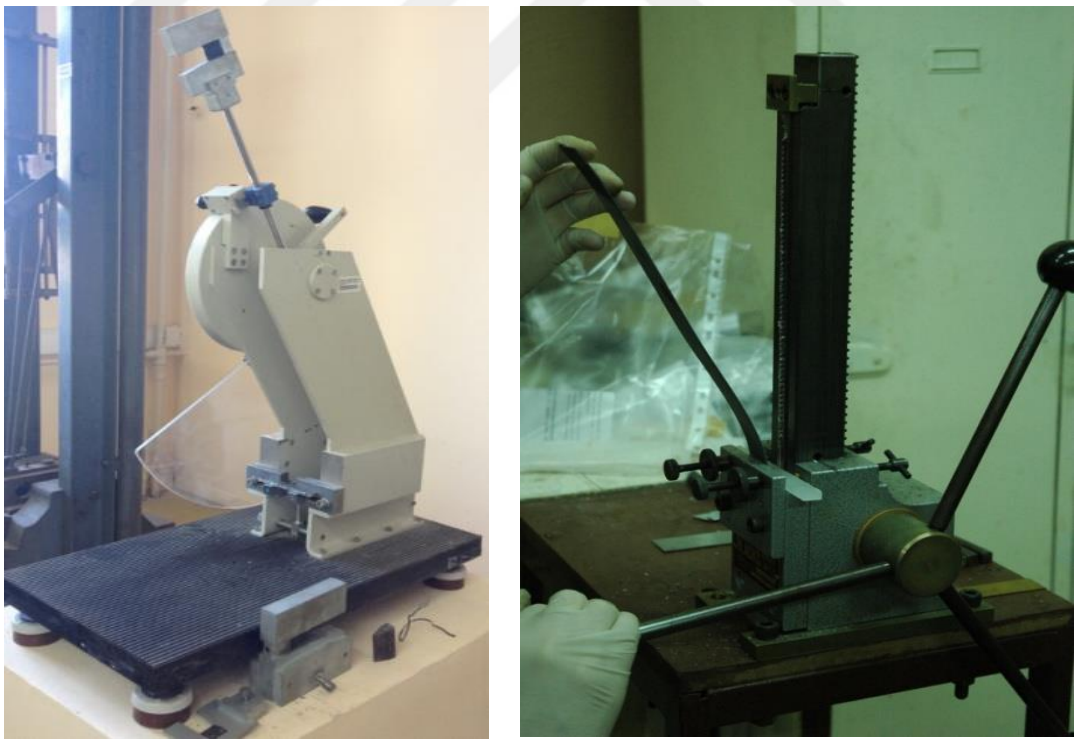

Figure 4.14 : (a) Devotrans charpy test machine, (b) notching machine.

Equation 4.4 was used to calculate the Charpy impact strength of notched specimen (a_{cN}).

$$a_{cn} = W \times \frac{10^3}{h \times b_n} \quad (4.4)$$

where W is the corrected energy absorbed by breaking the test specimen (J), h is the thickness of the test specimen (mm) and b_n is the remaining width at the notch base of the test specimen (mm).

4.2.6 Statistical analysis

The statistical analysis of the results was performed by using Minitab 18 software program. Full-factorial experiments are the experiments in which the effects of more than one factor on response are investigated. Factorial designs are mostly used to examine the effects of experimental factors and the interactions between those factors, that is, how the effect of one factor varies with the level of the other factors in a response. Also, the number of experiments geometrically increases with the increasing number of factors and levels (Bingol, Tekin, & Alkan, 2010; Öztürk & Kavak, 2004).

The full factorial experimental layout was designed in order to examine the main factors and their interactions on the tensile and impact properties of hybrid composite samples. One factor with two levels two factors with three levels and one factor with four levels were chosen to design the experimental study. The factors and levels are given in Table 4.5.

Table 4.5 : Sample codes of all composite samples.

Factors	Level 1	Level 2	Level 3	Level 4
Yarn (Material)Type	Jute/E-glass	Jute/carbon	E-glass/carbon	-
Fabric Direction	Warp	Weft		
Stacking Sequence	High strength inside	High strength outside	Alternately	
MWCNT Type	None	MWCNT	MWCNT-OH	MWCNT-COOH

The first factor was the yarn (material) type. Three types of fabrics (jute, E-glass and carbon) were used in this study. Primarily, four plied jute, four plied E-glass and four plied carbon fabric reinforced samples were manufactured and their mechanical properties were evaluated. After that, hybrid samples using two types of fabrics (jute/E-glass, jute/carbon and E-glass/carbon) were manufactured. The second factor was the fabric direction. The mechanical tests were done in two directions, those were; warp (longitudinal) and weft (transverse) directions. The third factor was the stacking

sequence of fabric layers in the composite sample. Three levels were chosen for this factor. At level 1, fabric layers which have higher strength were placed between low strength fabric layers. At level 2, fabric layers which have lower strength were placed between high strength fabric layers while at level 3, fabric layers were aligned alternately. The last factor was the MWCNT type. The level 1 did not contain any MWCNT whereas levels 2, 3 and 4 comprised pristine MWCNT, MWCNT-OH and MWCNT-COOH, respectively.

4.2.7 Morphological analysis

The interfacial surface morphologies of composite samples were observed by using a Scanning Electron Microscope (SEM) TS5130 Vega-Tescan (Figure 4.15) at 20 kV acceleration voltage. The samples were sputter coated with gold to increase the surface conductivity.

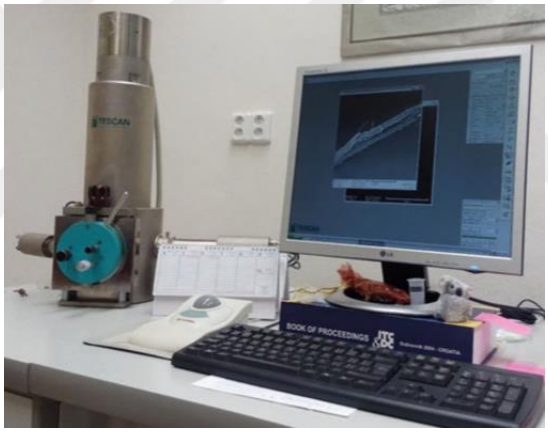

Figure 4.15 : Vega-Tescan TS5130 Scanning electron microscope.

5. RESULTS AND DISCUSSION

5.1 Reinforcement Materials (Fabric) Analysis Results

In order to determine the strength of the reinforcement materials, it was intended to perform tensile strength analysis of the fabric samples. Titan Universal Strength Tester and Shimadzu AG-IS Test Machine were used for this purpose but unfortunately, we could not obtain any results from these conventional testing devices. The high sliding tendency of E-glass and carbon yarns in the fabrics did not make it possible to fulfill the strength analysis of these fabric samples. After these inevitable failures, it was decided to measure the thermo-mechanical properties (dynamic mechanical properties) of fabric samples.

In this perpective, fabric sample analysis results are given in three sections: dynamic mechanical analysis, thermogravimetric analysis and differential scanning calorimetry analysis.

5.1.1 Dynamic mechanical analysis results

Dynamic mechanical properties of a material are stated in terms of storage modulus, loss modulus and tan delta (loss factor) (Jabbar et al., 2017, 2016).

5.1.1.1 Storage modulus

Storage modulus shows how stiff a material is and it is approximately similar to the Young modulus (S. Yang, Taha-Tijerina, Serrato-Diaz, Hernandez, & Lozano, 2007). It is proportional to the energy stored in course of a loading period (Jabbar et al., 2017)

Figure 5.1 shows the storage modulus comparisons of jute, E-glass and carbon fabrics taken from both warp and weft directions. Three samples from warp and three samples from weft direction were analyzed and optimum one was chosen to compare with other fabric types. It was obviously seen from the figure that carbon fabric has the highest storage modulus while jute fabric has the lowest at both directions. Storage moduli of jute, E-glass and carbon fabric samples at 25°C were about 0.06 GPa, 1.7 GPa and 3 GPa, respectively.

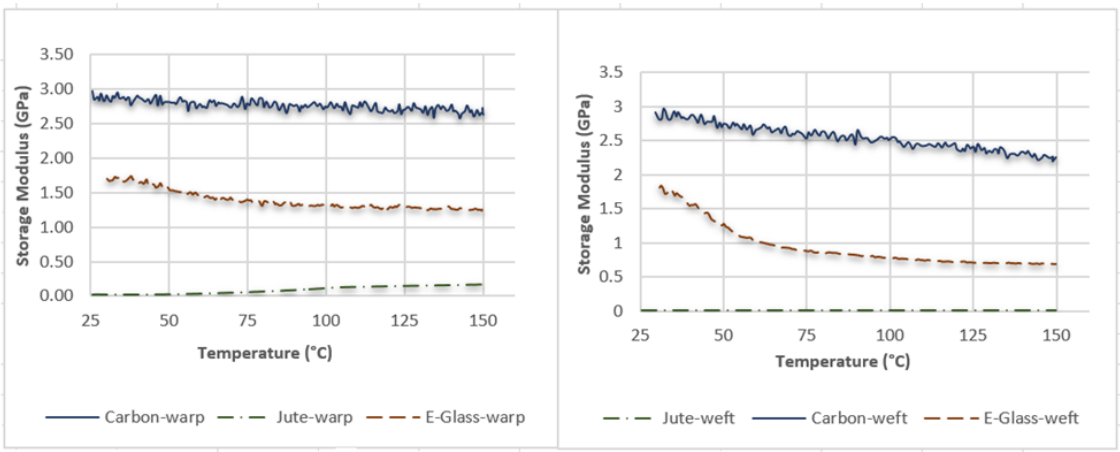

Figure 5.1 : Storage modulus results of fabric samples at (a) warp and (b) weft directions.

Besides, it was observed that while the storage moduli of E-glass and carbon fabrics decreased with increasing temperature, the storage modulus of jute fabric has increased. Resulting from the fact that storage moduli of E-glass and carbon fabrics were much higher than those of jute fabrics, the increase in the storage modulus of the jute fabric with ascending temperature did not appear clearly in Figure 5.1. Figure 5.2 demonstrates the storage moduli of jute fabrics from warp and weft directions with ascending temperature.

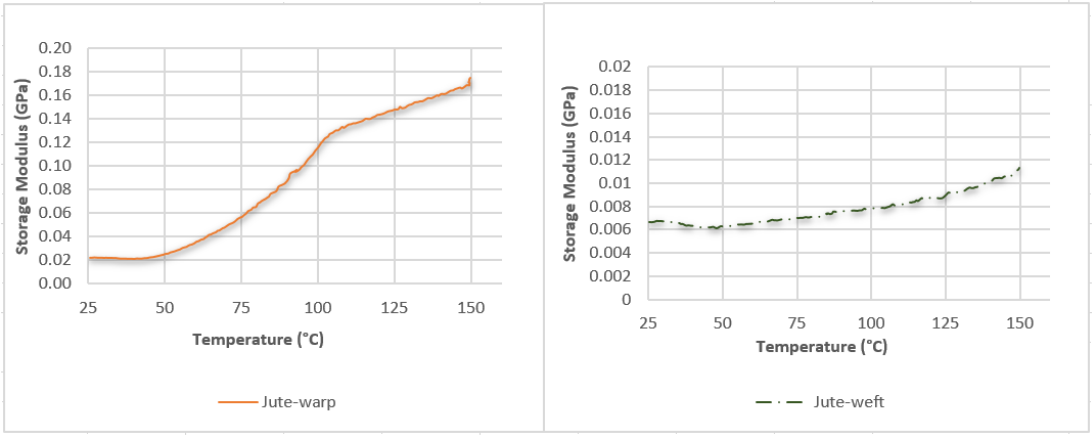

Figure 5.2 : Storage modulus results of jute fabric samples at (a) warp and (b) weft directions.

This is an inherent characteristic of some natural cellulosic fibers that their moduli decrease with increasing amount of water content (Baley, 2002). To this respect, it was thought that the reason of the increment of modulus could be the decreasing moisture content of jute fiber with ascending temperature. Moreover, it has been found that with increasing temperature, moduli decrements in E-glass and carbon fabrics were greater

in weft direction samples. In the case of jute fabrics, it was observed that the increment of storage modulus with increasing temperature was higher in the fabrics from warp direction.

5.1.1.2 Loss modulus

Loss modulus is related to the viscous behaviour of a material and is proportional to the energy dissipated per cycle (Ornaghi, Bolner, Fiorio, Zattera, & Amico, 2010).

Figure 5.3 displays the loss modulus comparisons of jute, E-glass and carbon fabrics. It was revealed from the results that, jute fabric had lower loss modulus value than other fabric types. When loss moduli of E-glass and carbon fabrics were examined, it has been found that although the loss moduli of warp and weft directions were similar at 25°C (≈0.40 GPa), the loss modulus of the sample taken from the weft direction decreased more with increasing temperature.

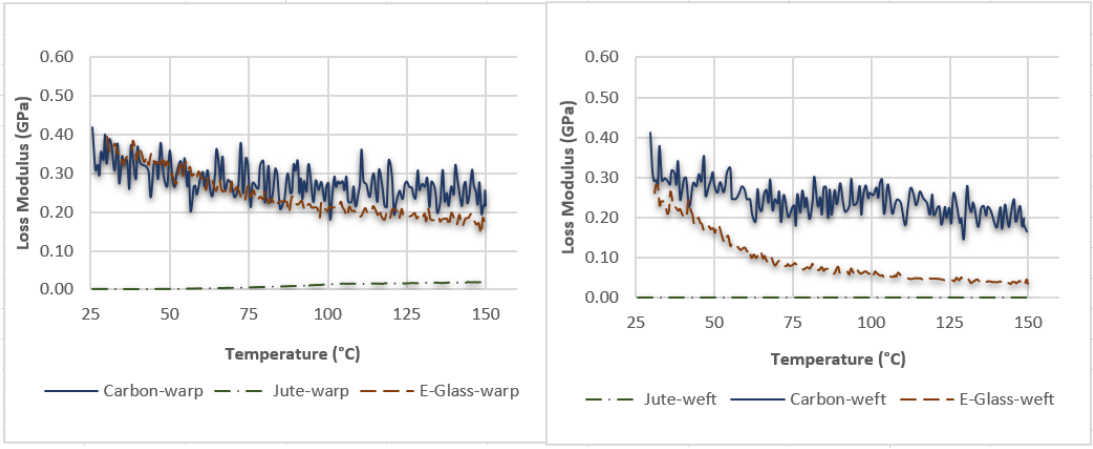

Figure 5.3 : Loss modulus results of fabric samples from (a) warp and (b) weft directions.

Similar to the storage modulus results, the loss moduli of jute fabric samples increased with ascending temperature (Figure 5.4). It was thought that, this fact was also related to the descending moisture content of jutes.

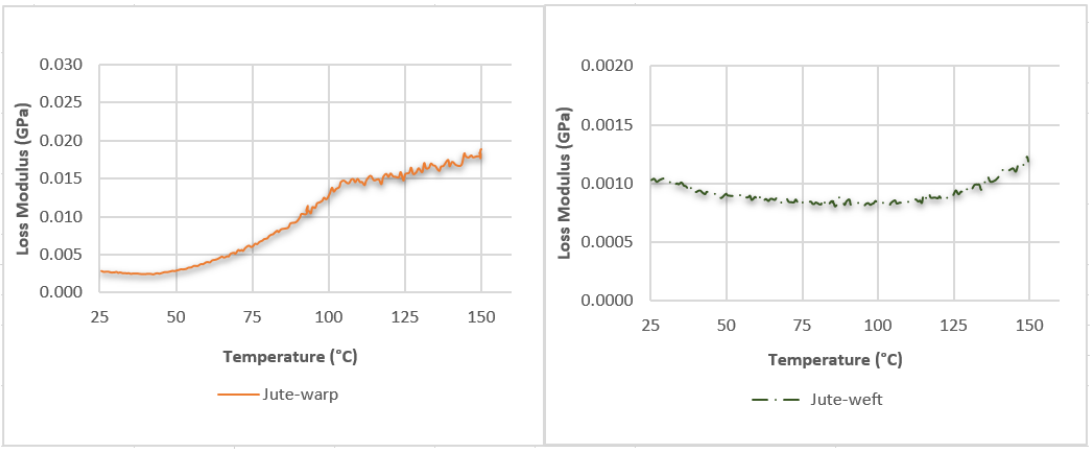

Figure 5.4 : Loss modulus results of jute fabric samples from (a) warp and (b) weft directions.

5.1.1.3 Tan delta

Tan delta (loss factor) is related to the damping properties of a material and it is the ratio of loss modulus to storage modulus (Ornaghi et al., 2010).

Tangent delta comparisons of fabrics samples are given in Figure 5.5. Tangent delta is the ratio of loss modulus to storage modulus. It is mostly used to determine the Tg of a material. The peak value of the curve demonstrates the Tg value of the material. Due to the fact that jute, E-glass and carbon fibers do not have Tg values, tan delta curves of fabric samples did not show a peak.

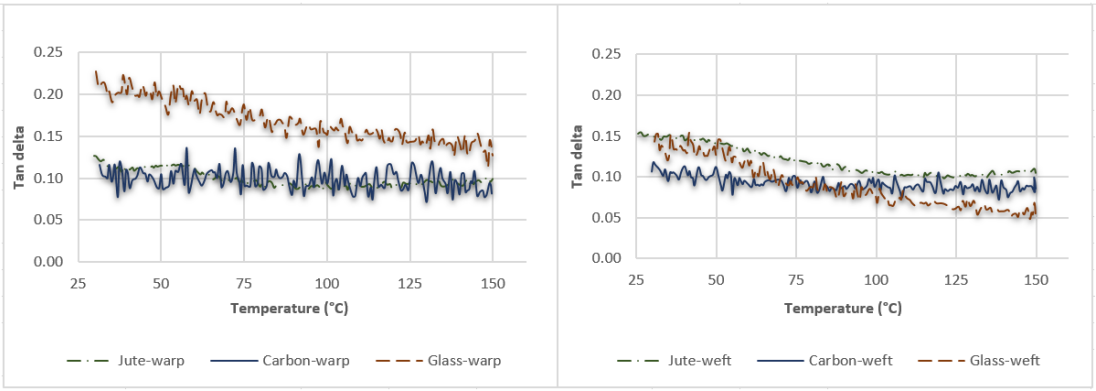

Figure 5.5 : Tan delta results of fabric samples.

E-glass fabric sample reached the highest tan delta value at warp direction, while they had approximately similar tan delta values at weft direction.

5.1.2 Thermogravimetric analysis

Figure 5.6 shows an example of a TGA graph of a fabric sample (carbon) that is achieved from Mettler Toledo Software Program. This graph shows the alteration in the weight of a sample with increasing temperature. Onset temperature that is marked in the figure is the temperature where a sharp decrease in the sample weight has commenced.

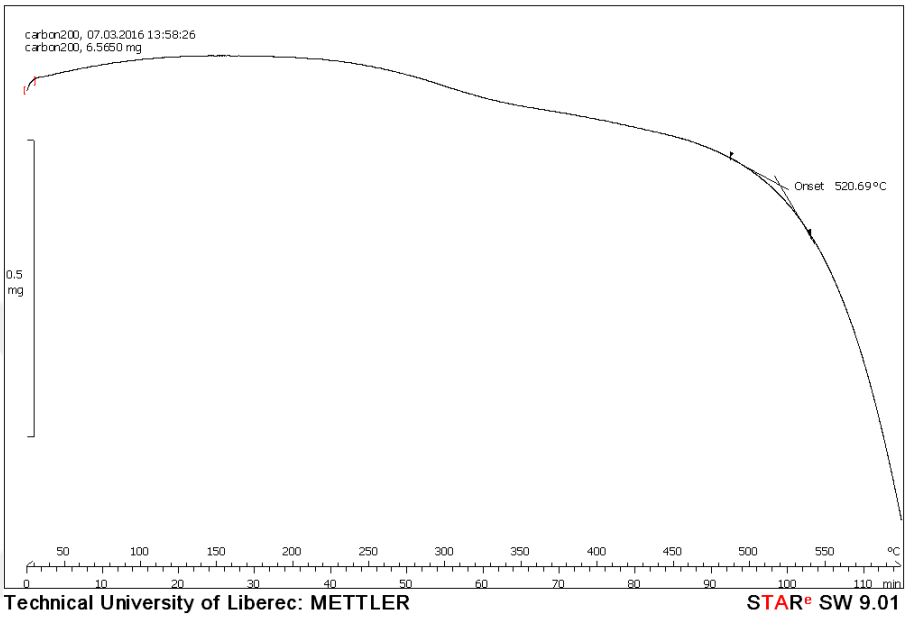

Figure 5.6 : TGA graph of carbon fabric.

Initial and final temperatures, weight losses and onset temperatures of fabric samples are given in Table 5.1. It was acquired that carbon fabric had a weight loss of 11% and its onset temperature was about 520°C while weight difference of E-glass fabric was 0.6 %. Due to the fact that E-glass fiber doesn't have a decomposition temperature (Zhou & Keller, 2005), E-glass fabric sample had nearly no weight loss and it did not have any onset temperature.

Table 5.1 : Weight loss and onset temperatures of fabric samples.

Fabric Type	Initial weight (mg)	Final weight (mg)	Weight loss (%)	Onset temperature (°C)
Jute	6.35	0.20	97	255.4 / 344.56
E-glass	6.28	6.24	0.6	-
Carbon	6.56	5.84	11	520.69

On the other hand, jute fabric sample had weight loss of 97% and it had two onset temperatures (255°C and 344°C). This could be due to the molecular content of jute fiber. It contains 15.86% lignin, 23.2% hemi-cellulose and 62.6% cellulose and they started to degrade at temperatures of 200°C, 180°C and 315°C, respectively (Lv, Wu, & Lou, 2010; Manikandan Nair, Thomas, & Groeninckx, 2001; Raghavendra et al., 2015; H. Yang, Yan, Chen, Lee, & Zheng, 2007). The onset temperature at 255°C was thought to be the degradation of lignin and hemicellulose, while the onset temprature at 344°C could be the cellulose degradation.

5.1.3 Differential scanning calorimetry analysis

Figure 5.7 shows the DSC graphs of jute, E-glass and carbon fabric samples. As it is seen from the figures, E-glass and carbon fabrics did not show any endothermic or exothermic reaction during both two heating and cooling cycles because they do not have any glass transition and melting temperatures and also their degradation temperatures are not in between 25°C - 200°C.

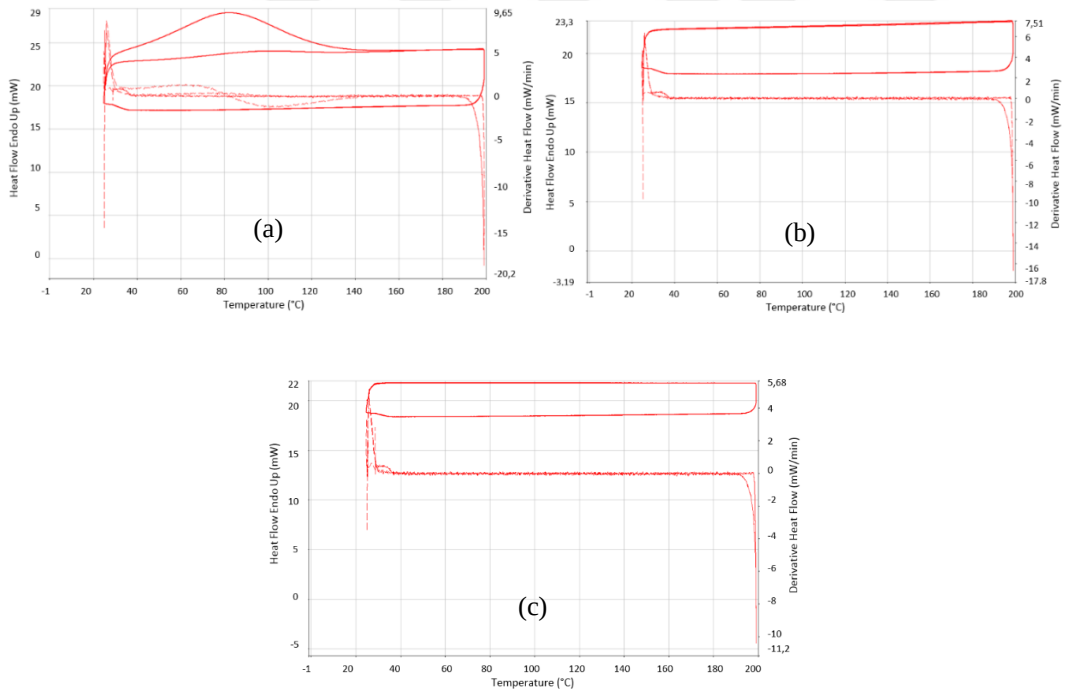

Figure 5.7 : DSC graphs of (a) jute ; (b) E-glass and (c) carbon fabric samples.

Jute fabric showed an endothermic reaction at the first cycle of heating at about 80°C, but when the second cycle was examined, it was in sight that jute fabrics did not demonstrate any endothermic or exothermic reactions. The endothermic reaction that

was seen in the first cycle was related to the impurities and the moisture located in the jute fabric. By heating the samples, these impurities and moisture were revolted from the fabric and this has revealed itself as the removal of endothermic reaction that occurred at 80°C.

5.2 Composite Structures Analysis Results

5.2.1 Fiber volume ratio and void fraction

Thicknesses, fiber weight and fiber volume ratios of composite laminates are given in Table 5.2. Due to high hydrophilic property of jute fiber, jute-reinforced composite contains high amount of polyester resin (81 wt.%, 84 vol.%). As a result of this fact, jute-reinforced composite has lower fiber weight and volume ratio than the others.

Table 5.2 : Thicknesses, fiber weight and fiber volume ratios of composite laminates.

Sample	Thickness (mm)	Jute Fabric		E-glass Fabric		Carbon Fabric		Total Fabric	
		Fiber Weight Ratio (%)	Fiber Volume Ratio (%)	Fiber Weight Ratio (%)	Fiber Volume Ratio (%)	Fiber Weight Ratio (%)	Fiber Volume Ratio (%)	Fiber Weight Ratio (%)	Fiber Volume Ratio (%)
JJJJ	3.0	19.0	16.0	-	-	-	-	19.0	16.0
GGGG	0.7	-	-	61.0	44.0	-	-	61.0	44.0
CCCC	1.5	-	-	-	-	62.0	52.0	62.0	52.0
JGGJ	1.5	23.0	22.5	23.0	12.5	-	-	46.0	35.0
GJJG	1.5	23.0	22.5	23.0	12.5	-	-	46.0	35.0
JGJG	1.5	21.5	21.0	21.5	12.0	-	-	43.0	33.0
JCCJ	2.0	22.5	21.0	-	-	22.5	17.0	45.0	38.0
CJJC	2.0	23.0	22.0	-	-	23.0	17.0	46.0	39.0
JCJC	2.0	21.5	20.0	-	-	21.6	16.0	43.0	36.0
GCCG	0.85	-	-	29.5	18.0	29.5	26.5	59.0	44.5
CGGC	0.85	-	-	30.5	19.0	30.5	27.6	61.0	46.6
GCGC	0.85	-	-	29.5	18	29.5	26.5	59.0	44.5

Pure E-glass and pure carbon fabric reinforced composite materials were found to contain almost same amount of fiber weight ratios (61-62 wt.%). However, E-glass fabric reinforced sample found to have lower fiber volume ratio (44 vol.%) than carbon fabric reinforced sample (52 vol.%) due to its higher density. In hybrid structures, the weight ratios of fibers vary between 43-46% in jute/E-glass and jute/carbon fabric reinforced samples, and between 59-61% in E-glass/carbon fabric reinforced samples.

Table 5.3 displays the experimental/theoretical densities and void fractions of pure and MWCNT treated one type of fabric reinforced samples. While pure E-glass and carbon fabric reinforced composite laminates have had void fractions of about 8%, pure jute fabric reinforced sample had a void fraction of 2.4%. Sreekala et al. mentioned in their study that void content increased with the increment of fiber content (Sreekala et al., 2002). When the fiber weight and volume ratios of our samples were taken into consideration, it could be said that those void fraction amounts were reasonable since the fiber weight and volume ratios of jute-reinforced composites were far less than those of others. Besides, owing to the hydrophilic property of jute fiber, jute fabric absorbed more resin than the other fabrics and thus resulted in less amount of void content.

Table 5.3 : Experimental densities, theoretical densities and void fractions of one type of fabric reinforced samples.

	Experimental density (g/cm^3)	Theoretical density (g/cm^3)	Void fraction (%)
JJJJ	1.22	1.25	2.4
JJJJ-MWCNT	1.24	1.25	0.8
JJJJ-MWCNT-OH	1.23	1.25	1.6
JJJJ-MWCNT-COOH	1.22	1.25	2.6
GGGG	1.64	1.78	7.86
GGGG-MWCNT	1.73	1.78	2.81
GGGG-MWCNT-OH	1.66	1.78	6.74
GGGG-MWCNT-COOH	1.73	1.78	2.81
CCCC	1.39	1.51	7.94
CCCC-MWCNT	1.42	1.51	5.96
CCCC-MWCNT-OH	1.40	1.51	7.28
CCCC-MWCNT-COOH	1.37	1.51	9.25

When the effects of different types of MWCNTs on the void content of the one type of fabric reinforced samples were examined, it was seen that at all fabric types with pristine MWCNT treated samples had the lowest void content.

The experimental/theoretical densities and void fractions of pure and MWCNTs treated jute/E-glass fabric reinforced hybrid samples are given in Table 5.4. The pure samples JGGJ, GJJG and JGJG had void fractions of 8.39%, 9.09% and 9.22%, respectively. The sample JGGJ, which had E-glass fabric plies at the inner layers, had the lowest void content among them. When the different MWCNT-treated samples were examined, it was seen that the lowest amount of void contents in the samples GJJG and JGJG were in the MWCNT-COOH treated samples while in the case of JGGJ the lowest void fraction was found in the sample treated with pristine MWCNT.

Table 5.4 : Experimental densities, theoretical densities and void fractions of jute/E-glass fabric reinforced hybrid samples.

	Experimental density (g/cm3)	Theoretical density (g/cm3)	Void fraction (%)
JGGJ	1.31	1.43	8.39
JGGJ-MWCNT	1.36	1.43	4.89
JGGJ-MWCNT-OH	1.30	1.43	9.09
JGGJ-MWCNT-COOH	1.34	1.43	6.29
GJJG	1.30	1.43	9.09
GJJG-MWCNT	1.33	1.43	7.08
GJJG-MWCNT-OH	1.31	1.43	8.39
GJJG-MWCNT-COOH	1.33	1.43	6.99
JGJG	1.28	1.41	9.22
JGJG-MWCNT	1.31	1.41	7.09
JGJG-MWCNT-OH	1.28	1.41	9.22
JGJG-MWCNT-COOH	1.32	1.41	6.38

Table 5.5 demonstrates the experimental/theoretical densities and void fractions of pure and MWCNT treated jute/carbon fabric reinforced hybrid samples. The void ratios of the JCCJ, CJJC and CJCJ samples were found to be 7.41%, 8.15% and 8.89%, respectively, and it was occured that the lowest void ratio was obtained with the sample in which the jute fabric layers were located in the outer layers of the composite structure similar to the E-glass-reinforced hybrid composite samples. Besides, the

lowest void ratio in the JCCJ reinforced composite specimen was observed in the MWCNT treated specimen while in the CJJC and JCJC specimens, it was acquired in the MWCNT-COOH treated sample. It is noteworthy that the highest void ratios of pure jute and pure carbon fabric reinforced composite samples were observed in the MWCNT-COOH treated ones but the lowest void ratios were obtained in the MWCNT-COOH treated samples formed by the hybridization of these two fabrics.

Table 5.5 : Experimental densities, theoretical densities and void fractions of jute/carbon fabric reinforced hybrid samples.

	Experimental density (g/cm^3)	Theoretical density (g/cm^3)	Void fraction (%)
JCCJ	1.25	1.35	7.41
JCCJ-MWCNT	1.30	1.35	3.70
JCCJ-MWCNT-OH	1.27	1.35	5.92
JCCJ-MWCNT-COOH	1.28	1.35	5.18
CJJC	1.24	1.35	8.15
CJJC-MWCNT	1.28	1.35	5.19
CJJC-MWCNT-OH	1.26	1.35	6.67
CJJC-MWCNT-COOH	1.31	1.35	2.96
JCJC	1.23	1.35	8.89
JCJC-MWCNT	1.28	1.35	5.19
JCJC-MWCNT-OH	1.31	1.35	2.96
JCJC-MWCNT-COOH	1.32	1.35	2.24

The experimental/theoretical densities and void fractions of pure and MWCNTs treated E-glass/carbon fabric reinforced hybrid samples are shown in Table 5.6. GCCG, CGGC and GCGC samples had void fractions of 6.63%, 6.02% and 7.83%, respectively. The addition of three different types of MWCNTs to the E-glass/carbon reinforced samples decreased the void contents of all samples compared to the pure ones. Moreover, MWCNT, which is the most effective additive in reducing the void ratio of pure E-glass and pure carbon reinforced composite materials, has been found to be highly effective in reducing the void ratio of E-glass/carbon fabric reinforced hybrid composites.

Table 5.6 : Experimental densities, theoretical densities and void fractions of E-glass/carbon fabric reinforced hybrid samples.

	Experimental density (g/cm^3)	Theoretical density (g/cm^3)	Void fraction (%)
GCCG	1.55	1.66	6.63
GCCG-MWCNT	1.59	1.66	4.22
GCCG-MWCNT-OH	1.58	1.66	4.82
GCCG-MWCNT-COOH	1.56	1.66	6.02
CGGC	1.56	1.66	6.02
CGGC-MWCNT	1.61	1.66	3.01
CGGC-MWCNT-OH	1.57	1.66	5.42
CGGC-MWCNT-COOH	1.59	1.66	4.22
GCGC	1.53	1.66	7.83
GCGC-MWCNT	1.58	1.66	4.82
GCGC-MWCNT-OH	1.55	1.66	6.63
GCGC-MWCNT-COOH	1.57	1.66	5.42

5.2.2 Thermal analysis results

5.2.2.1 Dynamic mechanical analysis results

Storage modulus results

Storage modulus demonstrates the elastic behaviour of a material and is proportional to the energy stored in one cycle (Tejyan, Patnaik, & Singh, 2013). Figure 5.8 shows the variation of storage moduli of one type of fabric reinforced composite samples (warp and weft directions) as a function of the temperature. It can be seen that the storage moduli of samples decreased with increase in temperature due to the transition from glassy region to the rubbery region. Materials are extremely immobile, highly packed and have strong intermolecular forces in glassy region, whereas they become mobile and loosely packed which results in decrease in storage modulus (Jabbar et al., 2017).

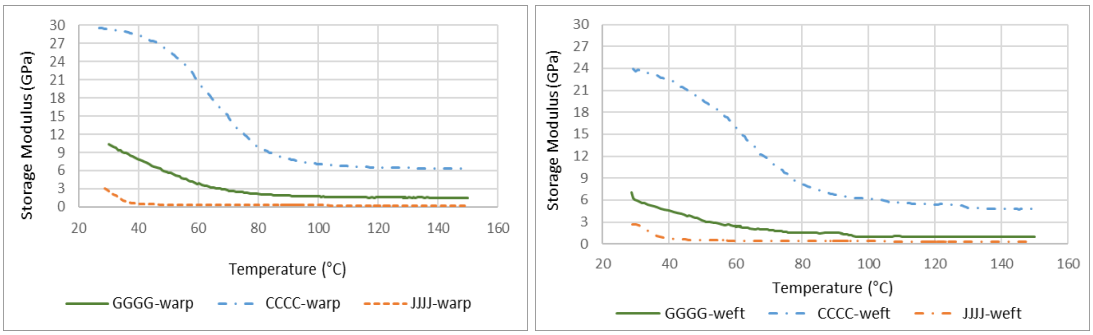

Figure 5.8 : The variation of storage moduli of one type of fabric reinforced samples.

When the storage moduli difference of warp direction samples at starting temperature (25°C) were examined, it was seen that while carbon fabric reinforced sample had a storage modulus of 30 GPa, E-glass and jute fabric reinforced samples had storage moduli of about 10 GPa and 3 GPa, respectively. Moreover, the storage moduli of carbon (6 GPa) and E-glass (2.2 GPa) reinforced samples became stable at about 80°C, whereas jute (0.4 GPa) reinforced sample became stable at about 40°C. At weft direction, again carbon fabric reinforced sample has reached the highest storage modulus value (24 GPa at 25°C). It was observed that storage moduli of carbon, E-glass and jute fabric reinforced samples became stable at about 6GPa, 1 GPa and 0.2 GPa with ascending temperature, respectively. Lastly, the storage moduli of samples that were taken from warp direction were higher than those of weft direction.

Figure 5.9 denotes the storage modulus curves of jute/E-glass fabric reinforced hybrid samples taken from both warp and weft directions. At both directions, the samples which have E-glass fabrics at the outer layers (GJJG) had higher storage modulus values (8.5 GPa – 7 GPa) than the other samples at the starting temperature. However, the storage modulus of GJJG-warp sample decreased sharply and approached to a lower storage modulus value than JGJG-warp sample after 60°C. Moreover, JGGJ samples (2.5 GPa – 2.1 GPa) had lowest storage modulus values throughout the testing.

Taking into consideration that four plied jute reinforced composite had storage modulus values of about 3 GPa around 27°C, it was surprising that storage modulus values of JGGJ-warp and JGGJ-weft samples were 2.5 GPa and 2.1 GPa, respectively.

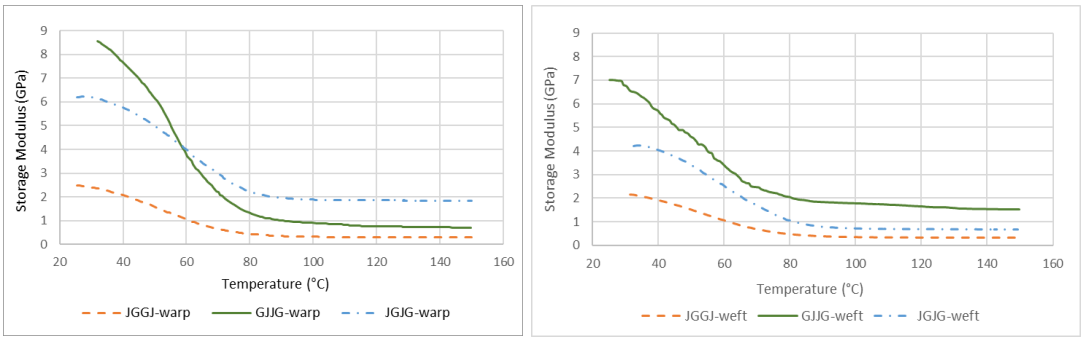

Figure 5.9 : Storage modulus curves of jute/E-glass fabric reinforced hybrid composite samples.

Storage modulus curves of jute/carbon fabric reinforced hybrid composites samples from warp and weft directions are given in Figure 5.10. Warp direction samples showed higher storage modulus than weft direction samples. Besides, samples which have carbon fabric plies at the outer layers of the structure (CJJC) attained higher modulus values than the other samples. Although there was great difference between the storage moduli of the samples at the initial temperature, it has approached to the same level around 100°C.

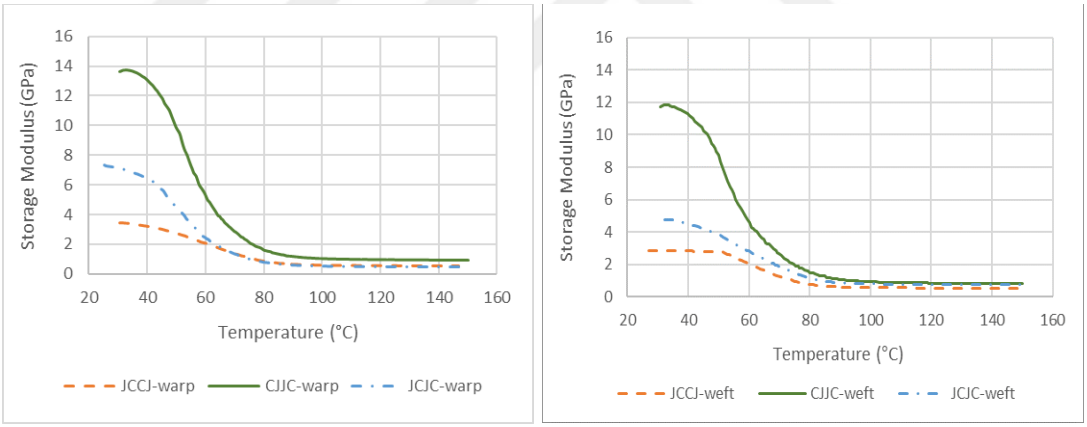

Figure 5.10 : Storage modulus curves of jute/carbon fabric reinforced hybrid composite samples.

The storage modulus curves of E-glass and carbon fabric reinforced hybrid composite samples are given in Figure 5.11. The CGGC and GCGC samples from warp and weft directions showed similar storage modulus values at the starting temperature, while GCCG samples had the lowest storage modulus. Warp direction samples had higher modulus values than the weft direction samples into the bargain,.

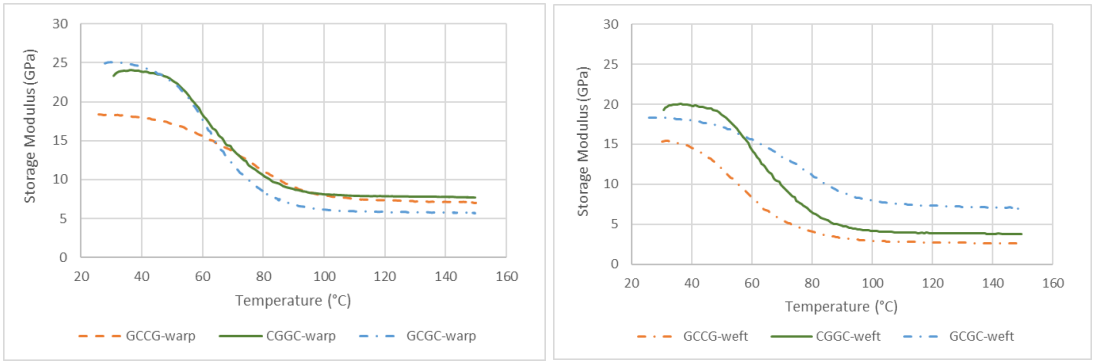

Figure 5.11 : Storage modulus curves of E-glass/carbon fabric reinforced hybrid composite samples.

The storage modulus variations of samples were examined after the addition of three different types of MWCNTs to the composite structures. Table 5.7 presents the storage modulus values of polyester resin and one type of fabric reinforced samples at 25°C and 100°C. As it can be seen from the results of the previous examples, the storage modulus started to decrease at about 60-70°C and stabilized at about 100°C. Therefore, the tables (Table 5.7 – 5.10) comparing the storage moduli of the composite specimens are given as the storage module values of 25°C and 100°C representing the test start and end moduli of those samples.

Table 5.7 : Storage modulus values of polyester and one type of fabric reinforced composites at 25°C and 100°C.

	Storage Modulus at 25°C (GPa)		Storage Modulus at 100°C (GPa)	
	Warp	Weft	Warp	Weft
Polyester	2.8	2.8	-	-
JJJJ	3.0	2.7	0.23	0.20
JJJJ-MWCNT	3.3	3.0	0.24	0.18
JJJJ-MWCNT-OH	3.1	2.9	0.22	0.18
JJJJ-MWCNT-COOH	2.4	2.6	0.16	0.22
GGGG	10.1	7.1	1.99	1.48
GGGG-MWCNT	13.2	11.9	4.01	3.57
GGGG-MWCNT-OH	13.0	11.0	4.20	3.72
GGGG-MWCNT-COOH	15.3	13.8	6.00	5.32
CCCC	28.1	24.2	5.46	4.71
CCCC-MWCNT	27.2	20.0	4.65	3.32
CCCC-MWCNT-OH	25.4	21.1	4.22	3.76
CCCC-MWCNT-COOH	22.1	20.9	3.95	3.84

When the storage modulus values of jute fabric reinforced samples were analyzed, it was observed that those samples had slightly higher storage modulus values than the polyester resin except JJJJ-MWCNT-COOH sample. It was understood that the nano-filled composites (except MWCNT-COOH reinforced sample) reached higher storage

modulus than the jute fabric reinforced composite without nano-filler, while the highest value at the initial temperature was obtained with the pristine MWCNT added sample. Furthermore, it was seen that the moduli of the samples taken from the warp direction were higher than those taken from the weft direction. The highest storage modulus value at 100°C was also obtained with pristine MWCNT added sample (JJJJ-MWCNT). The reason for not having the storage modulus value of polyester sample at 100°C was that the due to the softening of the sample at about 35°C, the DMA analysis could not accomplished.

In E-glass fabric reinforced specimens, storage moduli at both temperature values increased with addition of all three types of MWCNTs and also as distinct from jute fabric reinforced composites, the highest values were obtained with MWCNT-COOH added composite structures. Surprisingly, MWCNT supplements have been found to reduce the storage modulus of the carbon fabric reinforced materials. Among three nano-filled samples (CCCC-MWCNT, CCCC-MWCNT-OH and CCCC-MWCNT-COOH) the highest values were obtained with the pristine MWCNT added sample while the samples taken from the warp direction were found to reach higher modulus than the weft direction.

The storage modulus values of jute/E-glass fabric reinforced hybrid composite samples at 25°C and 100°C are given in Table 5.8. It was seen that the addition of different types of MWCNTs increased the storage moduli in all three different fabric sequences. When the storage modulus values of samples that have different fabric stacking sequences were compared, it was understood that the samples with E-glass fabrics in the outer layers had higher storage modulus while the lowest moduli were found in samples which have E-glass fabrics in the inner layers. In the samples with JGGJ and JGJG fabric alignments, the highest modulus values were obtained in pristine MWCNT added samples whereas in GJJG fabric ordered composites, the highest modulus was achieved with MWCNT-COOH added sample.Taking into consideration that the measurements were done at three-point bending configuration and the force was applied to the outer layers of the composite, this result (obtaining high modulus by placing high strength fabrics to the outer layers) was senseful.

Table 5.8 : Storage modulus values of jute/E-glass fabric reinforced hybrid composites at 25°C and 100°C.

	Storage Modulus at 25°C (GPa)		Storage Modulus at 100°C (GPa)	
	Warp	Weft	Warp	Weft
JGGJ	2.2	2.4	0.25	0.30
JGGJ-MWCNT	3.3	2.3	0.39	0.20
JGGJ-MWCNT-OH	2.4	2.8	0.27	0.31
JGGJ-MWCNT-COOH	2.5	3.3	0.28	0.38
GJJG	8.5	7.2	1.22	0.96
GJJG-MWCNT	8.7	7.6	0.94	0.75
GJJG-MWCNT-OH	10.4	8.0	1.14	0.84
GJJG-MWCNT-COOH	10.5	8.5	1.14	0.92
JGJG	6.5	4.3	0.85	0.75
JGJG-MWCNT	7.3	5.2	0.77	0.62
JGJG-MWCNT-OH	6.5	4.4	0.83	0.49
JGJG-MWCNT-COOH	6.7	5.0	0.70	0.56

Table 5.9 infers the storage modulus values of jute/carbon fabric reinforced hybrid composite samples at 25°C and 100°C. When the values in the table were examined it appeared that the addition of three types of MWCNTs increased the storage modulus of the samples (except JCCJ-MWCNT-COOH sample). It has been understood that higher storage moduli were obtained on samples where the higher modulus fabrics (carbon) were placed on the outer layers of structure like jute/E-glass reinforced hybrid specimens. Although there were huge differences between the storage moduli of the composite materials having different fabric stacking sequences at the initial temperature, it was seen that this difference was greatly reduced when the temperature reached 100°C.

Table 5.9 : Storage modulus values of jute/carbon fabric reinforced hybrid composites at 25°C and 100°C.

	Storage Modulus at 25°C (GPa)		Storage Modulus at 100°C (GPa)	
	Warp	Weft	Warp	Weft
JCCJ	3.5	2.8	0.54	0.39
JCCJ-MWCNT	4.5	3.5	0.46	0.30
JCCJ-MWCNT-OH	3.0	2.7	0.43	0.29
JCCJ-MWCNT-COOH	4.3	4.2	0.45	0.40
CJJC	14.0	13.0	1.07	0.83
CJJC-MWCNT	14.5	13.9	0.77	0.64
CJJC-MWCNT-OH	15.1	14.6	1.08	0.99
CJJC-MWCNT-COOH	19.5	18.0	1.04	0.99
JCJC	7.1	5.1	0.49	0.38
JCJC-MWCNT	7.5	5.6	0.50	0.41
JCJC-MWCNT-OH	7.8	5.9	0.45	0.42
JCJC-MWCNT-COOH	10.5	8.9	0.98	0.63

The storage modulus values of E-glass/carbon fabric reinforced hybrid composites at 25°C and 100°C are shown in Table 5.10. Unlike the previous samples, it was noteworthy that the E-glass/carbon fabric reinforced samples had very high storage modulus values at 100°C. Moduli of the samples taken from the warp direction were higher than those taken from the weft direction, while the highest modulus values were obtained in the pristine MWCNT added composite structures. When the storage moduli of samples with different fabric stacking sequences were compared, it was understood that the samples which have high modulus carbon fabrics at the outer layers reached higher storage modulus than the other samples.

Table 5.10 : Storage modulus values of E-glass/carbon fabric reinforced hybrid composites at 25˚C and 100˚C.

	Storage Modulus at 25°C (GPa)		Storage Modulus at 100°C (GPa)	
	Warp	Weft	Warp	Weft
GCCG	14.0	12.0	6.97	3.85
GCCG-MWCNT	18.0	14.0	5.76	4.00
GCCG-MWCNT-OH	16.0	12.3	5.45	2.77
GCCG-MWCNT-COOH	16.2	13.2	5.70	4.43
CGGC	23.5	20.0	6.68	5.53
CGGC-MWCNT	28.6	23.0	7.29	4.88
CGGC-MWCNT-OH	26.0	22.0	5.69	4.12
CGGC-MWCNT-COOH	25.0	23.1	6.09	5.03
GCGC	20.0	16.0	4.94	4.44
GCGC-MWCNT	24.0	18.2	5.10	4.04
GCGC-MWCNT-OH	24.0	22.9	5.23	4.48
GCGC-MWCNT-COOH	20.0	18.5	4.92	4.29

Loss modulus results

Loss modulus is related to the viscous behavior of a material and is proportional to the energy dissipated during a deformation period. The peak value of the loss modulus curve represents the glass transition temperature (Jabbar et al., 2017).

The variations of the loss modulus of one type of fabric reinforced composites (warp and weft direction samples) as a function of temperature is shown in Figure 5.12. The results showed that there is a big difference between the loss moduli of the three types of fabric reinforced composite samples. Carbon fabric reinforced samples had the highest loss modulus, followed by E-glass reinforced composites and jute fabric reinforced composites respectively. As it was mentioned before, the peak value of the loss modulus curve indicates the T_g value of the material. It was noteworthy that the curves of the E-glass reinforced composite samples did not have a peak while the other

two samples had peak points in the loss modulus curves. Moreover, samples taken from warp direction reached higher values than the weft direction samples.

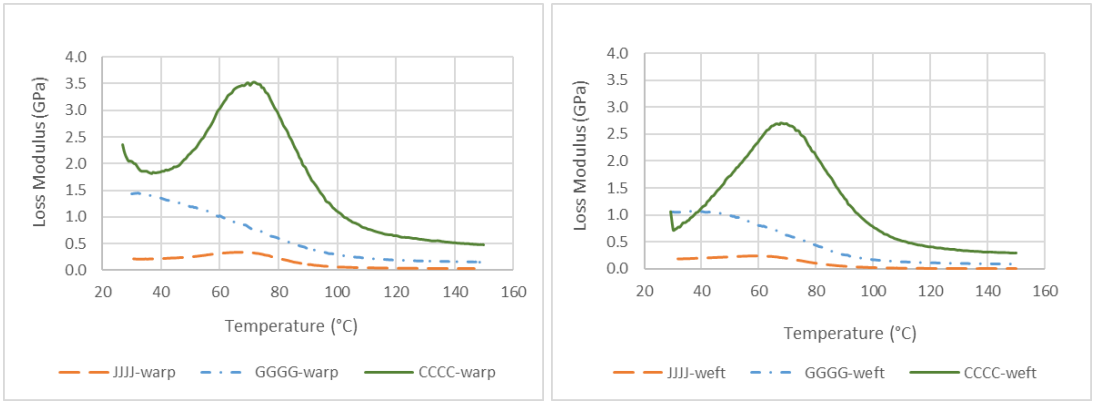

Figure 5.12 : Loss modulus curves of one type of fabric reinforced composite samples.

Since the T_g can also be obtained from the tan delta curves, the T_g values obtained from the loss modulus curves are given in the tables under the Tan delta heading for comparing both transition temperatures.

Figure 5.13 demonstrates the loss moduli of jute/E-glass fabric reinforced hybrid composites taken from warp and weft directions. It was seen that the samples with E-glass fabrics on the outer layers had higher loss modulus than the other samples. However, when approximately 100°C was reached, the differences between the modulus values of composite samples were decreased. Besides, the samples taken from the warp direction had reached the higher loss modulus values than the weft direction samples.

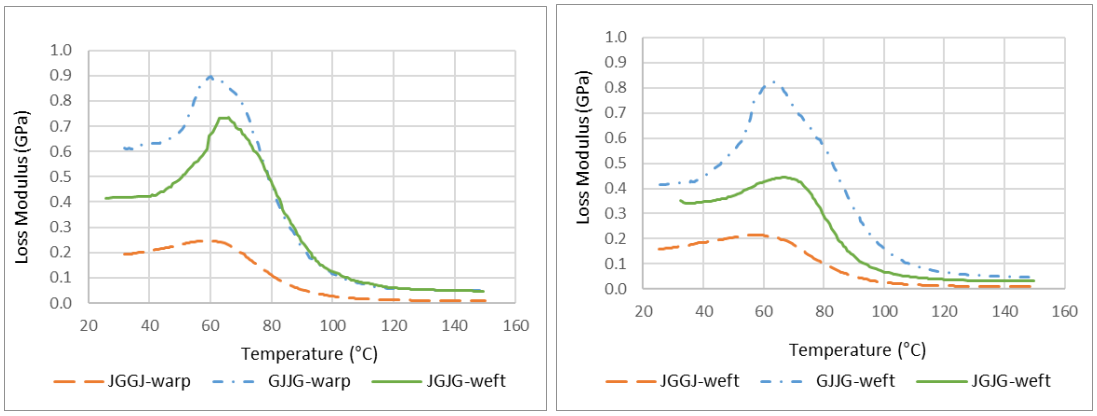

Figure 5.13 : Loss modulus curves of jute/E-glass fabric reinforced hybrid composite samples.

Loss modulus curves of jute/carbon fabric reinforced hybrid composites are given in Figure 5.14. Like other samples, again hybrid composites which have high modulus fabrics at the outer layers (CJJC) attained higher loss modulus values than the others. It was found that the decreasing loss modulus values (with increasing temperature) of the CJJC and JCJC hybrid composite materials, which have higher loss modulus values than the JCCJ sample, were higher than those of the JCCJ sample taken from the warp direction while the samples of the weft direction were found to have same level of loss modulus values at around 120°C.

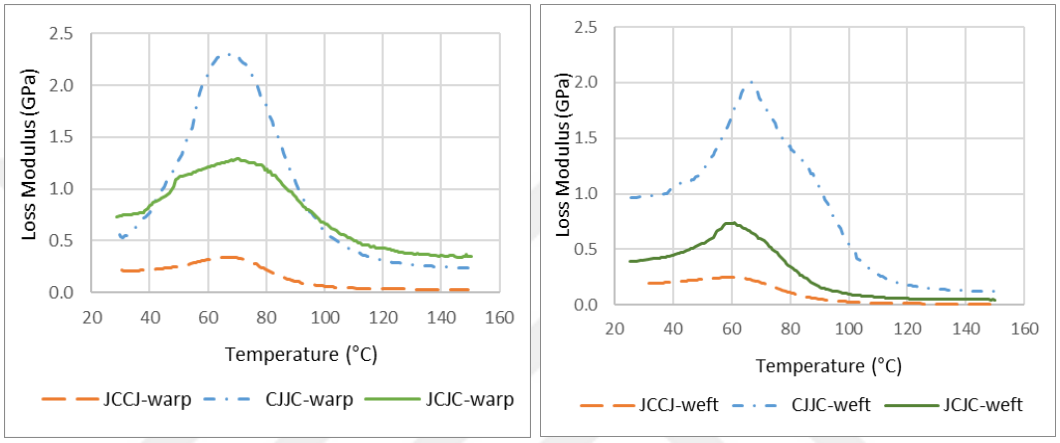

Figure 5.14 : Loss modulus curves of jute/carbon fabric reinforced hybrid composite samples.

Figure 5.15 shows the loss modulus curves of E-glass/carbon fabric reinforced hybrid composite samples. The samples with CGGC and GCGC fabric alignments obtained from the warp direction had approximately same loss modulus values (2.6 GPa), whereas the sample which has CGGC fabric alignment had the highest loss modulus value (2.2 GPa) among weft direction samples. And again, weft direction samples had lower modulus values than the warp direction samples.

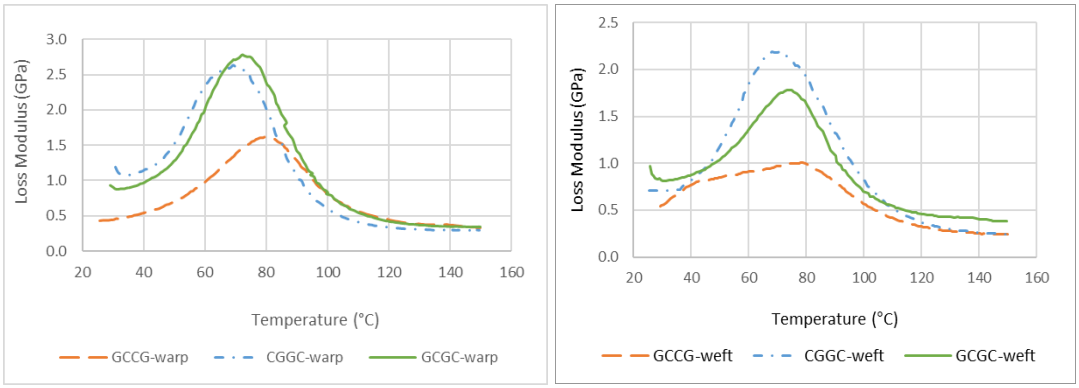

Figure 5.15 : Loss modulus curves of E-glass/carbon fabric reinforced hybrid composite samples.

The comparisons of the loss modulus values of the samples that were given above and different types of MWCNT added samples are shown in the following tables. Table 5.11 demonstrates the peak values of loss modulus curves of polyester resin and one type of fabric reinforced composites. Since the DMA measurement of polyester resin could not proceed after 35°C, it didn't have a peak point.

When the specimens reinforced with three different types of fabrics were examined, it was seen that the highest values were obtained with the carbon fabric reinforced sample while the lowest values attained with the jute fabric reinforced samples. It was also seen that the addition of different MWCNTs reduced the loss modulus values in all three types of fabric reinforced samples. The low tan delta value, which is an indicator of the high bonding strength between the matrix and the reinforcement material, is the ratio of loss modulus to the storage modulus of the material. The obtained nano-filled composite materials had lower loss modulus values than the non-treated samples, which is a sign of reduced tan delta value. This demonstrated that those nano fillers (MWCNT, MWCNT-OH and MWCNT-COOH) positively affected the bond strength between matrix and the reinforcement material.

Table 5.11 : Peak values of loss modulus curves of polyester and one type of fabric reinforced composite samples.

	Loss Modulus Peak (GPa)	
	Warp	Weft
Polyester Resin	-	-
JJJJ	0.34	0.24
JJJJ-MWCNT	0.31	0.30
JJJJ-MWCNT-OH	0.30	0.21
JJJJ-MWCNT-COOH	0.26	0.23
GGGG	1.40	1.10
GGGG-MWCNT	1.00	0.80
GGGG-MWCNT-OH	1.00	0.65
GGGG-MWCNT-COOH	1.20	0.85
CCCC	3.10	2.60
CCCC-MWCNT	2.70	2.20
CCCC-MWCNT-OH	2.80	2.30
CCCC-MWCNT-COOH	2.60	2.45

Table 5.12 infers the peak values of loss modulus curves of jute/E-glass fabric reinforced hybrid composite samples. It was found that, the addition of three types of MWCNTs had decreasing effect on the loss modulus values of those hybrid composite samples. At JGGJ and GJJG samples, the lowest values were attained with the MWCNT-COOH addition while the lowest values were found in the MWCNT-OH

added JGJG samples. Besides, samples taken from warp direction had higher loss modulus values than the weft direction samples.

Table 5.12 : Peak values of loss modulus curves of jute/E-glass fabric reinforced hybrid composite samples.

	Loss Modulus Peak (GPa)	
	Warp	Weft
JGGJ	0.25	0.23
JGGJ-MWCNT	0.24	0.21
JGGJ-MWCNT-OH	0.22	0.21
JGGJ-MWCNT-COOH	0.21	0.21
GJJG	0.90	0.80
GJJG-MWCNT	0.90	0.47
GJJG-MWCNT-OH	0.85	0.60
GJJG-MWCNT-COOH	0.73	0.67
JGJG	0.75	0.45
JGJG-MWCNT	0.55	0.38
JGJG-MWCNT-OH	0.43	0.38
JGJG-MWCNT-COOH	0.51	0.41

The peak values loss modulus curves of jute/carbon fabric reinforced hybrid composite samples are demonstrated in Table 5.13. The loss modulus values of the jute/carbon fabric reinforced hybrid samples were also reduced by the addition of different types MWCNTs. The highest reduction of loss modulus was obtained by the addition of MWCNT-OH in the samples with JCCJ and JCJC fabric alignments, whereas it was attained with pristine MWCNT addition in the sample with CJJC fabric alignment.

Table 5.13 : Peak values of loss modulus curves of jute/carbon fabric reinforced hybrid composite samples.

	Loss Modulus Peak (GPa)	
	Warp	Weft
JCCJ	0.37	0.25
JCCJ-MWCNT	0.36	0.24
JCCJ-MWCNT-OH	0.27	0.18
JCCJ-MWCNT-COOH	0.32	0.31
CJJC	2.20	2.00
CJJC-MWCNT	1.80	1.50
CJJC-MWCNT-OH	2.00	1.65
CJJC-MWCNT-COOH	2.30	2.30
JCJC	1.20	0.73
JCJC-MWCNT	1.00	0.71
JCJC-MWCNT-OH	0.95	0.72
JCJC-MWCNT-COOH	1.10	0.80

Table 5.14 displays the peak values of loss modulus curves of E-glass/carbon fabric reinforced hybrid composite sampes. The addition of nanofiller materials to the samples (except CGGC-MWCNT sample) reduced the loss modulus values. As in the

previous examples, it was understood that the samples taken from the warp direction had higher loss modulus values than the samples taken from the weft direction.

Table 5.14 : Peak values of loss modulus curves of E-glass/carbon fabric reinforced hybrid composite samples.

	Loss Modulus Peak (GPa)	
	Warp	Weft
GCCG	1.60	1.00
GCCG-MWCNT	1.00	0.80
GCCG-MWCNT-OH	1.15	0.82
GCCG-MWCNT-COOH	1.18	1.05
CGGC	2.60	2.30
CGGC-MWCNT	3.00	2.40
CGGC-MWCNT-OH	2.30	2.20
CGGC-MWCNT-COOH	2.50	2.30
GCGC	2.70	1.80
GCGC-MWCNT	1.90	1.65
GCGC-MWCNT-OH	2.30	2.00
GCGC-MWCNT-COOH	1.80	1.40

Damping factor (tan delta) results

The damping factor (tan δ) gives information about correlation of the viscous and elastic components of a viscoelastic material (S. Yang et al., 2007). It is the ratio of loss modulus to storage modulus (Tejyan, Patnaik, & Singh, 2013). T_g value can also be obtained from the peak point of tan delta curves but it was stated in the literature that Tg value that obtained from loss modulus curve is more accurate than T_g value obtained from tan delta curve. In the literature, it was reported that when the matrix and reinforcement material has high bonding strength, the mobility of molecular chains decreases and this causes reduction in damping factor (Pothan, Oommen, & Thomas, 2003).

The variation of the tan delta curves of one type of fabric reinforced composites as a function of temperature are shown in Figure 5.16. When the samples taken from both directions were examined, it was found that the jute fabric reinforced composites (0.35) had the highest tan delta values, whereas the tan delta values of the E-glass and carbon fabric reinforced samples (0.28-0.29) were so close to each other. The fact that adhesion of natural fibers to matrices is insufficient compared to traditional fibers explains this situation (Gassan & Bledzki, 1997; Tripathy et al., 2000).

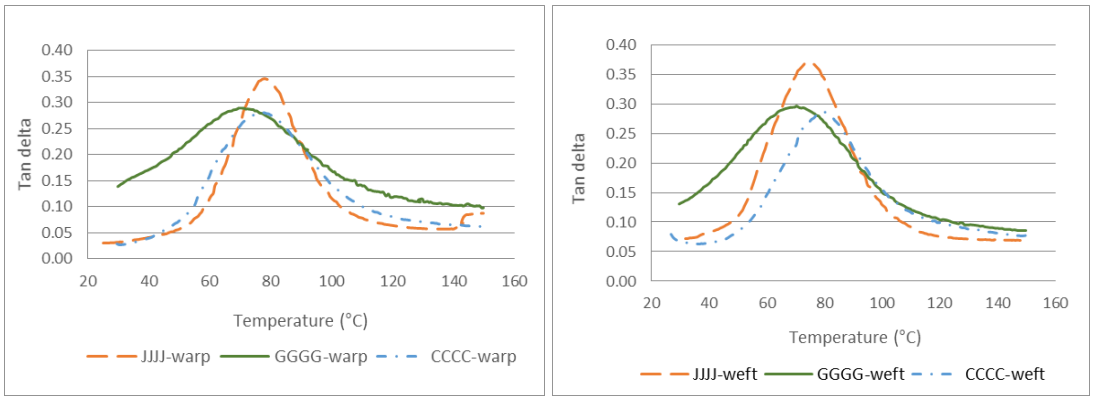

Figure 5.16 : Tan delta curves of one type of fabric reinforced composites.

Figure 5.17 demonstrates the tan delta curves of jute/E-glass fabric reinforced hybrid composite samples. Among those composite samples, the samples with the fabric stacking sequence of E-glass/jute/jute/E-glass (GJJG) had the lowest tan delta value, so, the highest matrix reinforcement bonding strength at both directions.

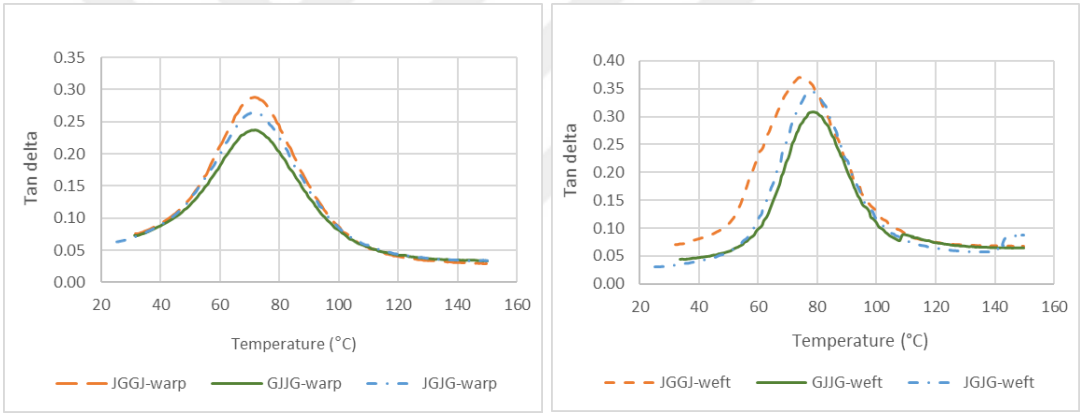

Figure 5.17 : Tan delta curves of jute/E-glass fabric reinforced hybrid composites.

The tan delta curves of jute/carbon fabric reinforced hybrid composite samples are given in Figure 5.18. As in the previous examples, the best result (low tan delta – high bonding strength) was obtained in hybrid composite specimens in which the high modulus carbon fabrics were placed on the outer layers (CJJC). Besides, the highest tan delta value was obtained with the sample having JCCJ fabric alignment.

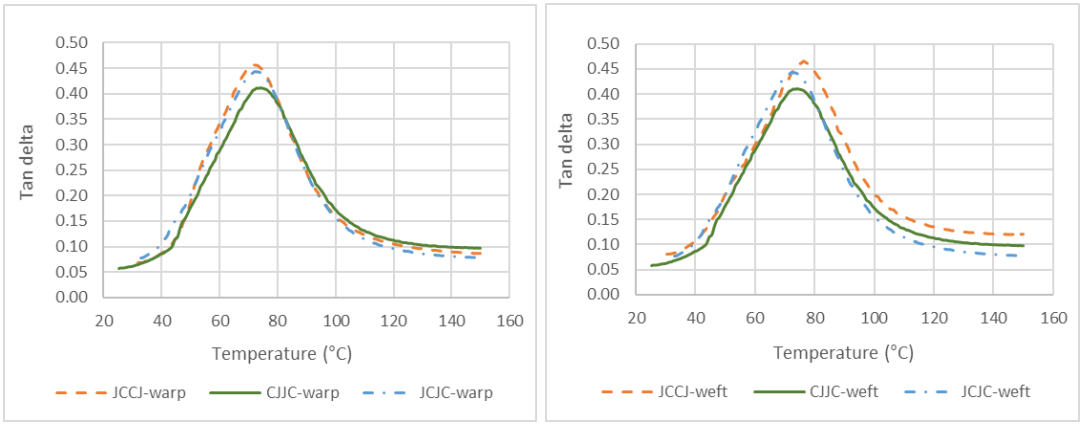

Figure 5.18 : Tan delta curves of jute/carbon fabric reinforced hybrid composites.

Figure 5.19 displays the tan delta curves of E-glass/carbon fabric reinforced hybrid composites. It has been found that the differences between the tan delta values of the E-glass/carbon fabric reinforced composite samples were larger than the those of previous samples. The lowest tan delta values were obtained with the configuration in which the high modulus carbon fabrics were placed in the outer layers.

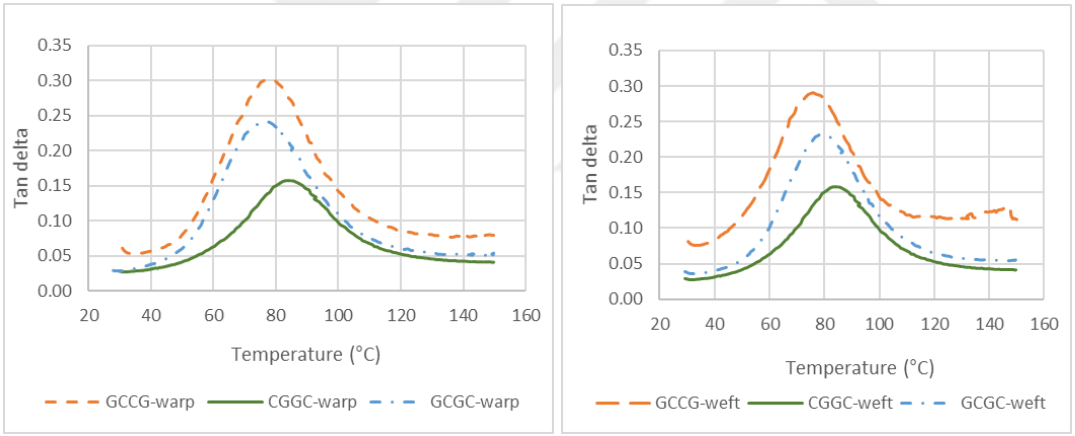

Figure 5.19 : Tan delta curves of E-glass/carbon fabric reinforced hybrid composites.

The peak values tan delta curves of non-treated and nano-filler added one type of fabric reinforced samples are given in Table 5.15. The tan delta value of unreinforced polyester resin plate could not be obtained because DMA measurements could not be performed to this plate above 35°C. When the values in the table were examined, it was seen that the addition of three types of MWCNTs in the samples reduced the tan delta values of the material, except carbon fabric reinforced samples. In the carbon fabric reinforced samples, addition of nanofiller materials (MWCNT, MWCNT-OH and MWCNT-COOH) had a decreasing effect on the tan delta value. Among the three

types of MWCNTs, pristine MWCNT was the one that greatly reduced the tan delta values.

The T_g values of these materials obtained from the loss modulus curves and tan delta curves are also given in the Table 5.15. Since the DMA measurements were carried out in two directions (warp and weft directions), the T_g values were given in the table as well, even though the glass transition temperature of the materials is not influenced by the orientation of the reinforcement material. The T_g values of the jute fabric reinforced samples obtained from the loss modulus curves were around 65-70°C, while the ones that obtained from the delta curves were between 76-80°C. The T_g values of E-glass fabric reinforced samples could not be obtained from loss modulus curves since the loss modulus curves do not make peak points. The values obtained from tan delta curves varied between 69-74°C. Finally, for carbon-reinforced samples, the T_g values obtained from the loss modulus curves range from 68 to 72°C, while the T_g values from tan delta curves range from 76 to 82°C. It appeared that the added MWCNTs did not significantly change the T_g value of the materials.

Table 5.15 : Peak values of tan delta curves, T_g values from loss modulus and tan delta curves of one type of fabric reinforced composites.

	Peak Value of Tan delta Curve (GPa)		T_g from Loss Modulus Curve		T_g from Tan delta Curve	
	Warp	Weft	Warp	Weft	Warp	Weft
Polyester Resin	-	-	-	-	-	-
JJJJ	0.34	0.37	69.9	65.2	78.7	76.3
JJJJ-MWCNT	0.30	0.34	72.3	68.9	79.9	77.7
JJJJ-MWCNT-OH	0.32	0.35	71.8	69.2	78.1	77.9
JJJJ-MWCNT-COOH	0.31	0.34	70.7	68.7	79.0	76.8
GGGG	0.29	0.30	-	-	68.9	70.3
GGGG-MWCNT	0.23	0.25	-	-	74.1	73.6
GGGG-MWCNT-OH	0.25	0.27	-	-	72.7	72.9
GGGG-MWCNT-COOH	0.26	0.27			72.5	72.5
CCCC	0.28	0.28	72.0	70.2	77.9	82.2
CCCC-MWCNT	0.32	0.31	67.8	65.8	76.7	78.6
CCCC-MWCNT-OH	0.29	0.29	68.0	67.9	76.9	79.1
CCCC-MWCNT-COOH	0.29	0.28	67.7	65.4	75.5	78.4

Table 5.16 shows the peak values of tan delta curves and T_g values of jute/E-glass fabric reinforced hybrid samples from los modulus and tan delta curves. All MWCNT types added to composite materials decreased the tan delta values while pristine MWCNT was the most effective one. Tan delta values of the composite samples taken from the weft direction were higher than those taken from the warp direction. T_g values

obtained from tan delta curves were found to be higher than T_g values obtained from loss modulus curves. The T_g values of the samples with JGGJ fabric alignments ranged between 60-63°C (loss modulus) and 70-77°C (tan delta), while the samples with GJJG fabric stacking sequences had T^g values of 62-64°C (loss modulus) and 74-80°C (tan delta) and those with JGJG alignment had T_g values of 66-69°C (loss modulus) and 73-80°C (tan delta). The obtained results showed that changing the fabric stacking sequence and adding different MWCNTs to the composite structure did not have an significant effect on the T_g value of the composite material.

Table 5.16 : Peak values of tan delta curves, T_g values from loss modulus and tan delta curves of jute/E-glass fabric reinforced hybrid composites.

	Peak value of Tan delta Curve (GPa)		T_g from Loss Modulus Curve		T_g from Tan delta Curve	
	Warp	Weft	Warp	Weft	Warp	Weft
JGGJ	0.29	0.37	60.9	60.7	72.4	75.7
JGGJ-MWCNT	0.26	0.34	62.6	63.0	74.4	76.8
JGGJ-MWCNT-OH	0.28	0.36	61.2	62.6	73.9	77.1
JGGJ-MWCNT-COOH	0.27	0.36	62.1	62.4	73.7	76.9
GJJG	0.23	0.31	61.6	62.9	73.3	80.1
GJJG-MWCNT	0.19	0.27	63.1	64.2	74.7	80.2
GJJG-MWCNT-OH	0.21	0.28	62.7	64.1	75.9	79.5
GJJG-MWCNT-COOH	0.21	0.27	62.0	63.7	76.7	79.7
JGJG	0.26	0.34	66.6	68.8	73.0	79.8
JGJG-MWCNT	0.22	0.29	68.1	68.9	75.6	79.8
JGJG-MWCNT-OH	0.24	0.29	67.9	69.2	75.4	80.0
JGJG-MWCNT-COOH	0.23	0.31	68.0	69.1	74.9	79.9

The peak values of tan delta curves and T_g values of jute/carbon fabric reinforced samples from loss modulus and tan delta curves are given in Table 5.17. The higher tan delta values of the jute/carbon fabric reinforced hybrid samples compared to the previous samples indicated that those samples hold the matrix and reinforcing materials together with a weaker bond than the other samples. It has been understood that the Tg values obtained from tan delta curves were higher than those obtained from the loss modulus curves and the positions of the fabric layers within the material did not have effect on the T_g value of the composite samples. Moreover, addition of various MWCNT types did not have a significant effect on the T_g values of the samples.

Table 5.17 : Peak values of tan delta curves, Tg values from loss modulus and tan delta curves of jute/carbon fabric reinforced hybrid composites.

	Peak value of Tan delta Curve (GPa)		Tg from Loss Modulus Curve		Tg from Tan delta Curve	
	Warp	Weft	Warp	Weft	Warp	Weft
JCCJ	0.45	0.46	69.8	61.4	72.7	77.0
JCCJ-MWCNT	0.41	0.41	70.8	62.6	74.8	77.8
JCCJ-MWCNT-OH	0.42	0.43	70.6	62.7	74.9	76.8
JCCJ-MWCNT-COOH	0.42	0.42	71.4	63.1	73.8	77.0
CJJC	0.41	0.44	69.3	66.3	72.9	75.0
CJJC-MWCNT	0.37	0.40	70.7	67.8	74.5	75.9
CJJC-MWCNT-OH	0.38	0.38	69.8	68.4	73.9	77.4
CJJC-MWCNT-COOH	0.37	0.38	70.6	67.4	74.1	76.7
JCJC	0.44	0.42	72.0	61.6	74.3	77.4
JCJC-MWCNT	0.40	0.39	71.7	62.8	76.4	78.0
JCJC-MWCNT-OH	0.42	0.41	72.6	61.9	76.1	77.9
JCJC-MWCNT-COOH	0.42	0.41	72.9	62.7	75.7	78.1

Table 5.18 demonstrates the peak values of tan delta curves and T_g values of E-glass/carbon fabric reinforced hybrid composite samples from loss modulus and tan delta curves. Samples which have fabric stacking sequences of carbon/E-glass/E-glass/carbon (CGGC) had the lowest tan delta value (highest bonding strength between matrix and reinforcemen materials) among all hybrid composite specimens. Besides, it was acquired that E-glass/carbon fabric reinforced samples had higher T_g values than other samples.

Table 5.18 : Peak values of tan delta curves, Tg values from loss modulus and tan delta curves of E-glass/carbon fabric reinforced hybrid composites.

	Peak value of Tan delta Curve (GPa)		Tg from Loss Modulus Curve		Tg from Tan delta Curve	
	Warp	Weft	Warp	Weft	Warp	Weft
GCCG	0.30	0.28	79.5	77.5	83.9	80.3
GCCG-MWCNT	0.24	0.24	82.3	79.8	84.0	82.3
GCCG-MWCNT-OH	0.26	0.24	83.2	80.1	83.5	83.0
GCCG-MWCNT-COOH	0.27	0.25	82.7	80.2	84.1	83.9
CGGC	0.16	0.16	67.8	70.8	84.0	84.8
CGGC-MWCNT	0.14	0.13	69.1	71.0	85.9	85.2
CGGC-MWCNT-OH	0.15	0.14	67.9	72.4	85.1	85.1
CGGC-MWCNT-COOH	1.14	0.14	68.3	72.5	84.7	84.8
GCGC	0.24	0.23	73.9	73.4	78.0	80.3
GCGC-MWCNT	0.21	0.21	75.2	76.0	80.2	81.9
GCGC-MWCNT-OH	0.22	0.21	74.3	75.3	79.6	81.3
GCGC-MWCNT-COOH	0.22	0.22	74.9	74.9	79.4	81.0

5.2.2.2 Thermogravimetric analysis results

Table 5.19 demonstrates the amounts of weight losses and onset temperatures of polyester resin and jute fabric reinforced composites. Polyester resin lost 97% of its weigth by heating from 25°C to 600°C and its degradation started at 305°C. When degradation temperatures of jute fabric reinforced composite samples were compared, it was observed that while pure jute fabric reinforced composite has an onset temperature of 300°C, pristine MWCNT, -OH functionalized MWCNT treated and –COOH functionalized MWCNT treated samples have onset temperatures of 321°C, 320°C and 316°C, respectively. The addition of MWCNTs to jute fabric reinforced composites increased the degradation temperatures at an amount of 20°C. Moreover, it was observed that the weight loss percentage of jute fabric reinforced composite decreased from 92% to 89% by addition of MWCNTs.

Table 5.19 : The percentage of weight loss and onset temperatures of polyester resin and jute fabric reinforced composites.

Sample Code	Initial Weight (mg)	Final Weight (mg)	Weight Loss (%)	Onset Temperature (°C)
Polyester	6.53	0.22	97	305
JJJJ	6.53	0.50	92	300
JJJJ-MWCNT	6.74	0.69	89	321
JJJJ-MWCNT-OH	6.65	0.7	89	320
JJJJ-MWCNT-COOH	6.26	0.69	88	316

Table 5.20 shows the percentages of weight losses and onset temperatures of polyester resin and E-glass fabric reinforced composites. The onset temperatures of neat polyester resin and pure E-glass fabric reinforced composites were approximately at same level due to the high temperature resistance of E-glass fiber. Addition of MWCNTs to E-glass fabric reinforced composites results in ascending onset temperatures. It was observed that highest onset temperature (334°C) was achieved with MWCNT-COOH added sample.

When weight loss percentages of samples were taken into consideration, it was unexpectedly occurred that addition of MWCNTs promoted the amount of weight loss of E-glass fabric reinforced composite.

Table 5.20 : The percentage of weight loss and onset temperatures of polyester resin and E-glass fabric reinforced composites.

Sample Code	Initial Weight (mg)	Final Weight (mg)	Weight Loss (%)	Onset Temperature (°C)
Polyester	6.53	0.22	97	305
GGGG	6.57	5.08	23	306
GGGG-MWCNT	6.68	4.91	26	327
GGGG-MWCNT-OH	6.91	4.68	32	327
GGGG-MWCNT-COOH	6.91	5.22	24	334

Table 5.21 displays the percentages of weight losses and onset temperatures of polyester resin and carbon fabric reinforced composites. The onset temperature of polyester resin increased from 305°C to 320°C by reinforcing with carbon fabric. Also, it was obtained from the results that again MWCNT-COOH added sample had the highest onset temperature (330°C) among carbon fabric reinforced samples.

When weight loss percentages of samples were handled, it was occurred that addition of MWCNTs promoted the amount of weight loss of carbon fabric reinforced composite, like the E-glass fabric reinforced composites.

Table 5.21 : The percentage of weight loss and onset temperatures of polyester resin and carbon fabric reinforced composites.

Sample Code	Initial Weight (mg)	Final Weight (mg)	Weight Loss (%)	Onset Temperature (°C)
Polyester	6.53	0.22	97	305
CCCC	6.27	4.27	23	320
CCCC-MWCNT	6.61	4.04	39	323
CCCC-MWCNT-OH	6.43	4.10	36	324
CCCC-MWCNT-COOH	6.40	4.06	36	330

The weight loss percentages and onset temperatures of jute/E-glass fabric reinforced hybrid composites are given in Table 5.22. The maximum onset temperatures of JGGJ, GJJG and JGJG were attained when MWCNT-COOH, MWCNT-OH and MWCNT were added to these composite structures, respectively. While MWCNT and MWCNT-OH had higher effect on degradation temperature of jute fabric reinforced sample, MWCNT-COOH had higher effect on the degradation temperature of E-glass

fabric reinforced sample. Considering these results, it could be observed that the highest value of the onset temperature of the samples which have E-glass fabrics at the inner layers was achieved with MWCNT-COOH addition, while it was obtained with integration of MWCNT or MWCNT-OH in jute fabric reinforced samples. This could be result in the fact that fabric layers that were placed to the inner layers had more effect on the onset temperature of the samples.

Table 5.22 : Weight loss and onset temperatures of jute/E-glass fabric reinforced hybrid composites.

Sample Code	Initial Weight (mg)	Final Weight (mg)	Weight Loss (%)	Onset Temperature (°C)
JGGJ	6.57	2.08	68	310
JGGJ-MWCNT	6.75	1.83	73	312
JGGJ-MWCNT-OH	6.39	1.86	71	314
JGGJ-MWCNT-COOH	7.23	2.29	68	324
GJJG	6.69	2.11	68	312
GJJG-MWCNT	6.95	2.19	68	323
GJJG-MWCNT-OH	6.60	1.44	78	324
GJJG-MWNCT-COOH	6.84	1.48	78	315
JGJG	6.79	1.17	83	303
JGJG-MWCNT	5.83	1.19	79	318
JGJG-MWCNT-OH	6.47	1.07	83	312
JGJG-MWCNT-COOH	6.74	1.84	73	314

Table 5.23 presents the percentages of weight losses and onset temperatures of jute/carbon fabric reinforced hybrid composite samples. According to the obtained onset temperature values, it was seen that JCCJ-MWCNT-OH sample had the highest onset temperature among JCCJ samples, while CJJC-MWCNT-OH had the highest onset temperature among CJJC samples. Analogously to the results of jute/E-glass fabric reinforced samples, this could be again related to the fact that fabric layers that were placed to the inner layers had more effect on the onset temperature of the samples.

Table 5.23 : Weight loss and onset temperatures of jute/carbon fabric reinforced hybrid composites.

Sample Code	Initial Weight (mg)	Final Weight (mg)	Weight Loss (%)	Onset Temperature (°C)
JCCJ	6.68	1.95	71	310
JCCJ-MWCNT	6.89	1.65	76	316
JCCJ-MWCNT-OH	6.51	1.87	71	312
JCCJ-MWCNT-COOH	6.53	1.77	73	319
CJJC	6.52	1.82	72	308
CJJC-MWCNT	6.30	1.66	74	316
CJJC-MWCNT-OH	6.40	1.63	76	321
CJJC-MWCNT-COOH	6.64	1.22	81	311
JCJC	6.87	1.92	72	306
JCJC-MWCNT	6.45	1.75	73	312
JCJC-MWCNT-OH	6.52	1.79	72	314
JCJC-MWCNT-COOH	6.61	1.57	76	314

The weight loss amount of all samples were increased by addition of MWCNTs to the composite samples. The weight loss percentages and onset temperatures of E-glass/carbon fabric reinforced hybrid composite structures are given in Table 5.24.

Table 5.24 : Weight loss and onset temperatures of E-glass/carbon fabric reinforced hybrid composites.

Sample Code	Initial Weight (mg)	Final Weight (mg)	Weight Loss (%)	Onset Temperature (°C)
GCCG	6.35	4.02	37	316
GCCG-MWCNT	6.22	4.20	32	323
GCCG-MWCNT-OH	6.61	4.02	39	320
GCCG-MWCNT-COOH	6.18	4.15	33	331
CGGC	6.65	4.66	30	314
CGGC-MWNCT	6.60	4.31	37	322
CGGC-MWCNT-OH	6.57	4.23	35	323
CGGC-MWCNT-COOH	6.00	4.57	24	325
GCGC	6.78	4.73	30	316
GCGC-MWCNT	6.54	4.40	32	322
GCGC-MWCNT-OH	6.42	4.50	30	328
GCGC-MWCNT-COOH	6.18	4.22	32	330

At each configuration of fabric arrangements, the highest onset temperature was achieved with MWCNT-COOH treated sample (GCCG - 331°C, CGGC - 325°C, GCGC - 330°C). Given the fact that the maximum onset temperatures of pure E-glass reinforced sample and pure carbon reinforced sample were obtained by addition of MWCNT-COOH to the samples, it would not be an unexpected result that highest onset temperature of E-glass/carbon fabric reinforced hybrid sample was attained with MWCNT-COOH added sample.

Figure 5.20 shows the shape of a composite sample (CGGC) before and after testing. As it is seen from the figure, due to the high temperature (600°C) polyester resin of the sample was annihilated and only carbon and E-glass fibers remained in the crucible.

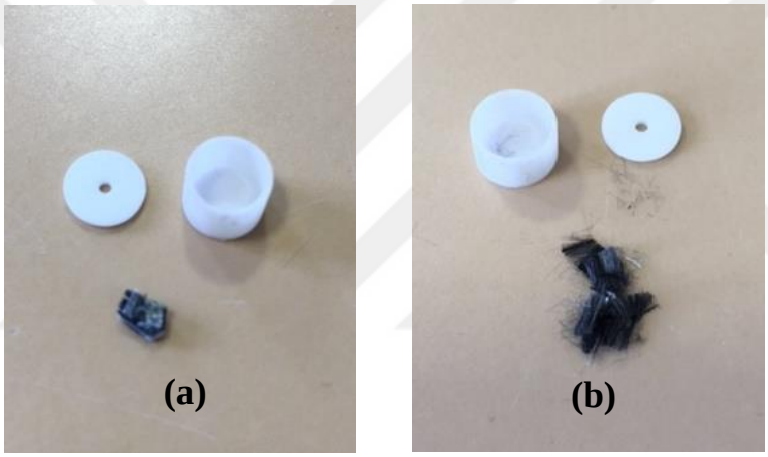

Figure 5.20 : Sample (a) before and (b) after thermogravimetric analysis.

5.2.2.3 Differential scanning calorimetry analysis results

Differential scanning calorimetry is a thermal analysis method that measures the heat flow rate as a function of time and temperature and this heat provides information regarding the physical and chemical transformations of the material. Figure 5.21 shows the DSC curves of polyester resin and one type of fabric reinforced composite samples. From DSC graph of polyester resin (Figure 5.21(a)) it was observed that an exothermic reaction started at about 260°C which infers the degradation of polyester resin. Moreover, an endothermic reaction was occured at about 390°C, which could be a sign of a change in the degradation process.

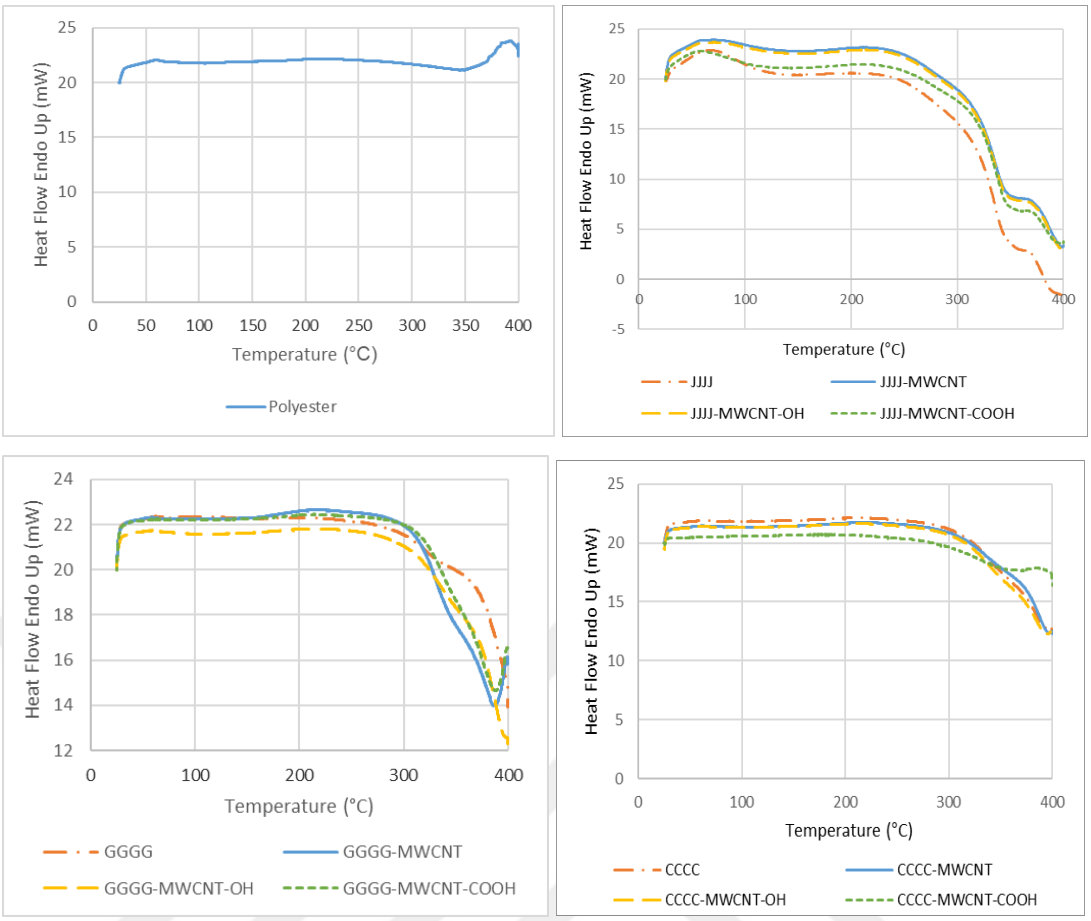

Figure 5.21 : DSC curves of polyester resin and one type of fabric reinforced composite samples.

The DSC curves of four-plied jute fabric reinforced composites (Figure 5.21(b)) show endothermic peaks centred at around 52°C. Those peaks were characterized by the removal of adsorbed moisture from the jute fabric. Jute (62.6% cellulose, 23.2% hemi-cellulose, 15.86% lignin) is majorly made up of cellulose therefore; its affinity to moisture is high since cellulose is hydrophilic in nature. At all samples an exothermic reaction started at around 260°C, which indicated the degradation of the polyester resin. Moreover, it was seen that at around 350°C, the exothermic reactions made peaks. As it was mentioned before, jute contains 62.6% cellulose and cellulose starts to degradate at around 315 °C. It was thought that these peaks infered the degradation of cellulose.

Figure 5.21(c) and 5.21(d) demonstrate the DSC graphs of E-glass and carbon fabric reinforced samples. It was seen from graphs that again the exothermic reaction started at about 260°C. As is known E-glass and carbon are so durable to heat and it could be said that exothermic reaction which started at around 260°C indicated the degradation

of only polyester resin. It has been understood that the addition of different types of MWCNTs do not have a significant effect on the phase changes of the composite materials.

Figure 5.22 demonstrates the DSC graphs of jute and E-glass fabric reinforced hybrid composite samples. In these twelve samples containing jute fabric, there were endothermic reactions at around 55°C that shows the removal of the moisture and impurities of the jute fabric. It has been seen that the degradation started at around 260°C and peaked at around 350°C similar to the four-fold jute fabric reinforced samples. As the glass fabric is very resistant to high temperatures and does not undergo any reaction up to 400 degrees, it was expected that samples with jute/E-glass fabric reinforcements show similar thermal characteristics to jute fabric reinforced samples at this temperature range.

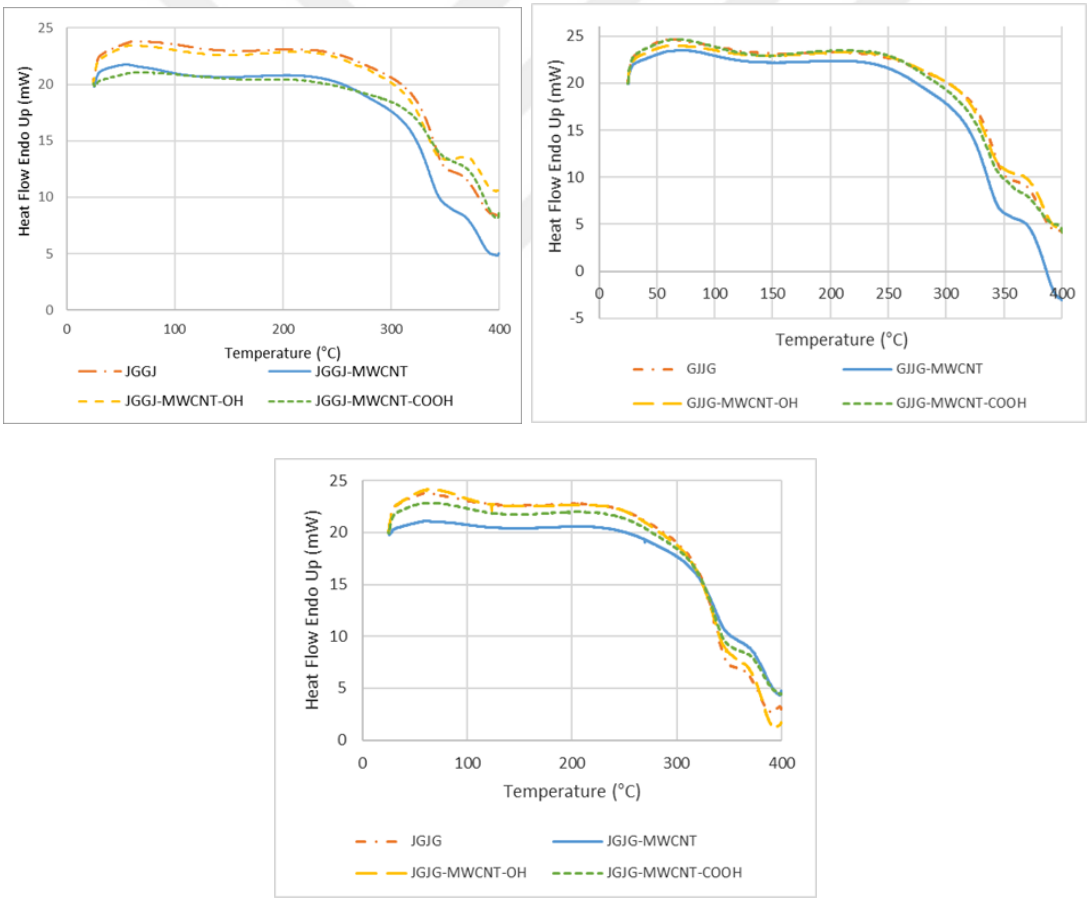

Figure 5.22 : DSC curves of jute/E-glass fabric reinforced hybrid composite samples.

Figure 5.23 screens the DSC curves of jute/carbon fabric reinforced hybrid composites. Similar to jute/E-glass reinforced hybrid composite samples, the

degradation appeared to start and peak at the same temperatures due to the high thermal stability of carbon fabric. It has also been understood that the addition of different MWCNTs does not have an effect on the degradation temperatures of the composite material.

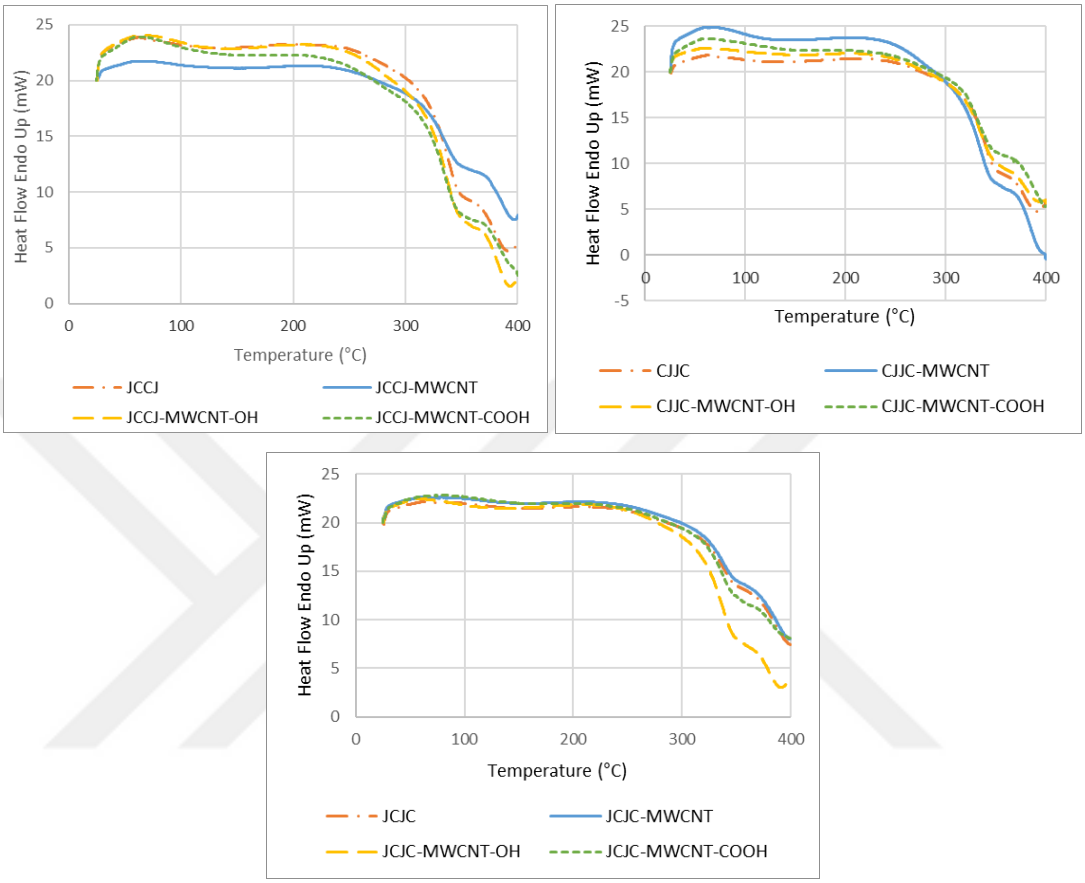

Figure 5.23 : DSC curves of jute/carbon fabric reinforced hybrid composite samples.

DSC graphs of E-glass/carbon fabric reinforced samples with different stacking sequences (GCCG, GCGC, CGGC) are given in Figure 5.24. As distinct from previous samples, E-glass/carbon fabric reinforced samples showed lower heat flows owing to their high durability to heat. It was occurred that at all samples demonstrated exothermic reactions which started at about 270 °C (degradation of polyester resin). Besides, it was seen that an endothermic reaction starts at about 390 °C at all samples which was also seen in the DSC graph of polyester resin (Figure 5.21(a)).

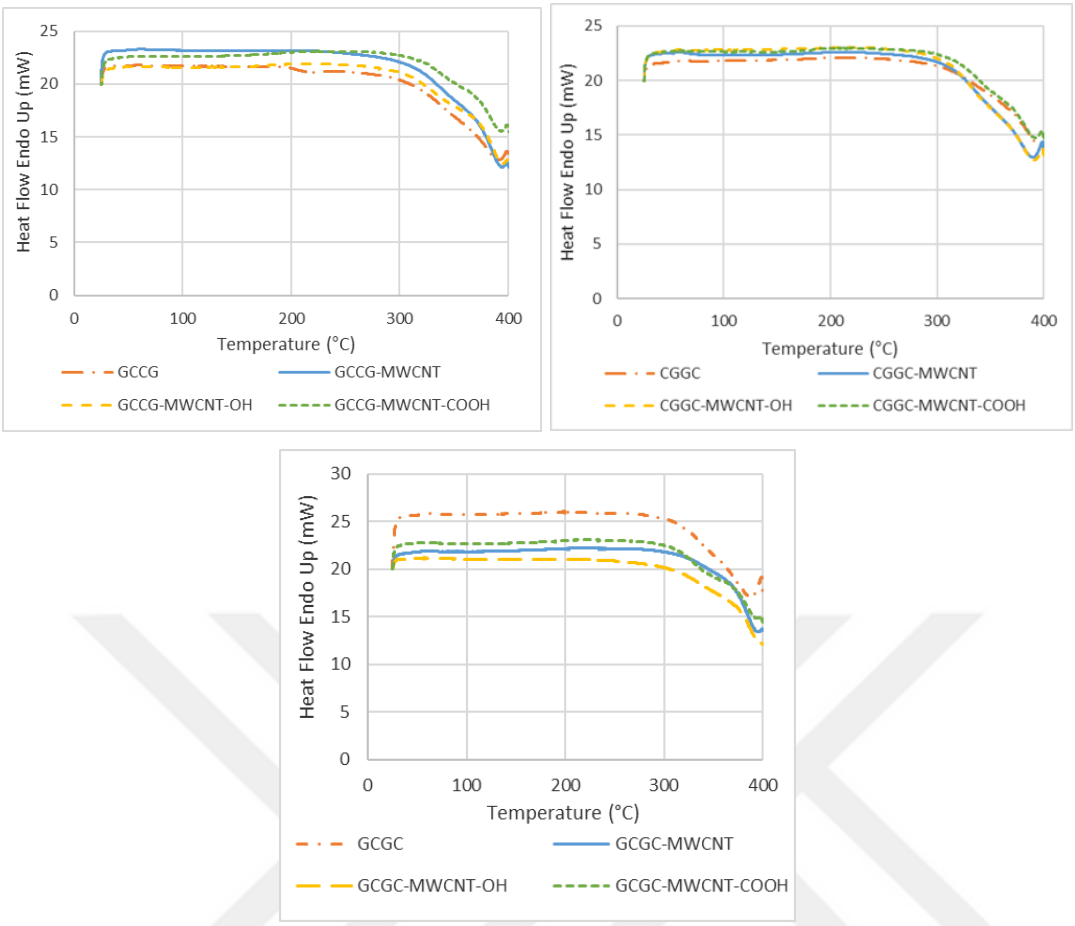

Figure 5.24 : DSC curves of E-glass/carbon fabric reinforced hybrid composite samples.

It was clearly understood that changing the fabric stacking sequences of the structures and addition of MWCNTs to the composite samples has almost no effect on the phase changes of the samples. Moreover, owing to the high thermal resistance of E-glass and carbon fabrics, the phase changes in the composite specimen obtained from these materials have been found to depend on the characteristics of the polyester resin and jute fabric reinforcement.

5.2.3 Mechanical analysis results

5.2.3.1 Tensile strength results

The tensile strength values of non-treated composite samples are given in Figure 5.25. When one-type fabric-reinforced samples were compared, it was seen that jute fabric-reinforced polyester composite had the lowest tensile strength (37.84–30.59 MPa) while the carbon fabric-reinforced composite had the highest (400.60–291.82 MPa) which was compatible with those fibers' tensile strength values (tensile strength of

carbon fiber is approximately 10 times higher than tensile strength of jute fiber). Moreover, tensile strength of polyester plate without reinforcement was also evaluated and it was about 21 MPa. Results showed that jute fabric reinforced composites had tensile strength values close to the tensile strength of polyester resin, while others had much higher values. When fiber weight (19%) and volume (16%) ratios of jute fabric reinforced composites were taken into consideration, this circumstance seems reasonable.

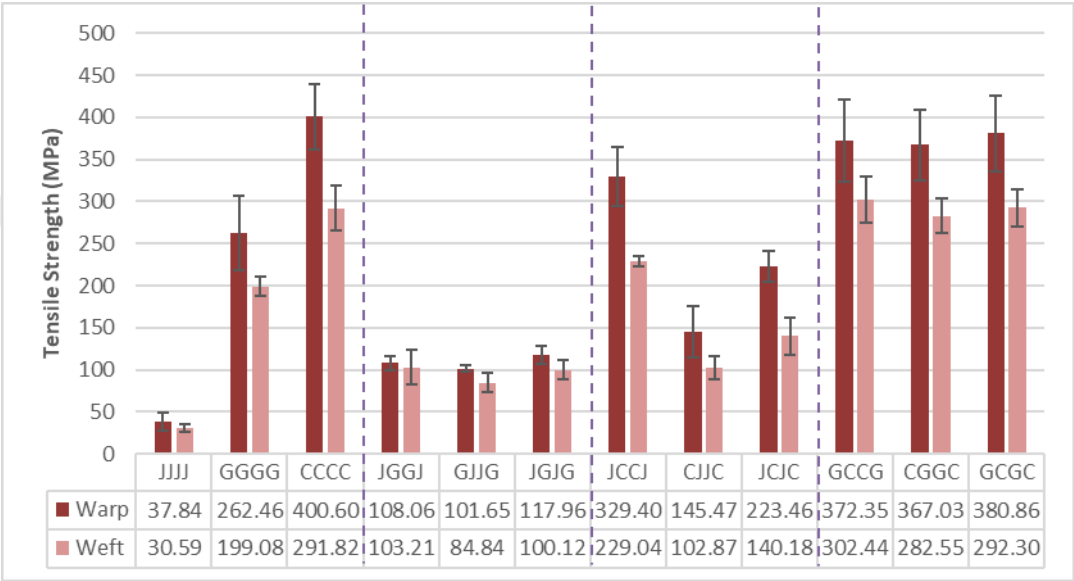

	JJJJ	GGGG	CCCC	JGGJ	GJJG	JGJG	JCCJ	CJJC	JCJC	GCCG	CGGC	GCGC
Warp	37.84	262.46	400.60	108.06	101.65	117.96	329.40	145.47	223.46	372.35	367.03	380.86
Weft	30.59	199.08	291.82	103.21	84.84	100.12	229.04	102.87	140.18	302.44	282.55	292.30

Figure 5.25 : Tensile strength results of non-treated composite samples.

When jute/E-glass hybrid samples were compared to jute reinforced composite, it was observed that tensile strength was increased from 30 MPa to 100 MPa. Besides, it was seen that there was not any significant difference between several stacking sequences of jute/E-glass hybrid composites. Unlike jute/E-glass hybrid composites, the tensile strength of jute/carbon hybrid composites differed by several stacking of fabric layers. It was occurred that while JCCJ sample, which has carbon fabrics in the inner layers, reached the highest tensile strength; CJJC sample, which has carbon fabrics in the outer layers, had the lowest tensile strength among all jute/carbon hybrid samples. This could be due to the fact that adhesion between carbon fabrics is stronger than the others and this steady bonding at the interface imparts higher tensile strength to the composite sample.

Also, it was investigated that composite samples that were taken from the warp direction had higher tensile strength values than the weft direction samples. This was

an expected result owing to the inherent characteristics of the biaxial woven fabric structures. As it was also observed, either thicker yarns or higher yarn densities were utilized at the warp directions which imparted higher tensile strength values to the reinforcements in this direction.

Figure 5.26 demonstrates the tensile strength results of one type of fabric reinforced composite samples. The tensile strength values of jute fabric reinforced composite specimens were between 30 and 60 MPa, while the tensile strength of E-glass fabric reinforced samples and carbon fabric reinforced specimens were between 200-300 MPa and 300-450 MPa, respectively. When the effects of MWCNTs on the tensile strength of samples were examined, it was seen that the highest tensile strength values were found in pristine MWCNT treated specimens in all three fabric reinforced composites. Moreover, tensile strengths were again found higher in the warp direction samples.

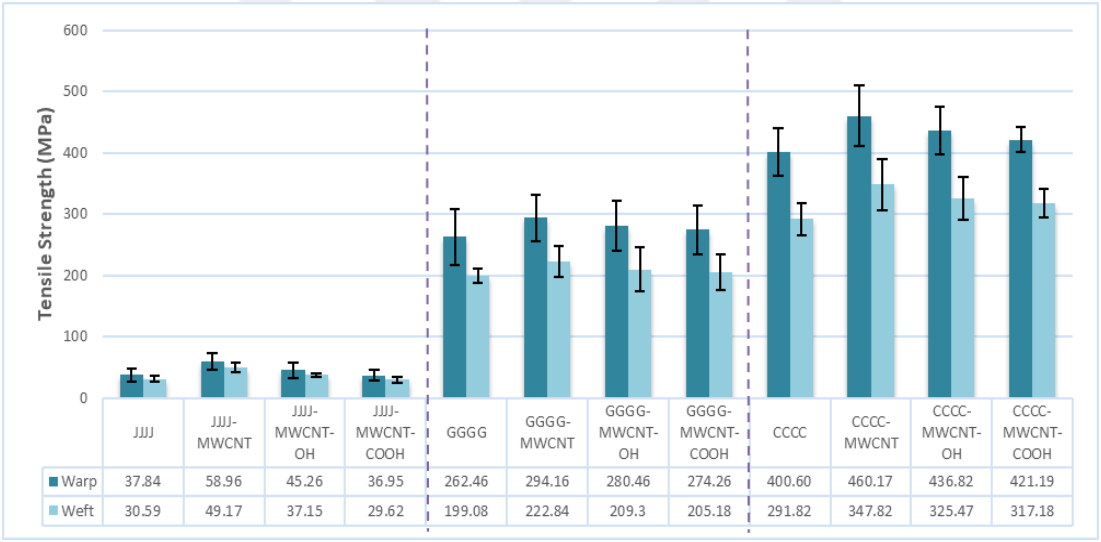

	JJJJ	JJJJ-MWCNT	JJJJ-MWCNT-OH	JJJJ-MWCNT-COOH	GGGG	GGGG-MWCNT	GGGG-MWCNT-OH	GGGG-MWCNT-COOH	CCCC	CCCC-MWCNT	CCCC-MWCNT-OH	CCCC-MWCNT-COOH
Warp	37.84	58.96	45.26	36.95	262.46	294.16	280.46	274.26	400.60	460.17	436.82	421.19
Weft	30.59	49.17	37.15	29.62	199.08	222.84	209.3	205.18	291.82	347.82	325.47	317.18

Figure 5.26 : Tensile strength results of one type of fabric reinforced composite samples.

It was investigated that when jute/E-glass and E-glass/carbon fabrics were used, there was not much difference between the tensile strength values at different levels of stacking sequences. However, it was observed that at all yarn (material) types the lowest tensile strength was occurred when the low strength fibers were put inside of the composite structure. Besides, there was a considerable difference between different levels of stacking sequences of jute/carbon fabric reinforced samples. It was noticed that when two carbon fabric plies were placed between jute fabric plies, the acquired tensile strength was about 330MPa (warp direction) and 230MPa (weft direction),

while they were about 145MPa (warp direction) and 100MPa (weft direction) when two jute fabric plies were placed between carbon fabric plies.

The tensile strength results of jute/E-glass fabric reinforced composite samples are given in Figure 5.27. In these samples with different fabric sequences, the highest values were obtained with pristine MWCNT treated samples (JGGJ-MWCNT, GJJG-MWCNT and JGJG-MWCNT) at all three fabric stacking sequences. When analyzing the same type of MWCNT treated composite samples with different fabric stacking sequences, it was observed that the highest strengths were obtained in the JGJG specimens, which have alternate fabric sequences. And again the highest tensile strengths were obtained in the samples taken from the warp direction.

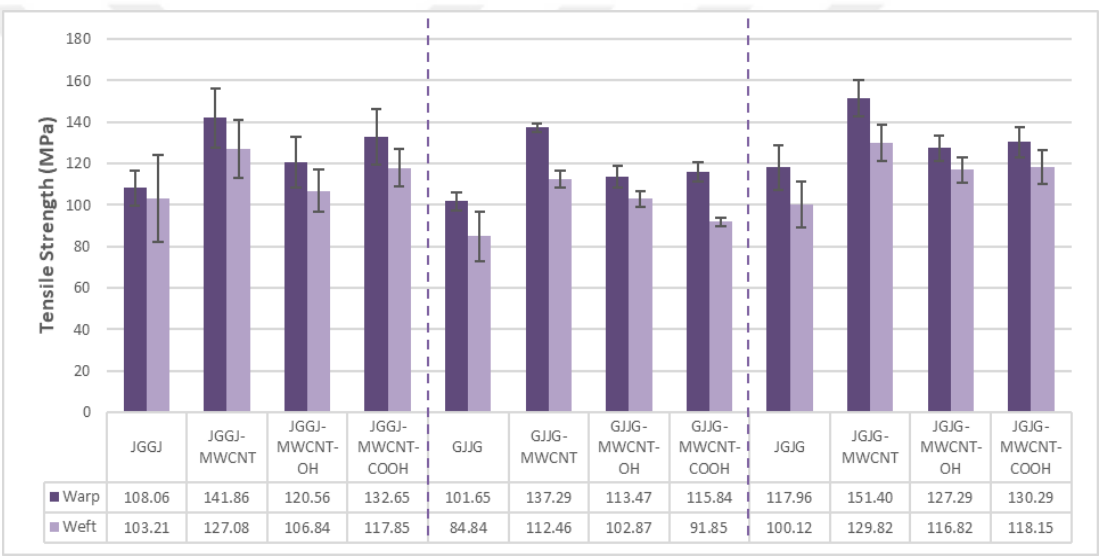

	JGGJ	JGGJ-MWCNT	JGGJ-MWCNT-OH	JGGJ-MWCNT-COOH	GJJG	GJJG-MWCNT	GJJG-MWCNT-OH	GJJG-MWCNT-COOH	JGJG	JGJG-MWCNT	JGJG-MWCNT-OH	JGJG-MWCNT-COOH
Warp	108.06	141.86	120.56	132.65	101.65	137.29	113.47	115.84	117.96	151.40	127.29	130.29
Weft	103.21	127.08	106.84	117.85	84.84	112.46	102.87	91.85	100.12	129.82	116.82	118.15

Figure 5.27 : Tensile strength results of jute/E-glass fabric reinforced composite samples.

Figure 5.28 indicates the tensile strength results of jute/carbon fabric reinforced composite samples. The MWCNT-COOH treated samples reached the maximum tensile strength values at all fabric stacking sequences. As in the pure samples, the highest tensile strength in the different types of MWCNT-treated specimens was acquired with the JCCJ specimen while the lowest strength was seen observed with the CJJC sample.

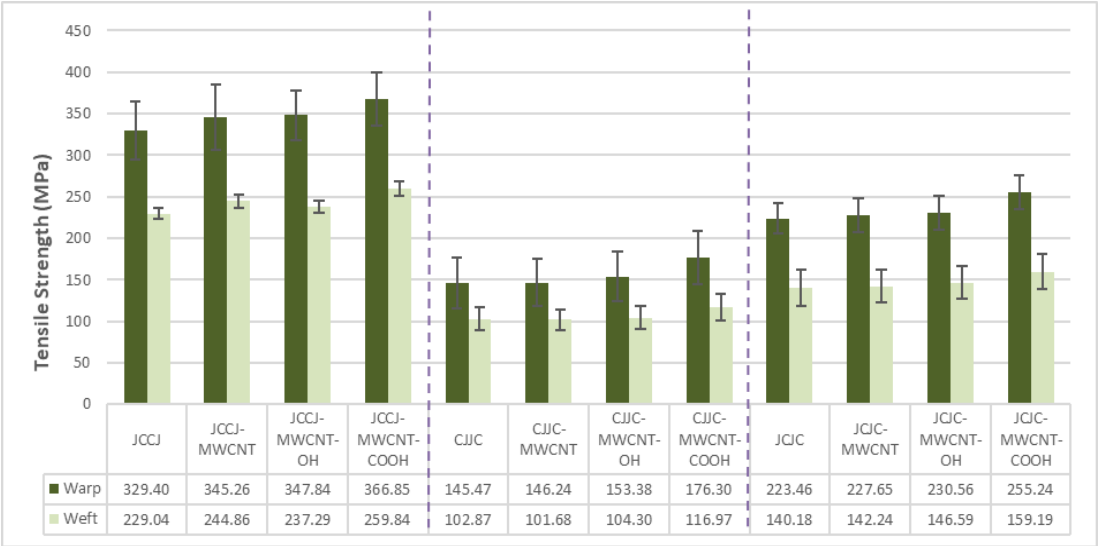

Figure 5.28 : Tensile strength results of jute/carbon fabric reinforced composite samples.

The tensile strength results of E-glass/carbon fabric reinforced samples are shown in Figure 5.29. It was noteworthy that as distinct from other hybrid samples, there was not much difference between the tensile strength results of three different fabric sequences in the E-glass/carbon hybrid samples. Besides, pristine MWCNT treated E-glass/carbon fabric reinforced hybrid samples attained higher tensile strength values than other samples.

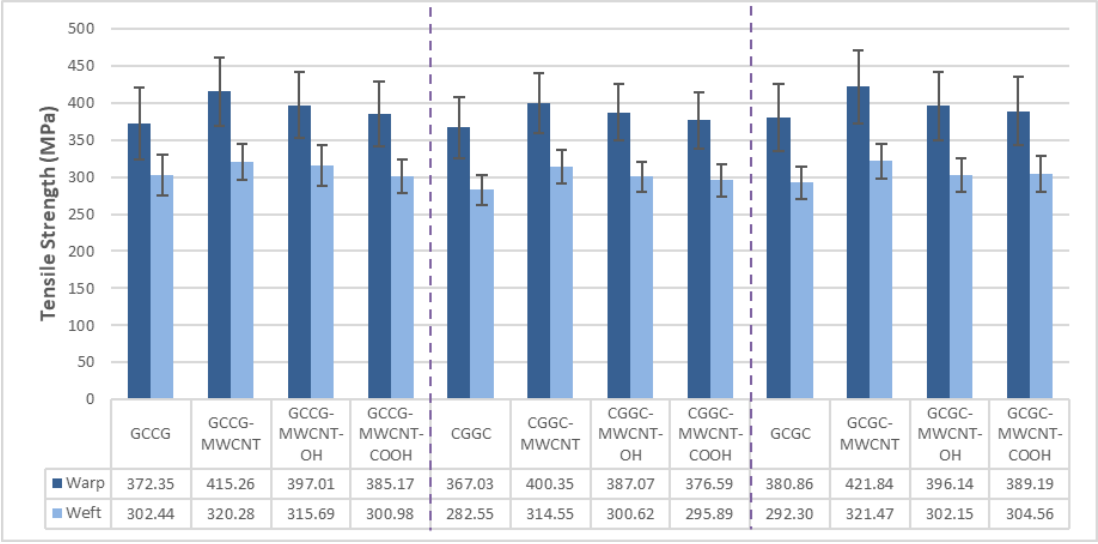

Figure 5.29 : Tensile strength results of E-glass/carbon fabric reinforced composite samples.

When a general assessment made about the tensile strength characteristics of the composite structures, it could be concluded that;

- Warp direction samples had higher tensile strength values than the weft direction samples.
- Carbon fabric reinforced samples had higher strength than other samples.
- Higher tensile strengths were achieved by incorporating higher strength fabrics to the inner layers of the structures.
- Addition of MWCNTs (MWCNT, MWCNT-OH and MWCNT-COOH) to the composite structure enhanced the tensile properties of composite materials.
- Among MWCNT types, the best results were achieved with pristine MWCNT treated composite samples.

5.2.3.2 Impact strength results

Figure 5.30 shows the impact resistances of the composite samples. It was seen that E-glass fabric reinforced composite had the highest impact resistance (262.11–190.42 kJ/m^2), while jute reinforced had the lowest (21.21-18.95 kJ/m^2). Moreover, impact strength of polyester plater without reinforcement was also measured and it was 14.83 kJ/m^2. When the effect of stacking sequence was examined, it was seen that among jute/E-glass-reinforced composites, GJJG sample (205.42 kJ/m^2 – 182.53 kJ/m^2) had the highest value while JGGJ sample had the lowest impact resistance (98.94 kJ/m^2 – 82.74 kJ/m^2). Besides, it was realized that although there was not a large difference among all jute/carbon hybrid composites' impact resistance values, CJJC sample which has carbon fabrics at the outer layers had a bit higher impact resistance than the others. As mentioned above, carbon fiber has low impact resistance compared to E-glass fiber and steel alloys; however, it has higher impact resistance than jute fiber. So, in this situation, placing carbon fabrics to the outer layers and jute fabrics to the inner layers leads to higher impact resistance values for jute/carbon hybrid composites. On the other hand, impact resistance values of jute/carbon hybrid composites were so close to the impact resistance value of carbon-reinforced composite. This unusual mechanical performance of composite laminates could be explained by void fractions and mechanics of the sliding behavior of the laminates under sudden impact and needs more attention in further studies.

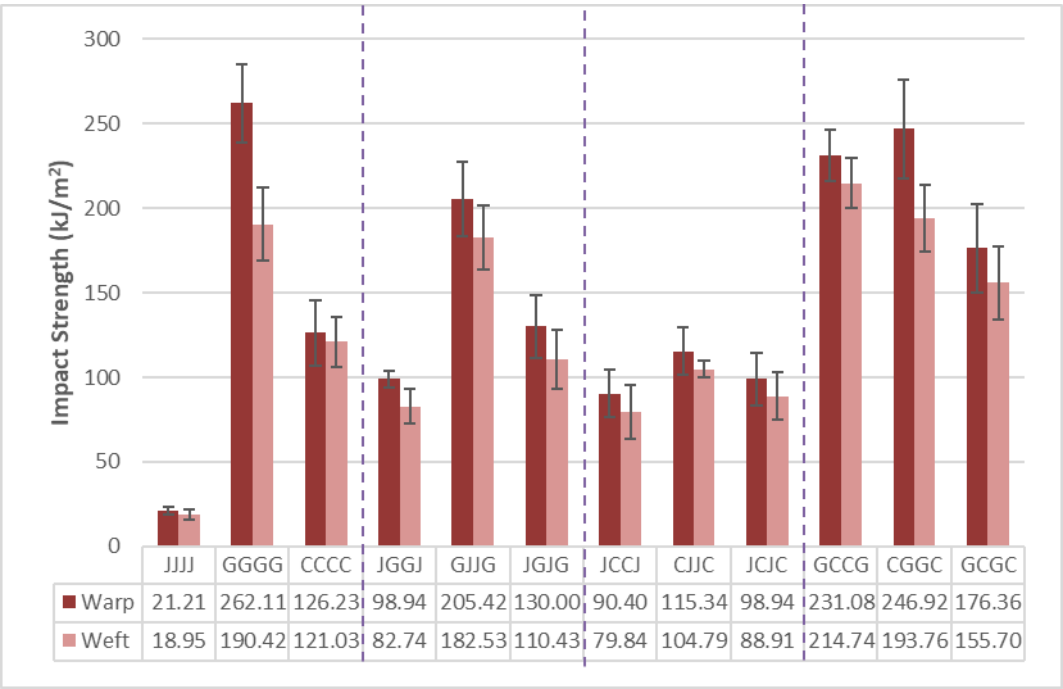

Figure 5.30 : Impact strength results of non-treated composite samples.

The impact strength results of one type of fabric reinforced composite samples are given in Figure 5.31. Results showed that while addition of MWCNT-OH and MWCNT-COOH to the composite structures had barely effect on the impact characteristics of the samples, pristine MWCNT addition had slightly higher influence on the impact strength results of jute, E-glass and carbon fabric reinforced composites. Jute fiber contains free hydroxyl groups in its amorphous region of cellulose, lignin and hemicellulose regions and this gives jute fiber an anionic structure (Ammayappan, Nayak, Ray, Das, & Roy, 2013). The two facts that anionic materials can not easily bond together and MWCNT-OH and MWCNT-COOH have anionic natures indicated that the bonding strength between these two nanofillers (MWCNT-OH and MWCNT-COOH) and jute fibers are not as robust as the bonding strength between jute fiber and pristine MWCNTs. Silica glass also contains hydroxyl groups and also it was stated in the literature that acids and alkalis causes brittleness in E-glass fibers (Norström, Watson, Engström, & Rosenholm, 2001; Plotnichenko, Sokolov, & Dianov, 2000; Tzounis, 2014). This fact could be the reason of achieving better impact properties with pristine MWCNT treated samples.

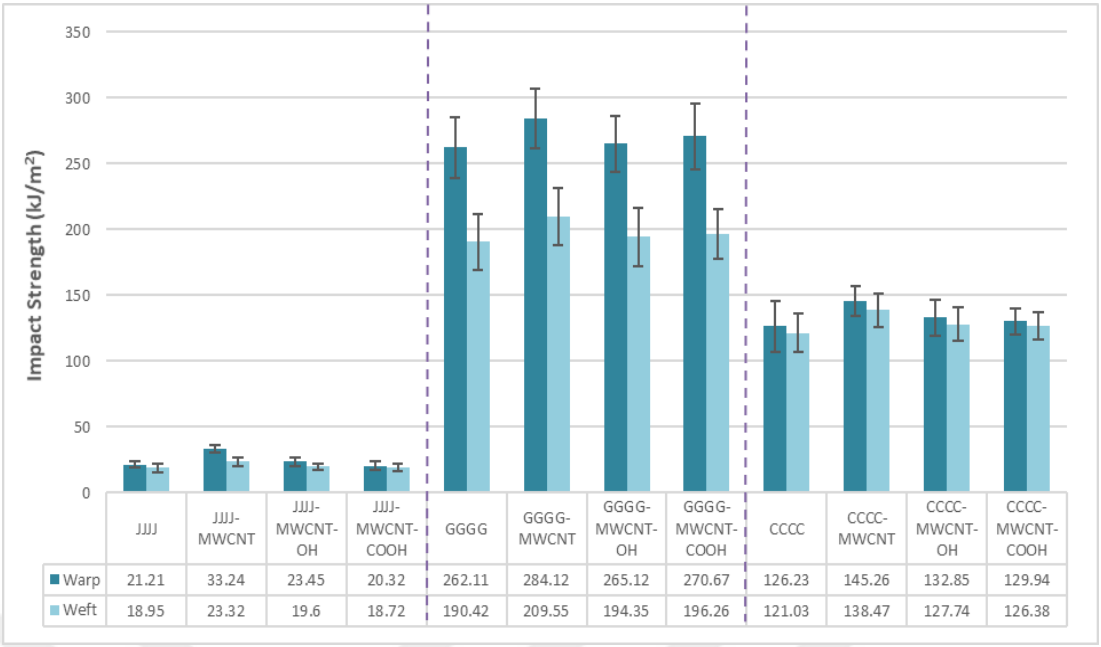

Figure 5.31 : Impact strength results of one type of fabric reinforced composite samples.

Figure 5.32 indicates the impact strength results of jute/E-glass fabric reinforced composite samples.

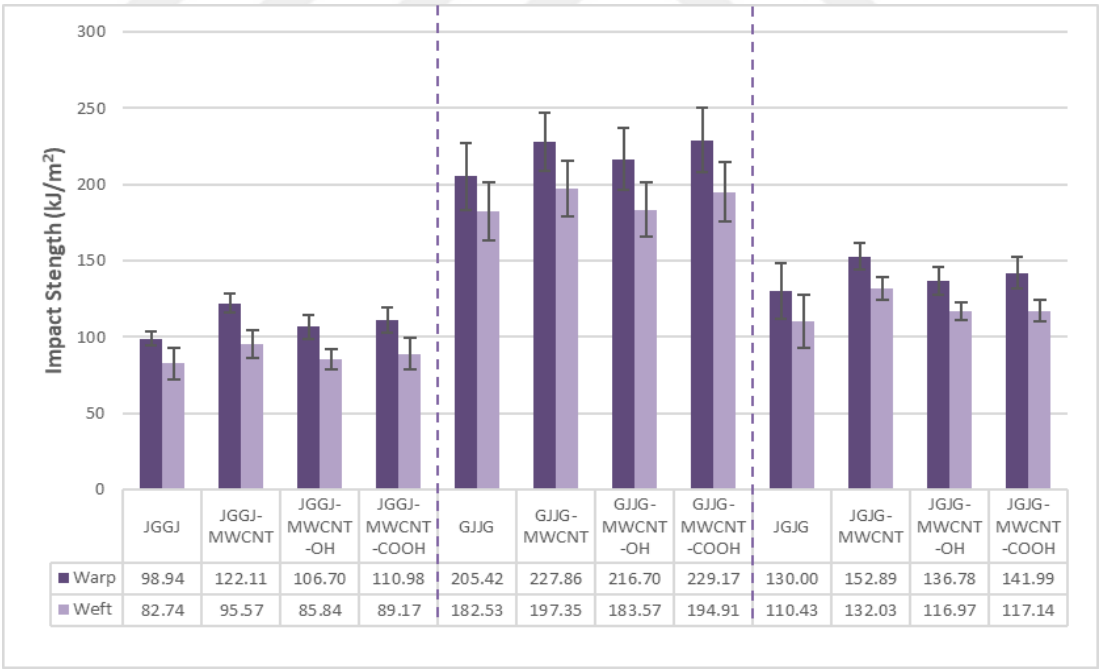

Figure 5.32 : Impact strength results of jute/E-glass fabric reinforced composite samples.

When three groups with different fabric sequences were examined, it was found that the highest impact strengths were obtained with pristine MWCNT treated specimens in the groups with JGGJ and JGJG fabric sequences, whereas the impact strength

values of the MWCNT and MWCNT-COOH reinforced specimens in the GJJG specimens were very close to each other and found higher than those of MWCNT-OH sample. It was once again seen that the samples obtained from the warp direction had higher strength than those taken from the weft direction.

The impact strength results of jute/carbon fabric reinforced composite samples are shown in Figure 5.33. When the samples in which the jute fabrics were placed to the outer layers of the composites (JCCJ) were examined, it was found that the highest strength was obtained with the MWCNT treated specimen (109.48 kJ/m^2 – 93.24 kJ/m^2) while the MWCNT (133.94 kJ/m^2 – 116.8 kJ/m^2) and MWCNT-COOH (134.26 kJ/m^2 – 112.7 kJ/m^2) treated specimens had higher impact strengths than MWCNT-OH treated sample among carbon/jute/jute/carbon fabric (JCJC) reinforced samples.

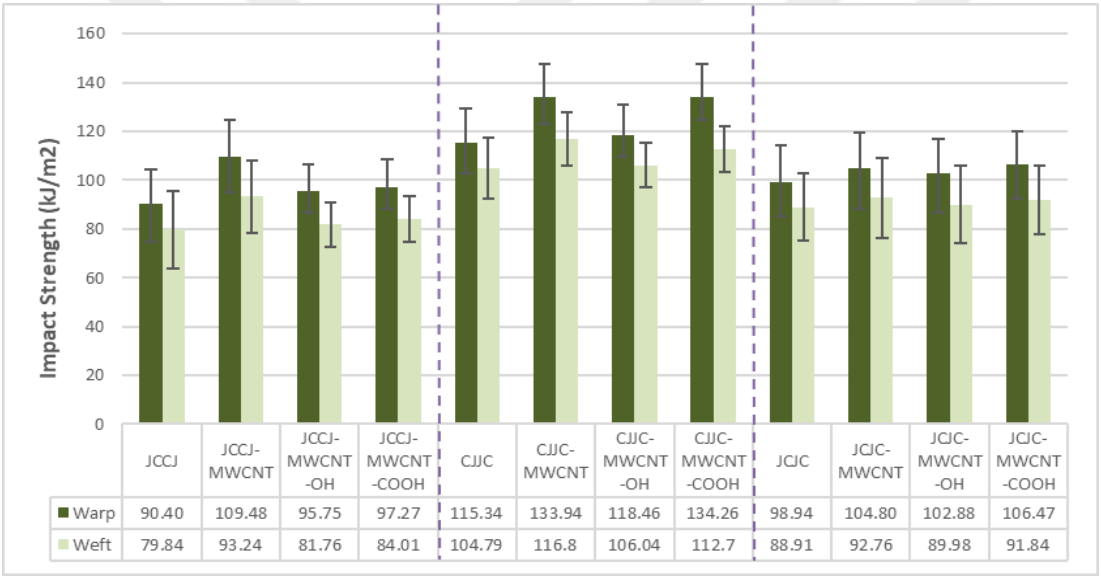

Figure 5.33 : Impact strength results of jute/carbon fabric reinforced composite samples.

Figure 5.34 shows the impact strength results of E-glass/carbon fabric reinforced composite samples. As in previous samples, it was understood that the addition of MWCNTs (MWCNT, MWCNT-OH and MWCNT-COOH) to the composite material samples reinforced with E-glass and carbon fabrics was increased the impact resistance of the material and the most effective one was pristine MWCNT. Moreover, it was observed that warp direction samples had higher impact resistance values than weft direction samples due to the inherent characteristics of biaxial woven fabric structures.

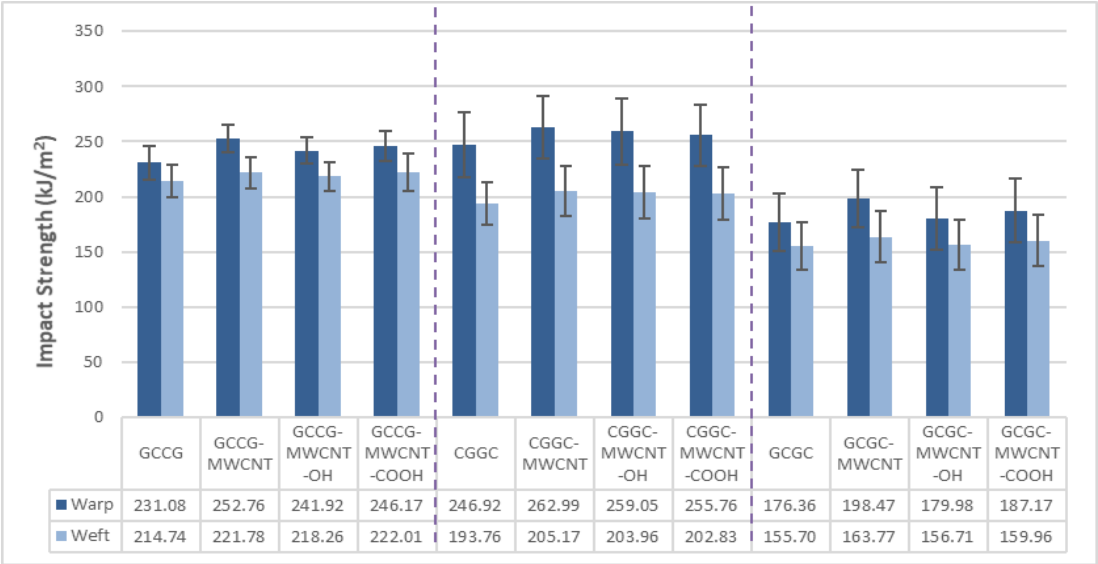

Figure 5.34 : Impact strength results of E-glass/carbon fabric reinforced composite samples.

As a conclusion, it could be sum up as;

- Samples from the warp direction had higher impact strength than samples taken from the weft direction.
- E-glass fabric reinforced composites had higher impact strength than carbon and jute fabric reinforced samples.
- Placing high strength fabrics to the outer layers of the composite enhanced the impact properties of the structures.
- Addition of MWCNTs enhanced the impact characteristics of all samples.
- Among different MWCNT types, pristine MWCNT added samples acquired higher impact strength.

5.2.4 Statistical analysis of mechanical properties

A full factorial analysis was performed on the results of tensile and impact tests to support the mechanical results with statistical analysis and to determine the statistically significance of the results.

5.2.4.1 Statistical analysis of tensile strength results

Tables 5.25 demonstrates the full-factorial experimental design layout of the tensile strength results given by Minitab 18 software program.

Table 5.25 : The full-factorial experimental design layout of the tensile strength results.

Sample Code	Yarn Type	Fabric Direction	Stacking Sequence	MWCNT type	Tensile Strength (MPa)
JGGJ-warp	1	1	1	1	108.06
JGGJ-MWCNT-warp	1	1	1	2	141.86
JGGJ-MWCNT-OH-warp	1	1	1	3	120.56
JGGJ-MWCNT-COOH-warp	1	1	1	4	132.65
GJJG-warp	1	1	2	1	101.65
GJJG-MWCNT-warp	1	1	2	2	137.29
GJJG-MWCNT-OH-warp	1	1	2	3	113.47
GJJG-MWCNT-COOH-warp	1	1	2	4	115.84
JGJG-warp	1	1	3	1	117.96
JGJG-MWCNT-warp	1	1	3	2	151.40
JGJG-MWCNT-OH-warp	1	1	3	3	127.29
JGJG-MWCNT-COOH-warp	1	1	3	4	130.29
JGGJ-weft	1	2	1	1	103.21
JGGJ-MWCNT-weft	1	2	1	2	127.08
JGGJ-MWCNT-OH-weft	1	2	1	3	106.84
JGGJ-MWCNT-COOH-weft	1	2	1	4	117.85
GJJG-weft	1	2	2	1	84.84
GJJG-MWCNT-weft	1	2	2	2	112.46
GJJG-MWCNT-OH-weft	1	2	2	3	102.87
GJJG-MWCNT-COOH-weft	1	2	2	4	91.85
JGJG-weft	1	2	3	1	100.12
JGJG-MWCNT-weft	1	2	3	2	129.82
JGJG-MWCNT-OH-weft	1	2	3	3	116.82
JGJG-MWCNT-COOH-weft	1	2	3	4	118.15
JCCJ-warp	2	1	1	1	329.40
JCCJ-MWCNT-warp	2	1	1	2	345.26
JCCJ-MWCNT-OH-warp	2	1	1	3	347.84
JCCJ-MWCNT-COOH-warp	2	1	1	4	366.85
CJJC-warp	2	1	2	1	145.47
CJJC-MWCNT-warp	2	1	2	2	146.24
CJJC-MWCNT-OH-warp	2	1	2	3	153.38
CJJC-MWCNT-COOH-warp	2	1	2	4	176.30
JCJC-warp	2	1	3	1	223.46
JCJC-MWCNT-warp	2	1	3	2	227.65
JCJC-MWCNT-OH-warp	2	1	3	3	230.56
JCJC-MWCNT-COOH-warp	2	1	3	4	255.24
JCCJ-weft	2	2	1	1	229.04
JCCJ-MWCNT-weft	2	2	1	2	244.86
JCCJ-MWCNT-OH-weft	2	2	1	3	237.29
JCCJ-MWCNT-COOH-weft	2	2	1	4	259.84
CJJC-weft	2	2	2	1	102.87
CJJC-MWCNT-weft	2	2	2	2	101.68
CJJC-MWCNT-OH-weft	2	2	2	3	104.30

Table 5.25 (continued) : The full-factorial experimental design layout of the tensile strength results.

Sample Code	Yarn Type	Fabric Direction	Stacking Sequence	MWCNT type	Tensile Strength (MPa)
CJJC-MWCNT-COOH-weft	2	2	2	4	116.97
JCJC-weft	2	2	3	1	140.18
JCJC-MWCNT-weft	2	2	3	2	142.24
JCJC-MWCNT-OH-weft	2	2	3	3	146.59
JCJC-MWCNT-COOH-weft	2	2	3	4	159.19
GCCG-warp	3	1	1	1	372.35
GCCG-MWCNT-warp	3	1	1	2	415.26
GCCG-MWCNT-OH-warp	3	1	1	3	397.01
GCCG-MWCNT-COOH-warp	3	1	1	4	385.17
CGGC-warp	3	1	2	1	367.03
CGGC-MWCNT-warp	3	1	2	2	400.35
CGGC-MWCNT-OH-warp	3	1	2	3	387.07
CGGC-MWCNT-COOH-warp	3	1	2	4	376.59
GCGC-warp	3	1	3	1	380.86
GCGC-MWCNT-warp	3	1	3	2	421.84
GCGC-MWCNT-OH-warp	3	1	3	3	396.14
GCGC-MWCNT-COOH-warp	3	1	3	4	389.90
GCCG-weft	3	2	1	1	302.44
GCCG-MWCNT-weft	3	2	1	2	320.28
GCCG-MWCNT-OH-weft	3	2	1	3	315.69
GCCG-MWCNT-COOH-weft	3	2	1	4	300.98
CGGC-weft	3	2	2	1	282.55
CGGC-MWCNT-weft	3	2	2	2	314.55
CGGC-MWCNT-OH-weft	3	2	2	3	300.62
CGGC-MWCNT-COOH-weft	3	2	2	4	295.89
GCGC-weft	3	2	3	1	292.30
GCGC-MWCNT-weft	3	2	3	2	321.47
GCGC-MWCNT-OH-weft	3	2	3	3	302.15
GCGC-MWCNT-COOH-weft	3	2	3	4	304.56

Table 5.26 shows the ANOVA response table of tensile strength results. In an ANOVA table, DF, Adj SS and Adj MS represent the degree of freedom, adjusted sum of squares and adjusted mean squares, respectively. DF of each source is one number less than the level of that factor and DF of interaction factors are calculated by multiplying the factors DF. Adj MS is calculated by dividing the Adj SS of each source to its degree of freedom. While F value is the ratio of MS for the variable to the MS of the error, the p-value is the area under the appropriate null sampling distribution of F that is bigger than the observed F-statistic. Based on 95% confidence interval, the parameters with a p value<0.05 denotes that the effect of that parameter on the given experimental

layout is statistically significant (Al-Hassani, Abbas, & Wan Daud, 2014; Sezgin, Bahadir, Boke, & Kalaoglu, 2016).

Table 5.26 : Analysis of variance response table of tensile strength results.

Source	DF	Adj SS	Adj MS	F	*p*
Linear	8	767508	95939	*	*
Yarn (Material) Type	2	649270	324635	*	*
Fabric Direction	1	66315	66315	*	*
Stacking Sequence	2	46677	23338	*	*
MWCNT type	3	5246	1749	*	*
2-Way Interactions	23	88662	3855	*	*
Yarn Type*Fabric Direction	2	18470	9235	*	*
Yarn Type*Stacking Sequence	4	65523	16381	*	*
Yarn Type*MWCNT type	6	3571	595	*	*
Fabric Direction*Stacking Sequence	2	894	447	*	*
Fabric Direction*MWCNT type	3	136	45	*	*
Stacking Sequence*MWCNT type	6	68	11	*	*
3-Way Interactions	28	3107	111	*	*
Yarn Type*Fabric Direction*Stacking Sequence	4	2503	626	*	*
Yarn Type*Fabric Direction*MWCNT type	6	206	34	*	*
Yarn Type*Stacking Sequence*MWCNT type	12	323	27	*	*
Fabric Direction*Stacking Sequence*MWCNT type	6	75	13	*	*
4-Way Interactions	12	135	11	*	*
Yarn Type*Fabric Direction*Stacking Sequence*MWCNT type	12	135	11	*	*
Error	0	*	*		
Total	71	859412			

As it is seen from the table, due to the fact that DF of the error is zero, F and p values could not be obtained in ANOVA table. Then, Adj SS values were taken into consideration to find out the parameters that have less effect on the result. Adj SS value represents the effect of the parameters on the result, if a parameter has a high-SS value, it means that it has a high effect on the result (Fisher & others, 1949). When Table 5.26 was examined, it was seen that two way interaction of stacking sequence and MWCNT type (Adj SS : 68) and three way interaction of fabric direction, stacking sequence and MWCNT type (Adj SS : 75) had the least effects on the tensile strength results and they were send to the error (Table 5.27).

Table 5.27 : Reduced analysis of variance response table of tensile strength results.

Source	DF	Adj SS	Adj MS	F	*p*
Linear	8	767508	95939	8019.78	0.000
Yarn Type	2	649270	324635	27137.21	0.000
Fabric Direction	1	66315	66315	5543.44	0.000
Stacking Sequence	2	46677	23338	1950.93	0.000
MWCNT type	3	5246	1749	146.19	0.000
2-Way Interactions	17	88594	5211	435.64	0.000
Yarn Type*Fabric Direction	2	18470	9235	771.97	0.000
Yarn Type*Stacking Sequence	4	65523	16381	1369.32	0.000
Yarn Type*MWCNT type	6	3571	595	49.75	0.000
Fabric Direction*Stacking Sequence	2	894	447	37.36	0.000
Fabric Direction*MWCNT type	3	136	45	3.79	0.040
3-Way Interactions	22	3032	138	11.52	0.000
Yarn Type*Fabric Direction*Stacking Sequence	4	2503	626	52.32	0.000
Yarn Type*Fabric Direction*MWCNT type	6	206	34	2.86	0.057
Yarn Type*Stacking Sequence*MWCNT type	12	323	27	2.25	0.087
4-Way Interactions	12	135	11	0.94	0.543
Yarn Type*Fabric Direction*Stacking Sequence*MWCNT type	12	135	11	0.94	0.543
Error	12	144	12		
Total	71	859412			

Model Summary: R-sq = 99.98%, R-sq(adj) = 99.90%, R-sq(pred) = 99.40%

When the Adj SS values of the linear factors were examined, it was observed that yarn (material) type (Adj SS : 649270) had the highest influence on the tensile strength of composite samples. Figure 5.35 demonstrates the main effect plots for tensile strength results. It was observed that the difference between the mean values of tensile strengths of different yarn (material) types was greater than the others. It was occured that tensile strength of jute/E-glass fabric reinforced samples were approximately around 110 MPa, while tensile strength of jute/carbon fabric reinforced samples and E-glass/carbon fabric reinforced samples were around 200MPa and 350 MPa, respectively. Carbon fiber has a tensile strength of 3.5–5 GPa while E-glass and jute have tensile strengths of 1.8–2.7 GPa and 0.45–0.55 GPa, respectively (Alves et al., 2011). The differences between these values also supported the tensile strength results of composite samples and revealed the fact that the type of reinforcement material has a huge effect on the tensile strength of the composite materials.

From the ANOVA table it was understood that the most effective factor on the tensile strength of composite structures after the yarn (material) type was the fabric direction

(Adj SS : 66315). Furthermore, when the main effect graph was taken into consideration (Figure 5.35), it was seen that the samples taken from the warp direction (250 MPa) had higher strengths than the samples taken from the weft direction (190MPa).

Fabric stacking sequence (Adj SS : 46677) and MWCNT type (Adj SS : 5246) also had significant effect on tensile strength of the composite samples. When the different fabric stacking sequences were analyzed, it came out that higher tensile strengths were achieved by placing high strength fabrics to the inner layers (250 MPa) of composite instead of placing outer layers (190 MPa) or putting alternatively (225 MPa).

Among all main factors, MWCNT type had the least effect on tensile strength. When main effect plot for tensile strength was examined, it was occurred that pristine MWCNT treated samples had higher tensile strength than other samples but the difference between the levels were not as high as the those of other factors. Moreover, the *p* values of all four main factors were 0.000 and this indicated that their effects on tensile strength are statistically significant.

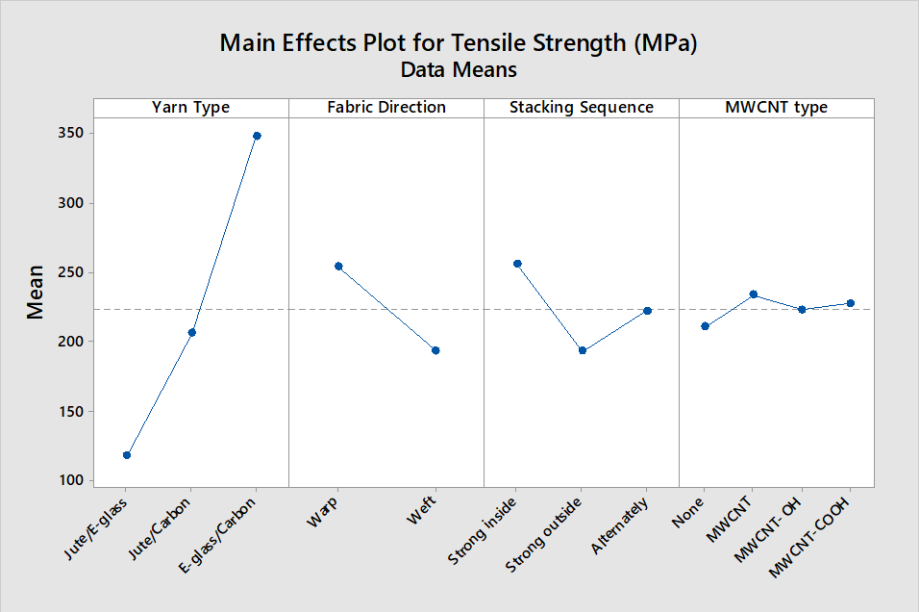

Figure 5.35 : Main effects plot for tensile strength.

Besides, it was acquired from Figure 5.35 that, the highest tensile strength was achieved with the third level of yarn (material) type (E glass/carbon), the first level of fabric direction (warp), first level of stacking sequence of fabric plies (strong fiber inside) and second level of MWCNT type (pristine MWCNT).

When two-way interactions were taken into consideration from reduced ANOVA table, it appeared that although some of them were not as effective as linear factors, their effects were also statistically significant (p<0.05). Adj SS values of two-way interactions revealed that the interactions of yarn type*fabric direction and yarn type*stacking sequence had higher influence on tensile strength by comparison with main factor MWCNT type.

Figure 5.36 shows the interaction plot for tensile strength. In interaction plots, if the lines are parallel to each other, this means that there is no interaction between these factors. Moreover, the degree of interaction increases with the increment of the difference in slope between the lines ('What is an interaction?', n.d.). As it was mentioned above, the combined effect of stacking sequence and MWCNT type on the tensile strength of composite samples was so low and send to the error. This fact was also proved by the interaction plot (lines are parallel to each other).

When we examined the other intersection curves, it was seen that the curves that indicated the fabric direction and MWCNT type were not exactly parallel to each other but just as parallel. Also, when we look at the p value from the ANOVA table, the p value of the intersection of fabric direction and the MWCNT type was 0.040 when the p value of other two way interactions were 0.000.

The intersection of yarn type*fabric direction*stacking sequence (Adj SS: 2503, p: 0.000) had the uttermost effect on tensile strength of samples between 3 way intersections. The low Adj SS values and high p values of yarn type*fabric direction*MWCNT type (Adj SS: 206, p: 0.057) and yarn type*stacking sequence*MWCNT type (Adj SS: 323, p: 0.087) demonstrated their low effect on tensile strength. Moreover, the combined effect of these four factors had very low Adj SS value (135) and very high p value (0.543) which indicates its nearly no effect on tensile strength.

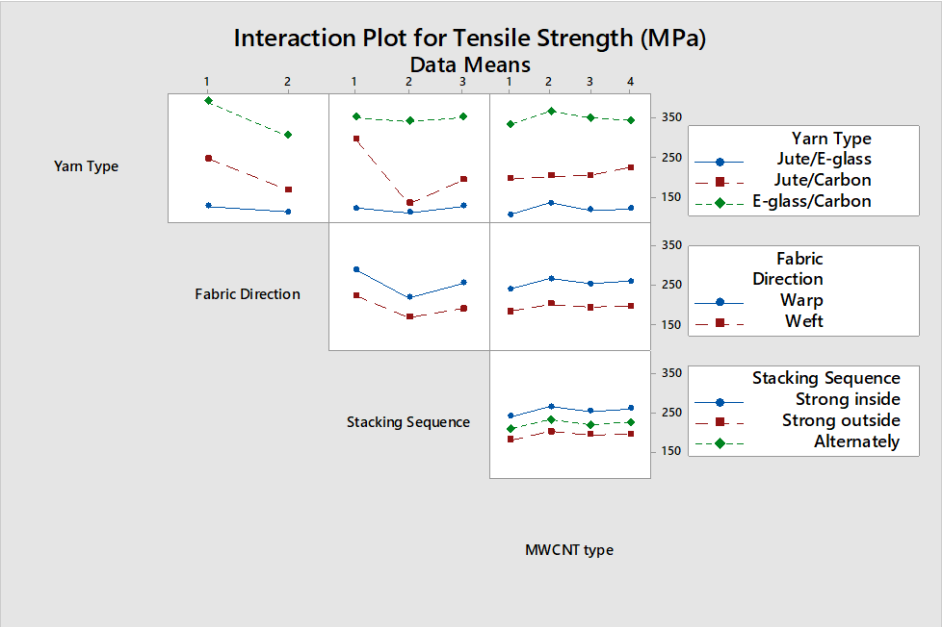

Figure 5.36 : Interaction plots for tensile strength.

Besides, in this model, R-sq (0.9998), adjusted R-sq (0.9990) and predicted R-sq (0.9940) were in reasonable agreement and close to 1. This indicated the adequacy of the model.

5.2.4.2 Statistical analysis of impact strength results

Tables 5.28 demonstrates the full-factorial experimental design layout of the impact strength results given by Minitab 18 software program. The reason to design two different experimental design layouts was that while carbon fabric reinforced composite sample had the highest tensile strength, E-glass fabric reinforced composite sample had the highest impact strength. So, the level 1 and 2 of the third factor differs for each situation.

Table 5.29 presented the ANOVA response table of the impact strength results. Similar to the previous ANOVA table, F and p values could not be obtained due to the fact that DF of error was zero. By examining the Adj SS values, the interaction of fabric direction*stacking sequence*MWCNT type (Adj SS : 31) was sent to the error due to its low effect.

Table 5.28 : Full-factorial experimental design layout of impact strength results.

Sample Code	Yarn Type	Fabric Direction	Stacking Sequence	MWCNT Type	Impact Strength (kJ/m^2)
JGGJ-warp	1	1	1	1	98.94
JGGJ-MWCNT-warp	1	1	1	2	122.11
JGGJ-MWCNT-OH-warp	1	1	1	3	106.70
JGGJ-MWCNT-COOH-warp	1	1	1	4	110.98
GJJG-warp	1	1	2	1	205.42
GJJG-MWCNT-warp	1	1	2	2	227.86
GJJG-MWCNT-OH-warp	1	1	2	3	216.70
GJJG-MWCNT-COOH-warp	1	1	2	4	229.17
JGJG-warp	1	1	3	1	130.00
JGJG-MWCNT-warp	1	1	3	2	152.89
JGJG-MWCNT-OH-warp	1	1	3	3	136.78
JGJG-MWCNT-COOH-warp	1	1	3	4	141.99
JGGJ-weft	1	2	1	1	82.74
JGGJ-MWCNT-weft	1	2	1	2	95.57
JGGJ-MWCNT-OH-weft	1	2	1	3	85.84
JGGJ-MWCNT-COOH-weft	1	2	1	4	89.17
GJJG-weft	1	2	2	1	182.53
GJJG-MWCNT-weft	1	2	2	2	197.35
GJJG-MWCNT-OH-weft	1	2	2	3	183.57
GJJG-MWCNT-COOH-weft	1	2	2	4	194.91
JGJG-weft	1	2	3	1	110.43
JGJG-MWCNT-weft	1	2	3	2	132.03
JGJG-MWCNT-OH-weft	1	2	3	3	116.97
JGJG-MWCNT-COOH-weft	1	2	3	4	117.14
JCCJ-warp	2	1	1	1	90.40
JCCJ-MWCNT-warp	2	1	1	2	109.48
JCCJ-MWCNT-OH-warp	2	1	1	3	95.75
JCCJ-MWCNT-COOH-warp	2	1	1	4	97.27
CJJC-warp	2	1	2	1	115.34
CJJC-MWCNT-warp	2	1	2	2	133.94
CJJC-MWCNT-OH-warp	2	1	2	3	118.46
CJJC-MWCNT-COOH-warp	2	1	2	4	134.26
JCJC-warp	2	1	3	1	98.94
JCJC-MWCNT-warp	2	1	3	2	104.8
JCJC-MWCNT-OH-warp	2	1	3	3	102.98
JCJC-MWCNT-COOH-warp	2	1	3	4	106.47
JCCJ-weft	2	2	1	1	79.84
JCCJ-MWCNT-weft	2	2	1	2	93.24
JCCJ-MWCNT-OH-weft	2	2	1	3	81.76
JCCJ-MWCNT-COOH-weft	2	2	1	4	84.01
CJJC-weft	2	2	2	1	104.79
CJJC-MWCNT-weft	2	2	2	2	116.80

Table 5.28 (continued) : Full-factorial experimental design layout of impact strength results.

Sample Code	Yarn Type	Fabric Direction	Stacking Sequence	MWCNT Type	Impact Strength (kJ/m^2)
CJJC-MWCNT-OH-weft	2	2	2	3	106.04
CJJC-MWCNT-COOH-weft	2	2	2	4	112.70
JCJC-weft	2	2	3	1	88.91
JCJC-MWCNT-weft	2	2	3	2	92.76
JCJC-MWCNT-OH-weft	2	2	3	3	89.98
JCJC-MWCNT-COOH-weft	2	2	3	4	91.84
CGGC-warp	3	1	1	1	246.92
CGGC-MWCNT-warp	3	1	1	2	262.99
CGGC-MWCNT-OH-warp	3	1	1	3	259.05
CGGC-MWCNT-COOH-warp	3	1	1	4	255.76
GCCG-warp	3	1	2	1	231.08
GCCG-MWCNT-warp	3	1	2	2	252.76
GCCG-MWCNT-OH-warp	3	1	2	3	241.92
GCCG-MWCNT-COOH-warp	3	1	2	4	246.17
GCGC-warp	3	1	3	1	176.36
GCGC-MWCNT-warp	3	1	3	2	198.47
GCGC-MWCNT-OH-warp	3	1	3	3	179.98
GCGC-MWCNT-COOH-warp	3	1	3	4	187.17
CGGC-weft	3	2	1	1	193.76
CGGC-MWCNT-weft	3	2	1	2	205.17
CGGC-MWCNT-OH-weft	3	2	1	3	203.96
CGGC-MWCNT-COOH-weft	3	2	1	4	202.83
GCCG-weft	3	2	2	1	214.74
GCCG-MWCNT-weft	3	2	2	2	221.78
GCCG-MWCNT-OH-weft	3	2	2	3	218.26
GCCG-MWCNT-COOH-weft	3	2	2	4	246.01
GCGC-weft	3	2	3	1	155.70
GCGC-MWCNT-weft	3	2	3	2	163.77
GCGC-MWCNT-OH-weft	3	2	3	3	156.71
GCGC-MWCNT-COOH-weft	3	2	3	4	159.96

Table 5.29 : Analysis of variance response table of impact strength results.

Source	DF	Adj SS	Adj MS	F	*p*
Linear	8	198326	24790.8	*	*
Yarn Type	2	146630	73314.8	*	*
Fabric Direction	1	10098	10098.3	*	*
Stacking Sequence	2	39149	19574.4	*	*
MWCNT Type	3	2450	816.5	*	*
2-Way Interactions	23	32049	1393.5	*	*
Yarn Type*Fabric Direction	2	1111	555.3	*	*
Yarn Type*Stacking Sequence	4	29991	7497.8	*	*
Yarn Type*MWCNT Type	6	140	23.3	*	*
Fabric Direction*Stacking Sequence	2	348	173.9	*	*
Fabric Direction*MWCNT Type	3	125	41.6	*	*
Stacking Sequence*MWCNT Type	6	335	55.9	*	*
3-Way Interactions	28	1627	58.1	*	*
Yarn Type*Fabric Direction*Stacking Sequence	4	1261	315.3	*	*
Yarn Type*Fabric Direction*MWCNT Type	6	129	21.4	*	*
Yarn Type*Stacking Sequence*MWCNT Type	12	206	17.2	*	*
Fabric Direction*Stacking Sequence*MWCNT Type	6	31	5.2	*	*
4-Way Interactions	12	166	13.8	*	*
Yarn Type*Fabric Direction*Stacking Sequence*MWCNT Type	12	166	13.8	*	*
Error	0	*	*		
Total	71	232168			

Table 5.30 displays the reduced ANOVA table of impact strength results. When the linear factors were examined, it was noticed that all factors had statistically significant effect (*p* : 0.000) on impact strength of composite samples. While yarn (material) type had the highest effect (Adj SS : 146630), MWCNT type (Adj SS : 2450) had the least influence among linear factors. This fact was also seen from the main effects plot for impact strength (Figure 5.37). The difference between the levels of yarn (material) types was higher than the other factors. Taking into account that impact strengths of these three yarn (material) types (jute, E-glass and carbon) are so different from each other, it was not surprising that their binary combinations in hybrid composite structures also showed dissimilar impact strength results.

The fabric direction had lesser effect than yarn (material) type and stacking sequence. While the mean impact strength at warp direction was about 160 kJ/m^2, it was about

145 kJ/m^2 at weft direction samples (Figure 5.37). During testing, impact was given from lateral surface of the sample. So, both warp and weft yarns were exposed to a nearly same amount of impact. So, the less effect of fabric direction on the impact strength of samples could be due to this situation.

Table 5.30 : Reduced analysis of variance response table of impact strength results.

Source	DF	Adj SS	Adj MS	F-Value	P-Value
Linear	8	198326	24790.8	4759.83	0.000
Yarn (Material) Type	2	146630	73314.8	14076.45	0.000
Fabric Direction	1	10098	10098.3	1938.88	0.000
Stacking Sequence	2	39149	19574.4	3758.28	0.000
MWCNT Type	3	2450	816.5	156.77	0.000
2-Way Interactions	23	32049	1393.5	267.54	0.000
Yarn Type*Fabric Direction	2	1111	555.3	106.61	0.000
Yarn Type*Stacking Sequence	4	29991	7497.8	1439.57	0.000
Yarn Type*MWCNT Type	6	140	23.3	4.47	0.045
Fabric Direction*Stacking Sequence	2	348	173.9	33.40	0.001
Fabric Direction*MWCNT Type	3	125	41.6	7.99	0.016
Stacking Sequence*MWCNT Type	6	335	55.9	10.73	0.005
3-Way Interactions	22	1596	72.5	13.93	0.002
Yarn Type*Fabric Direction*Stacking Sequence	4	1261	315.3	60.54	0.000
Yarn Type*Fabric Direction*MWCNT Type	6	129	21.4	4.12	0.055
Yarn Type*Stacking Sequence*MWCNT Type	12	206	17.2	3.30	0.077
4-Way Interactions	12	166	13.8	2.65	0.120
Yarn Type*Fabric Direction*Stacking Sequence*MWCNT Type	12	166	13.8	2.65	0,120
Error	6	31	5.2		
Total	71	232168			

Model summary: R-sq = 99.99%, R-sq(adj) = 99.84%, R-sq(pred) = 98.06%

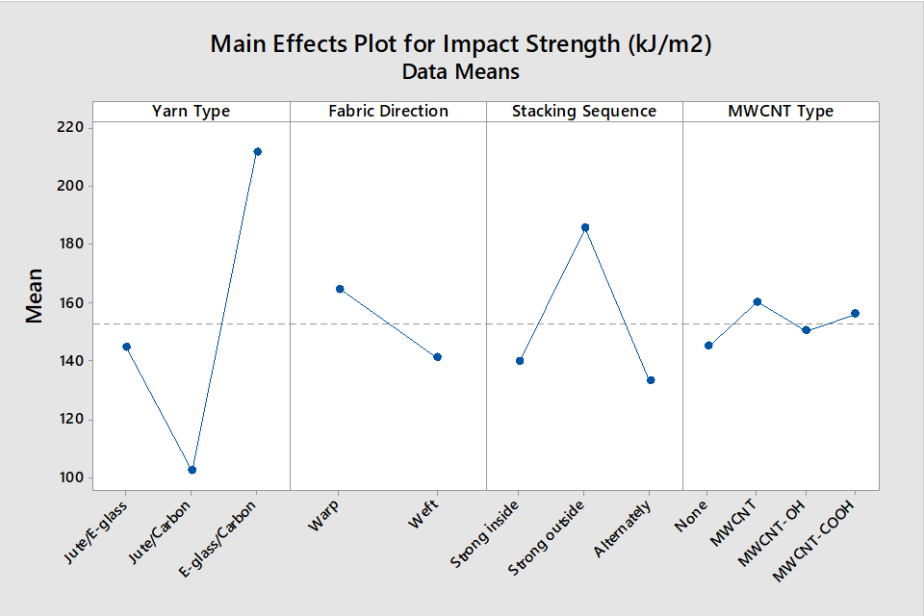

Figure 5.37 : Main effects plot for impact strength.

Distinct from the tensile strength results, the highest impact strength was obtained by placing high strength fabrics to the outer layers (Mean impact strength : 180 kJ/m^2) of the composite structures instead of placing inside (Mean impact strength : 140 kJ/m^2). When the effects of different levels of MWCNT types were considered, it was understood that the highest impact strength was obtained with pristine MWCNT treated sample, similar to the tensile strength results. However, it was both seen from ANOVA table and main effects plot that type of MWCNT had the least influence on impact strength.

From Figure 5.37, it could be concluded that higher impact strength was achieved with the third level of yarn type (E-glass/carbon), the first level of fabric direction (warp), the second level of stacking sequence of fabric plies (low strength fabric inside) and the second level of MWCNT type (pristine MWCNT).

Moreover, it was revealed that the combined effect of yarn (material) type and stacking sequence had the highest statistically significant effect on the impact strength (Adj SS : 29991, p : 0.000). Considering the fact that by changing the stacking sequence of fabric plies, we were changing the places of the different yarn (material) types in composite structure. So, this also showed us that these two factors had really strong interaction between each other. Also, all two way interactions had statistically significant effect ($p<0.05$) on impact strength. The interaction of yarn type*MWCNT type had an Adj SS of 140 and p value of 0.045 which showed us that its effect was at

borderline of statistically significance level. Moreover, the similar slopes of yarn type*MWCNT type curves in interaction plot promoted this result (Figure 5.38).

Among three way interactions, only the interaction of yarn type*fabric direction*MWCNT type had statistically significant effect on the impact strength. Moreover, the combined effect of these four factors had very low Adj SS value (166) and a high *p* value (0.120) which indicated its nearly no effect on tensile strength.

In this model, R-sq (0.9999), adjusted R-sq (0.9984) and predicted R-sq (0.9806) were in reasonable agreement, which indicated the adequacy of the model.

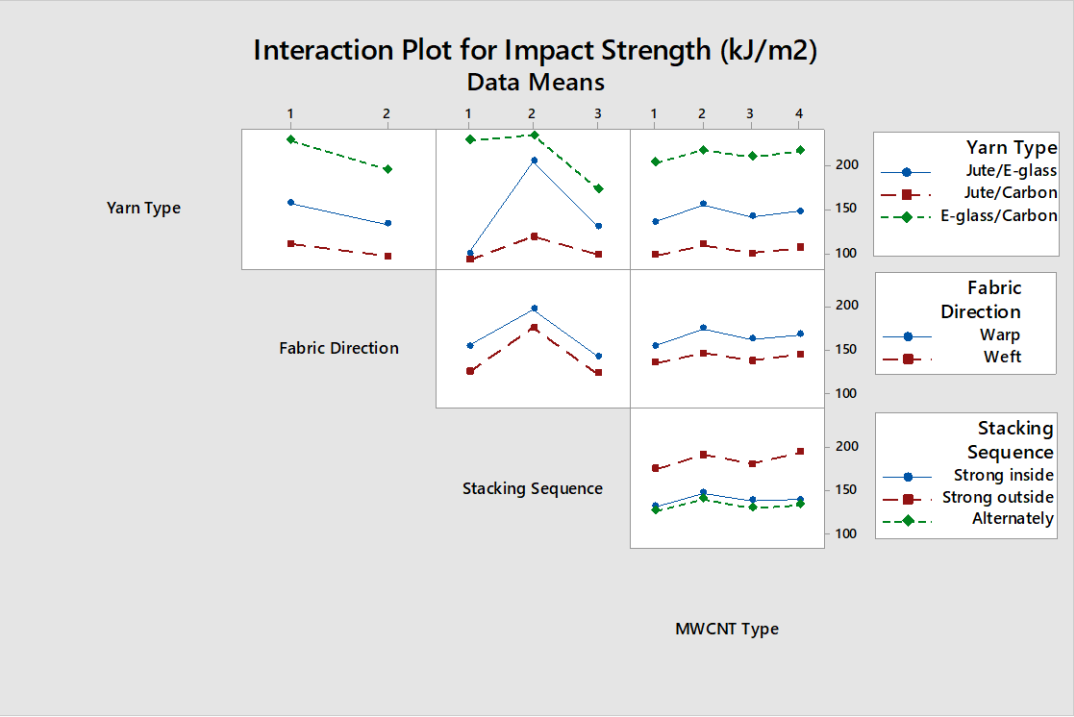

Figure 5.38 : Interaction plots for impact strength.

5.2.5 Morphological analysis

The morphological analysis of the composite samples were realized by using SEM images. In this section, SEM images of composite materials were examined by taking into consideration of the mechanical properties of the composite materials and the void ratios they possess.

Figure 5.39 demontrates the SEM images of JJJJ and JJJJ-MWCNT and JJJJ-MWCNT-COOH samples. In the samples JJJJ and JJJJ-MWCNT-COOH, the weak bonding areas of the matrix and reinforcement materials (voids) were seen, while the

composite sample of JJJJ-MWCNT was more tightly packed (almost no void area). The obtained void ratio values of those samples also supported the results. The void ratios of the JJJJ and JJJJ-MWCNT-COOH samples were 2.4% and 2.6%, respectively, while the void ratio of the JJJJ-MWCNT sample was 0.8%.

Figure 5.39 : SEM images of (a) JJJJ, (b) JJJJ-MWCNT and (c) JJJJ-MWCNT-COOH samples.

The SEM images of GGGG, GGGG-MWCNT, GGGG-MWCNT-OH and GGGG-MWCNT-COOH samples are given in Figure 5.40. The void ratio measurement results showed that the GGGG sample had the highest void ratio (7.86%), while the GGGG-MWCNT sample (2.81%) had the lowest. When the SEM images were examined, it was seen that in GGGG sample the matrix and reinforcement materials were bonded weakly and the amount of voids were higher than the other samples. This was also reflected in the mechanical properties of the materials. The GGGG-MWCNT specimen showed the highest tensile (294.16 MPa – 222.84 MPa) and impact strengths (284.12 kJ/m^2 – 209.55 kJ/m^2) in warp and weft directions while the GGGG specimen

showed the lowest tensile (262.46 MPa – 199.08 MPa) and impact strength (262.11 kJ/m^2 – 190.42 kJ/m^2).

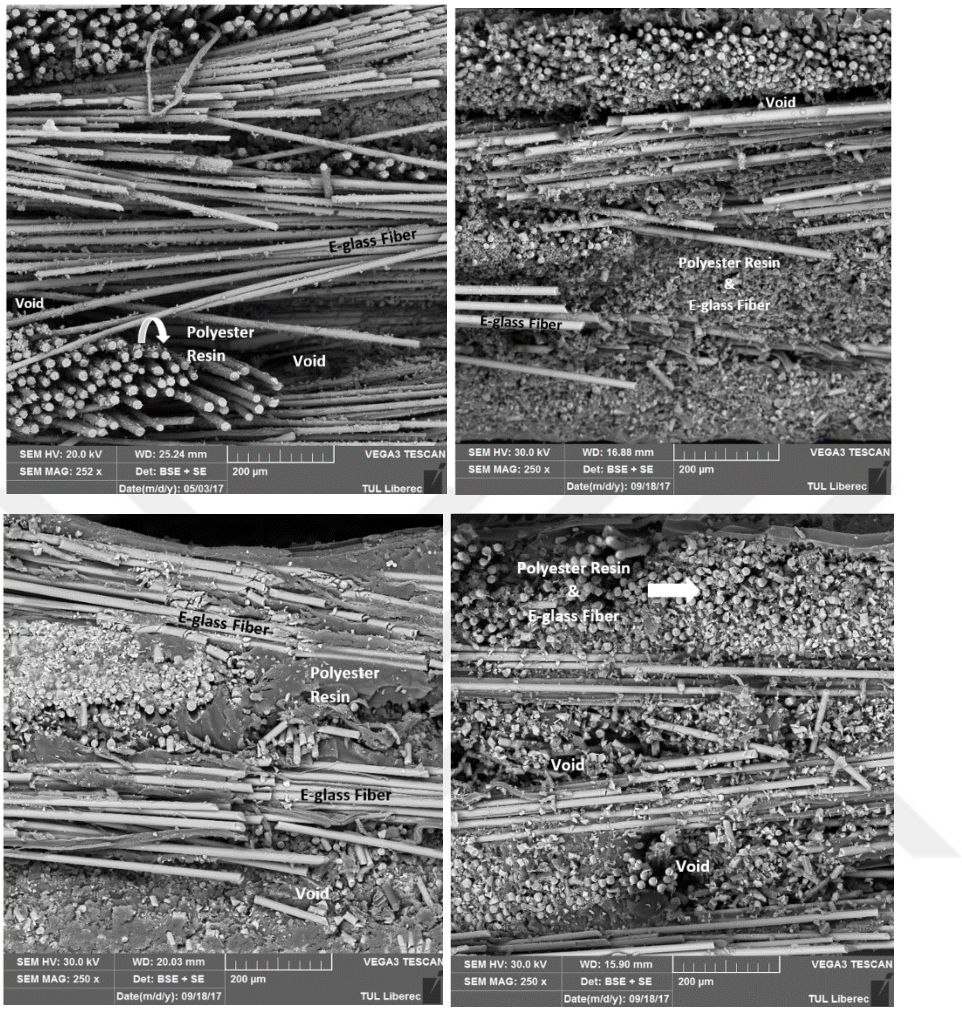

Figure 5.40 : SEM images of (a) GGGG, (b) GGGG-MWCNT, (c) GGGG-MWCNT-OH and (d) GGGG-MWCNT-COOH samples.

It was stated that the addition of different MWCNTs to the composite material reduced the void ratio in almost all samples. In some samples, however, the addition of MWCNTs negatively affected the void ratio of the composite structures. CCCC-MWCNT-COOH sample was a case for this situation. While the void ratio of the CCCC sample was 7.94%, this value increased to 9.25% by the addition of MWCNT-COOH. The SEM image of the CCCC-MWCNT-COOH sample is given in Figure 5.41, along with the SEM image of the CCCC sample. Although there is not a big difference between these two images, the matrix and th resin look to be held together in the CCCC sample.

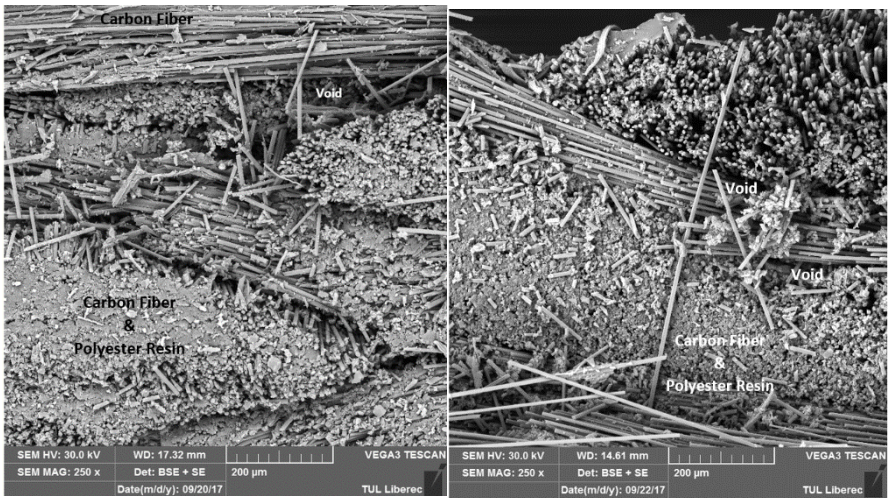

Figure 5.41 : SEM images of (a) CCCC and (b) CCCC-MWCNT-COOH samples.

Figure 5.42 shows the SEM images of cross sections of CJJC and JCCJ samples. It was seen from images that there were some voids at the sample, which has two jute fabric plies at the inner layer (CJJC). This fact indicated the low adhesion between the jute fabric plies and fabric/resin. This induced a low strength in the composite structure. Moreover, it came out that while carbon fibers had smooth and unbeaten surface, jute fibers showed a damaged structure.

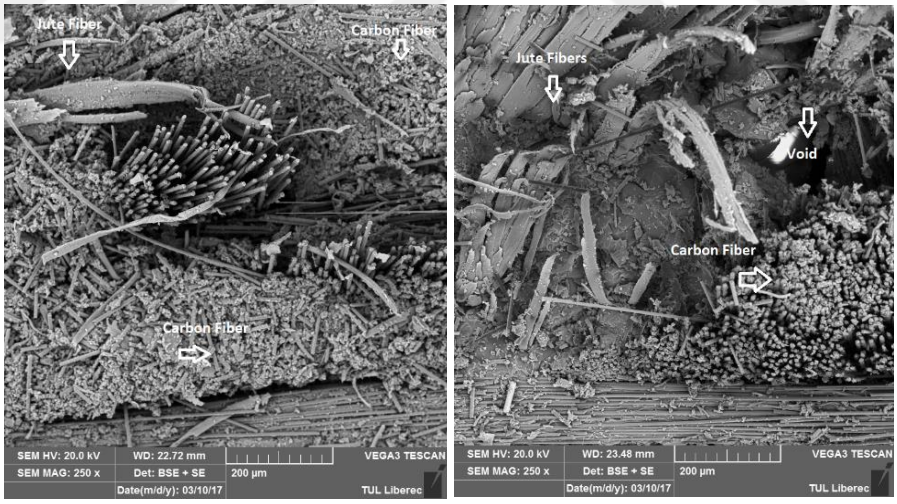

Figure 5.42 : SEM images of (a) JCCJ and (b) CJJC samples.

The SEM images of cross sections of CGCG, CGGC and GCCG samples are demonstrated in Figure 5.43. It was seen that in CGGC sample, the matrix and the reinforcements were more tightly bonded to each other among other E-glass/carbon samples. When the SEM image of CGGC sample was compared to other samples, it was clearly seen that there was no void in CGGC sample. Fiber and resin coalesced

into a compact structure which shows the high bonding strength between the fiber and the resin. The higher bonding strength in this sample could be the reason of higher impact strength.

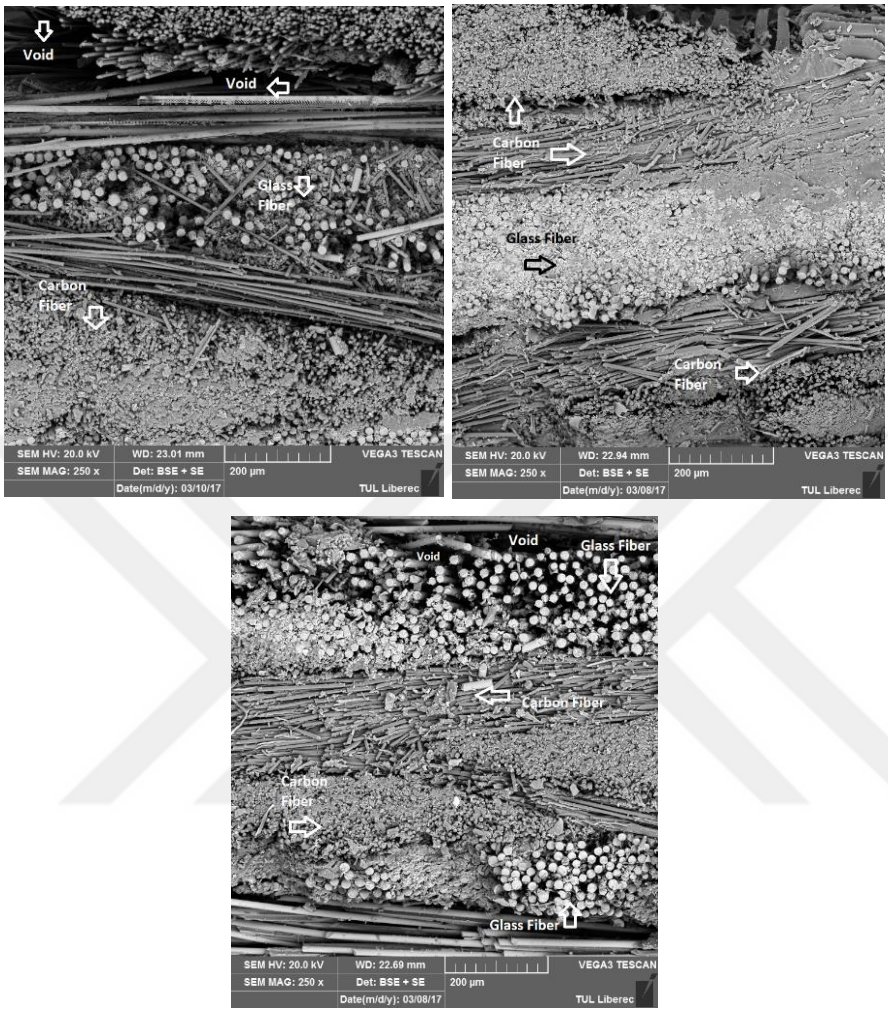

Figure 5.43 : SEM images of (a) CGCG, (b) CGGC and (c) GCCG samples.

Figure 5.44 infers the SEM images of JGGJ, GJJG and JGJG samples. It was known from previous calculations of the void ratio that the JGGJ sample (8.39 %) had the lowest void ratio and the JGJG sample (9.22 %) had the highest void ratio among those samples. When the SEM images were investigated, it could be seen that in all three samples, the matrix and the reinforcement material had some weakly bonded regions, but in the GJJG and JGJG samples those regions were more and larger.

Figure 5.44 : SEM images of (a) JGGJ, (b) GJJG and (c) JGJG samples.

The incorporation of different MWCNTs into hybrid composites resulted in the highest void fraction reduction in jute/carbon fabric reinforced hybrid composite specimens among all hybrid specimen. SEM images of jute/carbon fabric reinforced hybrid composite structures with different fabric sequences are given in Figures 5.45-5.46-5.47 in order to visually examine these reductions.

The SEM images of JCCJ, JCCJ-MWCNT and JCCJ-MWCNT-COOH samples are given in Figure 5.45. While the best bonding between the matrix and reinforcement material was found in the JCCJ-MWCNT specimen from the SEM images, the void ratio results also supported this outcome. The JCCJ sample had a void ratio of 7.41% while the JCCJ-MWCNT sample had a void ratio of 3.70%. When the mechanical properties of those samples were taken into account, it was understood that the lowest impact and tensile strengths were obtained with the JCCJ specimen, while the JCCJ-

MWCNT specimen had the highest impact strength and the JCCJ-MWCNT-COOH specimen had highest tensile strength .

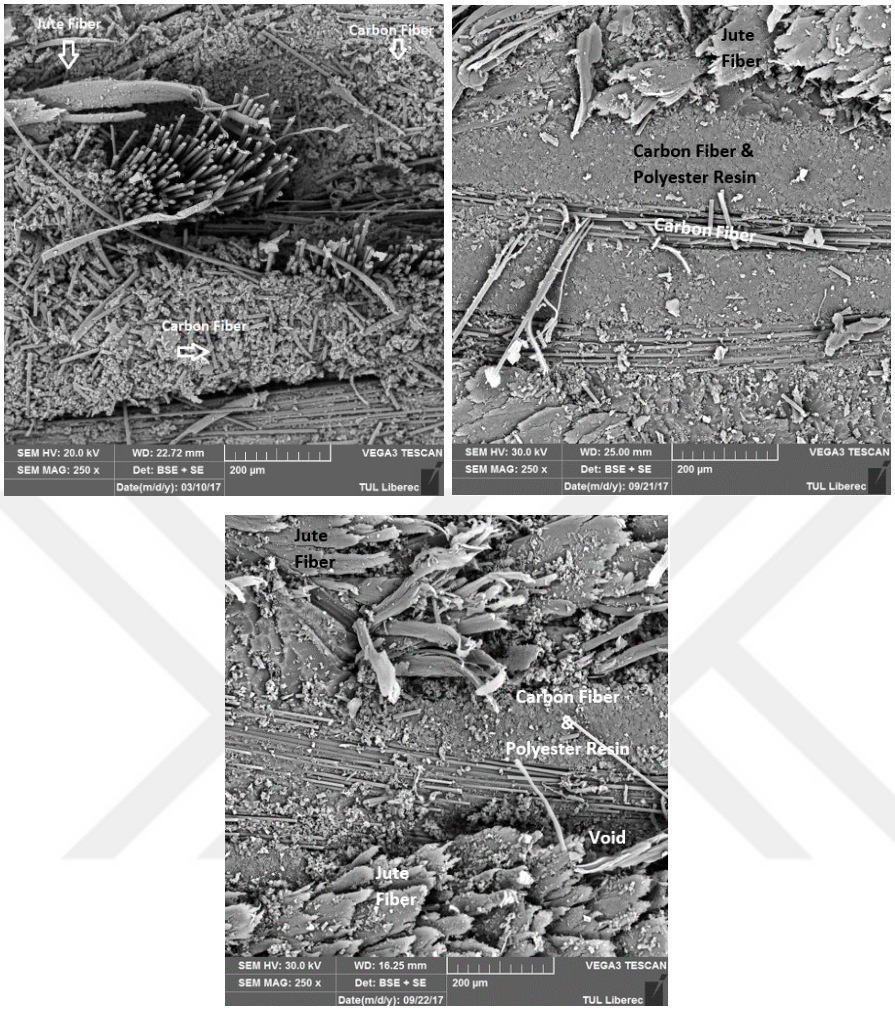

Figure 5.45 : SEM images of (a) JCCJ, (b) JCCJ-MWCNT and (c) JCCJ-MWCNT-COOH samples.

Figure 5.46 screens the SEM images of CJJC and CJJC-MWCNT-COOH samples. The addition of MWCNT-COOH to the CJJC hybrid composite sample resulted in a decrement of void ratio from 8.15% to 2.96%. In the CJJC-MWCNT-COOH sample, the resin and the reinforcement materials integrated with each other, while the jute fibers appeared separated in polyester resin in the CJJC sample.

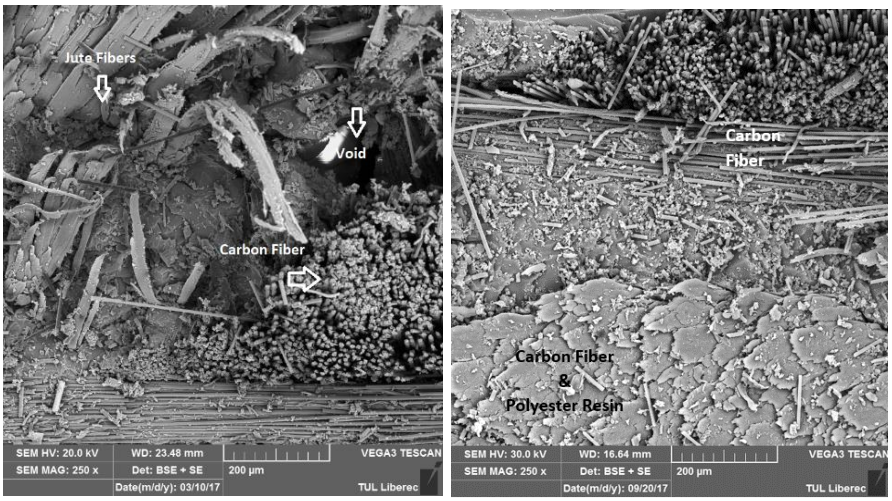

Figure 5.46 : SEM images of (a) CJJC and (b) CJJC-MWCNT-COOH samples.

The SEM images of JCJC and JCJC-MWCNT-COOH samples are presented in Figure 5.47. As in the case of CJJC fabric stacking sequence, the addition of MWCNT-COOH to the composite material resulted in a significant reduction in the void ratio of JCJC sample, which was also clearly seen from the SEM images.

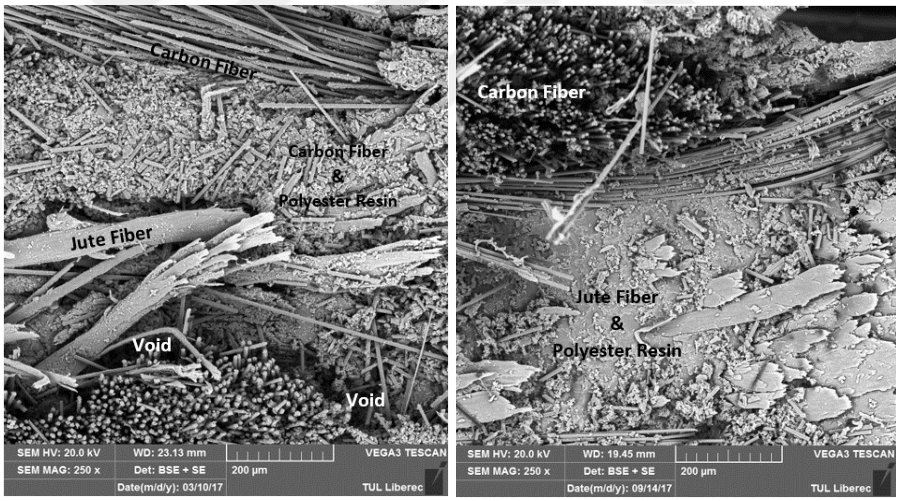

Figure 5.47 : SEM images of (a) JCJC and (b) JCJC-MWCNT-COOH samples.

6. CONCLUSIONS AND RECOMMENDATIONS

The mechanical and thermal properties of textile reinforced polyester hybrid composites, which were designed and fabricated in the scope of this thesis, were investigated and accordingly their properties were improved by the addition of nanofiller materials (MWCNT, MWCNT-OH and MWCNT-COOH). The results that were obtained throughout this study, can be summarized as follows;

- In the previous studies, the mechanical properties of the unidirectional fabric reinforced composite materials were examined at two (0° and 90°) directions, by taking into account that these fabrics show different properties at these two directions. However, according to our knowledge, such type of investigations have not been found in similar studies which were made on woven (bidirectional) fabric reinforced composite structures. In this research, the tests were carried out considering both warp and weft directions of the fabric reinforcement. As a result, the specimens taken from the warp direction showed comparatively higher mechanical properties than the samples taken from the weft direction as expected.

- It is concluded that, high tensile strength can be achieved by placing high tensile strength fabrics to the inner layers of composites, while high impact strength can be achieved by placing high impact strength fabrics to the outer layers of hybrid composites.
- It was also found that the tensile strengths of the jute/carbon fabric reinforced hybrid composite specimens (JCCJ) were close to the tensile strengths of the carbon fabric reinforced specimens and the impact strengths of the jute/E-glass fabric reinforced specimens (GJJG) were close to the those of the E-glass fabric reinforced specimens. This shows that E-glass and carbon fabric reinforced composite structures that are hybridized with jute fabric reinforcement, which considerably reduces both weight and cost, are highly suitable materials for the automotive industry.

- To the best of our knowledge, there are no studies on dynamic mechanical analysis of fabrics in the literature. The dynamic mechanical analysis of fabric structures that performed within the scope of this thesis is the first known study in this subject.
- The high storage and loss modulus values obtained from the dynamic mechanical analysis were achieved in the samples where high modulus fabric structures were placed on the outer layers of the composite material as well as in the impact strength results.
- There were some studies done with the addition of pristine MWCNT and MWCNT-NH_2 to improve the mechanical properties of composite samples in the literature, on the other hand according to our knowledge, there was no study on the benefits of MWCNT-OH and MWCNT-COOH for the modification of composites for this purpose. Taking into consideration of this fact, MWCNT-OH and MWCNT-COOH, which were not used in previous studies on textile reinforced composites, were used as nanofillers in order to understand their response in the material. Consequently, the results indicate that these nanofiller materials improve the mechanical properties of the composite structure, but it has been shown that pristine MWCNT gives better results than functionalized MWCNTs. Jute fiber contains free hydroxyl groups in its amorphous region and this gives jute fiber an anionic structure. Moreover, silica glass also contains hydroxyl groups and it was stated in the literature that acids and alkalis causes brittleness in E-glass fibers. The fact that anionic materials can not easily bond together could be the reason of achieving better results with pristine MWCNT treated samples.
- When the influence of MWCNT addition on the dynamic mechanical properties of composite material is examined, it is understood that these nanofiller materials decrease the storage moduli of composite materials and increase their loss moduli. The damping value, which is the ratio of the loss modulus to the storage modulus and an indicator of the adhesion of the matrix and reinforcing material in the composite structures, decreases with these changes in the moduli, showing that MWCNT addition strengthens the bonds in the composite structures.

- Besides improving the mechanical properties, MWCNTs are also seen to decrease the void ratio in the fabric reinforced composite materials.
- The results of TGA showed that the addition of nanofiller materials increased the degradation temperature of the composite structure to some extent, whereas DSC analysis results showed that the addition of MWCNTs did not lead to a change in the degradation temperature of the material.
- It has been understood that the replacement of the fabric layers in the composite structure has no effect on the thermal properties of the composite material.

It was considered that composite specimens developed within the scope of this thesis may find use in the automotive sector. Since the jute fabric reinforced specimens have lower mechanical properties than the others, it was thought that these composite structures can be used in automobile interior door panels, floor panels and glove compartments, while E-glass and carbon fabric reinforced composites are considered suitable for use in automobile exterior panels, drive shafts and leaf springs.

The main advantages that composite materials offer in the automotive applications are especially reducing the weight of the vehicle without comprising the safety issues which means “less energy”, “same or better safety” and “less CO_2 emission”. The main target of the automotive industry is to improve environmentally friendly, energy efficient and lighter vehicles, due to the rise in the fuel oil prices and growing awareness about carbon dioxide emission and global warming. Most of these problems have been overcome with the utilization of composite structures and also it is assumed that by developing innovative composite materials with enhanced properties will provide much more advantageous in the automotive industry.

This study and its results pave the way for several possibilities for future research. Some of the important ones are given below;

* Textile reinforced composite materials can be produced by using autoclave system instead of VARTM method, so that composite structures with higher mechanical properties can be obtained by applying high temperature and pressure.

* By modifying the amounts of MWCNT’s used, the effect on mechanical properties can be examined in the future studies.

* In the composite materials produced in this study all of the woven fabrics were placed in the same direction and as a result higher mechanical values were obtained along the warp direction of the fabrics. Taking this into consideration, thellll woven fabric layers can be placed in different directions within the composite structure, as in the case of unidirectional fabric reinforced composite material production, in order to obtain mechanical properties close to each other in both directions.

REFERENCES

Acha, B. A., Marcovich, N. E., & Reboredo, M. M. (2005). Physical and mechanical characterization of jute fabric composites. *Journal of Applied Polymer Science*, *98*(2), 639–650. https://doi.org/10.1002/app.22083

Advani, S. G., & Hsiao, K.-T. (2012). *Manufacturing techniques for polymer matrix composites (PMCs)*. Elsevier.

Agarwal, G., Patnaik, A., Sharma, R. kumar, & Agarwal, J. (2014). Effect of stacking sequence on physical, mechanical and tribological properties of glass-carbon hybrid composites. *Friction*, *2*(4), 354–364. https://doi.org/10.1007/s40544-014-0068-9

Ahmed, K. S., & Vijayarangan, S. (2006). Elastic property evaluation of jute-glass fibre hybrid composite using experimental and CLT approach. *IJEMS Vol.13(5) [October 2006]*. Retrieved from http://nopr.niscair.res.in/handle/123456789/7582

Ahmed, K. S., & Vijayarangan, S. (2007). Experimental characterization of woven jute-fabric-reinforced isothalic polyester composites. *Journal of Applied Polymer Science*, *104*(4), 2650–2662. https://doi.org/10.1002/app.25652

Ahmed, K. S., & Vijayarangan, S. (2008). Tensile, flexural and interlaminar shear properties of woven jute and jute-glass fabric reinforced polyester composites. *Journal of Materials Processing Technology*, *207*(1–3), 330–335. https://doi.org/10.1016/j.jmatprotec.2008.06.038

Ahmed, K. S., Vijayarangan, S., & Naidu, A. C. B. (2007). Elastic properties, notched strength and fracture criterion in untreated woven jute–glass fabric reinforced polyester hybrid composites. *Materials & Design*, *28*(8), 2287–2294. https://doi.org/10.1016/j.matdes.2006.08.002

Alavudeen, A., Rajini, N., Karthikeyan, S., Thiruchitrambalam, M., & Venkateshwaren, N. (2015). Mechanical properties of banana/kenaf fiber-reinforced hybrid polyester composites: Effect of woven fabric and random orientation. *Materials & Design (1980-2015)*, *66*, *Part A*, 246–257. https://doi.org/10.1016/j.matdes.2014.10.067

Alexopoulos, N. D., Bartholome, C., Poulin, P., & Marioli-Riga, Z. (2010). Structural health monitoring of glass fiber reinforced composites using embedded carbon nanotube (CNT) fibers. *Composites Science and Technology*, *70*(2), 260–271. https://doi.org/10.1016/j.compscitech.2009.10. 017

Alves, C., Dias, A. P. S., Diogo, A. C., Ferrão, P. M. C., Luz, S. M., Silva, A. J., … Freitas, M. (2011). Eco-composite: the effects of the jute fiber treatments on the mechanical and environmental performance of the composite materials. *Journal of Composite Materials*, *45*(5), 573–589. https://doi.org/10.1177/0021998310376111

Alves, C., Ferrão, P. M. C., Silva, A. J., Reis, L. G., Freitas, M., Rodrigues, L. B., & Alves, D. E. (2010). Ecodesign of automotive components making use of natural jute fiber composites. *Journal of Cleaner Production*, *18*(4), 313–327. https://doi.org/10.1016/j.jclepro.2009.10.022

Ammayappan, L., Nayak, L. K., Ray, D. P., Das, S., & Roy, A. K. (2013). Functional Finishing of Jute Textiles—An Overview in India. *Journal of Natural Fibers*, *10*(4), 390–413. https://doi.org/10.1080/15440478.2013 .824849

Araújo, A. L., Correia, J. R., & Soares, C. M. (2015). Mechanical Properties of Polypropylene Matrix Composites with Jute Fiber Fabric.

Ary Subagia, I. D. G., Kim, Y., Tijing, L. D., Kim, C. S., & Shon, H. K. (2014). Effect of stacking sequence on the flexural properties of hybrid composites reinforced with carbon and basalt fibers. *Composites Part B: Engineering*, *58*, 251–258. https://doi.org/10.1016/j.compositesb.2013.10.027

Ashworth, S., Rongong, J., Wilson, P., & Meredith, J. (2016). Mechanical and damping properties of resin transfer moulded jute-carbon hybrid composites. *Composites Part B: Engineering*, *105*, 60–66. https://doi.org/10.1016/j.compositesb.2016.08.019

Ataş, A. (2017). *Dokuma fiber takviyeli paralel pim delikli tabakalı polyester kompozit plakaların statik yük altındaki davranışlarının incelenmesi* (Master Thesis). Balıkesir University, Turkey.

Aziz, S. H., & Ansell, M. P. (2004). The effect of alkalization and fibre alignment on the mechanical and thermal properties of kenaf and hemp bast fibre composites: Part 1 – polyester resin matrix. *Composites Science and Technology*, *64*(9), 1219–1230. https://doi.org/10.1016/j.compscitech.2003. 10.001

Bakis, C. E., Bank, L. C., Brown, Vl., Cosenza, E., Davalos, J. F., Lesko, J. J., … Triantafillou, T. C. (2002). Fiber-reinforced polymer composites for construction—state of the art review. *Journal of Composites for Construction*, *6*(2), 73–87.

Balcioğlu, E., Kaya, M. T., Akyildiz, H. K., & Aktas, M. (2013). Kürleme Sıcaklığı ve Süresinin Dokuma Cam/Polyester Tabakalı Kompozitlerin Çekme Mukavemetlerine Etkisi. Presented at the II. Ulusal Ege Kompozit Malzemeler Sempozyumu, İzmir.

Baley, C. (2002). Analysis of the flax fibres tensile behaviour and analysis of the tensile stiffness increase. *Composites Part A: Applied Science and Manufacturing*, *33*(7), 939–948. https://doi.org/10.1016/S1359-835X(02)00040-4

Banerjee, S., & Sankar, B. V. (2014). Mechanical properties of hybrid composites using finite element method based micromechanics. *Composites Part B: Engineering*, *58*, 318–327. https://doi.org/10.1016/j.compositesb.2013.10.065

Begum, K., & Islam, M. (2013). Natural fiber as a substitute to synthetic fiber in polymer composites: a review. *Research J Eng Sci*, *2278*, 9472.

Behnia, S., Daghigh, V., Nikbin, K., Fereidoon, A., & Ghorbani, J. (2016). Influence of Stacking Sequence and Notch Angle on the Charpy Impact Behavior of Hybrid Composites. *Mechanics of Composite Materials*, *52*(4), 489–496. https://doi.org/10.1007/s11029-016-9599-7

Bekyarova, E., Thostenson, E. T., Yu, A., Kim, H., Gao, J., Tang, J., … Haddon, R. C. (2007). Multiscale Carbon Nanotube−Carbon Fiber Reinforcement for Advanced Epoxy Composites. *Langmuir*, *23*(7), 3970–3974. https://doi.org/10.1021/la062743p

Bernstein, R., & Carpi, A. (2015). Properties of Solids | Chemistry. Retrieved 23 December 2017, from https://www.visionlearning.com/en/library/Chemistry/1/Properties-of-Solids/209

Bilisik, K., & Yolacan, G. (2015). Short beam strength properties of multistitched biaxial woven E-glass/polyester nano composites. *Journal of Industrial Textiles*, *45*(2), 199–221. https://doi.org/10.1177/1528083714528017

Bily, M. A., Kwon, Y. W., & Pollak, R. D. (2010). Study of Composite Interface Fracture and Crack Growth Monitoring Using Carbon Nanotubes. *Applied Composite Materials*, *17*(4), 347–362. https://doi.org/10.1007/s10443-009-9124-4

Bindal, A., Singh, S., Batra, N. K., & Khanna, R. (2013). Development of glass/jute fibers reinforced polyester composite. *Indian Journal of Materials Science*, *2013*, 1–6.

Bingol, D., Tekin, N., & Alkan, M. (2010). Brilliant Yellow dye adsorption onto sepiolite using a full factorial design. *Applied Clay Science*, *50*(3), 315–321. https://doi.org/10.1016/j.clay.2010.08.015

Blackketter, D. M., Walrath, D. E., & Hansen, A. C. (1993). Modeling Damage in a Plain Weave Fabric-Reinforced Composite Material. *Journal of Composites, Technology and Research*, *15*(2), 136–142. https://doi.org/10.1520/ CTR10364J

Bodaghi, M., Cristóvão, C., Gomes, R., & Correia, N. C. (2016). Experimental characterization of voids in high fibre volume fraction composites processed by high injection pressure RTM. *Composites Part A: Applied Science and Manufacturing*, *82*, 88–99. https://doi.org/10.1016/j.compositesa.2015.11.042

Boroujeni, A. Y., Tehrani, M., Nelson, A. J., & Al-Haik, M. (2014). Hybrid carbon nanotube–carbon fiber composites with improved in-plane mechanical properties. *Composites Part B: Engineering*, *66*, 475–483. https://doi.org/10.1016/j.compositesb.2014.06.010

Bukhari, S. M., Kandasamy, J., & Hussain, M. M. (2017). Investigations on drilling process parameters of Hybrid Composites with different stacking sequence. *Materials Today: Proceedings*, *4*(2), 2184–2193.

Campbell, F. C. (2010). *Structural Composite Materials*. ASM International.

Cech, V., Palesch, E., & Lukes, J. (2013). The glass fiber–polymer matrix interface/interphase characterized by nanoscale imaging techniques. *Composites Science and Technology*, *83*(Supplement C), 22–26. https://doi.org/10.1016/j.compscitech.2013.04.014

Célino, A., Freour, S., Jacquemin, F., & Casari, P. (2014). The hygroscopic behavior of plant fibers: a review. *Frontiers in Chemistry*, *1*. https://doi.org/10.3389/fchem.2013.00043

Chambers, A. R., Earl, J. S., Squires, C. A., & Suhot, M. A. (2006). The effect of voids on the flexural fatigue performance of unidirectional carbon fibre composites developed for wind turbine applications. *International Journal of Fatigue*, *28*(10), 1389–1398. https://doi.org/10.1016/j.ijfatigue.2006.02.033

Chandrasekaran, V. C. S., Advani, S. G., & Santare, M. H. (2010). Role of processing on interlaminar shear strength enhancement of epoxy/glass fiber/multi-walled carbon nanotube hybrid composites. *Carbon*, *48*(13), 3692–3699. https://doi.org/10.1016/j.carbon.2010.06.010

Chen, X. L., & Liu, Y. J. (2004). Square representative volume elements for evaluating the effective material properties of carbon nanotube-based composites. *Computational Materials Science*, *29*(1), 1–11. https://doi.org/10.1016/S0927-0256(03)00090-9

Coleman, J. N., Khan, U., Blau, W. J., & Gun'ko, Y. K. (2006). Small but strong: A review of the mechanical properties of carbon nanotube–polymer composites. *Carbon*, *44*(9), 1624–1652. https://doi.org/10.1016/j.carbon. 2006.02.038

Composite materials guide: Resin Systems - Polyester Resins | NetComposites. (n.d.). Retrieved 24 November 2017, from https://netcomposites.com/guide-tools/guide/resin-systems/polyester-resins/

Cui, H., & Kessler, M. R. (2014). Pultruded glass fiber/bio-based polymer: Interface tailoring with silane coupling agent. *Composites Part A: Applied Science and Manufacturing*, *65*(Supplement C), 83–90. https://doi.org/10.1016/j.compositesa.2014.05.021

Das, S., & Bhowmick, M. (2015). Mechanical Properties of Unidirectional Jute-Polyester Composite. *Journal of Textile Science & Engineering*, *5*(4), 1–6. https://doi.org/10.4172/2165-8064.1000207

Demir, A., Seki, Y., Bozaci, E., Sarikanat, M., Erden, S., Sever, K., & Ozdogan, E. (2011). Effect of the atmospheric plasma treatment parameters on jute fabric: The effect on mechanical properties of jute fabric/polyester composites. *Journal of Applied Polymer Science*, *121*(2), 634–638. https://doi.org/10.1002/app.33220

Dicker, M. P. M., Duckworth, P. F., Baker, A. B., Francois, G., Hazzard, M. K., & Weaver, P. M. (2014). Green composites: A review of material attributes and complementary applications. *Composites Part A: Applied Science and Manufacturing*, *56*, 280–289. https://doi.org/10.1016/j.compositesa.2013.10.014

Díez-Pascual, A. M., Ashrafi, B., Naffakh, M., González-Domínguez, J. M., Johnston, A., Simard, B., … Gómez-Fatou, M. A. (2011). Influence of carbon nanotubes on the thermal, electrical and mechanical properties of poly(ether ether ketone)/glass fiber laminates. *Carbon*, *49*(8), 2817–2833. https://doi.org/10.1016/j.carbon.2011.03.011

Ding, Y. Q., Yan, Y., McIlhagger, R., & Brown, D. (1995). Comparison of the fatigue behaviour of 2-D and 3-D woven fabric reinforced composites. *Journal of Materials Processing Technology*, *55*(3), 171–177. https://doi.org/10.1016 /0924-0136(95)01950-2

Dittenber, D. B., & GangaRao, H. V. S. (2012). Critical review of recent publications on use of natural composites in infrastructure. *Composites Part A: Applied Science and Manufacturing*, *43*(8), 1419–1429. https://doi.org/10.1016/j.compositesa.2011.11.019

Doan, T.-T.-L., Brodowsky, H., & Mäder, E. (2012). Jute fibre/epoxy composites: Surface properties and interfacial adhesion. *Composites Science and Technology*, *72*(10), 1160–1166. https://doi.org/10.1016/j.compscitech.2012. 03.025

Donnet, J.-B., & Bansal, R. C. (1998). *Carbon Fibers, Third Edition,*. CRC Press.

Elanchezhian, C., Ramnath, B. V., & Hemalatha, J. (2014). Mechanical Behaviour of Glass and Carbon Fibre Reinforced Composites at Varying Strain Rates and Temperatures. *Procedia Materials Science*, *6*, 1405–1418. https://doi.org/10.1016/j.mspro.2014.07.120

Fan, Z., Santare, M. H., & Advani, S. G. (2008). Interlaminar shear strength of glass fiber reinforced epoxy composites enhanced with multi-walled carbon nanotubes. *Composites Part A: Applied Science and Manufacturing*, *39*(3), 540–554. https://doi.org/10.1016/j.compositesa.2007.11.013

Fisher, R. A., & others. (1949). The design of experiments. *The Design of Experiments.*, (Ed. 5).

Friedrich, K., & Almajid, A. A. (2013). Manufacturing Aspects of Advanced Polymer Composites for Automotive Applications. *Applied Composite Materials*, *20*(2), 107–128. https://doi.org/10.1007/s10443-012-9258-7

Gamze Karsli, N., Yesil, S., & Aytac, A. (2014). Effect of hybrid carbon nanotube/short glass fiber reinforcement on the properties of polypropylene composites. *Composites Part B: Engineering*, *63*, 154–160. https://doi.org/10.1016/j.compositesb.2014.04.006

Gassan, J., & Bledzki, A. K. (1997). The influence of fiber-surface treatment on the mechanical properties of jute-polypropylene composites. *Composites Part A: Applied Science and Manufacturing*, *28*(12), 1001–1005. https://doi.org/10.1016/S1359-835X(97)00042-0

Gassan, J., & Bledzki, A. K. (1999). Possibilities for improving the mechanical properties of jute/epoxy composites by alkali treatment of fibres. *Composites Science and Technology*, *59*(9), 1303–1309. https://doi.org/10.1016/S0266-3538(98)00169-9

Ghiasi, H., Fayazbakhsh, K., Pasini, D., & Lessard, L. (2010). Optimum stacking sequence design of composite materials Part II: Variable stiffness design. *Composite Structures*, *93*(1), 1–13. https://doi.org/10.1016/j.compstruct. 2010.06.001

Godara, A., Gorbatikh, L., Kalinka, G., Warrier, A., Rochez, O., Mezzo, L., … Verpoest, I. (2010). Interfacial shear strength of a glass fiber/epoxy bonding in composites modified with carbon nanotubes. *Composites*

Science and Technology, *70*(9), 1346–1352. https://doi.org/10.1016/j.compscitech.2010.04.010

Gojny, F. H., Wichmann, M. H. G., Fiedler, B., Bauhofer, W., & Schulte, K. (2005). Influence of nano-modification on the mechanical and electrical properties of conventional fibre-reinforced composites. *Composites Part A: Applied Science and Manufacturing*, *36*(11), 1525–1535. https://doi.org/10.1016/j.compositesa.2005.02.007

Gopinath, A., Kumar, M. S., & Elayaperumal, A. (2014). Experimental Investigations on Mechanical Properties Of Jute Fiber Reinforced Composites with Polyester and Epoxy Resin Matrices. *Procedia Engineering*, *97*, 2052–2063. https://doi.org/10.1016/j.proeng.2014.12.448

Gorowara, R. L., Kosik, W. E., McKnight, S. H., & McCullough, R. L. (2001). Molecular characterization of glass fiber surface coatings for thermosetting polymer matrix/glass fiber composites. *Composites Part A: Applied Science and Manufacturing*, *32*(3), 323–329. https://doi.org/10.1016/S1359-835X(00)00112-3

Gujjala, R., Ojha, S., Acharya, S. K., & Pal, S. K. (2014). Mechanical properties of woven jute–glass hybrid-reinforced epoxy composite. *Journal of Composite Materials*, *48*(28), 3445–3455. https://doi.org/10.1177/0021998313501924

Gupta, M. K., & Deep, V. (2017). Effect of Stacking Sequence on Flexural and Dynamic Mechanical Properties of Hybrid Sisal/Glass Polyester Composite. *American Journal of Polymer Science & Engineering*, *5*(1), 53–62.

Hagstrand, P.-O., Bonjour, F., & Månson, J.-A. E. (2005). The influence of void content on the structural flexural performance of unidirectional glass fibre reinforced polypropylene composites. *Composites Part A: Applied Science and Manufacturing*, *36*(5), 705–714. https://doi.org/10.1016/j.compositesa. 2004.03.007

Hameed, N., Sreekumar, P. A., Francis, B., Yang, W., & Thomas, S. (2007). Morphology, dynamic mechanical and thermal studies on poly(styrene-co-acrylonitrile) modified epoxy resin/glass fibre composites. *Composites Part A: Applied Science and Manufacturing*, *38*(12), 2422–2432. https://doi.org/10.1016/j.compositesa.2007.08.009

Hamouda, T., Hassanin, A. H., Kilic, A., Candan, Z., & Bodur, M. S. (2015). Hybrid composites from coir fibers reinforced with woven glass fabrics: Physical and mechanical evaluation. *Polymer Composites*, n/a-n/a. https://doi.org/10.1002/pc.23799

Haque, P., Barker, I. A., Parsons, A., Thurecht, K. J., Ahmed, I., Walker, G. S., … Irvine, D. J. (2010). Influence of compatibilizing agent molecular structure on the mechanical properties of phosphate glass fiber-reinforced PLA composites. *Journal of Polymer Science Part A: Polymer Chemistry*, *48*(14), 3082–3094. https://doi.org/10.1002/pola.24086

Hasan, K. F., Islam, M., Morshed, M. N., Iqbal, M. I. I., & Wu, J.-H. W. (2016). Dynamic mechanical behavior & analysis of the jute-glass fiber reinforced polyester hybrid composites. *American Journal of Applied Physics*, *1*(1), 1–12.

Hearle, J. W. (2001). *High-performance fibres*. Elsevier.

Holbery, J., & Houston, D. (2006). Natural-fiber-reinforced polymer composites in automotive applications. *JOM*, *58*(11), 80–86. https://doi.org/10.1007/s11837-006-0234-2

Horoschenkoff, A., & Christner, C. (2012). Carbon Fibre Sensor: Theory and Application. https://doi.org/10.5772/50504

Hossain, M. K., Hossain, M. E., Dewan, M. W., Hosur, M., & Jeelani, S. (2013). Effects of carbon nanofibers (CNFs) on thermal and interlaminar shear responses of E-glass/polyester composites. *Composites Part B: Engineering*, *44*(1), 313–320. https://doi.org/10.1016/j.compositesb.2012.05.006

Hosur, M. V., Adbullah, M., & Jeelani, S. (2005). Studies on the low-velocity impact response of woven hybrid composites. *Composite Structures*, *67*(3), 253–262. https://doi.org/10.1016/j.compstruct.2004.07.024

Huang, H., & Talreja, R. (2005). Effects of void geometry on elastic properties of unidirectional fiber reinforced composites. *Composites Science and Technology*, *65*(13), 1964–1981. https://doi.org/10.1016/j.compscitech.2005. 02.019

Ikbal, M. H., Ahmed, A., Qingtao, W., Shuai, Z., & Wei, L. (2016). Hybrid composites made of unidirectional T600S carbon and E-glass fabrics under quasi-static loading. *Journal of Industrial Textiles*, 1528083715624259. https://doi.org/10.1177/1528083715624259

Jabbar, A., Militký, J., Wiener, J., & Karahan, M. (2016). Static and dynamic mechanical properties of novel treated jute/green epoxy composites. *Textile Research Journal*, *86*(9), 960–974. https://doi.org/10.1177/004051751 5596936

Jabbar, A., Militký, J., Wiener, J., Madhukar Kale, B., Ali, U., & Rwawiire, S. (2017). Nanocellulose coated woven jute/green epoxy composites: Characterization of mechanical and dynamic mechanical behavior. *Composite Structures*, *161*, 340–349. https://doi.org/10.1016/j.compstruct.2016.11.062

Jawaid, M., & Abdul Khalil, H. P. S. (2011). Cellulosic/synthetic fibre reinforced polymer hybrid composites: A review. *Carbohydrate Polymers*, *86*(1), 1–18. https://doi.org/10.1016/j.carbpol.2011.04.043

Jawaid, M., Abdul Khalil, H. P. S., Hassan, A., Dungani, R., & Hadiyane, A. (2013). Effect of jute fibre loading on tensile and dynamic mechanical properties of oil palm epoxy composites. *Composites Part B: Engineering*, *45*(1), 619–624. https://doi.org/10.1016/j.compositesb.2012.04.068

Jawaid, M., Khalil, H. P. S. A., Bakar, A. A., & Khanam, P. N. (2011). Chemical resistance, void content and tensile properties of oil palm/jute fibre

reinforced polymer hybrid composites. *Materials & Design*, *32*(2), 1014–1019. https://doi.org/10.1016/j.matdes.2010.07.033

Jensen, R. E., & McKnight, S. H. (2006). Inorganic–organic fiber sizings for enhanced energy absorption in glass fiber-reinforced composites intended for structural applications. *Composites Science and Technology*, *66*(3), 509–521. https://doi.org/10.1016/j.compscitech.2005.06.004

Joseph, P. V., Joseph, K., Thomas, S., Pillai, C. K. S., Prasad, V. S., Groeninckx, G., & Sarkissova, M. (2003). The thermal and crystallisation studies of short sisal fibre reinforced polypropylene composites. *Composites Part A: Applied Science and Manufacturing*, *34*(3), 253–266. https://doi.org/10.1016/S1359-835X(02)00185-9

Jusoh, M. S. M., Santulli, C., Yahya, M. Y. M., Hussein, N. S., & Ahmad, H. A. I. (2016). Effect of Stacking Sequence on the Tensile and Flexural Properties of Glass Fibre Epoxy Composites Hybridized with Basalt, Flax or Jute Fibres. *Mater. Sci. Eng. Adv. Res*, *1*(4), 19–25.

Kaka, D. O., Rongong, J. A., Hodzic, A., & Lord, C. E. (2015). Dynamic mechanical properties of woven carbon fibre reinforced thermoplastic composite. In *Proceedings of the 20th International Conference on Composite Materials*. ICCM.

Karaduman, Y., & Onal, L. (2013). Dynamic mechanical and thermal properties of enzyme-treated jute/polyester composites. *Journal of Composite Materials*, *47*(19), 2361–2370. https://doi.org/10.1177/0021998312457885

Karapappas, P., Vavouliotis, A., Tsotra, P., Kostopoulos, V., & Palpetis, A. (2009). Enhanced Fracture Properties of Carbon Reinforced Composites by the Addition of Multi-Wall Carbon Nanotubes. *Journal of Composite Materials*. https://doi.org/10.1177/0021998308097735

Kargarzadeh, H., M. Sheltami, R., Ahmad, I., Abdullah, I., & Dufresne, A. (2015). Cellulose nanocrystal: A promising toughening agent for unsaturated polyester nanocomposite. *Polymer*, *56*(Supplement C), 346–357. https://doi.org/ 10.1016/j.polymer.2014.11.054

Kaufmann, A., Hampel, S., Rieger, C., Kunhardt, D., Schendel, D., Füssel, S., … Erdmann, K. (2017). Systematic evaluation of oligodeoxynucleotide binding and hybridization to modified multi-walled carbon nanotubes. *Journal of Nanobiotechnology*, *15*, 53. https://doi.org/10.1186/s12951-017-0288-z

Khan, J. A., Khan, M. A., Islam, R., & Gafur, A. (2010). Mechanical, Thermal and Interfacial Properties of Jute Fabric-Reinforced Polypropylene Composites: Effect of Potassium Dichromate. *Materials Sciences and Applications*, *01*(06), 350. https://doi.org/10.4236/msa.2010.16051

Khayyam, H., Fakhrhoseini, S. M., Church, J. S., Milani, A. S., Bab-Hadiashar, A., Jazar, R. N., & Naebe, M. (2017). Predictive modelling and optimization of carbon fiber mechanical properties through high temperature furnace. *Applied Thermal Engineering*, *125*(Supplement C), 1539–1554. https://doi.org/10.1016/j.applthermaleng.2017.06.071

Kim, H.-H., Kim, S.-Y., Kim, D.-H., Oh, C.-Y., & Jo, N.-J. (2014). Effect of Silane Coupling Agent on the Flexural Property of Glass Fiber Reinforced Composite Film. *Journal of Materials Science and Chemical Engineering*, *2*(10), 38.

Kim, J.-K., Sham, M.-L., Sohn, M.-S., & Hamada, H. (2001). Effect of hybrid layers with different silane coupling agents on impact response of glass fabric reinforced vinylester matrix composites. *Polymer*, *42*(17), 7455–7460. https://doi.org/10.1016/S0032-3861(01)00246-4

Ku, H., Wang, H., Pattarachaiyakoop, N., & Trada, M. (2011). A review on the tensile properties of natural fiber reinforced polymer composites. *Composites Part B: Engineering*, *42*(4), 856–873. https://doi.org/10.1016/j.compositesb. 2011.01.010

Lee, D. G., & Suh, N. P. (2006). *Axiomatic Design and Fabrication of Composite Structures: Applications in Robots, Machine Tools, and Automobiles*. Oxford University Press, USA.

Li, W., Dichiara, A., Zha, J., Su, Z., & Bai, J. (2014). On improvement of mechanical and thermo-mechanical properties of glass fabric/epoxy composites by incorporating CNT–Al 2 O 3 hybrids. *Composites Science and Technology*, *103*, 36–43.

Li, X., Tabil, L. G., & Panigrahi, S. (2007). Chemical Treatments of Natural Fiber for Use in Natural Fiber-Reinforced Composites: A Review. *Journal of Polymers and the Environment*, *15*(1), 25–33. https://doi.org/10.1007/s10924-006-0042-3

Liao, L., Wang, X., Fang, P., Liew, K. M., & Pan, C. (2011). Interface Enhancement of Glass Fiber Reinforced Vinyl Ester Composites with Flame-Synthesized Carbon Nanotubes and Its Enhancing Mechanism. *ACS Applied Materials & Interfaces*, *3*(2), 534–538. https://doi.org/10.1021/am101114t

Liu, L., Yu, J., Cheng, L., & Qu, W. (2009). Mechanical properties of poly(butylene succinate) (PBS) biocomposites reinforced with surface modified jute fibre. *Composites Part A: Applied Science and Manufacturing*, *40*(5), 669–674. https://doi.org/10.1016/j.compositesa.2009.03.002

Luo, W., Wang, X., Huang, R., & Fang, P. (2014). Interface enhancement of glass fiber/unsaturated polyester resin composites with nano-silica treated using silane coupling agent. *Wuhan University Journal of Natural Sciences*, *19*(1), 34–40. https://doi.org/10.1007/s11859-014-0975-7

Lv, G.-J., Wu, S.-B., & Lou, R. (2010). KINETIC STUDY FOR THE THERMAL DECOMPOSITION OF HEMICELLULOSE ISOLATED FROM CORN STALK. *BioResources*, *5*(2), 1281–1291. https://doi.org/10.15376/biores.5.2.1281-1291

Mallick, P. K. (2007). *Fiber-Reinforced Composites: Materials, Manufacturing, and Design, Third Edition*. CRC Press.

Manfredi, L. B., Rodríguez, E. S., Wladyka-Przybylak, M., & Vázquez, A. (2006). Thermal degradation and fire resistance of unsaturated polyester, modified acrylic resins and their composites with natural fibres.

Polymer Degradation and Stability, *91*(2), 255–261. https://doi.org/10.1016/j.polymdegradstab .2005.05.003

Manikandan Nair, K. C., Thomas, S., & Groeninckx, G. (2001). Thermal and dynamic mechanical analysis of polystyrene composites reinforced with short sisal fibres. *Composites Science and Technology*, *61*(16), 2519–2529. https://doi.org/10.1016/S0266-3538(01)00170-1

Mao Sheng Chang. (2010). An investigation on the dynamic behavior and thermal properties of MWCNTs/FRP laminate composites. *Journal of Reinforced Plastics and Composites*, *29*(24), 3593–3599. https://doi.org/10.1177/073168 4410379510

Mei, Z., & Chung, D. D. L. (2000). Glass transition and melting behavior of carbon fiber reinforced thermoplastic composite, studied by electrical resistance measurement. *Polymer Composites*, *21*(5), 711–715. https://doi.org/10.1002/pc.10224

Militký, J., & Jabbar, A. (2015). Comparative evaluation of fiber treatments on the creep behavior of jute/green epoxy composites. *Composites Part B: Engineering*, *80*, 361–368. https://doi.org/10.1016/j.compositesb.2015.06.014

Mishra, V., & Biswas, S. (2013). Physical and Mechanical Properties of Bi-directional Jute Fiber Epoxy Composites. *Procedia Engineering*, *51*, 561–566. https://doi.org/10.1016/j.proeng.2013.01.079

Misnon, M. I., Islam, M. M., Epaarachchi, J. A., & Lau, K. T. (2013). Textile material forms for reinforcement materials - a review. In *Third Malaysian Postgraduate Conference (MPC) 2013* (p. 105).

Mohan, K., & Rajmohan, T. (2017). Fabrication and Characterization of MWCNT Filled Hybrid Natural Fiber Composites. *Journal of Natural Fibers*, *14*(6), 864–874. https://doi.org/10.1080/15440478.2017.1300115

Mohanty, A. K., Khan, M. A., & Hinrichsen, G. (2000). Surface modification of jute and its influence on performance of biodegradable jute-fabric/Biopol composites. *Composites Science and Technology*, *60*(7), 1115–1124. https://doi.org/10.1016/S0266-3538(00)00012-9

Munikenche Gowda, T., Naidu, A. C. B., & Chhaya, R. (1999). Some mechanical properties of untreated jute fabric-reinforced polyester composites. *Composites Part A: Applied Science and Manufacturing*, *30*(3), 277–284. https://doi.org/10.1016/S1359-835X(98)00157-2

Murugan, R., Ramesh, R., & Padmanabhan, K. (2014). Investigation on Static and Dynamic Mechanical Properties of Epoxy Based Woven Fabric Glass/Carbon Hybrid Composite Laminates. *Procedia Engineering*, *97*, 459–468. https://doi.org/10.1016/j.proeng.2014.12.270

Murugan, R., Ramesh, R., Padmanabhan, K., Jeyaraam, R., & Krishna, S. (2014). Experimental investigation on static mechanical properties of glass/carbon hybrid woven fabric composite laminates. *Advanced Materials Research*, *903*, 96–101.

Norström, A., Watson, H., Engström, B., & Rosenholm, J. (2001). Treatment of E-glass fibres with acid, base and silanes. *Colloids and Surfaces A:*

Physicochemical and Engineering Aspects, *194*(1), 143–157. https://doi.org/10.1016/S0927-7757(01)00783-X

Ornaghi, H. L., Bolner, A. S., Fiorio, R., Zattera, A. J., & Amico, S. C. (2010). Mechanical and dynamic mechanical analysis of hybrid composites molded by resin transfer molding. *Journal of Applied Polymer Science*, *118*(2), 887–896. https://doi.org/10.1002/app.32388

Ornaghi Jr., H. L., da Silva, H. S. P., Zattera, A. J., & Amico, S. C. (2011). Hybridization effect on the mechanical and dynamic mechanical properties of curaua composites. *Materials Science and Engineering: A*, *528*(24), 7285–7289. https://doi.org/10.1016/j.msea.2011.05.078

Öztürk, N., & Kavak, D. (2004). Boron Removal from Aqueous Solutions by Adsorption on Waste Sepiolite and Activated Waste Sepiolite Using Full Factorial Design. *Adsorption*, *10*(3), 245–257. https://doi.org/10.1023/B:ADSO.0000046361.62180.c6

Pandita, S. D., Yuan, X., Manan, M. A., Lau, C. H., Subramanian, A. S., & Wei, J. (2013). Evaluation of jute/glass hybrid composite sandwich: Water resistance, impact properties and life cycle assessment. *Journal of Reinforced Plastics and Composites*, 0731684413505349. https://doi.org/10.1177/073 1684413505349

Pandya, K. S., Veerraju, C., & Naik, N. K. (2011). Hybrid composites made of carbon and glass woven fabrics under quasi-static loading. *Materials & Design*, *32*(7), 4094–4099. https://doi.org/10.1016/j.matdes.2011.03.003

Park, S.-J., & Jin, J.-S. (2001). Effect of Silane Coupling Agent on Interphase and Performance of Glass Fibers/Unsaturated Polyester Composites. *Journal of Colloid and Interface Science*, *242*(1), 174–179. https://doi.org/10.1006/jcis.2001.7788

Patel, V. A., Bhuva, B. D., & Parsania, P. H. (2008). Performance Evaluation of Treated–Untreated Jute–Carbon and Glass–Carbon Hybrid Composites of Bisphenol-C based Mixed Epoxy–Phenolic Resins. *Journal of Reinforced Plastics and Composites*. https://doi.org/10.1177/0731684408093973

Peterson, A. M., Jensen, R. E., & Palmese, G. R. (2011). Thermoreversible and remendable glass–polymer interface for fiber-reinforced composites. *Composites Science and Technology*, *71*(5), 586–592. https://doi.org/10.1016/j.compscitech.2010.11.022

Pıhtılı, H., & Tosun, N. (2002). Investigation of the wear behaviour of a glass-fibre-reinforced composite and plain polyester resin. *Composites Science and Technology*, *62*(3), 367–370. https://doi.org/10.1016/S0266-3538(01)00196-8

Plotnichenko, V. G., Sokolov, V. O., & Dianov, E. M. (2000). Hydroxyl groups in high-purity silica glass. *Journal of Non-Crystalline Solids*, *261*(1), 186–194. https://doi.org/10.1016/S0022-3093(99)00654-7

Portella, E. H., Romanzini, D., Angrizani, C. C., Amico, S. C., Zattera, A. J., Portella, E. H., … Zattera, A. J. (2016). Influence of Stacking

Sequence on the Mechanical and Dynamic Mechanical Properties of Cotton/Glass Fiber Reinforced Polyester Composites. *Materials Research*, *19*(3), 542–547. https://doi.org/10.1590/1980-5373-MR-2016-0058

Pothan, L. A., Oommen, Z., & Thomas, S. (2003). Dynamic mechanical analysis of banana fiber reinforced polyester composites. *Composites Science and Technology*, *63*(2), 283–293. https://doi.org/10.1016/S0266-3538(02)00254-3

Protz, R., Kosmann, N., Gude, M., Hufenbach, W., Schulte, K., & Fiedler, B. (2015). Voids and their effect on the strain rate dependent material properties and fatigue behaviour of non-crimp fabric composites materials. *Composites Part B: Engineering*, *83*, 346–351. https://doi.org/10.1016/j.compositesb .2015.08.018

Puska, M., Zhang, M., Matinlinna, J. P., & Vallittu, P. K. (2014). Silane-Treated E-Glass Fiber-Reinforced Telechelic Macromer-Based Polymer-Matrix Composites. *Silicon*, *6*(1), 57–63. https://doi.org/10.1007/s12633-013-9155-1

Qiu, J., Zhang, C., Wang, B., & Liang, R. (2007). Carbon nanotube integrated multifunctional multiscale composites. *Nanotechnology*, *18*(27), 275708. https://doi.org/10.1088/0957-4484/18/27/275708

Raghavendra, G., Kumar, K. A., Kumar, M. H., RaghuKumar, B., & Ojha, S. (2015). Moisture absorption behavior and its effect on the mechanical properties of jute-reinforced epoxy composite. *Polymer Composites*, n/a-n/a. https://doi.org/10.1002/pc.23610

Rajesh, M., Jeyaraj, P., & Rajini, N. (2016). Mechanical, Dynamic Mechanical and Vibration Behavior of Nanoclay Dispersed Natural Fiber Hybrid Intra-ply Woven Fabric Composite. In M. Jawaid, A. el K. Qaiss, & R. Bouhfid (Eds.), *Nanoclay Reinforced Polymer Composites* (pp. 281–296). Singapore: Springer Singapore. Retrieved from http://link.springer.com/10.1007/978-981-10-0950-1_12

Ramesh, M., Palanikumar, K., & Reddy, K. H. (2013a). Comparative Evaluation on Properties of Hybrid Glass Fiber- Sisal/Jute Reinforced Epoxy Composites. *Procedia Engineering*, *51*, 745–750. https://doi.org/10.1016/j.proeng .2013.01.106

Ramesh, M., Palanikumar, K., & Reddy, K. H. (2013b). Mechanical property evaluation of sisal–jute–glass fiber reinforced polyester composites. *Composites Part B: Engineering*, *48*, 1–9. https://doi.org/10.1016/j.compositesb.2012.12.004

Ray, D., Sarkar, B. K., Rana, A. K., & Bose, N. R. (2001). Effect of alkali treated jute fibres on composite properties. *Bulletin of Materials Science*, *24*(6), 129–135.

Rodrigues, E. F., Maia, T. F., & Mulinari, D. R. (2011). Tensile strength of polyester resin reinforced sugarcane bagasse fibers modified by estherification. *Procedia Engineering*, *10*, 2348–2352. https://doi.org/10.1016/j.proeng.2011.04.387

Roe, P. J., & Ansell, M. P. (1985). Jute-reinforced polyester composites. *Journal of Materials Science*, *20*(11), 4015–4020. https://doi.org/10.1007/BF00552393

Romanzini, D., Lavoratti, A., Ornaghi Jr., H. L., Amico, S. C., & Zattera, A. J. (2013). Influence of fiber content on the mechanical and dynamic mechanical properties of glass/ramie polymer composites. *Materials & Design*, *47*, 9–15. https://doi.org/10.1016/j.matdes.2012.12.029

Russo, P., Acierno, D., Simeoli, G., Iannace, S., & Sorrentino, L. (2013). Flexural and impact response of woven glass fiber fabric/polypropylene composites. *Composites Part B: Engineering*, *54*, 415–421. https://doi.org/10.1016/j. compositesb.2013.06.016

Saha, A. K., Das, S., Bhatta, D., & Mitra, B. C. (1999). Study of jute fiber reinforced polyester composites by dynamic mechanical analysis. *Journal of Applied Polymer Science*, *71*(9), 1505–1513.

Sapuan, S. M., & Maleque, M. A. (2005). Design and fabrication of natural woven fabric reinforced epoxy composite for household telephone stand. *Materials & Design*, *26*(1), 65–71. https://doi.org/10.1016/j.matdes.2004.03.015

Seyhan, A. T., Gojny, F. H., Tanoğlu, M., & Schulte, K. (2007). Critical aspects related to processing of carbon nanotube/unsaturated thermoset polyester nanocomposites. *European Polymer Journal*, *43*(2), 374–379. https://doi.org/10.1016/j.eurpolymj.2006.11.018

Sezgin, H., & Berkalp, O. B. (2016). The effect of hybridization on significant characteristics of jute/glass and jute/carbon-reinforced composites. *Journal of Industrial Textiles*. https://doi.org/10.1177/1528083716644290

Shah, D. U. (2013). Developing plant fibre composites for structural applications by optimising composite parameters: a critical review. *Journal of Materials Science*, *48*(18), 6083–6107. https://doi.org/10.1007/s10853-013-7458-7

Shah, D. U., Schubel, P. J., Licence, P., & Clifford, M. J. (2012). Determining the minimum, critical and maximum fibre content for twisted yarn reinforced plant fibre composites. *Composites Science and Technology*, *72*(15), 1909–1917. https://doi.org/10.1016/j.compscitech.2012.08.005

Shahinur, S., Hasan, M., Ahsan, Q., Saha, D. K., & Islam, M. S. (2015). Characterization on the Properties of Jute Fiber at Different Portions. *International Journal of Polymer Science*, *2015*, e262348. https://doi.org/10.1155/2015/262348

Shalin, R. E. (2012). *Polymer Matrix Composites*. Springer Science & Business Media.

Shanmugam, D., & Thiruchitrambalam, M. (2013). Static and dynamic mechanical properties of alkali treated unidirectional continuous Palmyra Palm Leaf Stalk Fiber/jute fiber reinforced hybrid polyester composites. *Materials & Design*, *50*, 533–542. https://doi.org/10.1016/j.matdes.2013.03.048

Shen, Z., Bateman, S., Wu, D. Y., McMahon, P., Dell'Olio, M., & Gotama, J. (2009). The effects of carbon nanotubes on mechanical and thermal properties of woven glass fibre reinforced polyamide-6 nanocomposites. *Composites Science and Technology*, *69*(2), 239–244. https://doi.org/10.1016/j. compscitech.2008.10.017

Shokrieh, M. M., Saeedi, A., & Chitsazzadeh, M. (2013). Mechanical properties of multi-walled carbon nanotube/polyester nanocomposites. *Journal of Nanostructure in Chemistry*, *3*(1), 20. https://doi.org/10.1186/2193-8865-3-20

Simsek, Y., Ozyuzer, L., Seyhan, A. T., Tanoglu, M., & Schulte, K. (2007). Temperature dependence of electrical conductivity in double-wall and multi-wall carbon nanotube/polyester nanocomposites. *Journal of Materials Science*, *42*(23), 9689–9695. https://doi.org/10.1007/s10853-007-1943-9

Sinha, E., & Rout, S. K. (2009). Influence of fibre-surface treatment on structural, thermal and mechanical properties of jute fibre and its composite. *Bulletin of Materials Science*, *32*(1), 65. https://doi.org/10.1007/s12034-009-0010-3

Smole, M. S., Hribernik, S., Kleinschek, K. S., & Kreže, T. (2013). Plant Fibres for Textile and Technical Applications. https://doi.org/10.5772/52372

Song, J. H. (2016). Bending properties of carbon/glass and carbon/aramid fabric composites with various stacking structures by the VARTM method. *Fibers and Polymers*, *17*(4), 600–607. https://doi.org/10.1007/s12221-016-5931-z

Song, Y. S., Lee, J. T., Ji, D. S., Kim, M. W., Lee, S. H., & Youn, J. R. (2012). Viscoelastic and thermal behavior of woven hemp fiber reinforced poly(lactic acid) composites. *Composites Part B: Engineering*, *43*(3), 856–860. https://doi.org/10.1016/j.compositesb.2011.10.021

Spitalsky, Z., Tasis, D., Papagelis, K., & Galiotis, C. (2010). Carbon nanotube–polymer composites: Chemistry, processing, mechanical and electrical properties. *Progress in Polymer Science*, *35*(3), 357–401. https://doi.org/10.1016/j.progpolymsci.2009.09.003

Sreekala, M. S., George, J., Kumaran, M. G., & Thomas, S. (2002). The mechanical performance of hybrid phenol-formaldehyde-based composites reinforced with glass and oil palm fibres. *Composites Science and Technology*, *62*(3), 339–353. https://doi.org/10.1016/S0266-3538(01)00219-6

Su, F.-H., Zhang, Z.-Z., Wang, K., Jiang, W., Men, X.-H., & Liu, W.-M. (2006). Friction and wear properties of carbon fabric composites filled with nano-Al2O3 and nano-Si3N4. *Composites Part A: Applied Science and Manufacturing*, *37*(9), 1351–1357. https://doi.org/10.1016/j.compositesa .2005.08.017

Suhas, Gupta, V. K., Carrott, P. J. M., Singh, R., Chaudhary, M., & Kushwaha, S. (2016). Cellulose: A review as natural, modified and activated carbon adsorbent. *Bioresource Technology*, *216*(Supplement C), 1066–1076. https://doi.org/10.1016/j.biortech.2016.05.106

Tajvidi, M., Falk, R. H., & Hermanson, J. C. (2006). Effect of natural fibers on thermal and mechanical properties of natural fiber polypropylene composites studied by dynamic mechanical analysis. *Journal of Applied Polymer Science*, *101*(6), 4341–4349. https://doi.org/10.1002/app.24289

Tejyan, S., Patnaik, A., & Singh, T. (2013). Effect of fibre weight percentage on thermo-mechanical properties of needle punched nonwoven reinforced polymer composites. *InternatIonal Journal of Research in MechanIcal EngIneerIng & Technology*, *3*(2), 41–44.

Thomas, S., Joseph, K., Malhotra, S. K., Goda, K., & Sreekala, M. S. (2012). *Polymer Composites: Macro- and Microcomposites*. Hoboken, GERMANY: John Wiley & Sons, Incorporated. Retrieved from http://ebookcentral.proquest.com/lib/itup/detail.action?docID=867652

Thostenson, E. T., Ren, Z., & Chou, T.-W. (2001). Advances in the science and technology of carbon nanotubes and their composites: a review. *Composites Science and Technology*, *61*(13), 1899–1912. https://doi.org/10.1016/S0266-3538(01)00094-X

Thwe, M. M., & Liao, K. (2003). Durability of bamboo-glass fiber reinforced polymer matrix hybrid composites. *Composites Science and Technology*, *63*(3), 375–387. https://doi.org/10.1016/S0266-3538(02)00225-7

Tripathy, S. S., Di Landro, L., Fontanelli, D., Marchetti, A., & Levita, G. (2000). Mechanical properties of jute fibers and interface strength with an epoxy resin. *Journal of Applied Polymer Science*, *75*(13), 1585–1596. https://doi.org/10.1002/(SICI)1097-4628(20000328)75:13<1585::AID-APP4>3.0.CO;2-Q

Tugrul Seyhan, A., Tanoglu, M., & Schulte, K. (2008). Mode I and mode II fracture toughness of E-glass non-crimp fabric/carbon nanotube (CNT) modified polymer based composites. *Engineering Fracture Mechanics*, *75*(18), 5151–5162. https://doi.org/10.1016/j.engfracmech.2008.08.003

Tzounis, L. (2014, July 2). *Glass and Jute fibers modified with CNT-based functional coatings for high performance composites*. University of Ioannina & Aristotle University of Thessaloniki.

Unterweger, C., Brüggemann, O., & Fürst, C. (2014). Synthetic fibers and thermoplastic short-fiber-reinforced polymers: Properties and characterization. *Polymer Composites*, *35*(2), 227–236. https://doi.org/10.1002/pc.22654

Varga, C., Miskolczi, N., Bartha, L., & Lipóczi, G. (2010). Improving the mechanical properties of glass-fibre-reinforced polyester composites by modification of fibre surface. *Materials & Design*, *31*(1), 185–193. https://doi.org/10.1016/j.matdes.2009.06.034

Wang, R.-M., Zheng, S.-R., & Zheng, Y.-P. (2011a). Elementary mechanical properties of composite materials. In *Polymer Matrix Composites and Technology* (pp. 357–548). Woodhead Publishing. https://doi.org/10.1533/9780857092229.3.357

Wang, R.-M., Zheng, S.-R., & Zheng, Y.-P. (2011b). Interface of polymer matrix composites. In *Polymer Matrix Composites and Technology* (pp. 169–548). Woodhead Publishing. https://doi.org/10.1533/9780857092229.1.169

Wang, R.-M., Zheng, S.-R., & Zheng, Y.-P. (2011c). Other mechanical properties of composite materials. In *Polymer Matrix Composites and Technology* (pp. 455–548). Woodhead Publishing. https://doi.org/10.1533/9780857092229.3.455

Warrier, A., Godara, A., Rochez, O., Mezzo, L., Luizi, F., Gorbatikh, L., … Verpoest, I. (2010). The effect of adding carbon nanotubes to glass/epoxy composites in the fibre sizing and/or the matrix. *Composites Part A: Applied Science and Manufacturing*, *41*(4), 532–538. https://doi.org/10.1016/j. compositesa.2010.01.001

Wu, H. F., Dwight, D. W., & Huff, N. T. (1997). Effects of silane coupling agents on the interphase and performance of glass-fiber-reinforced polymer composites. *Composites Science and Technology*, *57*(8), 975–983. https://doi.org/10.1016/S0266-3538(97)00033-X

Yang, H., Yan, R., Chen, H., Lee, D. H., & Zheng, C. (2007). Characteristics of hemicellulose, cellulose and lignin pyrolysis. *Fuel*, *86*(12–13), 1781–1788. https://doi.org/10.1016/j.fuel.2006.12.013

Yang, S., Taha-Tijerina, J., Serrato-Diaz, V., Hernandez, K., & Lozano, K. (2007). Dynamic mechanical and thermal analysis of aligned vapor grown carbon nanofiber reinforced polyethylene. *Composites Part B: Engineering*, *38*(2), 228–235. https://doi.org/10.1016/j.compositesb.2006.04.003

Yasar, I., & Aslan, F. (2000). Cam Elyaf Takviyeli Polyester Matrisli Kompozitlerde Elyaf Hacim Oranı ve Elyaf Doğrultusunun Tribolojik Özelliklere Etkisi. *Turkish Journal of Engineering and Environmental Sciences*, *24*(181–191).

Zhang, J., Chaisombat, K., He, S., & Wang, C. H. (2012). Hybrid composite laminates reinforced with glass/carbon woven fabrics for lightweight load bearing structures. *Materials & Design (1980-2015)*, *36*, 75–80. https://doi.org/10.1016/j.matdes.2011.11.006

Zhang, J., Zhuang, R., Liu, J., Mäder, E., Heinrich, G., & Gao, S. (2010). Functional interphases with multi-walled carbon nanotubes in glass fibre/epoxy composites. *Carbon*, *48*(8), 2273–2281. https://doi.org/10.1016/j.carbon.2010.03.001

Zhang, L., & Miao, M. (2010). Commingled natural fibre/polypropylene wrap spun yarns for structured thermoplastic composites. *Composites Science and Technology*, *70*(1), 130–135. https://doi.org/10.1016/j.compscitech.2009.09.016

Zhang, X., Wang, P., Neo, H., Lim, G., Malcolm, A. A., Yang, E.-H., & Yang, J. (2016). Design of glass fiber reinforced plastics modified with CNT and pre-stretching fabric for potential sports instruments. *Materials & Design*, *92*(Supplement C), 621–631. https://doi.org/10.1016/j.matdes.2015.12.051

Zhao, Z., Teng, K., Li, N., Li, X., Xu, Z., Chen, L., … Liu, Y. (2017). Mechanical, thermal and interfacial performances of carbon fiber reinforced composites flavored by carbon nanotube in matrix/interface. *Composite Structures*, *159*(Supplement C), 761–772. https://doi.org/10.1016/j.compstruct.2016.10. 022

Zhou, A., & Keller, T. (2005). Structural responses of FRP elements under combined thermal and mechanical loadings: experiments and analyses. Presented at the Fourth International Conference on Composites in Fire (CIF-4), New Castle, UK. Retrieved from https://infoscience.epfl.ch/record/109228

Zhu, J., Imam, A., Crane, R., Lozano, K., Khabashesku, V. N., & Barrera, E. V. (2007). Processing a glass fiber reinforced vinyl ester composite with nanotube enhancement of interlaminar shear strength. *Composites Science and Technology*, *67*(7–8), 1509–1517. https://doi.org/10.1016/j.compscitech.2006. 07.018

Zhu, P., Sui, S., Wang, B., Sun, K., & Sun, G. (2004). A study of pyrolysis and pyrolysis products of flame-retardant cotton fabrics by DSC, TGA, and PY–GC–MS. *Journal of Analytical and Applied Pyrolysis*, *71*(2), 645–655. https://doi.org/10.1016/j.jaap.2003.09.005

CURRICULUM VITAE

Name Surname **:** Hande SEZGİN

Place and Date of Birth **:** Trabzon, 11.08.1986

E-Mail **:** sezginh@itu.edu.tr

EDUCATION **:**

- **B.Sc.** **:** 2009, Istanbul Technical University, Textile Technologies and Design Faculty, Textile Engineering Department
- **M.Sc.** **:** 2012, Istanbul Technical University, Textile Technologies and Design Faculty, Textile Engineering Department

PROFESSIONAL EXPERIENCE AND REWARDS:

- 2011-2018, Research Assistant at Textile Technologies and Design Faculty in Istanbul Technical University.

PUBLICATIONS, PRESENTATIONS AND PATENTS ON THE THESIS:

Book Chapters

- **Sezgin H.,** Berkalp O.B. 2018. Textile Reinforced Composites for Automotive Industry, *Composites and Advanced Materials for Industrial Applications*, IGI Global (in press).

Articles

- **Sezgin H.,** Berkalp O.B. 2017. Analysis of the effects of fabric reinforcement parameters on the mechanical properties of textile-based hybrid composites by full factorial experimental design method, *Journal of Industrial Textiles*, doi: 10.1177/1528083717740764.

- **Sezgin H.,** Berkalp O.B., Mishra R., Militky J. 2017. Examination of the Thermo-mechanical Properties of E-Glass/Carbon Composites, *Tekstilec*, 60(4), 263-268.
- **Sezgin H.,** Berkalp O.B., Mishra R., Militky J. 2017. Thermo-mechanical Analysis of Jute, E-glass and Carbon Fabrics, Çukurova Üniversitesi Mühendislik Mimarlık Fakültesi Dergisi, 32(2), 183-194.
- **Sezgin H.,** Berkalp O.B. 2016. The Effect of Hybridization on Significant Characteristics of Jute/Glass and Jute/Carbon-Reinforced Composites, *Journal of Industrial Textiles*, doi: 10.1177/1528083716644290.
- **Sezgin H.,** Yalçın Eniş İ., Berkalp O.B. 2016. The Impact Of Biaxial Square Woven Jute Fabric Reinforcement on The Mechanical Performance pf Polyester Based Composites, *Indian Journal of Fiber and Textile Research* (accepted as short communication).

Presentations

- **Sezgin H.,** Berkalp O.B., Mishra R., Militky J. 2017: Effect Of Different Stacking Sequences Of Fabric Plies On The Thermo-Mechanical Properties Of Hybrid Composites, XIVth International Izmir Textile and Apparel Symposium, October 26-28, 2017 İzmir, Turkey.
- **Sezgin H.,** Berkalp O. B., Mishra R., Militky J. 2016: Investigation of Dynamic Mechanical Properties of Jute/Carbon Reinforced Composites, ICCM 2016 :18th International Conference on Composite Materials, December 26-27, 2016 Dubai, BAE.
- Berkalp O.B., **Sezgin H.,** Mishra R., Militky J. 2016: Dynamic Mechanical Analysis of Jute/E-Glass Composite Structures, CHEMTECH 16/ 4th International Chemical Engineering and Technologies Conference, November 17-18, 2016 Istanbul, Turkey.
- **Sezgin H.,** Berkalp O. B. 2015: Examination of Stacking Sequence Effect on Mechanical Properties of Woven Glass/Jute Hybrid Composites, 5th International Istanbul Textile Congress 2015: Innovative Technologies "Inspire to Innovate", September 11-12, 2015 Istanbul, Turkey.
- **Sezgin H.,** Berkalp OB. 2015: Investigation of the Mechanical Properties of Glass/Carbon Hybrid Composites, Applied Mechanics and Materials Conference, June 29 - July 1, 2015 Seattle, Washington, ABD.
- **Sezgin H.,** Berkalp O. B. 2015: Mechanical Properties of Woven Jute-Glass Hybrid Composites, 15th AUTEX World Textile Conference, June 10-12, 2015 Bucharest, Romania.

OTHER PUBLICATIONS, PRESENTATIONS AND PATENTS:

Book Chapters

- Yalçın Eniş İ., Küçükali Öztürk M., **Sezgin H.** 2017. Textile Waste Production, Treatment and Recycling, Environmental Chemistry for a Sustainable World, Springer (in press).

Articles

- Yalçın Eniş İ., **Sezgin H.,** Gök Sadıkoğlu T. 2017. Full Factorial Experimental Design for Mechanical Properties of Electrospun Vascular Grafts, *Journal of Industrial Textiles*, doi: 10.1177/1528083717690614.
- Yalcin Enis I., Kucukali Ozturk M., **Sezgin H.,** Ismar E., 2017. An Overview of Nanotoxicology, *Engineering Sciences*, 12(1), 57-65, doi:10.12739/NWSA. 2017.12.1.1A0373.
- **Sezgin H.,** Kurşun Bahadır S., Böke Y. E., Kalaoğlu F. 2015. Investigation of Heating Behaviour of E-textile Structures, *International Journal of Environmental, Chemical, Ecological, Geological and Geophysical Engineering*, 9(5), 474-477.
- **Sezgin H.,** Kurşun Bahadır S., Böke Y. E., Kalaoğlu F. 2014. Thermal analysis of e-textile structures using full-factorial experimental design method, *Journal of Industrial Textiles*, doi: 10.1177/1528083714540699.
- **Sezgin H.,** Yalçın I., Berkalp Ö. B. 2012. Re-evaluation of Cotton and E-glass Fibre Wastes in The Manufacture of Hybrid Composites. *Journal of International Scientific Publications: Materials Methods & Technology*, 6(2), 296-302.
- **Sezgin H.,** Yalçın I., Küçükali Öztürk M., Kızıldağ N. 2012. Nanomaterials In Textile Applications. *Journal of International Scientific Publications: Materials Methods & Technology*, 6(2), 303-317.
- **Sezgin H.,** Civelek O., Suvari H. O., Kalaoğlu F. 2009. Altı Sigma Araçları ile Bir Üretim Bandında Verimlilik Analizi- Efficiency Analysis of a Production Line With Six Sigma Tools, *Tekstil Teknoloji*, 14 (161) 72-81.

Presentations

- Yalçın Eniş I., Kızıldağ N., Küçükali Öztürk M., **Sezgin H.** 2017: Fibrous Scaffolds For Peripheral Nerve Regeneration, 3rd International Congress On Healthcare And Medical Textiles, October 26-28, 2017 Izmir, Turkey.
- **Sezgin H.,** Küçükali Öztürk M., Kızıldağ N., Yalçın Eniş I. 2017: Textile Based Materials For Wound Healing Applications, 3rd International Congress On Healthcare And Medical Textiles, 26-28 Ekim 2017, Izmir, Turkey.
- Yalçın Eniş I., **Sezgin H.** 2015: Spider Silk in Textile Industry, Advances in Material Engineering, December 1-2, 2015 Liberec, Czech Republic.
- Kucukali Ozturk, M., Yalcin Enis, I., Kizildag, N., **Sezgin H.** 2015: Ekolojik Tekstillerin Bebek Giysilerindeki Önemi, 15. Tekstil Teknolojisi ve Kimyasındaki Son Gelişmeler Sempozyumu, May 14-16, 2015 Bursa, Turkey.
- Kizildag, N., **Sezgin H.,** Kucukali Ozturk, M., Yalcin Enis, I. 2015: Nanoiplikler, 15. Tekstil Teknolojisi ve Kimyasındaki Son Gelişmeler Sempozyumu, May 14-16, 2015 Bursa, Turkey .
- **Sezgin H.,** Kizildag, N., Yalcin Enis, I., Kucukali Ozturk, M. 2015: Tıbbi Tekstillerde Nanoteknoloji, 15. Tekstil Teknolojisi ve Kimyasındaki Son Gelişmeler Sempozyumu, May 14-16, 2015 Bursa, Turkey.

- Yalcin Enis, I., **Sezgin H.,** Kucukali Ozturk, M., Kizildag, N. 2015: Tekstil Sektöründe Organik Pamuk, 15. Tekstil Teknolojisi ve Kimyasındaki Son Gelişmeler Sempozyumu, May 14-16, 2015 Bursa, Turkey.
- **Sezgin H.,** Yalçın I., Gocek, I., Berkalp O. B. 2014: Design of a Flame Retardant Tubular Woven Cloth Construction, 14th AUTEX World Textile Conference, May 26-28, 2014 Bursa, Turkey.
- Yalçın İ., **Sezgin H.,** Gok Sadıkoğlu T., Berkalp O. B. 2014: Comfort and Mechanical Performance Analysis of Spunlaced Nonwoven Fabrics, 14th AUTEX World Textile Conference, May 26-28, 2014 Bursa, Turkey.
- **Sezgin H.,** Yalçın I., Gok Sadıkoğlu T., Berkalp O. B. 2014: Design of a Composite Reinforced with Shredded Cotton Fabric Wastes, The Fiber Society Spring 2014, May 21-23, 2014 Liberec, Czech Republic.
- Yalçın I., **Sezgin H.,** Gok Sadıkoğlu T., Berkalp O. B. 2014: The Use of Nonwovens as Capillary Mineral Bags for Indoor Landscaping, The Fiber Society Spring 2014, May 21-23, 2014 Liberec, Czech Republic.
- **Sezgin H.,** Yalçın I., Berkalp O. B., Ozcan, G., Gok Sadıkoğlu T. 2014: Design of a UV-Protected Nonwoven Fabric with Anti-mosquito Property, Nanotech MEETs Tunusia, April 23-27, 2014 Tunusia.
- **Sezgin H.,** Yalcin I, Kizildag N., Kucukali Ozturk M. 2013: Horn As A Biomaterial, AMWC, 2013, Izmir, Turkey.
- Kucukali Ozturk M., **Sezgin H.,** Yalcin I, Kizildag N. 2013: Sound Absorption Materials, AMWC, 2013, Izmir, Turkey.
- Yalcin I, Kizildag N., Kucukali Ozturk M., **Sezgin H.** 2013: Biomaterials For The Construction of Vascular Grafts, AMWC, 2013, Izmir, Turkey.
- Kizildag N., Kucukali Ozturk M., **Sezgin H.,** Yalcin I. 2013: Applications of Electrospun Silk Fibroin Nanowebs, Sound Absorption Materials, AMWC, 2013, Izmir, Turkey.
- **Sezgin H.,** Kursun Bahadir S., Böke Y. E., Kalaoğlu F., 2013: Thermal Profile Analysis of E-textile Structures, The International Istanbul Textile Congress, 2013, Istanbul, Turkey.
- **Sezgin H.,** Yalcin I., Iridag Beceren Y., Berkalp O. B. 2012: Electrospinning of Polyacrylonitrile (PAN) Nanofibers: Optimization of Process Parameters with Full Factorial Experimental Design, 7th Central European Conference, September 15-17, 2012 Portorose, Slovenia.
- Yalcin I., Gok Sadikoglu T., **Sezgin H.,** Berkalp O. B. 2012: Design of a Tea Tray from Textile Waste Reinforced Composite, 7th Central European Conference, September 15-17, 2012 Portorose, Slovenia.
- **Sezgin H.,** Kursun Bahadir S., Böke Y. E., Kalaoğlu F. 2012: Effect of Different Conductive Yarns on Heating Behaviour of Fabrics, The 4th RMUTP International Conference: Textiles & Fashion, June 3-4, 2012 Bangkok, Thailand.
- **Sezgin H.,** Kursun Bahadir S., Böke Y. E., Kalaoğlu F. 2011: Examination of the Heat Manner of a Conductive Yarn with a Woven Fabric, 1st SMARTEX-Egypt

2011 World Textiles Conference, November 22–24, 2011 Kafrelsheikh University, Egypt.